Table 5-6: Table of Coefficients, P_N Equation		
b_1	b_2	b_3
0.0612	0.53648	-0.2778

Table 5-7: Elements of the P_N Variance-Covariance Matrix, R_{ij}, where i = row, j =column (Symmetric)		
0.13643		
-0.13024	0.14081	
-0.14613	0.13181	0.17452

Table 5.8.
Mixed Mode Burst Test Results and Ratios of Mixed Mode to Axial Crack Burst Pressures

Test No.	Sy + Su (ksi)	0.60" Long Circ Depth (%)	Axial Depth (%)	Axial Length (inch)	Burst Test Seal System	Measured Burst Pressure (psi)	Adjusted BP for Material Prop.(1)	Factor for Adj. BP to Nominal Depth(2)	Adjusted BP for Nominal Depth	Average Burst Pressure	Ratio MM/Axial Burst Pressure
0.80" Long, 72% Nominal Depth Axial Slot											
L Shape											
1-T1-1	164.0	0.0	72.2	0.80	None	4074	4074	1.005	4093	4211	1.000
1-T1-2	164.0	0.0	71.2	0.80	None	4374	4374	0.982	4295		
1-T1-3	164.0	0.0	75.0	0.80	None	3951	3951	1.074	4243		
1-T2-1	164.0	53.0	76.5	0.80	None	3337	3337	1.115	3722	4112	0.977
1-T2-2	164.0	51.2	76.5	0.80	None	3749	3749	1.115	4182		
1-T2-3	164.0	58.2	73.8	0.80	None	4251	4251	1.043	4434		
1-T3-1	164.0	66.0	71.5	0.80	None	4118	4118	0.989	4071	4062	0.965
1-T3-2	164.0	67.0	69.5	0.80	None	4300	4300	0.946	4068		
1-T3-3	164.0	69.8	71.3	0.80	None	4113	4113	0.984	4047		
1-T4-1	164.0	82.8	68.4	0.80	None	4899	4899	0.924	4527	4318	1.026
1-T4-2	164.0	84.2	69.2	0.80	None	4108	4108	0.940	3861		
1-T4-3	164.0	82.4	72.2	0.80	None	4546	4546	1.005	4567		
1-T5-1	164.0	100.0	72.7	0.80	Bladder	3843	3843	1.016	3906	3802	0.903
1-T5-2	164.0	100.0	71.5	0.80	Bladder	3553	3553	0.989	3513		
1-T5-3	164.0	100.0	71.2	0.80	Bladder	4059	4059	0.982	3986		
T Shape											
3-T15-1	165.9	73.8	68.2	0.80	None	4236	4187	0.920	3852	4205	0.999
3-T15-2	165.9	76.4	72.3	0.80	None	4609	4556	1.007	4588		
3-T15-3	165.9	83.1	72.3	0.80	None	4192	4144	1.007	4173		
0.60" Long, 79% Nominal Depth Axial Slot											
2-T6-1	166.1	0.0	77.6	0.60	Bladder	3857	3908	0.967	3682	4094	1.000
2-T6-2	166.1	0.0	78.3	0.60	Bladder	4398	4343	0.983	4269		
2-T6-3	166.1	0.0	78.7	0.60	Bladder	4069	4018	0.993	3988		
4-T19-1	161.8	0.0	80.9	0.60	Bld.,Foil	3897	3949	1.039	4103		
4-T19-2	161.8	0.0	83.8	0.60	Bld.,Foil	4118	4173	1.039	4336		
4-T19-3	161.8	0.0	80.5	0.60	Bld.,Foil	3980	4033	1.038	4187		
2-T7-1	166.1	61.7	77.2	0.60	Bladder	3946	3896	0.958	3731	3969	0.970
2-T7-2	166.1	62.8	79.4	0.60	Bladder	4324	4270	1.010	4312		
2-T7-3	166.1	61.0	77.6	0.60	Bladder	4049	3998	0.967	3865		
2-T8-1	166.1	71.1	80.1	0.60	None	3803	3755	1.028	3860	3756	0.917
2-T8-2	166.1	70.8	79.1	0.60	None	3572	3527	1.002	3536		
2-T8-3	166.1	73.2	78.3	0.60	None	3857	3808	0.983	3744		
2-T9-3	166.1	72.5	78.3	0.60	None	4000	3950	0.983	3883		
2-T9-1	166.1	84.5	80.1	0.60	None	3322	3280	1.028	3372	3308	0.808
2-T9-2	166.1	84.5	79.1	0.60	None	3278	3237	1.002	3245		
2-T10-1	166.1	100.0	81.2	0.60	Bladder	2211	2183	1.039	2267	2482	0.606
2-T10-2	166.1	100.0	78.7	0.60	Bladder	2786	2751	0.993	2731		
2-T10-3	166.1	100.0	80.9	0.60	Bladder	2388	2358	1.039	2449		

Table 5.8.
Mixed Mode Burst Test Results and Ratios of Mixed Mode to Axial Crack Burst Pressures

Test No.	Sy + Su (ksi)	0.60" Long Circ Depth (%)	Axial Depth (%)	Axial Length (inch)	Burst Test Seal System	Measured Burst Pressure (psi)	Adjusted BP for Material Prop.(1)	Factor for Adj. BP to Nominal Depth(2)	Adjusted BP for Nominal Depth	Average Burst Pressure	Ratio MM/Axial Burst Pressure
0.60" Long, 100% TW Axial Slot											
3-T13-1	165.9	0.0	100	0.60	Bld.,Foil	4182	4135	1.000	4135	4165	1.000
3-T13-2	165.9	0.0	100	0.60	Bld.,Foil	4059(3)					
3-T13-3	165.9	0.0	100	0.60	Bld.,Foil	4241	4194	1.000	4194		
3-T14-1	165.9	82.8	100	0.60	Bld.,Foil	2727	2697	1.000	2697	2697	0.648
3-T14-2	165.9	75.3	100	0.60	Bld.,Foil	3002	2969	1.000	2969	3080	0.740
3-T14-3	165.9	74.2	100	0.60	Bld.,Foil	3228	3192	1.000	3192		
0.24" Long, 100% TW Axial Slot											
3-T11-1	165.9	0.0	100	0.24	Bld.,Foil	7656	7571	1.000	7571	7584	1.000
3-T11-2	165.9	0.0	100	0.24	Bld.,Foil	7637	7552	1.000	7552		
3-T11-3	165.9	0.0	100	0.24	Bld.,Foil	7715	7629	1.000	7629		
3-T12-1	165.9	72.3	100	0.24	Bld.,Foil	6885	6808	1.000	6808	6904	0.910
3-T12-2	165.9	73.8	100	0.24	Bld.,Foil	7126	7047	1.000	7047		
3-T12-3	165.9	74.2	100	0.24	Bld.,Foil	6934	6857	1.000	6857		

Notes:

1. All measured burst pressures adjusted to Sy + Su = 164 ksi based on ratio of material properties.
2. Partial depth burst pressures adjusted to nominal depth to facilitate data comparisons. Adjustment based on ratio of nominal to actual axial notch depth burst pressures based upon applying the Westinghouse burst correlation.
3. Bad data due to incomplete burst. Data not included in overall evaluation.

Table 5.9. Burst Test Results for Mixed Mode Separation Distance Evaluation										
Test No.	**Axial Length**	**Axial Depth**	**Circ. Length**	**Circ. Depth**	**Axial Sep. Distance**	**Sep. Distance Flaw Depth**	**Burst Pressure (Note 1) (psig)**	**Burst Pressure Average (psig)**	**Adjusted Burst Pressure (Note 2)**	**Mixed Mode Ratio**
MM-11-01	0.50"	100%	None				4863			
MM-11-02	0.50"	100%	None				4927	4928	4928	1.000
MM-11-03	0.50"	100%	None				4995			
MM-12-01	0.50"	100%	120°	100%	0.250"	0.0%	4409			
MM-12-02	0.50"	100%	120°	100%	0.250"	0.0%	4473	4513	4513	0.916
MM-12-03	0.50"	100%	120°	100%	0.250"	0.0%	4658			
MM-13-01	0.50"	100%	120°	100%	0.250"	≈20.0%	4282			
MM-13-02	0.50"	100%	120°	100%	0.250"	≈20.0%	4092	4184	4184	0.849
MM-13-03	0.50"	100%	120°	100%	0.250"	≈20.0%	4180			
MM-12-04	None		None				11272			
4-T16-1	0.50"	100%	120°	100%	0.350"	9.7%	4241			
4-T16-2	0.50"	100%	120°	100%	0.350"	10.5%	4192	4218	4193	0.851
4-T16-3	0.50"	100%	120°	100%	0.350"	10.5%	4221			
4-T17-1	0.50"	100%	120°	71.2%	0.250"	12.3%	4491			
4-T17-2	0.50"	100%	120°	68.5%	0.250"	10.9%	4698	4549	4521	0.917
4-T17-3	0.50"	100%	120°	69.7%	0.250"	≈15.0%	4457			
4-T21-1	None		None				11340			

Notes:
1. Burst tests for 100% throughwall axial notches performed with a bladder and reinforcing brass foil over the axial notch.
2. Burst pressures for 4-T test series adjusted to MM series by ratio of undegraded burst pressures.

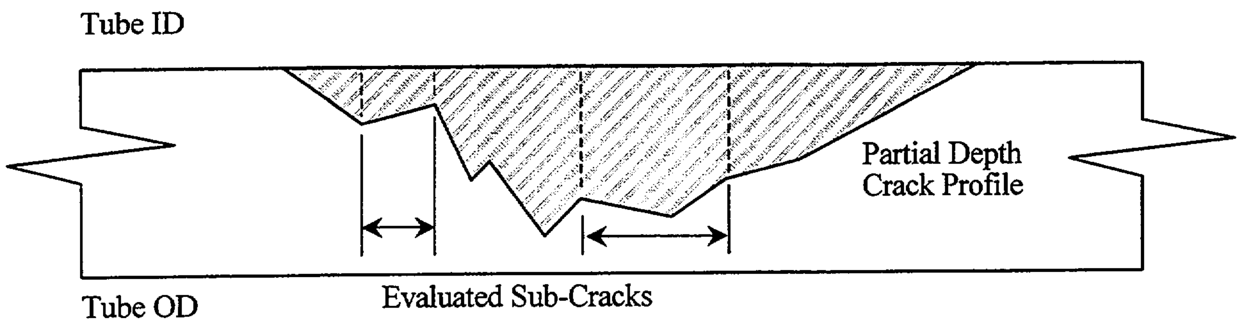

Figure 5-1(a): Representative part-throughwall axial crack profile.

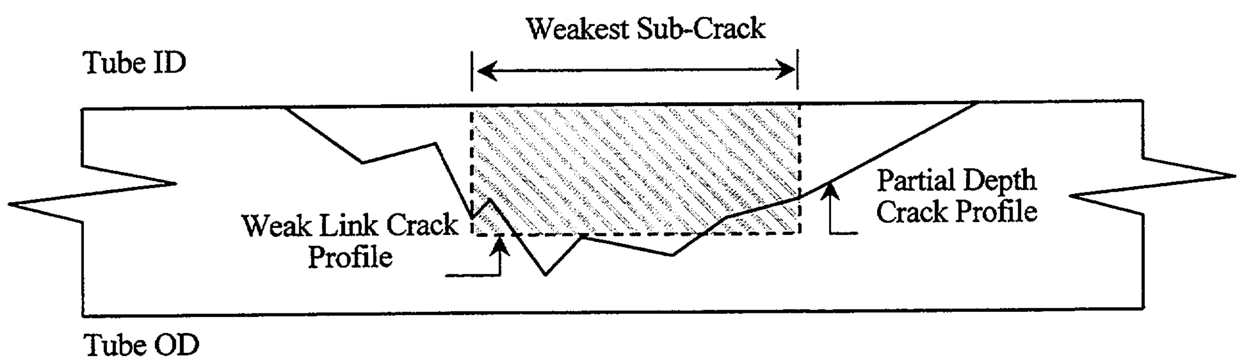

Figure 5-1(b): Representative part-throughwall axial crack profile with the Weak Link (weakest sub-crack) profile shown.

b,c

Figure 5-2

Figure 5-3

b,c

Figure 5-4

Figure 5-5

b,c

Figure 5-6

Figure 5-7

b,c

[ ]

Figure 5-8

Burst Pressure vs. Crack Length

7/8" x 0.050", Alloy 600 MA SG Tubes, σ_f = 68.8 ksi (650°F Mean)

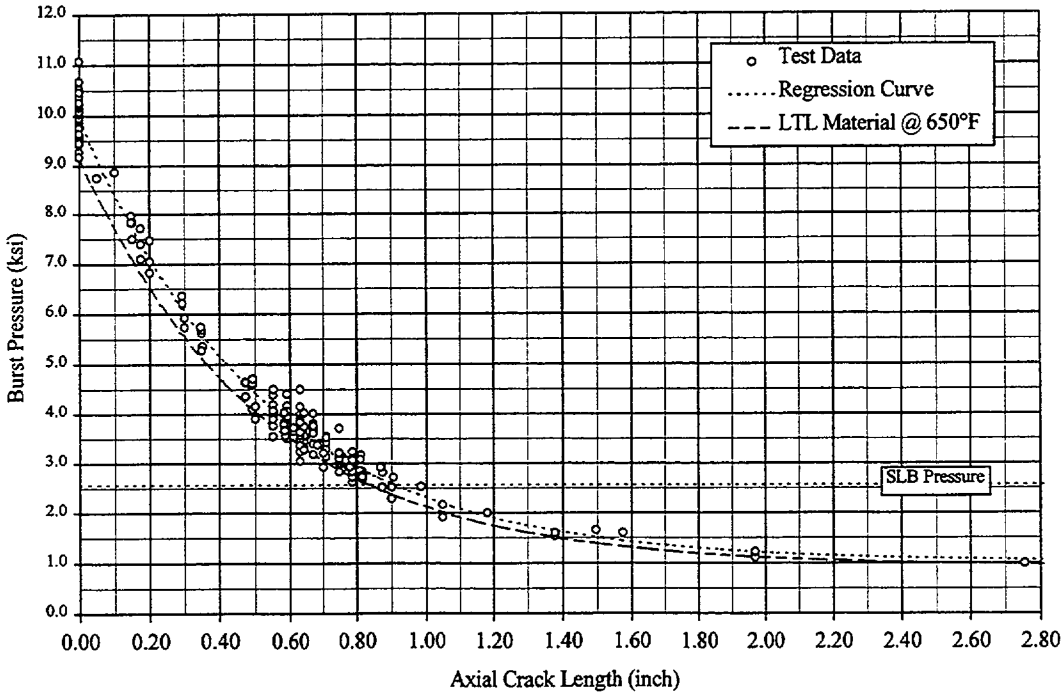

Figure 5-9

Figure 5-10. Mixed Mode Burst Pressure Reduction vs. Circumferential Depth

Ligament Tearing Tests of Intersecting L-shaped (one T-shaped test) EDM Slots

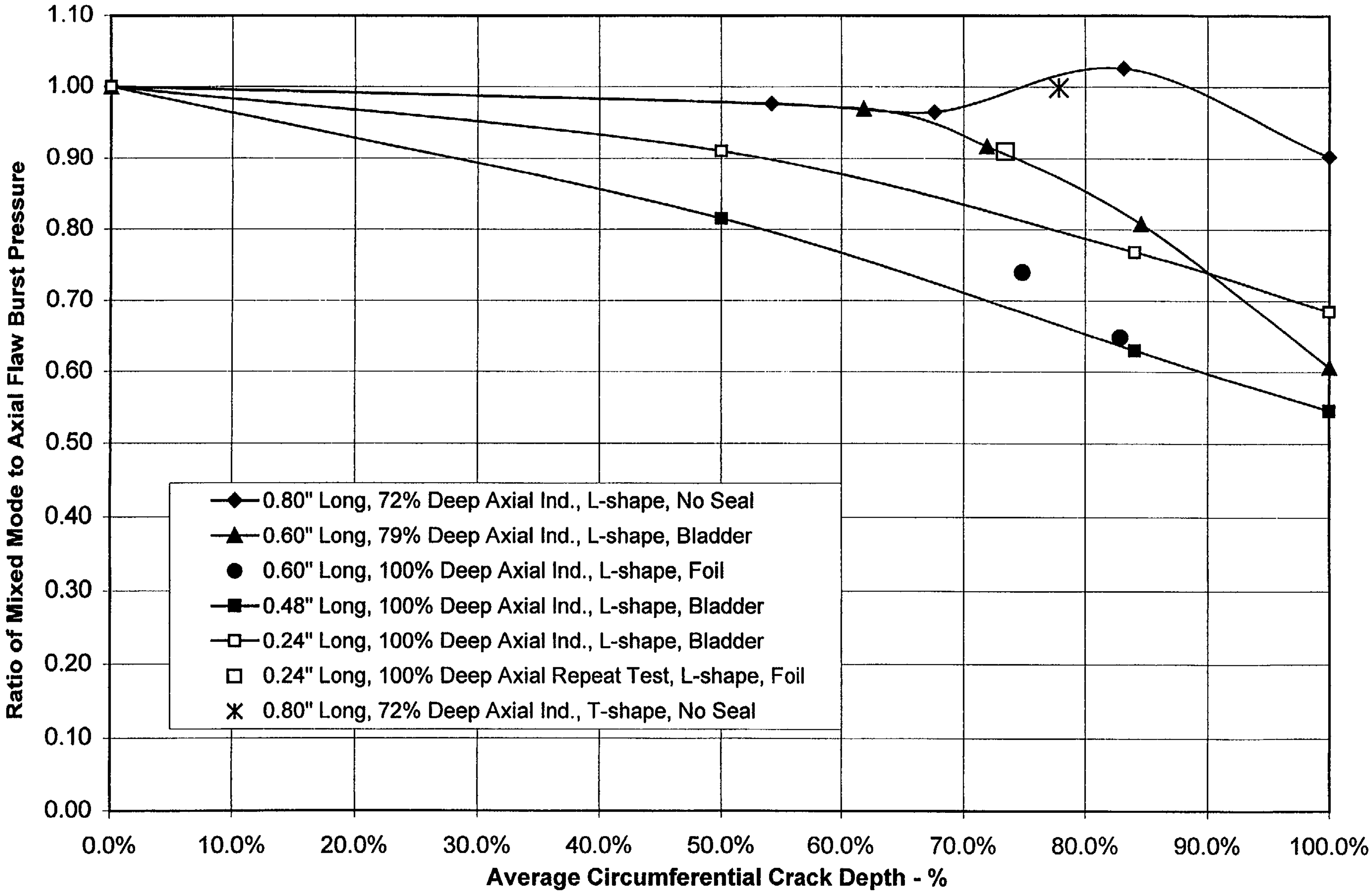

Figure 5-11. Comparisons of Throughwall Burst Pressures with ANL Model Ligament Tearing Pressures - Nominal Material Properties

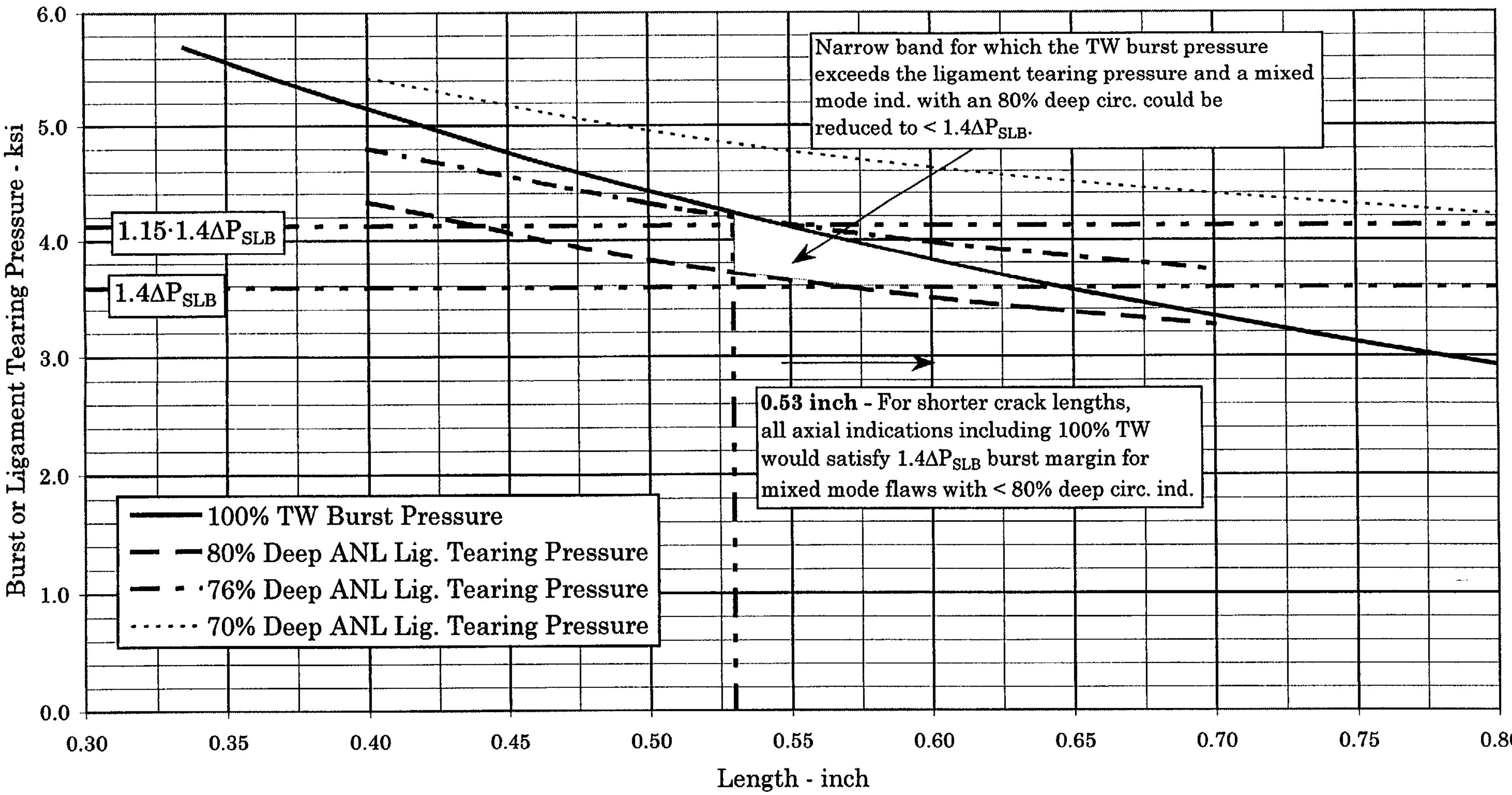

Figure 5-12

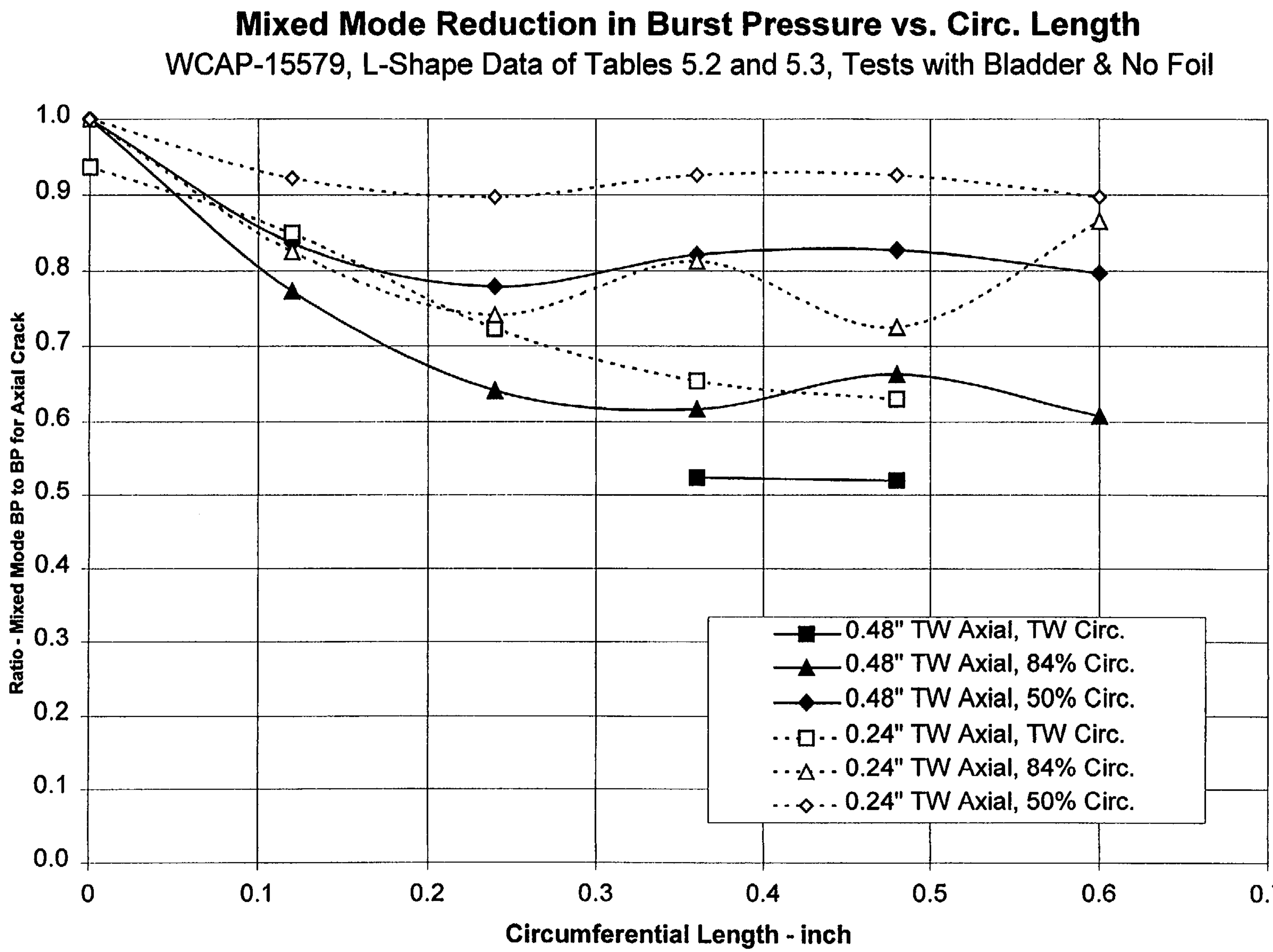
Mixed Mode Reduction in Burst Pressure vs. Circ. Length
WCAP-15579, L-Shape Data of Tables 5.2 and 5.3, Tests with Bladder & No Foil
Ratio - Mixed Mode BP to BP for Axial Crack
1.0
0.9
0.8
0.7
0.6
0.5
0.4
0.3
0.2
0.1
0.0
0
0.1
0.2
0.3
0.4
0.5
0.6
0.7
Circumferential Length - inch
0.48" TW Axial, TW Circ.
0.48" TW Axial, 84% Circ.
0.48" TW Axial, 50% Circ.
0.24" TW Axial, TW Circ.
0.24" TW Axial, 84% Circ.
0.24" TW Axial, 50% Circ.

6.0 SLB LEAK RATE ANALYSIS

This section develops a correlation between measured leak rates and leak rates calculated using the CRACKFLO code. The resulting leak rate correlation is then used to support condition monitoring and operational assessment leak rate analyses. The CRACKFLO code and alternate correlations of measured to calculated leak rates are described in Section 6.2. Section 6.3 provides the correlation applied for leak rate analyses in support of this report. Since the CRACKFLO leak rates are correlated to measured leak rates, the leak rates predicted with the correlation are not strongly dependent upon the specific use of the CRACKFLO code, although the uncertainties in the correlation can be dependent upon the analytical model used to develop the correlation. The ligament tearing model used to predict the throughwall length resulting from breakthrough of wall thickness ligaments is described in Section 6.4.

6.1 Leak Rate Calculation Methodology

For a number of years, leak rates for free span cracks have been calculated using the CRACKFLO Code. This code calculates a crack opening area based on the primary to secondary pressure differential acting on a tube with a given crack length and material properties. Fluid mechanics relations are applied to the pressure opened crack and assumed crack surface geometry such as roughness and tortuosity of the crack flow path. Leak rates are a function of the primary pressure and temperature. Secondary pressure also affects the flow if choking does not occur.

6.2 Leak Rates for Free Span Cracks

In this section, the available crack leak rate database is used to validate the CRACKFLO Code at steam line break conditions. The data base will also be used to assess the effect of various CRACKFLO user specified input parameters. The validation approach will be to develop a correlation including uncertainties between measured crack leak rates (i.e., "truth") and CRACKFLO Code predictions at SLB conditions. SLB leak rates with defined uncertainties can then be determined from the correlation using the CRACKFLO leak rates and a measured crack depth profile. Thus the correlation can support both deterministic and probabilistic leak rate analyses.

6.2.1 CRACKFLO Code Model Description

<u>Crack Leakage Model</u>

The crack leakage model assumes one-dimensional flow and accounts for crack entrance pressure losses, tube wall friction and flashing. The flow experiences a sudden contraction on entering from the primary side. The flashing of liquid to vapor generates an acceleration pressure drop while surface roughness and number of flow path turns along the flow path (tortuosity) result in a friction loss. The total pressure drop is the sum or these pressure losses, determining the pressure at the exit of the crack. For non-critical flow the crack exit pressure will equal the secondary side pressure of the steam generator, while for critical flow, this pressure will be higher than the secondary pressure.

Critical flow is evaluated according to Henry's non-equilibrium model, References 8-22 & 8-23. This method accounts for non-equilibrium effects due to finite flashing rates. This is expected to be particularly important for flow through large cracks where the fluid transit time is short.

The governing equation for flow through an axial crack is the one-dimensional momentum equation for a homogeneous two-phase fluid.

$$\frac{dP}{dy}=\frac{1}{A_c}\frac{d}{dy}\left(\frac{G^2A_c}{\rho}\right)+\frac{f}{2D}\frac{G^2}{\rho} \qquad 6\text{-}1$$

where

P = Static pressure
y = Flow coordinate
A_c = Crack opening area
G = Mass flux
ρ = Fluid density
D = Flow path hydraulic diameter
f = Friction Factor

The first term on the right hand side of equation 6-1 is the is the acceleration pressure drop, while the second term represents friction pressure drop. The acceleration pressure drop can be expanded into component drops due to area and phase change. Assuming isenthalpic conditions, Equation 6-1 can be integrated analytically to give the pressure drop components:

Entrance

$$\Delta P_e=\frac{G_c^2 v_{fo}}{2C_D^2}\left(\frac{A_c}{A_o}\right)^2 \qquad 6\text{-}2$$

Phase change

$$\Delta P_{ae}=G_c^2\left(\frac{A_c}{A_i}\right)\left[v_{fc}+x_c\left(v_{gc}-v_{fc}\right)-v_{fo}\right] \qquad 6\text{-}3$$

Area change

$$\Delta P_{aa}=\frac{G_c^2 v_{fo}}{2}\left\{\left(\frac{A_c}{A_i}\right)^2-\left(\frac{A_c}{A_o}\right)^2\right\}+\frac{G_c^2\left[\overline{v_f}+\overline{x}\left(\overline{v_g}-\overline{v_f}\right)\right]}{2}\left\{1-\left(\frac{A_c}{A_i}\right)^2\right\} \qquad 6\text{-}4$$

Friction

$$\Delta P_f=\left(\frac{12f}{2}\right)\left(\frac{G_c^2A_c^2 v_{fo}}{A_oA_i}\right)+\frac{f}{2}\left(\frac{L}{D}-12\right)\frac{G_c^2A_c}{A_i}\left[\overline{v_f}+\overline{x}\left(\overline{v_g}-\overline{v_f}\right)\right] \qquad 6\text{-}5$$

where

L = Crack depth

ν = Specific volume
x = Steam quality
C_D = Orifice discharge coefficient

Subscripts f & g refer to liquid and vapor phases while o, i & c refer to crack inlet, L/D = 12 (limit of non-equilibrium flow) and crack exit. The overbar indicates average property values.

For tight cracks, short lengths and or low pressure difference, the wall thickness can comprise a large number of L/D's, often in excess of 100. For these cracks friction loss, consisting of wall shear and flow path tortuosity, predominates. Tortuosity is treated using a method proposed by Shrock (Reference 8-24), in which it is represented by a number of fluid expansions, contractions and bends. The equivalent friction factor is given by

$$f = f_p + D\sum_i n_i k_i \qquad 6\text{-}6$$

where pipe friction, f_p, is given by the modified von Karman relation

$$f_p = \left(2\log\frac{D}{2\varepsilon} + 1.74\right)^{-2} \qquad 6\text{-}7$$

and also

n = Number of turns, contractions or expansions
k = Loss coefficient for turns, contractions or expansions
ε = Crack surface roughness

<u>Critical Flow Model</u>

For crack leakage flows, critical flow is possible. When it occurs, the rate of discharge has a maximum value, for a given crack opening, dependent on primary side conditions. Due to its importance in accident analysis, two-phase critical flow has been studied extensively. Theoretical models can be divided into two general categories: 1) equilibrium models which assume thermodynamic equilibrium between both phases throughout the discharge and 2) models which account for non-equilibrium between the phases. Equilibrium models accurately predict the critical mass flow rate in long channels, L/D > 100, where there is sufficient time for thermodynamic equilibrium to be established and the interphase forces are sufficiently developed to maintain relative motion between the phases. For shorter channels, L/D < 20-30, there is insufficient time for the vapor formation to proceed to equilibrium. In this case, non-equilibrium models provide a better predictive tool for mass flow rate. Since crack geometry comprises both short and long flow channels, both equilibrium and non-equilibrium models are appropriate. A good representation of both flow regimes is provided by Henry's critical flow model, References 8-22 & 8-23. According to Henry, the critical mass flow is given by

$$G_c^2 = -\left(\left(\nu_g - \nu_{fo}\right)N \cdot \frac{dx_E}{dP}\right)_t^{-1} \qquad 6\text{-}8$$

for wall thickness to hydraulic diameter ratios less than 12 and

$$G_c^2=-\left(\frac{xv_g}{P}-\left(v_g-v_{fo}\right)N*\frac{dx_E}{dP}\right)_t^{-1} \qquad 6\text{-}9$$

for wall thickness to hydraulic diameter ratios greater than 12, where

G_c = Critical mass flux
x = Non-equilibrium quality
x_E = Equilibrium quality
N = Henry's non-equilibrium parameter

The subscript t on the large brackets in these equations refers to the throat or choking plane at the exit to the crack. The parameter N accounts for non-equilibrium effects due to finite evaporation rates. This is expected to be particularly important in flow through flow through large cracks, where the fluid transit time is short. For small cracks, characterized by a large wall thickness to hydraulic diameter ratio, non-equilibrium effects are not as important and Henry's model reduces to the equilibrium model.

Crack Opening Area Model

Crack opening area is determined from equations presented by Paris and Tada in Reference 8-25. For a tube subject to differential pressure, ΔP, the elastic crack opening area is given by

$$A_c=\frac{\sigma}{E}(2\pi R t_w)G(\lambda) \qquad 6\text{-}10$$

where $G(\lambda)$ is evaluated as

$$G(\lambda)=\lambda^2+0.625\lambda^2 \qquad 6\text{-}11a$$

for λ less than 1 and

$$G(\lambda)=0.14+0.36\lambda^2+0.72\lambda^3+0.405\lambda^4 \qquad 6\text{-}11b$$

for λ greater than or equal to 1. The crack geometric parameter, λ, is given by

[ ]a,c 6-12

and,

σ = Hoop stress
E = Young's modulus
R = Mean tube wall radius
t_w = Wall thickness
a = Crack half length

The effect of yielding near the crack tips is incorporated by the customary method of plastic zone corrections in which a and λ are replaced by a_{eff} and λ_{eff}, respectively. In essence, the size of the plastic zone ahead of the crack is a function of the applied stress intensity factor. However, the stress intensity factor is a function of the size of the crack. Hence, the initial stress intensity factor is used to estimate the size of the plastic zone ahead of the crack tip, which is then added to the crack length to calculate an effect length for the structural and leak rate analysis. The relationship between a_{eff} and λ_{eff} is as follows

$$a_{eff} = a + \left(\frac{1}{2\pi}\right)\left(\frac{K_I}{\sigma_f}\right)^2 \qquad \text{6-13a}$$

and,

$$\lambda_{eff} = \frac{a_{eff}}{\sqrt{Rt_w}} \qquad \text{6-13b}$$

where

K_I = Applied stress intensity factor
σ_f = Flow stress

The flow stress is the average of the yield and ultimate stresses. It is apparent from Equation 6-13a that the lower the flow stress the greater the plastic zone adjustment and the greater the predicted leak rate. The stress intensity factor is a function of the hoop stress, the crack half length and geometry parameter. It is given by

a,c

6-14a

for λ less than 1 and

6-14b

for λ greater than or equal to 1.

6.2.2 Leak Rate Data Base

The primary validation of CRACKFLO calculated leak rates is empirical. The six sets of crack leak rate data available are listed in Table 6-1. Of these, five have leak rates measured at SLB conditions, and were the ones used for this CRACKFLO validation. Sets 1, 3 & 6 were PWSCC cracks and Sets 4 & 5 were ODSCC. For Set 2, the fatigue cracks, no leak rates were measured at SLB conditions and these data are not used in the correlations of this report.

The data sets listed in Table 6-1 provide leak rates at specified primary and secondary side operating conditions. Crack lengths are defined for tube ID and OD or as maximum and through wall lengths. Tube material properties, principally flow stress, were sometimes available; otherwise, mean properties from Reference 8-26 were used for the Inconel 600 tube in question. Tube ID & OD were of course given for each data set.

Mean material properties were used for the leakage analyses when the specific tube material properties were not reported since the leak rates have only a modest sensitivity to material properties and the affect of high or low material properties on the correlation cannot be predicted prior to completing the work. The sensitivity of leak rates to flow stress is shown in Figure 6-8 and tabulated in Table 6-5 for mean properties and for the upper/lower 95%/95% confidence on the flow stress. The effect of flow stress is insignificant for throughwall crack lengths less than 0.2 inch and a modest effect for lengths greater than about 0.3 inch. A 0.5 inch throughwall crack bounds most of the data in the leak rate database, and would be expected to bound any field indication. From Table 6-5 for a 0.5 inch crack, the lower 95%/95% on flow stress results in an increased leak rate by 37% and the upper confidence results in a decreased leak rate by 20%. About 75% of the data used in the leak rate correlation has a throughwall length less than about 0.35 inch for which the flow stress effect is bounded by about 20% for the lower confidence on flow stress. These effects are small compared to the differences frequently found between measured and predicted leak rates. Before the predicted and experimental leak rates are quantitatively compared for each data point, it is not known whether a higher or lower flow stress will improve or reduce the agreement between test and calculation. Conceptually, knowledge of the flow stress for each specimen would reduce the difference between test and analysis, and, thereby, reduce uncertainty in the correlation. However, the differences between test and calculation are more influenced by variability in the test and analysis methods than by variations in flow stress about the mean value. Overall, it is concluded that the use of the mean flow stress in the analysis, when the actual flow stress is unknown, does not significantly influence the test versus calculation leak rate correlation.

For the data sources used in this evaluation as given in Table 6-1, all of the data used in the SLB leak rate correlation are for corrosion cracks since the fatigue data does not include SLB leak rates. The database for the SLB correlation is for pulled tubes and laboratory corrosion specimens included in 5 of the 6 data sets noted in the table. Data sets 4 and 5 were obtained from the EPRI ODSCC database used for the NRC GL 95-05 ARC and are comprised of laboratory specimens. The laboratory specimens were shown in the referenced reports to have corrosion cracks representative of ODSCC pulled tubes. The PWSCC laboratory specimens from Set 1 of Table 6-1 were generated in doped steam tests, for which this report and other work have shown crack morphologies typical of pulled tube specimens. The leakage correlation is based on throughwall crack length, which reduces the sensitivity of the correlation to crack morphology. The differences between PWSCC and ODSCC cracks are primarily due to increased tortuosity for ODSCC compared to PWSCC and some tendency for ODSCC to have more uncorroded ligaments in the crack face. Increased tortuosity factors are included for ODSCC in the correlation as described below in Section 6.2.3. The throughwall crack lengths used for the leakage specimens ignore small uncorroded ligaments between microcracks which would be expected to result in increased differences between analytical predictions and test results. Due to the relatively large crack openings for the longer cracks, the leak rates for long cracks (about > 0.4 inch) are not strongly sensitive to crack morphology (surface roughness, tortuosity) or the differences between PWSCC and ODSCC cracks. As a result, the differences between PWSCC and ODSCC are even less significant than for shorter cracks. In summary, the database used for the correlation is comprised of pulled tube and lab specimens prototypic of pulled tube crack morphologies. Thus, the leak rate data is consistent with flaws found in service.

The distribution of throughwall crack lengths for the specimens used in the correlation of test results to CRACKFLO predictions ranges from 0.03 to 0.6 inch. A number of the PWSCC specimens include more than one throughwall crack. These secondary cracks were dominantly 0.1 inch with a few up to 0.15 inch. The leak rate calculations sum the leak rate from all throughwall cracks for comparison with the test results.

6.2.3 Methodology for Predicting Measured Leak Rates

For calculation, the CRACKFLO Code requires input of a single crack length. Since the data sets provide ID & OD or maximum & through wall crack lengths, there is an option to input either the through wall or a mean value. There are two additional, user specified parameters which are not available with the data sets, crack surface roughness and tortuosity. In the CRACKFLO Code, tortuosity is assumed to be the number of 45° turns along the flow path. Selection of these parameters provides additional options when comparing predicted and measured leak rates.

The following three sets of CRACKFLO Code input assumptions, with respect to crack length, surface roughness and tortuosity, were tested against the data base.

Case 1: Mean crack length, CRACKFLO Code default roughness and tortuosity

Case 2: Mean crack length, increased roughness and tortuosity.

Case 3: Through wall crack length, increased roughness and tortuosity.

The choices above will significantly affect the relationship between predicted and measured values. However, as long as the selected choice is used for both the development of the correlation and the application of the correlation for field prediction, any of the choices can be used.

Crack Length Choice

Choosing either a mean length or a through wall length, as input into the CRACKFLO Code for comparison with a measured result, is a choice which significantly affects the predicted value. Often, the two measured lengths for a given crack are quite different, especially for short cracks.

Crack Roughness and Tortuosity Choice

The character of the crack surfaces and the tortuosity of the crack along the flow path through the tube wall are not measured for the available data but CRACKFLO input parameters for them are required. The default value for roughness is 0.0002 inches which is somewhat rougher than a smooth pipe. Tortuosity is input as the number of 45° turns in the flow path and the default value is zero. Both these values are conservative in the sense that they would yield higher predicted values than more realistic assumptions.

The input values for the three sets of assumptions listed above are defined in Table 6-2. The values for roughness are somewhat arbitrary. [

]^{a,c} Table 6-3 displays the roughness values used in relation to values found in Schrock, Reference 8-24, and a standard fluids text, Streeter, Reference 8-20.

The tortuosity is defined here as the number of 45° turns along the flow path. Schrock, Reference 8-24, based on studies with IGSCC cracks in a weld affected region of stainless steel pipe, gives the following relation for this number:

[ ]a,c 6-15

where, in the present application,

t_W = tube wall thickness - in.

δ = crack opening width - in.

The formula in equation 6-15 is assumed to give the tortuosity for ODSCC cracks. Because PWSCC cracks are less tortuous, an intermediate value between equation 6-15 and no tortuosity is used, given by Equation 6-16.

[ ]a,c 6-16

The above values and relations for crack surface roughness and tortuosity are reasonable for determining the impact of these parameters on CRACKFLO Code predictions in relation to the conservative default values used by the code.

6.2.4 Comparisons of Predicted and Measured Leak Rates

CRACKFLO Code predictions were made for each measured leak rate available in the data sets listed in Table 6-1. Three different predictions were made, corresponding to the 3 cases of CRACKFLO Code assumptions listed in Table 6-2.

Insofar as possible, all required CRACKFLO Code input not listed in Table 6-2, including geometry, operating conditions and material properties were take from the test data sheets and supporting materials. In some cases, material properties were not provided with the test data and were derived from Reference 8-26. The material property most important for calculating leak rate is flow stress; the best estimate value from Reference 8-26 was used. Young's modulus, which has a minimal effect on leak rate, used the ASME Code value.

Some leak tests using pulled tubes contained a number of cracks. For these cases, predictions for each crack were made and summed for comparison with the single measured leak rate.

<u>Comparison Results</u>

Figures 6-1 through 6-3 present comparisons of the crack the measured values with predicted leak rates for the corresponding test. Case 1 CRACKFLO assumptions, Figure 6-1, results in consistent over prediction of measured leak rates though the slope of the regression line is close to the slope of the predicted = measured line. The 95% confidence prediction upper bound follows the predicted = measured line closely. Adding more realistic roughness and tortuosity, Figure 6-2, reduces the degree of over prediction by CRACKFLO but at the same time increases the scatter of the data about the regression line. The slope of the regression continues to be close to the slope of the predicted = measured line. Using the through wall crack length for the predictions, Figure 6-3, further reduces the over prediction of the regression line, but also changes the slope to a value significantly different from the slope of the predicted = measured line and tends to further increase the scatter of the data in relation to the regression line.

In summary, Figure 6-4 presents the three regression lines in relation to the predicted = measured line. Using the Case 2 & 3 CRACKFLO assumptions increases flow resistance and/or reduces flow area. These effects reduce, as expected, the over prediction of the Case 1 conservative assumptions. Both these assumptions tend to reduce leak rate more for short cracks (low measured leak rates) than long cracks (high measured leak rates), explaining the decrease of the regression line slope for the Case 2 & 3 assumptions. The surface roughness contributes more significantly to leak rate reduction in short cracks with small opening width because the friction losses constitute a large part of the total pressure drop for these cracks. Similarly for tortuosity, the same turns on a crack surface contribute more to turn losses when the matching crack surfaces are close together, short cracks, than when they are farther apart. The Schrock relation for Number of 45° turns reflects this since the number is inversely proportional to crack opening width, Equations 6-15 & 6-16. With respect to the assumption of through wall crack length rather than the mean length, the effect is also larger for short cracks since the ratio of maximum length to through wall length is larger for these cracks. As cracks grow deeper, the ratio of maximum crack length to through wall length tends toward unity.

6.3 SLB Leak Rate Correlation

In this section the SLB measured leak rate data sets, reported in section 6.2, are used to define a leak rate correlation for calculating SLB leak rates for throughwall cracks. The throughwall crack model as used in this analysis can be easily applied in deterministic or Monte Carlo analyses using crack depth profiles. Given a crack profile, the throughwall (applied at less than throughwall to allow for radial ligament tearing) crack length can be readily determined for input to the leak rate calculation. The radial ligament breakthrough model applied for the leakage analysis is described in Section 6.4. Based on the statistical correlation given in Figure 6-3, the measured or "truth" leak rates can be obtained from the CRACKFLO Code calculated leak rates and developed to account for uncertainties. The predicted leak rates can be obtained at any confidence level from the correlation parameters for any given throughwall crack.

6.3.1 SLB Through Wall Crack Leak Rate and Confidence Bounds

Figure 6-3 shows the regression line or median leak rate, the arithmetic average leak rate from the regression analysis (for a log correlation, the average leak rate is not the regression correlation) and the 95% confidence prediction bounds for the measured leak rates at any given calculated leak rate. For any leak rate calculated by CRACKFLO (on the abscissa), the 95% confidence prediction upper bound line represents the conservative upper bound leak rate for that calculated value. CRACKFLO leak rates are calculated as a function of the throughwall crack length for standard SLB conditions. The correlation is then applied to obtain the predicted or "truth" leak rate from the CRACKFLO leak rate. The correlation is linear in the logarithms and given by:

[ ]a.c 6-18

The parameters for the correlation are given in Table 6-4. The correlation parameters of Table 6-4 can be used in Monte Carlo analyses for SLB leak rates as discussed in Section 7. The p-value for the slope of the correlation is seen to be on the order of 10^{-22} and readily satisfies statistical guidance for use of a correlation.

The distribution of the residual values of Q_{truth} is shown on Figures 6-5 and 6-6. The scatter plot on Figure 6-5 illustrates that the residuals are not correlated to the predicted values of leak rates. Finally, the normal probability plot on Figure 6-6 confirms that the residuals of the logarithm of the leak rate do not contradict the assumption of being from a normal, i.e., Gaussian, distribution.

6.3.2 CRACKFLO and Correlation SLB Leak Rates for PWSCC

The Steam Line Break conditions assumed for the leak rate calculation are as follows

Primary Temperature —	600°F
Primary Pressure —	2575 psia
Secondary Pressure —	15 psia

In addition, a 7/8" OD by 0.050" wall thickness tube with a mean flow stress from Reference 8-26 and Case 3 CRACKFLO assumptions for PWSCC from Table 6-2 are assumed. With these assumptions, a unique leak rate can be calculated as a function of throughwall crack length. The SLB leak rate calculated by CRACKFLO is tabulated in Table 6-5. Although the leak rates are calculated for operating temperature conditions, the resulting leak rates are converted to room temperature gpm for comparisons with acceptance limits given as room temperature values. Table 6-5 also includes the corresponding correlation nominal leak rate from the regression equation and the upper 95% confidence on the predicted leak rate for "truth". The correlation nominal leak rate is the regression line for the correlation of measured ("truth") and CRACKFLO leak rates and represents the regression median value or 50% probability at 50% confidence.

The correlation nominal, regression or arithmetic average and upper 95% SLB leak rates as a function of throughwall crack length given in Figure 6-7 to graphically illustrate the uncertainty levels associated with the correlation. As described in Section 7, condition monitoring and operational assessment analyses for SLB leak rates are expected to be performed by Monte Carlo analyses using the CRACKFLO leak rates of Table 6-5 and the correlation parameters of Table 6-4. A correction for flow stress, as described in the following section, is applied to the CRACKFLO leak rates of Table 6-5.

6.3.3 Leak Rate Correction for Material Flow Stress

The calculations in the previous section assumed a mean flow stress of 68.8 ksi for a 7/8" OD, mill annealed, Inconel 600 tube at 650°F (Reference 8-26). From the same reference, the lower tolerance limit (LTL) for flow stress is 63.0, 9.2% lower. Assuming an upper limit 9.2% above the mean results in a flow stress of 75.1 ksi. Flow stress values lower than the mean will result in higher leak rates than those defined in Figure 6-7 while higher values of flow stress will cause leak rates to be lower. Figure 6-8 shows the leak rate dependence on the LTL, mean and maximum flow stresses.

To use the values of leak rate plotted in Figure 6-7 for flow stress values different from the mean, a table of bounding correction factors has been developed using the results of Figure 6-8. These factors appear in Table 6-5, along with the numerical values of leak rate used to plot Figure 6-7. For small cracks, ≤ 0.2 inches, the correction factors are approximately inversely proportional to the flow stress. For this range the factor has been conservatively set to 1.0 for flow stresses larger than the mean and to the flow stress ratio for flow stresses smaller than the mean. For cracks larger than 0.2 inches, the effect on leak rate is greater and the bounding factors listed in Table 6-5 were calculated using CRACKFLO results for different values of flow stress.

For Monte Carlo leak rate analyses, the flow stress correction of Table 6-5 is interpolated for the specific flow stress and throughwall crack length of each Monte Carlo sample and the correction is applied to the CRACKFLO calculated leak rate obtained from the function of Figure 6-7.

The values for parameters needed to perform the leak rate modeling are given in Tables 6-4 and 6-5. Additional parameters for ligament tearing are given in Section 6.4.2 below.

6.4 Monte Carlo Calculation of the Radial Ligament Breakthrough Length at SLB Conditions

6.4.1 Monte Carlo Leakage Analysis Method

A Monte Carlo simulation model is applied for estimating the leak rate through degraded tubes during a postulated steam line break (SLB) event. The Monte Carlo model uses the NDE crack profiles obtained for each indication including simulation sample adjustments for maximum depth and length NDE uncertainties for condition monitoring and maximum depth NDE uncertainties, length NDE uncertainties and maximum depth growth for operational assessments. Calculations may be performed to obtain the leakage distribution for a single indication or for the entire SG indication distribution. The Monte Carlo leakage model includes:

1. The crack profile is searched for the longest lengths that would be predicted to break through by ligament tearing at SLB conditions. The profile is evaluated three times. In general, the weakest ligament of the crack will be near the center of the crack. Once that torn length has been identified, the profile of the crack above and below the torn length is evaluated to determine if a second or third location is anticipated to tear.

2. The ANL (Argonne National Laboratories) model for ligament tearing is used to estimate the throughwall length(s) of the indication(s) (See Section 6.4.2 below).

3. CRACKFLO is used to calculate a model value of the leak rate using the throughwall length(s) from the ANL model.

4. The leak rate correlation is applied to calculate a random value of the leak rate distributed about the regression line.

5. The distribution of leak rates from each of the random samples is developed and evaluated at the required confidence level (See Section 7 for ARC requirements on confidence levels) for the analysis.

6. The combined use of a ligament tearing model and CRACKFLO leak rates results in a conservative overestimate of the leak rate. As described in Section 6.2.1, the CRACKFLO crack opening model includes a calculation for crack extension at the crack tip, which is also effectively part of the ligament tearing effect. Leakage is therefore based on a longer length than

that obtained only from the ligament tearing model and the predicted leak rates are inherently conservative. In addition, PWSCC cracks are initiated as multiple microcracks which grow to link up with other microcracks to form the overall macrocrack. Crack depths vary significantly between microcracks such that non-throughwall depths vary sharply over short spans. As a consequence, leak tests of corrosion induced cracks rarely show ligament tearing for more than about 2% of the wall thickness where the depth is the largest. The ligament tearing models are based on uniform average depths and typically predict breakthrough at shallower depths and longer lengths than found in tests of corrosion cracks. This effect adds further conservatism to the predicted leak rates. That is, leak rates would be over-predicted due to the CRACKFLO crack extension beyond that of the ANO ligament tearing model and due to the analytical models predicting more ligament tearing than indicated by leak tests of corrosion cracks with non-uniform depth profiles.

6.4.2 Ligament Tearing (Breakthrough) Model

The ligament tearing model is based on the use of a hoop stress magnification factor approach as presented in Reference 8-27. For a single throughwall axial crack the pressure to cause burst of the tube, P_B, is given by,

$$P_B = \frac{P_0}{m}, \qquad 6\text{-}19$$

where P_0 is the burst pressure of the non-degraded tube and m is referred to as the hoop stress or stress intensity (in the fracture mechanics sense) magnification factor. The factor m is also referred to as the bulging factor because it accounts for radial deformation of the crack flanks as a function of the crack length, L, the mean radius of the tube, R_m, and the thickness of the tube, t. Reference 8-27 reported m to be

$$m = 0.614 + 0.386\,e^{-1.25\lambda} + 0.481\lambda, \quad 6\text{-}20$$

where λ is the normalized crack length given by,

$$\lambda = \frac{0.9089\,L}{\sqrt{R_m\,t}}. \qquad 6\text{-}21$$

The expression for m is the result of a regression analysis of data obtained from numerical solutions of theoretical models of axial cracks. Hence, it represents a theoretical solution to the problem of burst of axially cracked tubes. The constant in the numerator is a function of the Poisson's ratio of the material. Reference 8-28 reviewed several models for predicting the pressure required for tearing the remaining ligament based on modifying the above formulation to use a part-throughwall stress intensity magnification factor, m_p. The inverse of the stress intensity magnification factor is a failure pressure reduction factor, herein designated by ξ. Thus, the pressure required to tear the remaining radial ligament of a part-throughwall axial crack, P_T, is found as,

$$P_T = \frac{P_0}{m_p} = \xi\,P_0. \qquad 6\text{-}22$$

Reference 8-28 presented a review of various formulations for m_p and recommended a final expression for m_p as a function the relative depth of the crack, h (the ratio of the depth, d, to the thickness of the tube), and the throughwall axial crack magnification factor as,

$$m_p = \frac{1-\alpha h/m}{1-h}, \text{ where } \alpha = 1 + 0.85h^2\left(1-\frac{1}{m}\right). \qquad \text{6-23}$$

Reference 8-28 further designated this model as the ANL model. The coefficient of 0.85 used in equation 6-23 was originally reported as 0.9 in NUREG/CR-6511, Vol. 2. Subsequent examination of the original calculation revealed that some minor changes in the computation were required to account for temperature affects on the material properties (the tensile tests were performed at room temperature and the burst tests at 600°F), the radius used for the normalized crack length, the radius used for the non-degraded burst pressure, and the number of data for which ANL depth measurements were available. The revised coefficient was obtained via Reference 8-30. The non-degraded burst pressure is computed as,

$$P_0 = 0.595(S_Y + S_U)\frac{t}{R_m}, \qquad \text{6-24}$$

based on a large amount of Westinghouse and industry data, including the results used in the ANL computation, see Reference 8-13.

The limit of m_p as h goes to 1, i.e., corresponding to a throughwall crack, is infinity, and the ligament tearing pressure is then zero. Results obtained from the model for three different cracks lengths are illustrated on Figure 6-9. For very long cracks, say greater than 1.5", the model is linear between the non-degraded burst pressure for zero depth and zero for 100% depth. For shorter cracks the shape of the curve becomes more and more convex. As the length approaches zero, the location of the maximum rate of change of the slope, i.e., the *knee* of the curve, tends to the non-degraded burst pressure as the depth approaches 100%.

The critical crack length as a function of crack depth for the postulated SLB differential pressure for nominal and 95/95 lower tolerance limit (LTL) material properties is presented on Figure 6-10. A curve for the critical crack length under typical normal operating conditions is also presented. It may be concluded from the figure that the effect of material property variations is small for depths greater than about 90% throughwall.

The ligament tearing model was derived to predict the behavior of part-throughwall, rectangular shaped, axial cracks. The comments of Section 5 regarding the shape of real cracks also apply to the prediction of the ligament failure pressure. The approach used to predict the ligament tearing pressure is the same as that used to predict the tube burst pressure, with the exception that the ANL model is used. Since the intent is to predict ligament tearing, no calculations of the burst pressure of the resulting 100% throughwall axial crack are performed for the leak rate evaluations. Following the naming of the burst pressure algorithm, the leak rate algorithm was designated as the *weak leak* model.

The end goal of the weak leak model is different from that of the burst pressure model. In order to estimate the leak rate, the likely throughwall crack length for a given applied pressure must be known.

Hence, the model is applied to all possible sub-cracks from the original profile and the ligament tearing pressures are calculated. The length of the sub-crack with a ligament tearing pressure just less than (not more than) the SLB differential pressure may then be used for the leak rate calculation. Following identification of this longest throughwall length due to break through at SLB conditions, the crack profile is searched to identify the next two largest sub-lengths either above or below the longest throughwall length that would also be predicted to break through at SLB conditions. The lengths predicted to be throughwall are then included in the SLB leak rate analysis. Because the profile information is based on discrete increments, the appropriate sub-crack to evaluate is the one with the minimum tearing pressure that is greater than or equal to the given critical pressure. This means that the length returned is greater than or equal to that corresponding to the tearing pressure exactly matching the critical pressure. Because the leak rate from axial cracks varies approximately with the third to fourth power of the crack length, the subsequent leak rate calculation is conservative.

It is possible for multiple, distinct sub-cracks to exist with ligament tearing pressures equal to the SLB pressure. In this case the leak rate calculation would normally be performed for all such sub-cracks and the total leak rate found as the sum of the individual values. However, the presence of such cracks is judged to be a rare event although the model considers the longest and next two largest sub-cracks with a ligament tearing pressure nearest to, but greater than or equal to, the applied SLB pressure. For the rare case of two sub-cracks having the potential for ligament tearing, the longest sub-crack leak rate can be expected to be significantly higher than that of a shorter crack due to the leak rate dependence on throughwall crack length to a power of 3 to 4. Due to both low frequency of occurrence and lower leak rate of a second sub-crack with leakage, the leakage from a potential second sub-crack can be ignored. As discussed above in Section 6.4.1, the leakage model already incorporates conservative leak rate predictions and efforts to calculate the breakthrough length for a second, shorter sub-crack are not necessary, but is included in the analysis.

Additionally, there is a conservative shortcoming of the model associated with the representation of the crack as an equivalent rectangle. Consider the case where there is a 100% throughwall portion of the crack being evaluated. One of the crack segments analyzed will consist only of the 100% throughwall region (the ligament tearing pressure will be zero in this case). The next segment analyzed will consist of the 100% throughwall length plus the inspection increment at one end of that segment. To make a rectangular representation of the crack, the incremental material will be treated as being much narrower in order to extend it over the length of the rectangle while keeping the area of the crack constant. This means that the analysis will likely predict tearing of that incremental ligament even if it is quite wide. For example, consider a 7/8" by 0.050" SG tube with a 0.3" long throughwall axial crack segment, an inspection increment of 0.030", and an adjacent depth of 50%. The geometry of the throughwall portion and the next increment will be that of a rectangle with a length of 0.33" and a depth of 95%. It is likely that such a narrow ligament would be predicted to tear at a lower pressure than needed to actually extend the crack.

6.4.3 Simulation of the Torn Ligament Crack Length

The ANL ligament tearing relation involves the calculation of a constant in the expression for determining the bulging stress magnification factor, m_p. The evaluation of the test data indicate a mean error of –0.02 in predicting the inverse of the magnification factor. The error of the estimate, ε, is given by:

$$\varepsilon = \frac{\xi_t - \xi_c}{\xi_t} \text{ where } \xi = \frac{1}{m_p}, \qquad \text{6-25}$$

and the subscript t denotes the experimentally measured test failure pressure reduction factor and c denotes the predicted value from the empirical (ANL) equation. The negative value of the mean error indicates that the experimental failure pressure is usually slightly higher than the predicted failure pressure. The standard deviation of the error was calculated to be 0.05. Owing to the errors in the determination of ξ there will be an uncertainty associated with the value of m_p in the ligament tearing equation. The criterion for ligament tearing then becomes,

$$\frac{P_0}{m_p + \Delta m_p} \le P_{SLB} \text{ or, } \frac{P_0}{m_p} \le \left[1 - \frac{\Delta\xi}{\xi}\right] P_{SLB}, \qquad \text{6-26}$$

where $\Delta\xi$ is the uncertainty or error in determining $1/m_p$, and P_{SLB} is the primary-to-secondary differential pressure associated with a SLB event. The intent of the calculation is to account for the effect uncertainties associated with $1/m_p$ on the ligament tearing length from the ANL equation. The actual process of estimating the leak rate is to find the maximum length associated with any tearing pressure that is less than the critical accident pressure. The process is repeated for the remaining profile on either side of the initial maximum length to identify up to two additional maximum tearing lengths associated with the remainder of the profile. The relative error of $1/m_p$ is given in the square bracket of the above equation. Thus, uncertainties in $1/m_p$ may be translated to uncertainties in the length by adjusting the critical pressure for which the torn length is to be found. The simulation of the uncertainties in $1/m_p$ may be achieved by directly sampling (with replacement) the observed distribution of the errors. The observed relative errors, $\Delta\xi/\xi$, from the ANL data are listed in Table 6-6. The errors are approximately normally distributed as shown on Figure 6-11 and the errors are independent of the calculated value of $1/m_p$ as shown on Figure 6-12. This means that the simulation of the errors may be performed independent of the value of $1/m_p$ calculated.

For example, if the relative error of $1/m_p$ is negative, then the calculated tearing pressure, P_T, must be compared to a larger critical pressure to determine if ligament tearing occurs. The length of the torn ligament is calculated from the value of P_0/m_p that just satisfies or exceeds the criterion. Hence, increasing the criterion pressure results in the calculation of a longer crack length. This occurs when the error in ξ is negative. The converse is also true, if the relative error of ξ is positive, then the criterion pressure is reduced, consequently the applicable ligament tearing pressure is reduced as is the corresponding torn length.

In practice, a random error in ξ is selected for each indication in the SG. The critical pressure for ligament tearing is calculated as the right hand side of Equation 6-26. As the *WeakLeak* model calculation is performed, the ligament associated with the sub-crack with the minimum burst pressure that is still greater than the critical pressure is assumed to tear and the length used for the leak rate calculation. If no sub-cracks have ligament tearing pressures less than the critical value, the crack is assumed to not leak during a postulated SLB event.

6.4.4 Simulation of the Actual Leak Rate

Table 6-4 presents the results of performing a regression analysis of the measured leak rate on the leak rate predicted by the Westinghouse code CRACKFLO. The leak rate values simulated by the Monte Carlo code are predictions based on using the effective standard deviation of the log, i.e., logarithm, of the leak rate and the Student's *t* distribution. The method includes simulation of the uncertainties of the regression parameters.

Information presented in Section 6.3 documented the development of a regression model to be used for predicting the expected actual leak rate, Q_a, from a throughwall axial crack as a function of the leak rate predicted by the Westinghouse computer code CRACKFLO, Q_c. The regression equation is linear in the logarithms of the respective variables, i.e.,

$$\log(Q_a) = b_0 + b_1 \log(Q_c), \qquad 6\text{-}27$$

where b_0 and b_1 are the coefficients of the equation obtained from the regression analysis. The values of the coefficients are listed in Table 6-4. The available data are only a sample of some infinite population of pairs of leak rates. Therefore, the solution coefficients, and the standard deviation, s_r, of the residuals from the regression analysis, are estimates of the parameters of some "true" equation that would be obtained if the entire population of all possible leak rates were analyzed. If these were the true coefficients and standard deviation of the residuals, the parameters of the "true" relation, the distribution of a large number, *N*, of future values of the logarithm of the actual as a function of a predicted leak rate could be calculated as,

$$\log(Q_{a,i}) = b_0 + b_1 \log(Q_c) + Z_i\, s_r \; ; i = 1,\ldots,N, \qquad 6\text{-}28$$

where the subscript *i* indicates some i^{th} value, and the Z_i are random numbers from the standard normal distribution (mean of zero and standard deviation of one). However, the coefficients and standard deviation are obtained from the analysis of sample data. Therefore, the simulation must account for the potential statistical errors arising from the use of the sample data to estimate the population parameters.

One approach that has been approved by the staff for simulating the total leak rate from multiple indications is documented in Reference 8-10. The simulation proceeds as follows:

1. For each simulation of the indications in the SG in toto, a random value of the population standard deviation, σ, is estimated from the regression standard deviation, s_r, using a random value from the Chi-Square distribution (the distribution of variances of samples drawn from a normal population).

2. The population σ is then used to estimate a random value of the population intercept regression coefficient, β_0, corresponding to the sample estimate, b_0, as following a normal distribution with the known population standard deviation divided by the square root of the number of test values used in the correlation.

3. The population σ and β_0 are then used to estimate a random value of the population slope coefficient, β_1, corresponding to the sample estimates, b_1. The values of β_0 and β_1 follow a bi-variate normal distribution, hence the sampling of each value is not independent of the other.

4. A random value of the log of each leak rate for each indication in the SG is then calculated as,

$$\log(Q_j) = \beta_0 + \beta_1 \log(Q_{c,j}) + Z_{R,j}\,\sigma \qquad \text{6-29}$$

   where the $Z_{R,j}$ are independent random values from the standard normal distribution, and j varies from one to the number of indications.

5. The total leak rate from the simulation of all of the indications in the SG is then calculated and retained as the estimate from a single simulation.

6. The process is repeated many times, say 10,000, and the distribution of total leak rates characterized, mean, standard deviation, etc. A selected percentile, e.g., 95th, of the distribution of leak rates is then used to estimate the potential leakage that could occur during a postulated SLB event.

7. If that estimate exceeds a plant specific allowable value, additional tubes are removed from service until the 95th percentile prediction is less than the allowable. This approach simulates the uncertainties associated with estimating the regression parameters from the sample data. The approach using equation 6-29 is rigorous in accounting for all possible uncertainties associated with the prediction as long as the assumption of normally distributed residuals is valid.

If the number of data is large and the variance of the predictions small, the omission of the simulation of the uncertainties associated with the calculation of the parameters (the coefficients and the standard deviation of the residuals) may not significantly affect the simulation of the total leak rate. However, this has not been demonstrated to be the case for this problem and simulation of the uncertainties of the parameters was performed as part of the Monte Carlo analysis.

6.4.5 Conclusions

Monte Carlo simulations à la Equation 6-29 are performed to simulate the total leak rate from the SG. Due to the complexity of the equation for ligament tearing, the error in the predicted tearing pressure reduction factor is simulated using the actual distribution of errors associated with the qualification of the model, i.e., just as the growth rate is simulated.

6.5 Uncertainties in SLB Leak Rate Analyses

The following items address methods and uncertainties used in the SLB leak rate analyses relative to their increasing or decreasing the conservatism in the leakage analyses.

1. Leak rates based on calculated ligament tearing breakthrough length
   - Very conservative methodology for leak rate analysis based on leak rate correlation

- Effects of ligament tearing are already included in leak rate correlation as the difference between test and calculation since calculations are based only on the corrosion throughwall crack length with no breakthrough allowance. Net effect on correlation is to increase uncertainty since difference between test and calculation would increase if ligament tearing was significant.
- Calculated TW length will always equal or exceed corrosion TW length, thus uniformly increasing predicted leak rate.
- If ligament tearing was included in the correlation development, the calculated leak rates would increase, the mean regression correction to test results would decrease, and the uncertainty in the correlation would conceptually decrease. However, crack depth profiles are not available for more than 50% of the database and these data could not be used in a correlation based upon ligament tearing analyses.

2. Inclusion of uncertainties in the ligament tearing model
   - Conservative methodology
   - Further increases the larger leak rate predictions above the conservatism resulting from Item 1 above.

3. Inclusion of POD = 0.6 in leakage operational assessment
   - Very conservative methodology
   - Indications large enough to leak in the subsequent operating cycle can are expected to be detected with a POD much higher than 0.6 and likely approaching unity. This expectation is supported by the absence of any leaking PWSCC indications at dented TSP intersections in Sequoyah and Diablo Canyon SGs.
   - Based upon the POD adjustment applied as 1/POD to define the BOC indications, the effect of applying a POD = 0.6 is to increase the leak rate for indications left in service by 67%.
   - The 0.6 POD leaves in service 0.67 of an indication for each repaired indication. For depth based tube integrity assessments, this effect is excessively conservative and can lead to repaired indications leading to unacceptable leakage in the operational assessment. For example, if a few indications satisfy all condition monitoring requirements but are very close to throughwall or have negligible leakage, the addition of growth to 0.67 indication for each of these repaired indications could lead to exceeding the operational leakage limit for plugged tubes. In this case, repair of all indications would still lead to exceeding operational assessment limits.

4. Crack depth profiles are adjusted to 100% depth for indications with maximum amplitudes > 4.5 volts based on application of the data adjustment procedures
   - Conservative methodology intended to improve nominal leak rate predictions
   - PWSCC indications with finite throughwall lengths are expected to exceed 4.5 +Point volts as supported by the database of this report.
   - Addition of NDE uncertainties then increases the throughwall length and associated leakage
   - Further calculation of ligament tearing length will further increase throughwall length and leakage

5. Finite +Point coil resolution (0.16") tends to reduce very short maximum depths
   - Modest non-conservatism for leak rate analyses
   - Since the NDE uncertainties on maximum depth are also based on coil resolution averaging of destructive exam results, the NDE uncertainties do not adjust for this effect
   - Local maximum depths < 0.16" would have small leak rates of < 0.005 gpm based on nominal leak rate correlation of Table 6-5.
   - Since ligament tearing model is based upon average depths, the average depths for significant leakage of > 0.16" would not be affected by the finite coil resolution.

6. Use of mean flow stress in leak rate calculations when actual tube flow stress was not reported in leak test reports
   - Negligible effect on calculated leak rates
   - Calculated leak rates would be slightly lower or larger if the flow stress was higher or lower, respectively, than obtained using the mean stress. In general, knowledge of the flow stress would lead to improved agreement with the test value, such that use of the mean value would tend to conservatively increase the uncertainty in the leak rate correlation.
   - Additional discussion on the use of the mean flow stress is given in Section 6.2.2.

7. Use of ODSCC data in leak rate correlation applied for PWSCC leak rates
   - Minor conservatism
   - Use of throughwall length for leak rate correlation reduces the differences between ID and OD flaws in leak rate analyses. The principal difference between PWSCC and ODSCC is the more tortuous leak path for ODSCC, for which a correction is applied in the leak rate calculation
   - Specimens with the largest differences between test and calculation in the correlation are ODSCC indications, which increase the uncertainty in the correlation

The cumulative influence of the above methods and uncertainties on SLB leak rates is dominated by the conservatism of Items 1 and 3 above. Substantial conservatism results from incorporating a ligament tearing model in the analysis even though the effects of ligament tearing are incorporated in the uncertainties of the leak rate correlation as part of the difference between test and analysis. Incorporation of the ligament tearing model can be expected to increase all calculated leak rates even though the effects of ligament tearing are already indirectly included in the correlation. It would be more appropriate to include the ligament tearing model in the analyses used to develop the correlation. However, less than half of the leak rate data include the depth profiles necessary to calculate ligament tearing. As noted for item 3, the use of POD = 0.6 can lead to not satisfying operational assessment leakage limits even if all indications are plugged. The influence of Items 4 to 7 above have a negligible impact on the leak rate analyses compared to Items 1 to 3.

6.6. Methods for Mixed Mode SLB Leak Rate Adjustments

It is shown in Section 7.9 that there is a very low probability of occurrence for a mixed mode indication leading to a significant reduction in burst pressure or an increase in SLB leakage. However, Section 7.9.5 provides conditional criteria for requiring mixed mode adjustments to leakage in the unlikely event that a mixed mode indication large enough to potentially impact leakage is found in an inspection. This section defines the methods to be applied for mixed mode leak rate adjustments if the conditional criteria for a leakage adjustment are satisfied. Section 6.6.1 defines factors for increasing the isolated axial crack leak rate if intersected by a sufficiently deep circumferential crack. These factors can be applied directly to a mixed mode indication with axial leakage for condition monitoring assessments and are also included in the mixed mode increase in predicted leakage for an operational assessment. Section 6.6.2 develops the methods for adjusting axial leakage for mixed mode effects in an operational assessment.

The maximum pressure differential for leakage integrity evaluation is the SLB pressure differential of 2560 psi. At this low level of loading, the range of mixed mode geometries, which would develop leakage solely due to interaction effects (i.e., increased ligament tearing) without leaking as individual cracks, is very small. Consequently, a mixed mode evaluation for SLB leakage is not required unless the axial crack would be predicted to leak based on the analysis methods described above for axial indications.

6.6.1 Increased Leak Rates for Axial Cracks with Intersecting Circumferential Cracks

This section addresses mixed mode increases in the axial indication leak rate for both partial depth and throughwall intersecting circumferential indications. The leak rate factor for partial depth circumferential cracks is based on test measurements while the throughwall factor is based on analysis. Mixed mode defects could potentially increase leak rates without having any significant effect on structural integrity at SLB conditions. The relatively low SLB differential pressures compared to meeting burst margin requirements are sufficient to limit interaction effects to essentially in-plane crack openings rather than the development of a flap type opening.

Section 5.5.4 provides a leak rate adjustment factor based on measurements of the axial crack opening area ratio of a mixed mode axial indication to an isolated axial indication. The tests were performed for a 0.60 inch long 100% throughwall axial notch and for the same size axial notch intersected by a circumferential notch of 75% depth. The indications were pressurized using a bladder and the crack openings were measured at the SLB pressure differential of 2560 psi. The axial indication crack opening area for the intersecting mixed mode indication was found to be a factor of 1.4 larger than for the axial indication. The 1.4 factor for increased crack opening area leads to a factor of 1.7 increase in the SLB leak rate. The 0.60 inch throughwall axial indication in these measurements bounds throughwall indications meeting burst margin requirements and is expected to bound the EOC throughwall length of any PWSCC ARC indications. Thus, the 1.7 factor on SLB leak rates can be conservatively applied for all axial indication leak rates intersected by circumferential cracks up to about 80% average depth. Although tests were not performed as a function of circumferential depth, it is reasonable to expect no leakage impact for shallower circumferential indications such as about 50% average depth. When the criteria of Section 7.9.5 require a mixed mode adjustment to the axial leak rates, the 1.7 factor is applied for average circumferential depths between 50% and 80%.

Based on evaluations presented below and in EMECH-0738-SR-1 (Reference 8-35) supporting the TVA evaluation of Reference 8-39, intersecting 100% TW axial and circumferential cracks could potentially increase crack opening areas by a factor of 2. This could lead to increased leak rates by a factor of about 10 for an axial crack.

Given the nature of loading, a potentially intersecting crack will not experience much in the way of increased crack opening if the intersection point is some distance away from the crack tip. If the tip of a crack intersects a significantly longer crack, the situation is akin to a crack intersecting a free surface. This is shown in Figure 6-13. The crack tip is released and the tip could spring open. A straightforward center cracked/edge cracked panel fracture mechanics analogy shows that the upper bound effect is to develop a released tip crack opening equal to the center opening of a crack twice as long. The elastic crack opening area essentially doubles.

Figure 6-14 illustrates the increase in leak rates calculated by assuming the released crack tip leak rate is equivalent to one half of the leak rate of a crack twice as long. This increase ratio (released tip condition to isolated single crack) is a function of crack length. Also, the full free surface release effect is only realized if the released tip has intersected a crack much longer than itself. Figure 6-15 illustrates the fraction of the free surface released effect actually observed as a function of ratio of the length of intersected crack to the length of the crack with a released crack tip. The solid line in Figure 6-14 combines plasticity effects on crack opening and assumes that all axial cracks intersect circumferential cracks with a length of 0.25 inches and a depth of 100% TW. Accounting for plasticity is the same as lengthening the crack, hence the true leak rate increase factor for single cracks will be between the solid line and lower dotted line in Figure 6-14. A leak rate increase by a factor of about 10 is a conservative approach for axial cracks that undergo crack tip release.

The following summarizes the applicability of the mixed mode leak rate adjustment factors developed above.

- No mixed mode leak rate adjustment is required for average circumferential crack depths < 50%. Cracks < 50% average depth would not be expected, based on reasonable judgment, to have any influence on the axial crack leak rate given that 80% depth has only a 1.7 factor on leak rates.
- For average circumferential crack depths of 50% to 80%, a factor of 1.7 is applied to the axial crack leak rate
- For average circumferential crack depths of 81% to 100%, a factor of 10 is conservatively applied to the axial crack leak rate.
- For condition monitoring assessments, the above mixed mode leak rate factors would be directly applied to the calculated leak rate for the axial crack. The leak rate for the PWSCC axial crack is that calculated by the single indication Monte Carlo analysis for the mixed mode indication.
- For operational assessments, the factor is included in the methods described in Section 6.6.2.

6.6.2 Methodology for Mixed Mode Operational Assessment Leak Rate Adjustments

The multiplying factor to be applied to projected SLB leak rates for axial degradation in an operational assessment to account for the possibility of intersecting cracks is derived below. The following definitions, on a per steam generator basis, are used:

Q = projected ARC SLB leak rate for axial indications
L_F = factor from Section 6.6.1 for increasing axial leak rate for mixed mode effects
N = number of axial cracks
N_L = number of leaking axial cracks
N_i = number of leaking axial cracks intersected by a circumferential crack

N_{MM} = number of intersecting mixed mode indications
$f = N_{MM}/N$ = fraction of axial cracks that have intersecting circumferential indications
Q_T = total projected ARC SLB leak rate including mixed mode interaction effects
$M_L = Q_T/Q$ = multiplying factor applied to the ARC leak rate to obtain leak rate adjusted for mixed mode effects
$\alpha = N_L/N$ = fraction of axial cracks that leak
q_i = leak rate for an intersected crack.

The leak rate for an intersected crack is taken as a factor of L_F times the average crack leak rate, that is,

$$q_i = \frac{10Q}{N_L}$$

The average leak rate is applied for the analysis due to the low probability of mixed mode indications and the need to apply the correction for operational assessments for which a specific indication cannot be corrected. The intersections with a leaking crack are equal to the total number of crack intersections times the probability that the intersected crack is a leaker.

$$N_i = \alpha\, f\, N = N_L \frac{N_{MM}}{N} \quad = \quad N_L\, f$$

The total leaking rate is the sum of leak rates for cracks with intersections plus the leak rates of cracks without intersections.

$$Q_T = q_i N_i + \frac{Q}{N_L}(N_L - N_i)$$

$$Q_T = L_F \frac{Q}{N_L} N_i + \frac{Q}{N_L}(N_L - N_i)$$

Since $N_i = N_L f$, then:

$$Q_T = L_F Q f + Q(1-f),$$

$$\text{and, } Q_T = Q\{1 + (L_F - 1)f\},$$

$$\text{so, } M_L = 1 + (L_F - 1)f\ .$$

Thus, the multiplying factor, M_L, to be applied for mixed mode leak rate adjustments in operational assessments, when required per the criteria of Section 7.9.5, depends on the observed fraction (f) of intersecting axial and circumferential cracks and the required mixed mode leak rate adjustment factor, L_F. The above correction applies to axial cracks.

The appropriate L_F factor to be applied is described above in Section 6.6.1 and is dependent upon the average depth found for the interacting circumferential indication. The observed fraction (f) of intersecting axial and circumferential cracks will be determined based on the larger of the current outage inspection results or historical data. The multiplying factor, M_L, applied to each SG ARC leak rate for the PWSCC ARC, basically states that a fraction, f, of the projected leaking cracks leak at a rate L_F times the average leak rate per crack.

6.6.3 Application of Leak Rate Methodology

Using historical data at Diablo Canyon Units 1 and 2, the worst-case f is 0.0147 based on 1R9 data. In 1R9, there was one interacting (non-intersecting) mixed mode flaw (R21C33) and 68 axial PWSCC indications. Interacting indications (not satisfying separation distance requirements for evaluation as isolated indications) detected during inspections are conservatively treated as intersecting indications in the leak rate adjustment methodology. This is the only interacting mixed mode indication found to date in the Diablo Canyon SGs. The R21C33 average depths of the average and circumferential indications were 26% and 28%. The axial indication was too shallow to leak and the circumferential crack too shallow for a significant mixed mode effect. Therefore, no CM leak rate adjustment was required. To date, no mixed mode indications requiring a CM or OA leak rate adjustment have been found in the Diablo Canyon SGs.

Table 6-1. Crack Leak Rate Data Sources

Data Set	Source/ Set #	Sample Type	Tube OD/wall	Crack Length Info	---- Operating Conditions ---			
						T_o °F	P_o psia	P_b psia
W-IGASCC (PWSCC)	(1)	Lab	.75x043.	ID &OD	NOP SLB	616 616	2250 3000	1000 350
W-Fatigue	(2)	Lab	Variable	Single Value	NOP	550	2250	1000
McGuire-PWSCC	(3)	Pulled Tubes	.75x.043	ID &OD	NOP SLB	550 550	2650 2750	1350 100
ODSCC@TSP1	(4)	Lab	.875x.05	Max & T. Wall	NOP SLB	616 616	2250 3000	1000 350
ODSCC@TSP1	(5)	Lab	.75x.043	Max & T. Wall	NOP SLB	616 616	2250 3000	750 350
Farley-PWSCC	(6)	Pulled Tubes	.875x.05	Max & T Wall	NOP SLB	Variable Variable		

Sources
1) Calc TH-90-43 Attachment IV ("Begley Data")
2) Calc TH-88-81. See also WCAP-9922, Rev. 1, Pt. 3
3) TH-90-43 Attachment V
4) EPRI Report NP-7480-L,"SGT ODSCC @ TSP's Database for ARC, V1, Table 5-12
5) EPRI Report NP-7480-L,"SGT ODSCC @ TSP's Database for ARC, V2, Table 5-6
6) Roll Transition, Farley Pulled Tubes, Cullen

Definitions
NOP - Normal operating conditions
SLB - Steam line break conditions

a,c

Table 6-2. CRACKFLO Assumptions					
Assumption	Crack Length	Roughness and Tortuosity (# of 45° Turns)			
		PWSCC, Sets 1, 3, & 6		ODSCC, Sets 4 & 5	

* Reference 8-24

a,c

Table 6-3. Roughness Values	
Surface / Source	Roughness inches

b,c

Table 6-4. Parameters for Correlation of Predicted Leak Rates from CRACKFLO Leak Rates

Table 6-5. PWSCC SLB Leak Rates and Correction Factors for Flow Stress

b,c

TW Crack Length (inches)	CRACKFLO Leak Rate gpm @ RT	Nominal Leak Rate gpm @ RT Note 1	95% Confidence Leak Rate gpm @ RT Note 2	63.0 ksi σ_f	65.0 ksi σ_f	67.0 ksi σ_f	68.8 ksi σ_f	71.0 ksi σ_f	73.0 ksi σ_f	75.1 ksi σ_f

Notes:
1. Nominal leak rate represents regression line of correlation or 50% probability, 50% confidence on predicted ("truth") leak rate from CRACKFLO analysis.
2. Upper 95% prediction interval on correlation between predicted ("truth") leak rate and CRACKFLO leak rate.

Table 6-6: Distribution of Burst Reduction Factor Error (ANL Ligament Model)	
$1 / m_p$ Fractional Error	Median CDF
-0.2552	0.74%
-0.2308	1.80%
-0.1771	2.86%
-0.1633	3.92%
-0.1407	4.98%
-0.1379	6.04%
-0.1365	7.10%
-0.1192	8.16%
-0.1174	9.22%
-0.1117	10.28%
-0.1069	11.33%
-0.1051	12.39%
-0.1014	13.45%
-0.1002	14.51%
-0.0980	15.57%
-0.0970	16.63%
-0.0967	17.69%
-0.0931	18.75%
-0.0848	19.81%
-0.0825	20.87%
-0.0816	21.93%
-0.0794	22.99%
-0.0746	24.05%
-0.0733	25.11%
-0.0733	26.17%
-0.0729	27.22%
-0.0727	28.28%
-0.0698	29.34%
-0.0695	30.40%
-0.0680	31.46%
-0.0655	32.52%
-0.0646	33.58%
-0.0623	34.64%
-0.0589	35.70%
-0.0477	36.76%
-0.0452	37.82%
-0.0450	38.88%
-0.0434	39.94%
-0.0433	41.00%
-0.0425	42.06%
-0.0421	43.11%
-0.0406	44.17%
-0.0389	45.23%
-0.0381	46.29%
-0.0366	47.35%
-0.0337	48.41%
-0.0321	49.47%
-0.0310	50.53%
-0.0270	51.59%
-0.0175	52.65%

Table 6-6: Distribution of Burst Reduction Factor Error (ANL Ligament Model)	
$1 / m_p$ Fractional Error	Median CDF
-0.0174	53.71%
-0.0173	54.77%
-0.0172	55.83%
-0.0168	56.89%
-0.0147	57.94%
-0.0132	59.00%
-0.0106	60.06%
-0.0088	61.12%
-0.0073	62.18%
-0.0023	63.24%
0.0018	64.30%
0.0030	65.36%
0.0047	66.42%
0.0068	67.48%
0.0150	68.54%
0.0166	69.60%
0.0188	70.66%
0.0214	71.72%
0.0220	72.78%
0.0248	73.83%
0.0275	74.89%
0.0278	75.95%
0.0280	77.01%
0.0318	78.07%
0.0333	79.13%
0.0453	80.19%
0.0475	81.25%
0.0477	82.31%
0.0482	83.37%
0.0491	84.43%
0.0529	85.49%
0.0660	86.55%
0.0751	87.61%
0.0904	88.67%
0.1044	89.72%
0.1045	90.78%
0.1114	91.84%
0.1252	92.90%
0.1268	93.96%
0.1322	95.02%
0.1426	96.08%
0.1644	97.14%
0.1777	98.20%
0.2246	99.26%

Figure 6-1. Comparison of Measured to Predicted SLB Leak Rates, Case 1 CRACKFLO Assumptions

b,c

b,c

Figure 6-2. Comparison of Measured to Predicted SLB Leak Rates, Case 2 CRACKFLO Assumptions

b,c

Figure 6-3. Comparison of Measured to Predicted SLB Leak Rates, Case 3 CRACKFLO Assumptions

Figure 6-4. Regression Lines for Three CRACKFLO Assumption Cases

b,c

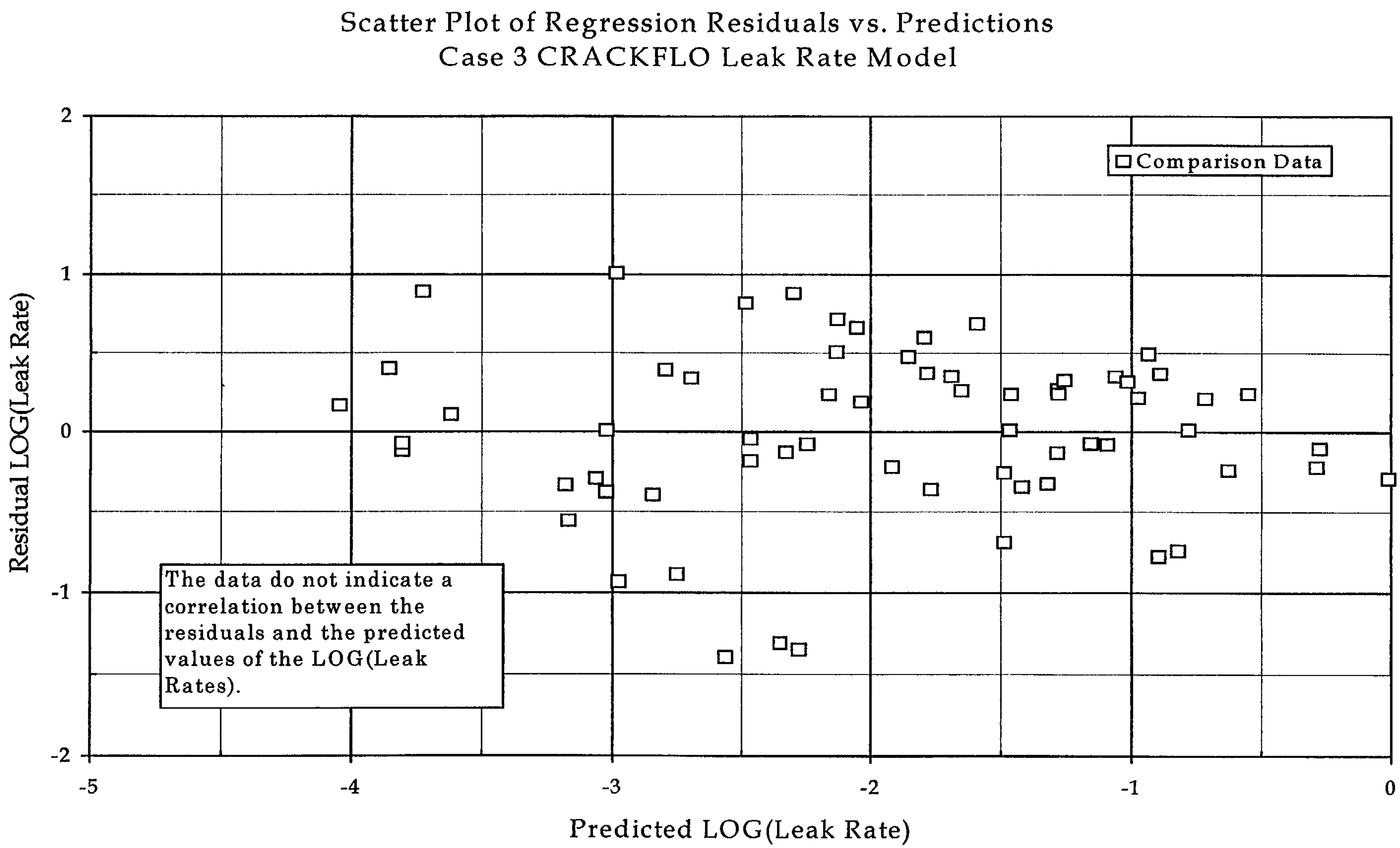

Figure 6-5. Scatter Plot of Regression Residuals versus Predictions

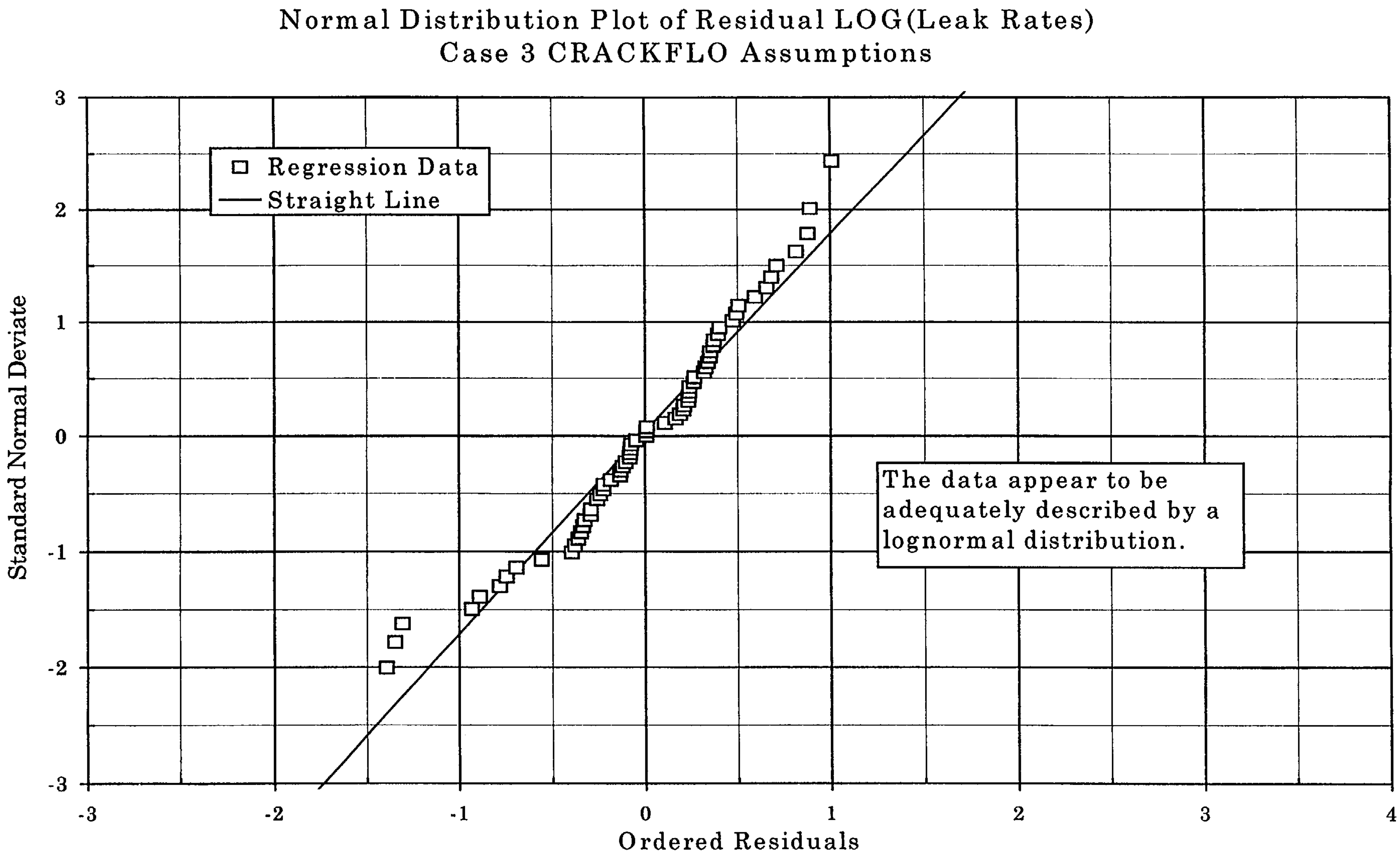

Figure 6-6. Normal Distribution of Residual Log of Leak Rates

[ ]b,c

b,c

Figure 6-8. Effect of Flow Stress on Thru-wall Crack Leakage

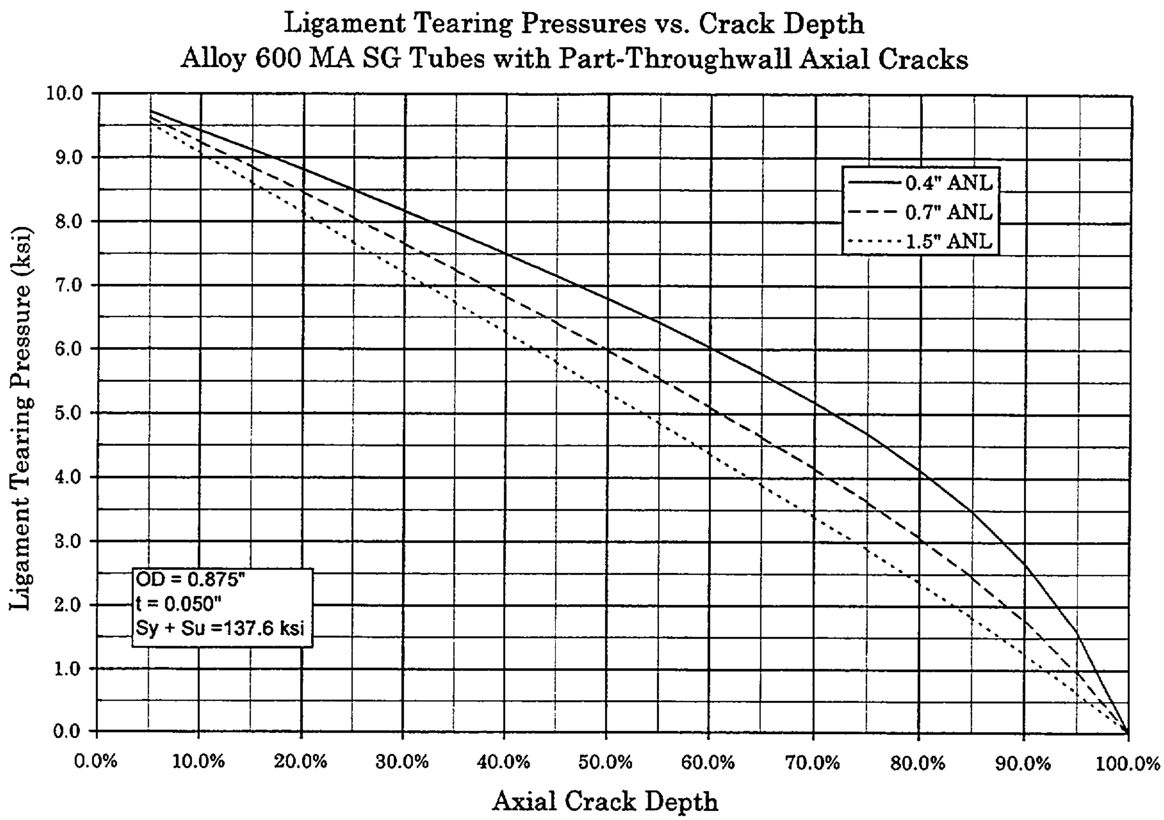

Figure 6-9

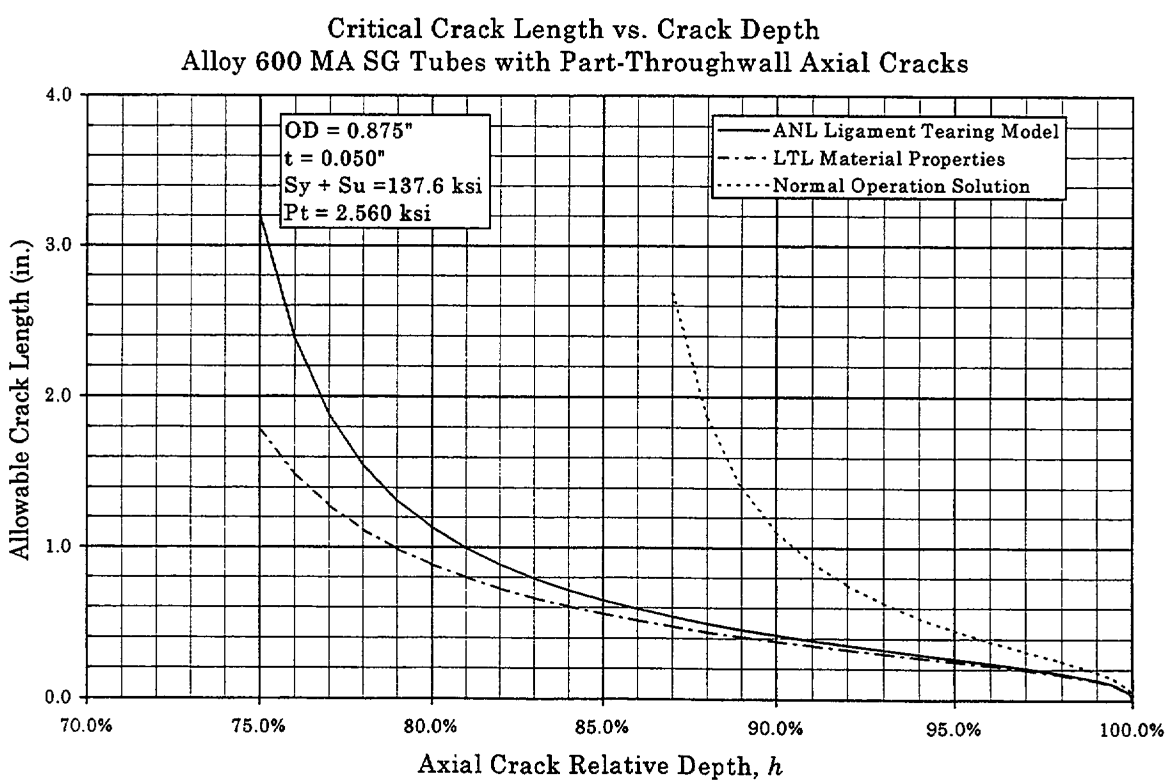

Figure 6-10

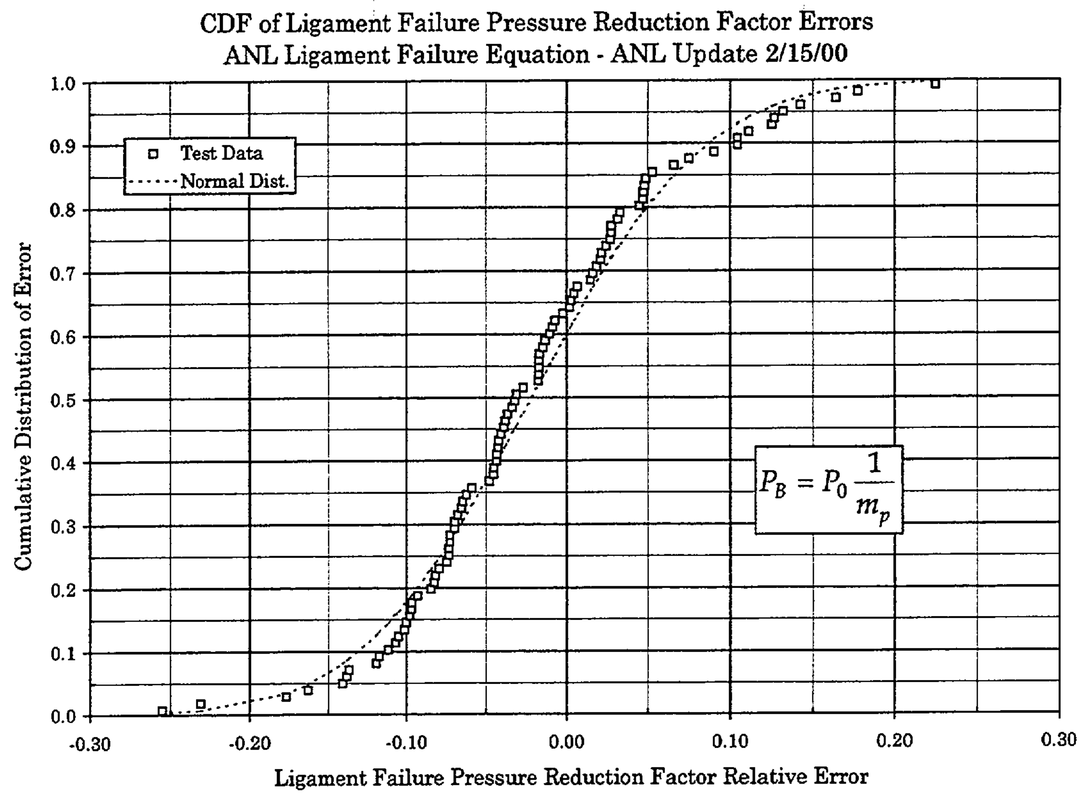

Figure 6-11

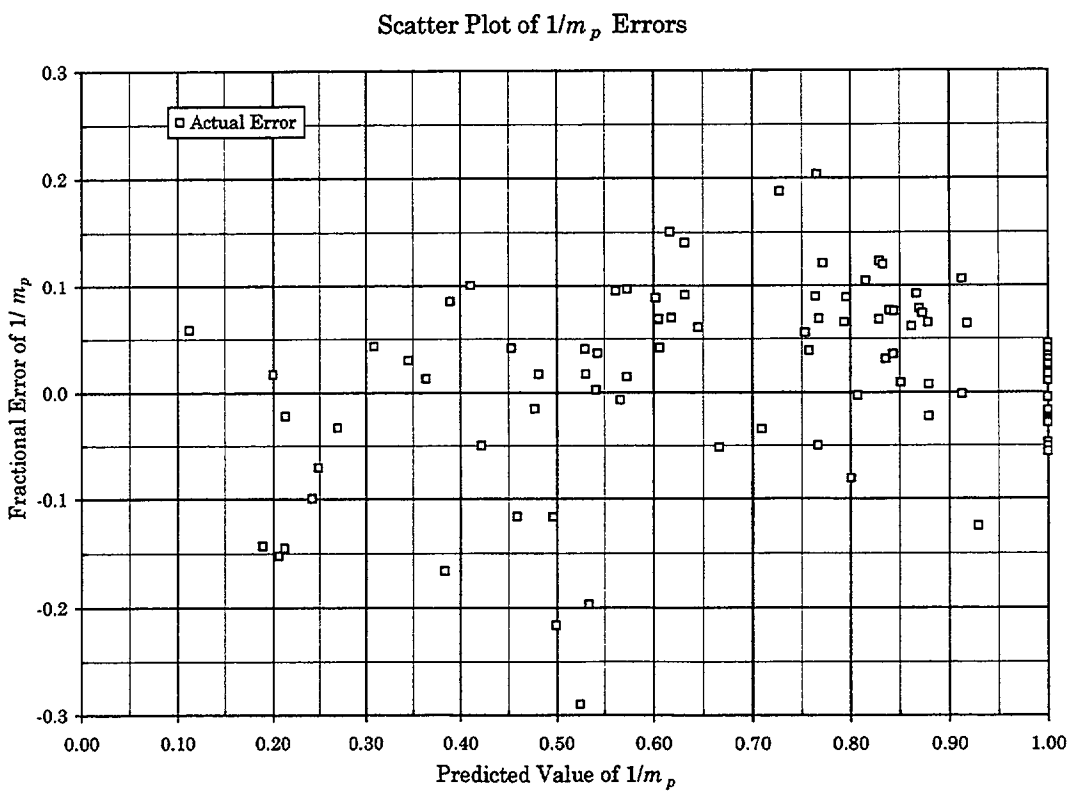

Figure 6-12

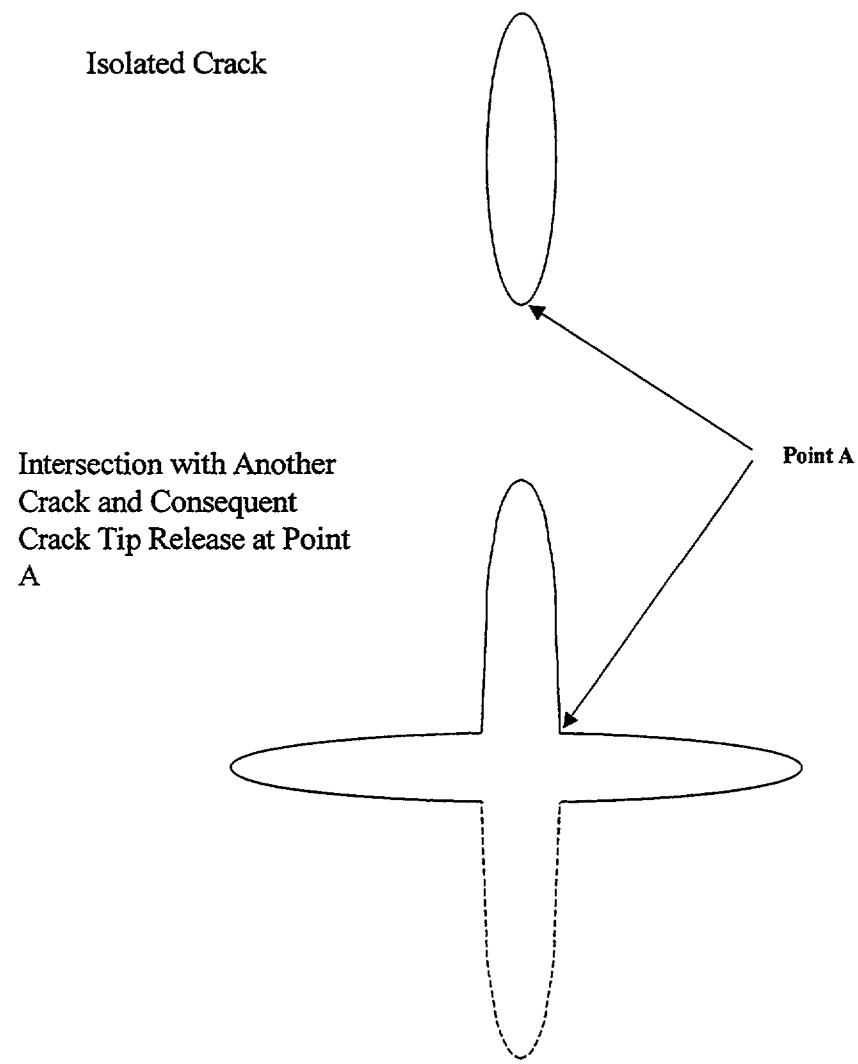

Figure 6-13. Illustration of Intersecting Cracks Leading to a Crack tip Opening Release and Creation of Increased Crack Opening Area for Leakage

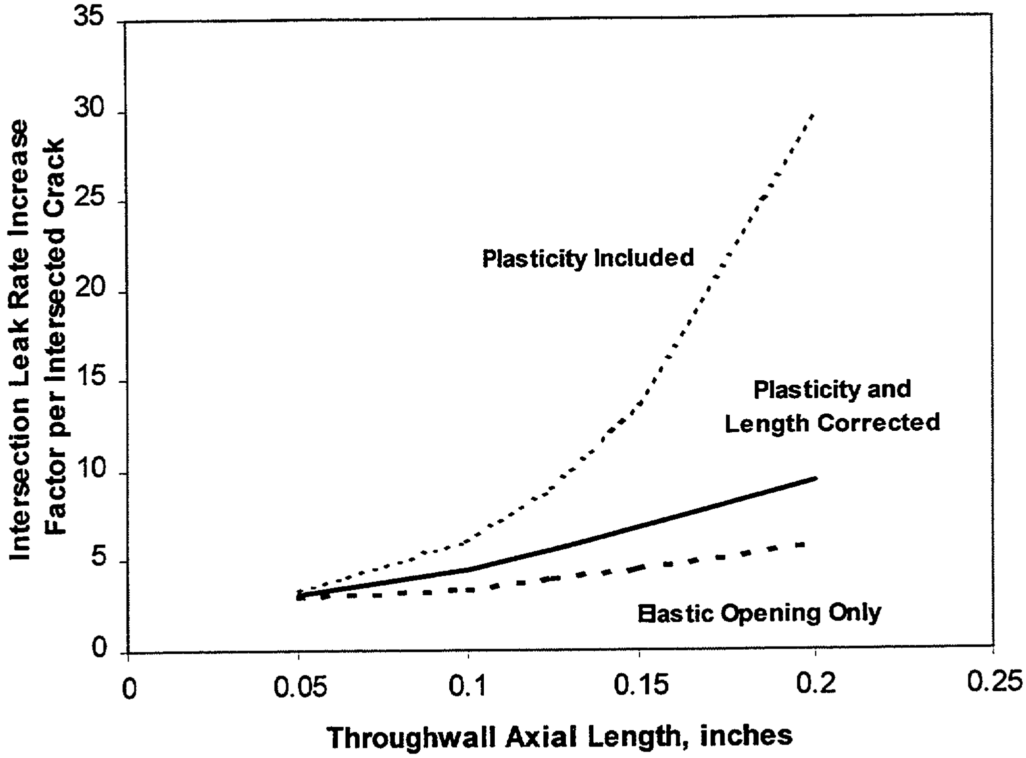

Figure 6-14. Leak Rate Increase Factor for an Intersected Crack versus Throughwall Axial Crack Length

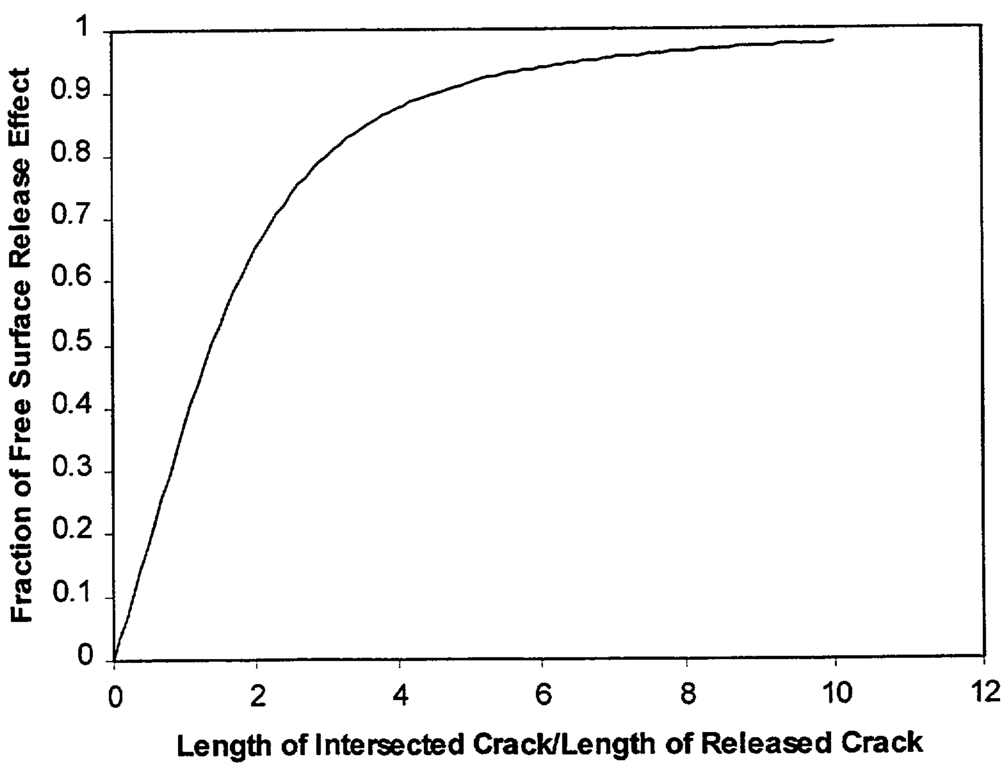

Figure 6-15. Fraction of Free Surface Release Effect Observed versus Relative Length of Intersecting Cracks

7.0 OVERVIEW OF ARC AND SUPPORTING ANALYSES FOR AXIAL PWSCC AT DENTED TSP INTERSECTIONS

This report provides the technical bases for a depth based ARC for axial PWSCC indications at dented TSP intersections. Repair limits are developed for indications within the dented TSP or with limited extension outside the TSP. The ARC repair limits of this report apply to axial PWSCC indications ≥ 40% maximum depth. Indications with < 40% maximum depth are left in service per the existing Technical Specification repair limit of 40% depth. The ARC and supporting requirements including inspection, burst analyses and leak rate analyses are described in this section. The ARC is conservatively based upon the assumption that the indications are freespan at SLB conditions and applies to axial indications that are located within or extending outside the TSP. However, crack extensions outside the TSP are required to be < 40% maximum depth. Requirements for including NDE uncertainties in the ARC analyses are also defined. The ARC satisfy steam generator tube integrity guidelines consistent with the requirements of NEI 97-06 (Reference 8-5), draft Regulatory Guide 1.121 (Reference 8-6) and the draft Regulatory Guide DG-1074 (Reference 8-7). The depth based repair limits are based upon establishing a high confidence that the indications will not burst or result in unacceptable leak rates under SLB conditions at the end of the operating cycle.

The ARC is based on the use of crack depth profiles obtained from a qualified and performance demonstrated +Point sizing technique. Burst pressures are calculated from the depth profiles by searching the total crack length for the partial length that results in the lowest burst pressure. Pending resolution of issues associated with burst correlations (Reference 8-2), the ANL ligament tearing model and EPRI throughwall burst pressure correlation are conservatively applied to define the burst pressure. The larger of the burst pressures obtained from ligament tearing or assuming the crack length is throughwall is used to obtain the burst pressure for the indication. Upon NRC concurrence that the burst pressure issue is resolved, the Westinghouse burst pressure model will be applied for all burst pressure analyses. The repair basis is obtained by projecting the crack profile to the end of the next operating cycle and determining if the burst pressure and SLB leakage for the projected profile satisfy acceptance requirements. If the projected EOC requirements are satisfied, the indication can be left in service. Thus, the repair basis assures that the operational assessment requirements are satisfied.

Applicable NDE uncertainties and growth rates are described in Sections 7.1 to 7.4. Repair limits for burst margins and potential leakage are developed in Section 7.5. The repair limits are based on single indication Monte Carlo analyses for the operational assessments to determine whether the projected EOC indications satisfy burst margin and leakage requirements. An option is provided to perform a total SG SLB leak rate operational assessment for comparison with the acceptance limits. Inspection requirements for application of the ARC are described in Section 7.6. Sections 7.7 and 7.8 describe supporting operational and condition monitoring assessment analysis methods for burst and leakage with an option for probabilistic condition monitoring analyses for indications dominantly within the TSP. Section 7.9 defines evaluation requirements for potential mixed mode indications. Requirements for pulling tubes in support of the ARC are given in Section 7.10. Section 7.11 provides a risk assessment for the ARC and Section 7.12 identifies NRC reporting requirements.

7.1 Tube Burst Margin Requirements and Burst Pressure Correlation

The proposed ARC of this report assumes that the TSPs are not present in a SLB event such that all indications at dented TSP intersections are freespan at SLB conditions. The structural limit for indications within the TSP is based on the presence of the TSPs under normal operating conditions such that the $1.4\Delta P_{SLB}$ burst margin requirement is applicable for indications within the TSP and for the total crack length if extending outside the TSP. The structural limit for the length of an indication totally outside the TSP is based on satisfying $3\Delta P_{NO}$ burst margin requirements. In the case of a crack extending from inside to outside the TSP, the structural limit is based upon the more limiting of $1.4\Delta P_{SLB}$ for the total crack length or $3\Delta P_{NO}$ for the length outside the TSP.

The burst correlations for partial throughwall, axial cracks are developed in Section 5. The Westinghouse burst pressure correlation is applied for the Monte Carlo condition monitoring assessment. For the operational assessments defining the need for tube repair, burst pressures are calculated as the larger of the ANL model ligament tearing pressure or the EPRI throughwall burst pressure correlation arbitrarily assuming the crack length is throughwall. The operational assessment burst margin analyses to determine the need for tube repair must be satisfied at 95% probability and 95% confidence given uncertainties in the burst correlation, material properties and NDE uncertainties on length and average depth. The condition monitoring burst margins must be satisfied at 95% probability and 50% confidence as further discussed in Section 7.8. These confidence level requirements are consistent with the guidance given in the draft NRC Regulatory Guide DG-1074 (Reference 8-7) and more conservative than the 90%/50% confidence required by the EPRI SG integrity guidelines of Reference 8-32. Based upon the guidance of Draft DG-1074, the limiting indication must satisfy the burst margin requirements. This guidance is satisfied by performing single indication Monte Carlo analyses for each indication to compare the predicted burst pressure at the specified confidence level against the burst margin requirements.

The normal operating pressure differential, ΔP_{NO}, is based on normal full power operating conditions. This bounds other normal operating conditions such as hot standby or power level adjustments for Westinghouse SGs. The primary and secondary side pressures to be used for determining ΔP_{NO} are the pressures near the location of the tube degradation. For Westinghouse Model 51 SGs with a primary side pressure of 2250 psia at the pressurizer, the primary pressure at the inlet to the SG is slightly higher than 2250 psia and the pressure at the top of the tubesheet is very close to 2250 psia. As elevation in the tube increases above the tubesheet, the primary pressure decreases faster than the secondary side pressure decreases. Therefore, the maximum primary to secondary hot leg pressure differential under normal operating conditions occurs at the top of the tubesheet. Secondary side steam pressure used to determine ΔP_{NO} should therefore be that at the top of the tubesheet. The burst margin requirements are then $1.4\Delta P_{SLB} = 3584$ psi and $3\Delta P_{NO} = 4383$ psi for a Diablo Canyon steam pressure of 789 psia at the top of the tubesheet.

7.2 SLB Leak Rate Requirements and Leak Rate Correlation

The SLB leak rate correlation and ligament tearing model developed in Section 6 are applied for the Monte Carlo condition monitoring and operational assessments. The operational assessment analyses performed to determine the need for tube repair must satisfy the allowable leakage limits at 95% probability and 95% confidence given uncertainties in the burst correlation, material properties and NDE uncertainties on length and depth. For condition monitoring, the allowable leak rate limits must be satisfied at 95% probability and 50% confidence as further discussed in Section 7.8. Leakage from the total crack length is constrained by the presence of the TSP except under the postulated SLB condition that the TSPs displace in a SLB event. The allowable limit for the total constrained leakage is the same as given in the licensing basis for the NRC GL 95-05 voltage based ARC. The total constrained leakage limit applies to the sum of leak rates from the PWSCC total crack length of this ARC, the GL 95-05 ARC for ODSCC at TSP intersections and indications within the tubesheet for application of the W*

ARC. The allowable leakage limit for freespan indications is 1 gpm. The total freespan leakage limit applies to the sum of leak rates from the PWSCC ARC crack length outside the TSP and any other freespan leakage from the operational assessments for other degradation mechanisms. The tube repair basis for SLB leakage is defined in Section 7.5.4.

7.3 NDE Uncertainties

NDE uncertainties are required on maximum depth, average depth and length to support the repair criteria based upon the operational assessment. The NDE uncertainties on average depth and length are used for the burst pressure analyses, and uncertainties on maximum depth and length are applied in the leakage analyses. Validated +Point sizing techniques based on a NDE Performance Test to develop the NDE uncertainties are described in Section 4 and the NDE uncertainties are developed in Section 4.7. The NDE uncertainties are developed as correlations between "truth" based on destructive exam data and NDE measurements. The NDE correlations are applied in the Monte Carlo burst pressure and SLB leak rate analyses. The resulting correlations are given below with the 95% confidence values given as a specific example of the magnitude of the uncertainties.

Average Depth NDE Uncertainty

Correlation: y (truth) = 0.914x + 0.687
Standard deviation = 7.8%
NDE Uncertainty at +95% confidence ($\Delta NDE_{AD95\%}$) = 10.1% for indication at ≈40% average depth

Maximum Depth NDE Uncertainty

Correlation: y (truth) = 0.939x – 0.923
Standard deviation = 14.2%
NDE Uncertainty at +95% confidence ($\Delta NDE_{MD95\%}$) = 19.1% for indication at 55% maximum depth

Length NDE Uncertainty

Correlation: y (truth) = 1.008x + 0.010
Standard deviation = 0.139 inch
NDE Uncertainty at +95% confidence ($\Delta NDE_{L95\%}$) = approximately 0.25 inch for indications between 0.75 and 1.25 inch length

7.4 Growth Rates

Growth rates for axial PWSCC at dented TSP intersections were developed in Section 4.8 based on data from Diablo Canyon SGs. Separate growth rate distributions were developed for average depth, maximum depth and length on an EFPY basis. The growth rate distributions are used in the Monte Carlo analyses with length and average depth used in the burst pressure analyses and length and maximum depth used in the leak rate analyses. The growth rates can be temperature dependent with a hot leg temperature of 603°F applicable to Diablo Canyon Unit 2 and 604.5°F applicable to Unit 1. Growth rates will be corrected for temperature as may be necessary for each operational assessment. As an example of the growth rate magnitudes, the 95% cumulative probability growth rates are (from Table 4-7):

Average depth growth at 95% probability ($\Delta G_{AD95\%}$) = 10.5% per EFPY for Diablo Canyon
Maximum depth growth at 95% probability ($\Delta G_{MD95\%}$) =12.5% per EFPY for Diablo Canyon
Length growth at 95% probability ($\Delta G_{L95\%}$) =0.081 inch per EFPY

Further discussion on updating the growth rate distributions is given in Section 7.5.5.

7.5 Tube Repair Limits

ARC tube repair limits are developed below for indications within the TSP, indications within and extending outside the TSP or at the edge of the TSP. Totally freespan indication repair limits are based on the Technical Specification repair limit of 40% maximum depth as described in Section 7.5.1. Similarly, indications < 40% maximum depth within the TSP or at the edge of the TSP are left in service per the existing Technical Specification repair limit of 40% depth and the additional ARC requirements for ≥ 40% depth indications are not applicable. Indications ≥ 40% maximum depth that can be left in service are limited to depths ≥ 40% only within the TSP. Separate repair bases are developed for burst and leakage considerations. Input to the repair limits are adjusted on an outage to outage basis as may be necessary to update growth rate distributions and steam pressures or account for changes in the cycle length or hot leg temperature from that used in the following development of the repair limits.

The ARC repair bases are limited to axial PWSCC at dented TSP intersections. If axial PWSCC is identified, a bobbin coil dent of any magnitude must be identifiable to leave the indication in service. NRC GL 95-05 would require repair of a TSP intersection found to have both PWSCC and ODSCC indications since the bobbin voltage response would not be limited to ODSCC indications.

7.5.1 Freespan Indication Repair Limits

The crack length outside the TSP will be repaired based on the current Technical Specification limit of 40% maximum depth. Although the 40% maximum depth repair limit is expected to result in acceptable conditions at the next EOC, the operational assessment performed to determine the potential need for tube repair evaluates the freespan length for acceptability as well as the total crack length.

The following is provided as a scoping demonstration of the acceptability of the 40% depth limit for freespan indications. Since NDE uncertainty on maximum depth is about 19% and growth at 95% is bounded by about 21% for a conservative 1.65 EFPY cycle length, the maximum depth at EOC would be about 80%. From Figure 6-9, a crack length of about 0.6 inch averaging 85% depth would be required for ligament tearing and potential leakage. Since 80% is the estimated maximum EOC depth, there is a low probability that a length of 0.6 inch averaging 85% depth would be present to permit ligament tearing and leakage. For a maximum depth of 40% and a typical maximum to average depth ratio of about 1.25, the average depth left in service would be on the order of 32%. With an average depth growth rate of about 17% (1.65 EFPY cycle length) at 95% probability, the EOC average depth would be about 49%. For a $3\Delta P_{NO}$ burst margin including allowances of 10% for NDE uncertainties, an EOC average depth of about 58% including uncertainties permits a long crack length of about 1.5 inch length based on ligament tearing (Figure 6-9). Thus the 40% maximum depth limit provides large margins against burst and leakage.

For indications < 40% maximum depth that are dominantly within the TSP, the structural margins are even larger than for freespan indications since the $1.4\Delta P_{SLB}$ structural margin requirement is applicable.

Consequently, the Technical Specification repair limit of 40% maximum depth can be applied to all axial PWSCC indications and the additional ARC requirements on location and length for indications < 40% maximum depth are not necessary. The ARC requirements for ≥ 40% depth are developed in Sections 7.5.2 to 7.5.6.

In summary, axial PWSCC indications at dented TSP intersections with maximum depths < 40% can be left in service independent of length or position relative to the TSP. Indications ≥ 40% maximum depth outside the TSP will be repaired. The operational assessment of Section 7.5.3 is performed for these indications to further demonstrate acceptability of the Technical Specification 40% repair limit.

7.5.2 Crack Length Limit for ≥ 40% Maximum Depth

A crack length limit for ≥ 40% Maximum Depth is defined to limit the potential length of a deep crack outside the TSP at EOC conditions. The ARC repair limit is established to require repair of any indication having a maximum crack depth ≥ 40% outside the TSP. This limit is established to provide large margins against burst or leakage for freespan indications outside the TSP. As discussed in Section 7.5.1, the maximum EOC depth outside the TSP would be less than 80% deep, except for a short length at the TSP edge resulting from growth of the crack inside the TSP to possible extension outside the TSP as discussed in the following. Growth in length at 95% probability is given in Section 7.3 as 0.081" per EFPY at 603°F. For a corresponding cycle length of 1.65 EFPY, the total growth in length would be 0.13 inch. The EOC length outside the TSP that could then be potentially more than about 80% depth would be about 0.13 inch under the conservative assumption that all growth occurred at the edge of the TSP. This potentially deeper, short length just outside the TSP together with the potentially longer length left in service at < 40% maximum depth would not challenge structural integrity at EOC conditions. Although no challenges to freespan burst margins at EOC conditions are expected, the operational assessment performed to identify repairable indications includes a burst pressure analysis for any crack length potentially extending outside the TSP.

Since crack positions are measured from the centerline of the TSP, the maximum allowable length that can be left in service at ≥ 40% maximum depth is 0.375 inch from the TSP centerline. This limit defines the edges of the TSP thickness of 0.75 inch for Model 51 SGs. It is acceptable for the crack to extend outside both edges of the TSP as long as the maximum depth of the crack outside the TSP is < 40% and burst margins at projected EOC conditions are acceptable per the structural assessment described in Section 7.5.3 below.

In summary, axial PWSCC indications at dented TSP intersections with ≥ 40% maximum depth at > 0.375 inch or < -0.375 from the TSP centerline will be repaired. Indications acceptable by this requirement are further evaluated against the burst pressure and SLB leakage repair bases of Sections 7.5.3 and 7.5.4.

7.5.3 Burst Pressure Repair Basis

The repair limit on maximum crack depth (≥ 40%) for the potential length outside the TSP (length not within ± 0.375 inch of TSP centerline) is developed above in Sections 7.5.1 and 7.5.2. If this limit is exceeded, the tube is repaired and the evaluation for tube repair described in this section is not required. However, an operational assessment will be performed for all PWSCC indications left in service at dented TSP intersections including indications with < 40% maximum depth within or extending outside the TSP. The crack profile must be evaluated to determine the partial length that results in the lowest burst pressure. Acceptability must be defined in terms of the projected EOC crack profile since growth in length and depth change the burst characteristics of the measured profile. Projecting the measured profile to the EOC is equivalent to performing an operational assessment for the indication. The measured profile is projected to EOC conditions by adding growth in length and growth in average depth. The projections to EOC conditions are performed using Monte Carlo analysis methods. Each simulated EOC profile is then searched for the lowest burst pressure using the combined ligament tearing and throughwall burst model of Section 5. This process results in the effective length (partial length of total crack length) and associated average depth of the indication that results in the lowest burst pressure. This process is separately performed for the total crack length and for the length of the crack outside the TSP. The resulting Monte Carlo burst pressure distribution for the total crack length evaluation is compared to the $1.4\Delta P_{SLB}$ acceptance limits at 95% probability and 95% confidence on the distribution. The resulting burst pressure distribution obtained from the evaluation of the length outside the TSP is evaluated against the appropriate $3\Delta P_{NO}$ limits at 95% probability and 95% confidence on the distribution. If the burst pressures from both evaluations are less than their associated acceptance limits, the indication is left in service subject to the results of the leakage evaluation. If either burst pressure acceptance limit is exceeded, the indication must be repaired. The Monte Carlo methods for performing the operational assessment for burst pressures are described in Section 7.7.

In summary, the ARC repair limits, other than maximum depth outside the TSP, are established to satisfy structural limits at the projected EOC. This process is an operational assessment and no further operational assessment is required. The repair limits are dependent upon growth rates and cycle length with the freespan lengths also dependent upon steam pressure. These parameters must be updated for each inspection or it must be demonstrated that the prior cycle values remain acceptable.

7.5.4 SLB Leakage Repair Basis

The leakage repair basis applies a Monte Carlo, SG operational assessment for leakage to demonstrate that accident condition acceptance limits for leakage are not exceeded at the specified confidence levels. If the total SG leak rate is found to exceed acceptance limits, single indication leak rate analyses may be performed to identify the indications with the largest leak rates for potential repair. For conservatism, the total SG leak rate is evaluated assuming a constant POD of 0.6 for the analysis. The total SG leakage is evaluated at 95%/95% confidence for operational assessments. The PWSCC leakage for the total crack length, representing TSP constrained leakage, must be added to other degradation mechanisms with constrained leakage such as ODSCC at TSP intersections and W* indications within the tubesheet. The total constrained leak rate must be less than the licensing basis allowable leakage limit for the faulted SG per GL 95-05 guidelines. The freespan leakage must be added to potential contributions from other degradation mechanisms in the overall operational assessment and the total freespan leakage must be less than or equal to the allowable limit maximum of 1 gpm. The constrained and freespan leak rates from the operational assessments must satisfy the allowable limits at 95% probability and 95% confidence. Contributions from separate degradation mechanisms may be individually evaluated at these confidence levels to satisfy the total leakage requirements. If either the constrained or freespan leakage limit is exceeded, indications with the largest leak rates will be repaired until the leakage limit is satisfied. For the Diablo Canyon SGs, the steamline break event (SLB) is the limiting accident condition for leakage. Any indications with known leakage will be repaired where known leakage may result from identification of the indication due to operational leakage or in situ testing.

The leakage model used in the Monte Carlo operational assessment is described in Section 6 of the report. The analyses are based on the use of crack depth profiles projected to EOC conditions. At SLB conditions, there is conceptually a potential that a near throughwall crack would "breakthrough" (ligament tearing) the remaining wall thickness ligament to result in a leak. No occurrences of breakthrough of more than a few percent wall thickness have been identified in available leak rate data for PWSCC cracks or the more extensive ODSCC database for indications at TSP intersections. However, the Monte Carlo analysis conservatively includes a ligament tearing analysis based on the ANL model including uncertainties as described in Section 6. Each simulated EOC profile for the total crack length is searched for the longest length that could potentially breakthrough at the SLB pressure differential of 2560 psi. If ligament tearing is predicted, the partial crack length estimated to tear through the remaining ligament is assumed to be throughwall in applying the SLB leak rate correlation described in Section 6. The resulting Monte Carlo SLB leak rate distribution for the indication is evaluated at the specified confidence level. A description of the Monte Carlo methods for the operational assessment is provided in Section 7.7.

The above formulations provide the basis for developing the need for tube repair based upon potential SLB leakage. The analyses are a function of growth rates, hot leg temperature and cycle length, which may have to be updated on an outage specific basis if changes occur in growth rates, hot leg temperature or cycle length.

7.5.5 Adjustments to Repair Limits for Changes in Operating Conditions

Prior to an inspection for which the depth based repair limits are to be applied, growth distributions are to be updated to include growth data from the previous inspection. In addition, changes in planned cycle lengths or steam pressure can change the repair limits. The updated growth rates, cycle lengths and steam pressures should be used to update the inputs to the Monte Carlo operational assessments per Sections 7.5.3 and 7.5.4 above for application during the inspection outage. Growth rates in average depth, maximum depth and length are developed for the indications found in the prior inspection. In addition, if the new growth data and deletion of the oldest cycle of growth data in the growth distribution result in a minimum of 200 growth points, the oldest cycle of growth data should be deleted from the growth distribution. However, data cannot be deleted from the last two cycles of growth data since it is necessary to utilize the largest growth distribution over the last two cycles of operation in the operational assessments.

The growth data from the Diablo Canyon SGs exceed 200 data points, and the plant specific growth distribution is applied for the Diablo Canyon analyses. The guidance noted above for updating the growth distributions applies to the plant specific growth data. If the last two cycles of plant specific data each have 200 growth points, the most conservative growth distribution (largest growth at +95% confidence) from the last two cycles of operation should be used to define the updated repair limits.

As a minimum, growth rates for large indications that could impact the upper tail of the growth distribution shall be evaluated during an inspection outage. If the new growth data cause the growth distribution above 90% probability to be more conservative, the new growth data shall be added to the growth distribution for the operational assessment. This assessment based on initially evaluating the large indications that could impact the tail of the distribution leads to a conservative growth distribution in the operational assessment. The complete growth distribution would reduce growth rates above the 90% value when the criterion is satisfied. The following examples help to clarify this conclusion. If all the largest growth rates found are less than the current 90% value, the probability of occurrence for the larger growth rates is reduced. If one or more indications above the 90% value are found, additional new growth data must be added to the distribution until the growth distribution above 90% bounds the old distribution. If the 90% value is more conservative when all growth data are included, the repair evaluations would be reassessed with the new growth distribution. This criterion on growth is added to reduce the likelihood of extending an outage time to obtain more growth data that has no impact on tube integrity. Prioritizing growth evaluations starting with the largest indication permits an earlier conclusion on the acceptability of the prior cycle growth distribution.

7.5.6 Exclusion Zones for Application of the Alternate Repair Criteria

LOCA + SSE

For the combined LOCA + SSE loading condition, the potential exists for yielding of the tube support plate in the vicinity of wedge groups, accompanied by potential deformation of the tubes and subsequent postulated in-leakage if the tube has significant degradation. In-leakage may occur if deep axial cracks are present and propagate throughwall as tube deformation occurs. This deformation may also lead to opening of preexisting tight throughwall cracks. Significant deformation for this potential in-leakage applies to indications left in service exceeding the current Technical Specification 40% maximum depth repair limit. In-leakage is a potential concern as modest leakage could have an adverse effect on the FSAR safety analysis results. Any tubes that are defined to be potentially susceptible to significant deformation under LOCA + SSE loads are excluded from consideration of the ARC.

No tubes are calculated to be susceptible to significant deformation in the Sequoyah SGs as shown in documentation supporting the voltage based repair limits for ODSCC at TSP intersections; therefore, no tubes are excluded from the application of the ARC. For the Diablo Canyon SGs, tube locations susceptible to significant deformation are identified in the NRC submittal of Reference 8-29. Although the referenced exclusion zone submittal is for the TSP ODSCC ARC, the exclusion zones for Diablo Canyon SGs are applicable to both the voltage based repair limits for ODSCC at TSP intersections and the depth based repair limits of this report. Revised exclusion zones are permissible with NRC concurrence.

FLB or SLB + SSE

Since the TSPs provide lateral support to potential tube deformation that may occur during postulated accident conditions, tube bending stress can be induced at the TSP intersections. This bending stress is distributed around the circumference of the tube cross section, tension on one side of the tube, compression on the other side and is oriented in the axial direction of the tube. Axial cracks at the TSP intersection could experience either a tension stress that tends to close the crack or a compressive stress that tends to open the crack. The compressive stress has the potential to reduce the burst capability of the cracked tube due to the crack opening if the stress level is sufficiently large. Test results (Reference 8-14) have shown that an OD bending stress on the order of 34 ksi, which is very close to the yield strength of the tube material at 650°F, will not have a significant effect on the burst capability of a cracked tube. In the absence of test data for bending stresses above the tube yield strength, it is conservatively assumed that high bending stresses (above yield) could have a degrading effect on tube burst pressure. In general, the potential for bending stresses exceeding yield in Westinghouse SGs is significant only at plants with relatively large SSEs in the design basis.

No tubes have been identified to have bending stresses exceeding the yield strength in the Sequoyah SGs and, therefore, no tubes are excluded from the application of the ARC. For the Diablo Canyon SGs, tube locations susceptible to bending stresses exceeding about 34 ksi have been identified at the top TSP for a FLB + SSE event. These locations are conservatively excluded from application of the alternate repair limits. The tube locations are defined as follows: 7^{th} TSP intersections in rows 11 through 15 and rows

36 through 46. These exclusion zones for Diablo Canyon SGs are applicable to both the voltage based repair limits for ODSCC at TSP intersections and the depth based repair limits of this report.

7.6 Inspection Requirements

To support the ARC for axial PWSCC at dented TSP intersections, inspection requirements are identified for the extent of inspection and NDE data analysis.

Extent of Inspection

The bobbin coil probe is applied for sizing of dent voltages and, optionally, for detection of axial PWSCC indications at TSP intersections with less than or equal to 2.0 volt dents for which the bobbin probe qualification is described in Section 4. The +Point probe is applied for sizing of bobbin detected indications and for detection and sizing at intersections with greater than 2.0 volt dents (or optionally lower than a 2.0 volt dent threshold). The extent of inspection required for the ARC is then:

- 100% bobbin coil inspection of all TSP intersections
- +Point coil inspection of all bobbin coil indications at dented TSP intersections
- +Point coil inspection of all prior PWSCC indications left in service.
- If bobbin coil is relied upon for detection of axial PWSCC in less than or equal to 2.0 volt dents, then on a SG basis perform +Point coil inspection of all TSP intersections having > 2.0 volt dents up to the highest TSP for which PWSCC has been detected in the prior two inspections or current inspection and 20% of dents > 2.0 volts at the next higher TSP. If a circumferential indication is detected in a dent of "x" volts in the prior two inspections or current inspection, +Point inspections will be conducted on 100% of dents greater than "x - 0.3" volts up to the affected TSP elevation in the affected SG, plus 20% of dents greater than "x - 0.3" volts at the next higher TSP. "x" is defined as the lowest dent voltage where a circumferential crack was detected.
- If bobbin coil is not relied upon for detection of axial PWSCC in less than or equal to 2.0 volt dents, then on a SG basis perform +Point coil inspection of all dented TSP intersections (no lower dent voltage threshold) up to the highest TSP for which PWSCC has been detected in the prior two inspections or current inspection and 20% of all dents at the next higher TSP.
- For any 20% sample, a minimum of 50 dents at the TSP elevation shall be inspected. If the population of dents is less than 50 at the TSP elevation, then 100% of the dents at the TSP elevation shall be inspected.

NDE Analysis Requirements

In addition to general reporting requirements such as tube location, TSP number and crack location relative to the center of the TSP, the following data are required from the inspection:

Bobbin Coil Probe

- Dent voltage if dented
  - When it is established that denting has been arrested and dents are not growing, dent voltages for TSP intersections can be established one time and applied for subsequent inspections. It is preferable that dent voltages be defined prior to the presence of an indication.
  - Dent voltages must be determined to at least a minimum of 2 volt dents in order to define the +Point inspection requirements.
  - If PWSCC is found at a TSP intersection for which no dent has previously been defined, the intersection must be reevaluated for denting. If no dent of any size is found in the reevaluation, the indication must be repaired.

- NDD or DSI (or equivalent code) if potential indication detected with associated bobbin flaw voltage

+Point Probe

- NDD, SAI or MAI for each dented intersection inspected

- Crack length versus depth and voltage profile with axial positions defined relative to the center of the TSP. The NDE profiles are adjusted for length and depth (if maximum voltage ≤ 1.0 or ≥ 4.5 volts) per the adjustment procedure given in Section 4.

- Identification of crack as ID or OD

- When PWSCC indications at dented TSP intersections are to be left in service, the +Point data shall be applied to evaluate the TSP for cracked ligaments. If cracked ligaments are detected, the PWSCC indication shall be repaired.

The NDE profile adjustment procedure of Section 4 has been applied to the +Point data used to develop NDE uncertainties and growth rates. The same procedure must therefore be applied to all field axial PWSCC indications for which the ARC of this report are applied. Tube repair limits are applied to the +Point sizing results.

7.7 Operational Assessments for Axial PWSCC Indications

The ARC operational assessment is performed to determine the indications requiring repair as described in Section 7.5. The analysis process for the operational assessment is outlined in this section utilizing flow charts to describe the methodology. Figures 7-1 to 7-4 show the flow charts outlining the operational assessment. All indications are conservatively assumed to be free span indications under SLB conditions for both the operational and condition monitoring assessments even if the indication is totally inside the TSP.

POD as a function of depth from the NDE Performance Tests discussed in Section 4 is not currently applicable for use in Monte Carlo analyses due to the high false call rate attained in the tests, and the need to confirm that field inspections will apply comparable calling criteria prior to application of PODs developed from the performance tests. The performance test results and field inspections following implementation of bobbin coil detection for axial PWSCC in dents support a conclusion that indications large enough to challenge structural integrity at the next inspection are being detected. The false call rate relates to calling indications at NDD intersections. A conservative objective of identifying small flaws detectable only as distorted dent signals was incorporated in the NDE analyst training. Flaws of significant length and depth tend to show a flaw phase response separable from the horizontal dent signal and do not require conservative calling criteria for detection. Bobbin detection for PWSCC in dents ≤ 2 volts has been implemented in DCPP Unit 2 in 2001. Only about 3% of the bobbin indications at dents reported in the last DCPP Unit 2 2001 inspection (excluding PWSCC indications reported in prior inspections) were confirmed as flaws by +Point inspection. Although the NDE evaluations and field experience show the adequacy of the bobbin inspection for small dents, a very conservative constant POD of 0.6 will be used for the SG Monte Carlo leak rate analyses. All burst pressure analyses to define the need for tube repair are based on single indication analyses for comparisons with the limiting indication burst margin requirements, and no SG analyses are applied for the structural assessment.

Preparations for the outage inspection and assessments are described in Figure 7-1. Growth rate distributions are updated to reflect growth data from the last inspections and for potential changes in the T_{hot} resulting from estimated tube repair or changes in operating conditions. The +Point inspection requirements for dents greater than 2 volts are defined based on the dent population found in the prior inspection.

Figure 7-2 describes ARC implementation for the inspection, evaluation for exclusion zones and for the evaluation of each indication against the criterion for repair of indications ≥ 40% depth outside of the TSP thickness of 0.375 inch. The upper boxes of the figure reflect the inspection requirements of Section 7.6 to identify the PWSCC axial indications and size the indications using +Point depth profiling. Each indication is evaluated for potential repair due to being located in the zones excluded from ARC application as discussed in Section 7.5.6. The exclusion zones apply only to Diablo Canyon SGs and indications located in the exclusion zone are repaired and a condition monitoring assessment is performed for the indication if one or more of the additional repair criteria are exceeded. If the maximum depth of the indication is < 40%, the indication is left in service per the existing Technical Specification repair limits and evaluations against the ARC repair limits are not required as described in Section 7.5.1. Indications with maximum depth outside the TSP ≥ 40% are repaired and a condition monitoring assessment is performed for the indication. A Monte Carlo operational assessment is then performed for the indications ≥ 40% maximum depth within the TSP. In addition, an operational assessment is performed for indications < 40% maximum depth left in service.

The Monte Carlo burst pressure operational assessment for comparison with the burst margin requirements is described in Figure 7-3. The following describes the Monte Carlo processing of NDE uncertainties and growth to obtain the EOC crack profile, where the order of the calculations is not important since the individual components are additive:

- Average depth NDE uncertainties and growth are added to the NDE profile. Average depth values are used for burst pressure analyses due to the dominant dependence of burst pressure on average depth. Depth NDE uncertainties and growth are added to each point in the depth profile so that the adjustments yield the correct average depth for the profile.
- The NDE uncertainties on length occur only at the ends of the crack due to difficulties in detecting shallow tails of the crack and/or coil lead-in and lead-out effects. The length adjustment for NDE uncertainty is conservatively applied at the end of the crack farthest from the TSP centerline, which maximizes the potential length outside the TSP. When a sample length uncertainty is obtained in the Monte Carlo analysis, the end points of the NDE crack profile having a spacing just greater than the uncertainty are scaled to correct for the uncertainty.

- Growth in length is applied to the profile by scaling all point-to-point spacings in the profile to correct for the sample growth value. The center point of the crack is held at a fixed position so growth occurs in both directions relative to the center of the crack.

As described in Section 5, the burst pressure is obtained for the partial length of the crack that results in the lowest burst pressure, which is called the burst effective length or the weak link of the crack. Burst pressures are calculated for both the total crack length and the freespan length outside the plate when the crack extends from the TSP. The burst pressure model for the operational assessment is based on calculating the ligament tearing pressure using the ANL model and the throughwall burst pressure using the EPRI correlation. For applying the throughwall correlation, the length of the crack is assumed to be throughwall. The burst pressure assigned to each Monte Carlo sample is the larger of the ligament tearing or throughwall burst pressure. Details of this combined ligament tearing and throughwall burst model are described in Section 5. The burst pressure distribution for total or constrained length is evaluated at 95%/95% confidence and compared to the $1.4\Delta P_{SLB}$ burst margin requirement as given in Section 7.1. If the burst pressure is less than the required margin, the indication is repaired and a condition monitoring assessment is performed for the indication. Similarly, if the freespan burst margin of $3\Delta P_{NO}$ is not satisfied, the indication is repaired and a condition monitoring assessment is performed. If the burst pressure exceeds the burst margin requirements, the indication is evaluated for leakage as described below.

The SLB leak rate operational assessment is described in Figure 7-4. A single indication Monte Carlo operational assessment is performed for both freespan and total length. If results of the single indication analyses show no leakage for condition monitoring and operational assessments, then the leakage analysis is complete and a total SG leak rate Monte Carlo operational assessment is not required. If the results of single indication analyses show leakage for condition monitoring or operational assessments for either freespan or total length, then a total SG leak rate Monte Carlo operational assessment is required for each SG that shows leakage. The total SG leak rate analysis compares total leakage against both constrained and freespan indication acceptance requirements. A conservative POD of 0.6 is used in the SG analysis. The 0.6 POD is sufficiently conservative to account for potential new indication contributions to the total SG leakage. Thus, leakage from new indications is effectively included in the SLB leak rate analysis. The Monte Carlo projection to obtain the EOC profile is the same as for burst pressure analyses except that maximum depth NDE uncertainties and growth are used in the leakage analysis. Maximum depth, rather than average depth, values are used to improve the projection of the deepest part of the crack for leakage analysis. As described in Sections 7.2 and 6.4, the projected EOC crack profile is searched for the longest length for which the remaining wall thickness ligament tears to throughwall at SLB pressure differentials. The partial crack length from the ligament tearing analysis is assumed to be throughwall for the leakage analysis. Based on available leak rate test data for non-throughwall corrosion cracks, which show ligament tearing only over a few percent depth, the use of the ligament tearing model is expected to result in significant conservatism in the calculated leak rates. The total crack length and freespan lengths (if present) are separately evaluated for ligament tearing and leakage to develop distributions of the leak rates. The total length or constrained leakage and the freespan leak rate are evaluated at 95%/95% confidence to define the leak rate for the indication. The PWSCC leak rate from the total SG Monte Carlo analysis, must be added to other degradation mechanisms found in the overall operational assessment to have projected EOC leakage. For the constrained leak rates associated with the total PWSCC crack length leakage, the PWSCC leak rates would be summed with the leak rates from the TSP ODSCC ARC of GL95-05 and from the W* ARC indications. Freespan leak rates are summed with the potential leak rates found in the operational assessments for other degradation mechanisms. The total constrained and freespan indication leak rates are then compared with the acceptance limits (see Section 7.5.4). If the acceptance limits are exceeded, additional ARC indications with the largest leak rates, but otherwise acceptable for continued service, are repaired until the resulting leakage satisfies the acceptance limits. If additional indications are repaired, the total SG Monte Carlo analysis would be repeated to confirm that the leakage acceptance limits are satisfied.

Single indication Monte Carlo analyses are performed as the +Point sizing data is obtained. The single indication analyses identify leaking indications that may require repair if the total SG leakage limits are not satisfied. A condition monitoring assessment is then performed for any indications found to leak in the single indication operational assessment.

If the condition monitoring assessments performed per Section 7.8 satisfy burst and leakage requirements, no adjustments of the repair limits developed per Section 7.5 are required other than for the changes in operating conditions described in Section 7.5.5. If the condition monitoring requirements are not satisfied for burst and/or leakage, the causative factors for EOC indications exceeding the expected values should be evaluated. In general, it would be expected that larger than expected growth rates would be the cause of not satisfying condition monitoring requirements. If the growth rate update developed from this causative factor evaluation is applied for an analysis of the prior cycle and results in acceptable comparisons with EOC conditions, this update of the growth would be a basis for performing an additional operational assessment. This update assessment would identify indications requiring repair for the inspection found to exceed condition monitoring requirements. If this growth update does not result in acceptable EOC conditions, additional causative factor evaluation is required and the results should be documented in the reports identified in Section 7.11.

7.8 Condition Monitoring Assessments for Axial PWSCC Indications

The condition monitoring assessment methods for axial PWSCC indications are described in Section 7.8.1. Comparisons of projected burst and leakage data with results based on the measured indications at the EOC inspection are given in Section 7.8.2

7.8.1 Condition Monitoring Assessment Methodology for Axial PWSCC Indications

The assessments described in Figures 7-2 to 7-4, and discussed above in Section 7.7, identify the indications requiring a condition monitoring assessment. Indications for which condition monitoring (CM) analyses will be performed include all indications with ≥ 40% maximum depth outside the TSP, indications requiring repair due to exceeding burst margins (CM burst analysis) and any indications found to have leakage in the operational assessment (CM leakage analysis). The condition monitoring analyses will also utilize Monte Carlo analyses, and Figures 7-5 and 7-6 show the logic diagrams for performing the analyses.

Figures 7-5 and 7-6 permit options for the use of a SG Monte Carlo analysis for the total crack length (constrained crack) burst probability and leak rate analyses. These condition monitoring SG analyses are performed assuming a POD of 1.0 on the basis that indications that could challenge structural and leakage integrity are detected in the inspection. This application of POD = 1.0 is consistent with NRC GL 95-05, Attachment 1, Section 2.c, Alternative Tube Integrity Calculation. This section of GL 95-05 requires that the actual indication distribution and NDE uncertainties be included in the calculation as well as uncertainties in the burst and leak rate analyses. The SG condition monitoring analyses of this report are consistent with these GL 95-05 requirements.

The logic followed for the condition monitoring burst pressure assessment is shown in Figure 7-5. The Monte Carlo analysis methods for condition monitoring are the same as for the operational assessment except that growth is not included in the analysis. In addition, the Westinghouse burst pressure correlation of Section 5 is also applied for condition monitoring analyses. Condition monitoring requirements are satisfied if the burst margin is met using the Westinghouse burst correlation. If the indication satisfies burst margins using the Westinghouse correlation but does not satisfy burst margin requirements using the conservative combined ligament tearing and throughwall crack model, the indication will be further evaluated in the 120 day report described in Section 7.11. This evaluation will utilize the latest available burst pressure information developed toward resolution of the burst issue of Reference 8-2. The principal differences from the operational assessment are the actions required if an indication does not satisfy the burst margin requirements. If the total length burst margin of $1.4\Delta P_{SLB}$ is not satisfied at 95%/50% confidence for one or more indications, a total SG Monte Carlo analysis should be performed to determine the tube burst probability at SLB conditions. The acceptance limit for the SLB burst probability for PWSCC alone is 1.0×10^{-2} at 95%/50% confidence based on the guidance of NRC GL95-05 for ODSCC at TSP intersections and the guidance of draft Regulatory Guide DG-1074 for condition monitoring. If this burst probability limit is exceeded, the condition monitoring total length burst margin requirement is not satisfied and the results must be reported to the NRC. The application of the SLB burst probability criterion is limited to the total length, constrained crack evaluation and cannot be applied to the freespan indication evaluation. If the freespan burst margin of $3\Delta P_{NO}$ is not satisfied for any PWSCC indication, the indication should be in situ pressure and leak tested. This criterion for defining the need for in situ pressure testing can only be applied to the freespan indication length and is applied in lieu of the EPRI In Situ Test Guidelines based on the detailed analyses performed to determine the need for in situ testing. If the in situ pressure test does not demonstrate satisfaction of the burst margin requirement, the condition monitoring freespan burst margin requirement is not satisfied and the results must be reported to the NRC.

Figure 7-6 outlines the condition monitoring SLB leak rate assessment for axial PWSCC. The Monte Carlo leakage analysis methods are also the same as for the operational assessment other than growth is not included in the condition monitoring assessment. As performed for the operational assessment, the sum of PWSCC leakage for the total crack length is added to that from other ARCs for comparison with the acceptance limits. If the total constrained leakage is less than the allowable dose based limit in the licensing basis, the condition monitoring leakage requirements on accident condition leakage are satisfied for constrained indications (ARC applications). If the constrained leakage limit is exceeded, a total SG Monte Carlo analysis should be performed for the total length leakage. This analysis with total SG leakage evaluated at 95%/50% confidence is a more accurate calculation and less conservative than summing all indication leakage values at their individual confidence levels. The results of this total SG analysis are then added to the leakage from other constrained mechanisms and compared to the acceptance limit. If the total constrained leakage limit is exceeded, condition monitoring leakage limits are not satisfied and the results must be reported to the NRC. In addition, a corrective action program must be initiated to identify the causative factors for exceeding the leakage limits. If any freespan leakage is predicted, the indication should be in situ pressure and leak tested. This requirement for in situ testing, which replaces application of the EPRI In Situ Guidelines for selection of indications for in situ testing, is applicable only to the freespan evaluation and cannot be applied to the total crack length evaluation. The sum of all freespan leak rates from analysis and in situ tests is added to the leakage from other freespan degradation mechanism condition monitoring assessments. If this leak rate exceeds the allowable limit of 1 gpm, NRC reporting and a corrective action program are required.

If in situ testing is performed for free span indications, the results of the tests are used in place of any analytical results such as described above. The measured leak rate would be added to the calculated

SLB leak rate from all other indications. In situ tests cannot be directly applied for the crack length inside the TSP due to the conservative ARC assumption that the TSPs are displaced in a SLB event.

7.8.2 Comparisons of Operational Assessment Predictions with Condition Monitoring Results

Although the PWSCC ARC has not been implemented at Diablo Canyon, comparisons of projected burst pressures and SLB leak rates can be made for indications left in service based on maximum depths < 40%. The 40% maximum depth repair limit has been implemented in consecutive outages (1R9 and 1R10, 2R9 and 2R10). This comparison was performed to provide an evaluation of the operational assessment methodology as described in this section.

In 1R9, 44 axial PWSCC indications at dented TSPs were left in service based on maximum depths less than 40%. Using both the Westinghouse burst model and the ANL/TW burst model, the OA burst pressures of these 44 indications exceeded 6100 psi. Due to computer storage considerations in the PWSCC ARC code, calculated burst pressures above 6100 psi are not stored in developing the burst pressure distribution. If the predicted burst pressure at the specified confidence level is > 6100 psi, the value is reported as 6100 psi. The OA leakage was 0.0 gpm. In 1R10, 41 of these 44 indications were detected (3 were not reportable). Using both the Westinghouse burst model and the ANL/TW burst model, the CM burst pressures of these repeat indications exceeded 6100 psi. The CM leakage was 0.0 gpm. In 1R10, 60 new indications were detected. Of the 60 new indications, 44 had been inspected by +Point in 1R9, and all were detectable based on reevaluation of the1R9 data given the knowledge of a flaw in 1R10. 12 of the new indications exceeded 40% maximum depth and required plugging in 1R10. Additionally, 7 new indications were plugged because of exclusion requirements. All but 2 of the new indications exceeded 6100 psi. The burst pressures of the 2 indications that did not exceed 6100 psi were 5789 psi and 5675 psi (using Westinghouse burst model), which are well above burst margin requirements. These two indications were >40% maximum depth and plugged in 1R10. These two indications were not inspected by +Point in 1R9, nor in any prior outage. The indications were located in less than 2 volt dents and were detected by bobbin in 1R10. Use of enhanced bobbin calling criteria in future Unit 1 outages should increase the probability of detected axial PWSCC indications in less than 2 volt dents that have never been inspected by +Point. Application of the enhanced bobbin criteria in Unit 2 during 2R10 resulted in high false call rates with only 3% of the bobbin calls being confirmed by +Point, and can be expected to lead to improved bobbin coil detection.

In 2R9, 34 axial PWSCC indications at dented TSPs were left in service based on maximum depths less than 40%. Using both the Westinghouse burst model and the ANL/TW burst model, the OA burst pressures of these 34 indications exceeded 6100 psi. The OA leakage was 0.0 gpm. In 2R10, all 2R9 indications left in service were detected. Using both the Westinghouse burst model and the ANL/TW burst model, the CM burst pressures of these repeat indications exceeded 6100 psi. The CM leakage was 0.0 gpm.

In 2R10, 21 new indications were detected. For these 21 TSP locations, 18 had been inspected by +Point in 2R9, and 16 indications were detectable based on a reevaluation of the 2R9 data given knowledge of the indication in the 2R10 inspection. Nine of the new indications exceeded 40% maximum depth and required plugging in 2R10. All but 1 of the new indications exceeded 6100 psi burst pressure. The burst pressure of the 1 indication that did not exceed 6100 psi was 4592 psi (using Westinghouse burst model), which is well above burst margin requirements. This indication was >40% maximum depth and plugged in 2R10. This indication was not inspected by Plus Point in 2R9, nor in any prior outage. The indication was detected by bobbin in less than a 2 volt dent in 2R10 as part of an enhanced bobbin calling criteria for less than 2 volt dents. Repeated use of the enhanced bobbin calling criteria in future Unit 2 outages should increase the probability of detecting axial PWSCC indications in less than 2 volt dents that have never been inspected by +Point.

Based on these comparisons, it is concluded that OA predictions of burst pressures and leak rates are adequately conservative. The OA analyses for both units predicted all burst pressures to exceed 6100 psi (upper bound for computer code) with no leakage and the subsequent CM analyses for both units yielded the same results.

7.9 Assessments for Mixed Mode Indications

This section addresses evaluations required for mixed mode indications. A mixed mode indication is defined as the presence of an axial and a circumferential indication at the same TSP intersection. An interacting mixed mode indication is defined as a mixed mode indication having the axial and circumferential indications separated by less than the required separation distance (0.25 inch) for negligible mixed mode effects on burst or leakage. An intersecting mixed mode indication is defined as the circumferential indication abutting or crossing the axial indication.

7.9.1 Overview of Approach to Mixed Mode Indications

Tests and analyses supporting evaluations of mixed mode indications are given in Sections 4.8, 4.10 to 4.14, 5.4, 5.5 and 6.6. These results are further developed below in Sections 7.9.2 to 7.9.7 to support assessments of the influence of mixed mode indications on application of the PWSCC ARC. It is shown that the probability of occurrence of a mixed mode indication leading to a reduction in the axial indication burst pressure below acceptance limits or significantly increasing SLB leak rates is negligible. This conclusion is particularly applicable to the expected range of circumferential crack depths, which can be expected (Section 7.9.2) to be smaller than the > 80% average depths required for significant influence of the mixed mode indication on burst and leakage integrity. The best estimate probability (see Section 7.9.4) of a significant mixed mode impact is about 10^{-7} per cycle with a potential range of about 10^{-4} to 10^{-7} per cycle dependent upon the benefits assumed for the dented TSPs preventing TSP displacement in a SLB event.

The following summary provides an overview of the mixed mode assessment and conclusions:

1. Negligible probability (about 10^{-4} to 10^{-7}) of a mixed mode indication leading to a reduction in the burst pressure below the burst margin requirements or significantly increasing SLB leakage (Section 7.9.4).

For a mixed mode indication to significantly impact burst or leakage integrity, the circumferential crack must be very deep (> 80% average depth), the axial indication burst pressure must be marginally above the burst margin requirement, and the near throughwall or throughwall circumferential crack must intersect the deepest part of the axial crack. The Diablo Canyon SG historical data show only shallow circumferential indications in modest numbers (63 indications in about 35,000 dented TSP inspections), only 5 TSP intersections having mixed mode indications (presence of both axial and circumferential cracks) for about 459 axial indications found to date, and only one of the 5 TSP intersections having shallow mixed mode circumferential and axial cracks close enough (< 0.25 inch separation distance) for a potential mixed mode interaction. However, the crack depths for the one indication with < 0.25" separation were too shallow for a mixed mode effect on burst pressure or leakage (See Section 7.9.8 below). All mixed mode indications found to date have been located within the TSP and it is expected that the potential intersection of the axial and circumferential cracks will remain within the TSP. There is a very high probability that the dented TSPs will not permit TSP displacement in a SLB event, and the presence of the TSP would prevent significant opening of the mixed mode crack. Collectively, these considerations lead to a very low probability (about 10^{-4} to 10^{-7}) of a significant mixed mode indication influence on burst and/or leakage integrity.

Given the low probability of occurrence for a significant mixed mode indication, there is no need to include any mixed mode effects in the tube repair basis for axial PWSCC. If a significant mixed mode impact is found in condition monitoring evaluations (Section 7.9.6), threshold limits requiring corrective action evaluations are given in Section 7.9.5.

2. Historical and Expected Circumferential Crack Sizes (Section 7.9.2)

The type of denting found in the Diablo Canyon and Sequoyah SGs is localized indentations with modest tube ovalization such that total dent deformation is typically from a few mils to about 10 mils diameter reduction. These small to modest dent sizes are in contrast to earlier SGs (since replaced) that had highly ovalized tubes leading to probe restrictions during inspections and somewhat larger (but < 180°) circumferential cracks. Pulled tubes show the circumferential cracks located near the localized dent with the OD indications tending toward the edges of the local dent. The circumferential cracks tend to be short and shallow, as described below, which is consistent with the small regions of high axial stresses associated with the localized dents. The axial tensile stresses can develop on both the ID and OD of the tube such that both PWSCC and ODSCC circumferential cracks may develop. Due to the short axial tensile stress fields at the localized dents, the circumferential cracks are expected to be short as found in the SG inspections. The circumferential cracks are located within the TSP since they are associated with local dents, which tend to be within the TSP as contrasted to overall tube ovalization which can extend outside the TSP. Ovalization of the cylindrical tube geometry leads to tube distortions longer in the axial direction than in the circumferential direction such that the axial cracks formed at the minor axis of tube ovalization can be longer than the short circumferential indications at the local dent locations.

In addition to dent geometry considerations for limiting the size of circumferential cracks at dented TSP intersections, crack sizes are also limited by the requirement to repair all circumferential indications upon detection. Any potential increase in tube integrity risk from mixed mode indications under the PWSCC ARC compared to no ARC is limited to intersections that have had a prior +Point inspection leading to an axial indication being left in service under the ARC. The +Point detectability applies for the potential of a mixed mode indication. It is shown below in Section 7.9.3 that +Point detectability is adequate to limit EOC circumferential average depths to ≤ 80% based upon indication sizes found to date, growth rates and EOC projections of circ crack sizes. Thus, any circumferential cracks found at EOC conditions can be expected to have average depths less than the > 80% depth required for significant mixed mode impact on tube integrity. If circumferential cracks > 80% depth are found in an inspection, corrective actions would be evaluated as described in Section 7.9.5.

3. Mixed Mode Burst Test Results

Burst tests of partial depth mixed mode indications were performed to quantify mixed mode effects for part throughwall axial indications. The test results for up to 80% circumferential average depth show no reduction in the axial indication burst pressure for part throughwall axial indications having a ligament tearing pressure higher than the burst pressure for a throughwall indication of the same length. In this case based upon testing of uniform depth slots, tearing of the ligament occurs over the total length of the notch and results in a tube burst since the throughwall length has a lower burst pressure than the ligament tearing pressure. The ligament tearing pressure of the axial crack is not significantly influenced by the presence of a partial depth circumferential crack. Reductions in the ligament tearing pressure can occur for very deep or throughwall circumferential indications due to reduced constraint against bulging of the axial indication. The higher ligament tearing condition corresponds to long and deep, but not throughwall axial indications and shallow, shorter axial indications. Some reduction in the axial indication burst pressure can occur when the ligament tearing pressure is less than the throughwall burst pressure. In this case, pressurization tears the axial ligament resulting in a throughwall indication for which tearing of the circumferential ligament can reduce the axial throughwall burst pressure. The potential for this condition reducing the burst pressure to less than burst margin requirements is limited to a narrow range of crack lengths (See Section 5.5.3).

The burst test results of Sections 5.5 (intersecting mixed mode tests) and 5.6 (separation distance tests) lead to the following conclusions on mixed mode effects on burst pressures:

- An average circumferential depth of ≤ 80% reduces mixed mode effects on burst pressures for intersecting indications to negligible levels (<10%) for partial depth axial indications and the probable range (less than about 0.25") of throughwall axial indications to be found for axial PWSCC. If the ligament tearing pressure exceeds the throughwall burst pressure for the same length crack (typical of long indications > 0.5" satisfying burst margins), there are no mixed mode effects on burst pressures for ≤ 80% average depth circumferential cracks. The modest burst pressure reductions of about 10% for average circumferential depths near 80% occur when the throughwall burst pressure exceeds the ligament tearing pressure. However, there is a very narrow range of crack lengths and depths for which the burst pressure could be reduced by up to 15% for 80% average circumferential depth.

- For throughwall axial indications longer than about 0.5" and ≤ 80% circumferential indications, the mixed mode effects can approach about 25% for intersecting indications but are reduced to <10% for a separation distance of 0.25 inch. Consequently, a separation distance for negligible mixed mode effects with ≤ 80% deep circumferential indications is required only for long throughwall axial indications. In this case, satisfaction of a 0.25 inch separation requirement is applied only to eliminate the need for a detailed mixed mode evaluation. If the separation distance is < 0.25", a mixed mode evaluation is required for which the results would be dependent on the lengths and depths of the indications.

- For throughwall axial indications longer than about 0.5" intersecting throughwall circumferential indications, mixed mode effects approach about 40%, but are reduced to about 15% with 0.25" separation. Demonstration of a 0.25" separation distance is acceptable to eliminate the need for a detailed mixed mode evaluation unless both the axial and circumferential indications are throughwall at any point. In this case when both indications are throughwall, a detail mixed mode evaluation is required independent of the separation distance although the mixed mode effects are bounded by about 15% with 0.25" separation.

- If the separation distance is greater than or equal to 0.25 inch including an allowance for undetected cracks (about 20% maximum depth within the separation distance), each component can be regarded as individual, isolated cracks for structural and leakage evaluations unless both indications are throughwall at any point.

If a mixed mode indication is found to cause a reduction in the axial indication burst pressure, corrective actions will be evaluated as described in Section 7.9.5.

4. SLB Leak Rate Considerations

To assess the potential impact of mixed mode indications on leakage, the widths of axial slots used for burst testing were measured (see Section 5.4) at SLB pressure differential for throughwall axial slots with and without a L-shaped 75% circumferential indication. The measurements performed for a 0.60 inch throughwall axial indication and an intersecting 75% circumferential indication show a crack opening area increase of only a factor of 1.4 leading to a leak rate increase by about a factor of 1.7 compared to the axial indication only.

If a circumferential indication > 50% and ≤ 80% average depth is found in an inspection to interact with a throughwall axial indication, or if a circumferential crack of > 80% average depth is found in an inspection, corrective actions will be evaluated for SLB leak rates as described in Section 7.9.5. Circumferential average depths measured in the field need to be adjusted for NDE uncertainty when comparing against the above average depth criteria.

5. Separation Distance

As noted in item 3 above, a separation distance of 0.25 inch is adequate to reduce mixed mode effects on burst pressures to acceptable levels except for the case when both the axial and circumferential indications are throughwall. The latter requires a separate mixed mode evaluation for any separation distance.

The required 0.25" separation distance can be confirmed by the presence of null points between the axial and circumferential RPC responses. The NDE conclusions on separation requirements can be summarized as the following requirements for the PWSCC ARC applications:

- About 0.075 inch null point spacing (about three null points for RPC spacing ≈0.025") are required to demonstrate acceptable separation for OD circumferential indications.
- About 0.050 inch null point spacing (about two null points if RPC spacing ≈0.025") between the axial and circumferential indications are required to demonstrate acceptable separation for ID circumferential indications.
- If, with allowances for NDE uncertainties, both the axial and circumferential indications are 100% throughwall at any point, the null point separation is not applied and a detailed mixed mode evaluation is required.
- With the exception of throughwall axial and circumferential indications, satisfaction of the null point requirements eliminates the need for a detailed mixed mode evaluation.

The above null point requirements include an additional null point beyond the requirements based on EDM notch tests in order to correct for the differences between EDM notches and cracks for RPC coil lead-in effects.

7.9.2 Evaluations of Circumferential Cracks Found at Dented TSP Intersections

The circumferential cracks found to date in the Diablo Canyon SGs are described in Section 4.12. The indications were sized using the techniques described in Section 4.10. The NDE uncertainties were obtained by testing five analysts expected to perform sizing at Diablo Canyon against pulled tube and laboratory corrosion specimen destructive exam data. Three of these analysts then sized the Diablo Canyon circumferential indications at dented TSPs. The uncertainties are thus directly applicable to the analysts performing the sizing. The following table provides the largest circumferential crack sizes found to date.

Diablo Canyon SG Circumferential Indications		
Quantity	**Largest Found to Date**	
	PWSCC	ODSCC
Average Depth	48.9%	57.2%
Maximum Depth	68%	72%
Length	77°	64°

As expected from the stress fields associated with the localized dents, the crack angles are small and≤ 75°. The largest average depth found to date is only 57%.

From Section 4.10, the average and maximum depth NDE uncertainty correlations for PWSCC circumferential cracks are:

$$D_{avg}(\text{truth}) = 0.673D_{avg}(\text{measured}) + 13.25 \qquad \text{PWSCC indications}$$
$$D_{max}(\text{truth}) = 0.725D_{max}(\text{measured}) + 16.71$$

The standard deviation on the PWSCC average depth uncertainty is 7.79% and a 49% measured average depth adjusted for NDE uncertainty at 95% probability is 58%. The standard deviation on the PWSCC maximum depth uncertainty is 11.25%

The average and maximum depth NDE uncertainty correlations for ODSCC circumferential cracks are:

$$D_{avg}(\text{truth}) = 0.631D_{avg}(\text{measured}) + 20.11 \qquad \text{ODSCC indications}$$
$$D_{max}(\text{truth}) = 0.731D_{max}(\text{measured}) + 19.43$$

The standard deviation on the ODSCC average depth uncertainty is 7.75% and a 57% measured average depth adjusted for NDE uncertainty at 95% probability is 69%. The standard deviation on the ODSCC maximum depth uncertainty is 9.54%

A discussion on applying the NDE uncertainties to measured flaw sizes to define circumferential indication depths for a comparison with requirements is given in Section 7.9.3. For mixed mode burst evaluations, average depth NDE uncertainties are applied while maximum depth uncertainties are applied for evaluations based on maximum depth such as leakage assessments.

The lengths and depths of the circumferential indications found at Diablo Canyon are compared with axial indication lengths and depths in Section 4.14. These comparisons show that the circumferential flaws look very much like the axial indications rotated 90°. The longest circumferential indications are shorter than the longest axial indications. Maximum and average depth distributions as well as the maximum to average depth ratios of the axial and circumferential indications are similar. Given the similarities of the indications at dented TSP intersections, the predictability of the flaw behavior can be expected to also be comparable. Based on tube repair upon +Point detection for circumferential indications, it can be expected that large and deep circumferential indications will not be found at TSP intersections.

7.9.3 Circumferential Crack Size Considerations

A conservative estimate for a projected circumferential crack size can be deterministically obtained by adjusting the largest measured depth found to date for NDE uncertainty at 95% probability. Adjustments for NDE uncertainties can also be performed using Monte Carlo methods. As given in Section 7.9.2 above, the largest measured circumferential average depths found to date are 49% for PWSCC and 57% for ODSCC, and when deterministically adjusted to 95% NDE uncertainties, the corresponding average depths are 58% and 69%. These depths are well below the > 80% average depth required for significant mixed mode interaction effects. The circumferential indications, as described in Section 4.12, do not show any increase in length or depth in the later inspections compared to the earlier inspections. The largest circumferential PWSCC indications detected at DCPP occurred in 1995 and 1996, during the first time use of Plus Point for inspection of dented TSPs. ODSCC indications were not found until later cycles. Consequently, the prior history provides a conservative estimate of the expected future indication size.

A detection threshold for a +Point inspection can be expected to be smaller than that for circumferential indications found in tubes pulled based on detected indications at dented TSP intersections. One tube was pulled from Diablo Canyon-1 for a PWSCC indication in a 28 volt dent and one tube was pulled from Sequoyah-1 for an ODSCC indication in a 2.9 volt dent. As described in Section 4.11, the laboratory specimen and pulled tube results support average depth detection thresholds of about 35% for ODSCC and about 25% for PWSCC. The detection thresholds can be projected to EOC conditions by adding growth at 95% cumulative probability. From Section 4.13, the circumferential growth rate at 95% is 29% for a conservative cycle length of 1.65 EFPY (21 month cycle length). Adding growth to the conservatively assumed 35% detection threshold would result in an EOC circumferential average depth of 64% (73% with 95% NDE uncertainty allowance to bound comparison with EOC measured indications). This average depth exceeds the largest ODSCC indication of 57% (69% with +95% NDE uncertainty) found in any inspection, which supports the conservatism in assuming a 35% detection threshold.

Both the deepest indication found to date and the deterministic EOC projections demonstrate that the EOC circumferential average depth is expected to be less than 69%. This depth is less than the 80% average depth found to have negligible mixed mode effects on burst and leakage for long PWSCC indications.

7.9.4 Probability for a Mixed Mode Burst Pressure Reduction

An estimate can be made of the probability for occurrence of a mixed mode indication leading to a significant reduction in the axial indication burst pressure. This estimate is provided in Table 7-1 which includes the probability quantity being estimated, the value for each component of the probability and comments supporting the probability estimate. The number of axial and circumferential indications as well as the number of interacting mixed mode indications form the principal basis for the probability estimate and are obtained from Diablo Canyon SG historical data as given in Table 7-1. Two conditional probabilities for finding deep axial indications near the burst margin requirements and for finding the circumferential crack intersecting the deep part of the axial crack must be estimated. The estimated values for these conditional probabilities are included in the table. Since the forces required to displace the TSP at a dented intersection are much higher than expected SLB loads across the plate, the probability that the plates would displace is very small and conservatively estimated to be 0.001. Since the circumferential cracks and most of the axial cracks (or most of the axial length) are located within the TSP, the presence of a dented TSP would prevent opening ('locked' TSPs) of the axial crack and exclude a mixed mode effect.

From Table 7-1, the probability per axial indication of a mixed mode reduction in the axial indication burst pressure ranges from $\approx 2x10^{-7}$ to $\approx 2x10^{-10}$, where the smaller value includes the 10^{-3} probability of TSP displacement in a SLB event and represents the best estimate probability. To obtain the probability per cycle, these values need to be multiplied by the number of axial indications left in service. It is estimated that the largest number of PWSCC axial indications left in service in any future cycle will be less than 400. The estimated probability per cycle of a mixed mode burst pressure reduction then ranges from $\approx 8x10^{-5}$ to $\approx 8x10^{-8}$.

The upper bound probability of about 10^{-4} supports the expectation that mixed mode indications will not contribute to challenging burst or leakage integrity at the Diablo Canyon SGs. Given the low probability of a mixed mode effect, there is no need to modify the PWSCC ARC repair limits for mixed mode effects. Rather, the emphasis is on evaluating circumferential and mixed mode indications at each inspection to demonstrate that the bases for the low probability estimates are valid. The requirements for these evaluations are described below in Section 7.9.5.

7.9.5 Circumferential Crack and Mixed Mode Evaluation Requirements

At each outage, all circumferential cracks are to be sized per the NDE analysis techniques described in Section 4.10. The measured average depths are to be adjusted by deterministic or Monte Carlo methods for NDE uncertainty at the upper 95% probability level to define the average circumferential crack depth for the mixed mode evaluations. If a mixed mode indication is found, the indication shall be evaluated for interaction based upon the null point NDE techniques of Section 4.8 and the 0.25 inch separation requirement of Section 5.5. If the mixed mode indication is found to be interacting (separation distance of 0.25" not demonstrated by NDE null points or both the axial and circ indications are throughwall at any point), the indication shall be evaluated for a reduction in the burst pressure below the acceptance limits based on the mixed mode test results of Section 5.4. If the mixed mode data is not adequate to assess the potential reduction in the axial indication burst pressure, additional burst tests may be performed to simulate the indication in order to measure the associated reduction in the axial indication burst pressure. Based upon the methods of Sections 4.8, 5.4 and 5.5, the following are examples of acceptable mixed mode indications:

- Two NDE null points (assumed 0.025" RPC pitch) for a PWSCC circumferential indication or three null points for a ODSCC circumferential indication exist between the axial and circumferential indication and the average circumferential crack depth is ≤ 80%.
- The calculated ligament tearing pressure for the axial indication is greater than that for an assumed 100% throughwall indication of the same length and the average circumferential crack depth is ≤ 80%. The test data show no burst pressure reductions in this case for circumferential crack average depths up to 80%.
- The calculated ligament tearing pressure for the axial indication is less than that for an assumed 100% throughwall indication of the same length and the average circumferential crack depth is ≤ 80%. The test data show negligible (<10%) burst pressure reductions in this case for circumferential crack average depths up to 80%, and up to 15% reduction for 80% circ crack average depth over a very small range of axial crack length and depth combinations.

Examples requiring evaluations for mixed mode effects based on the data of Section 5.5 would include interacting axial and circumferential indications having the average circumferential depth > 80% or an axial indication having a throughwall length > 0.25 inch.

A conditional requirement for corrective action is defined below in the unexpected event that a mixed mode indication significantly impacts the axial indication burst pressure.

- If an interacting mixed mode indication is found by the above evaluations to have led to a reduction in the axial indication burst pressure by more than 10% and to less than 4000 psi, or to have caused an indication to not satisfy burst margin requirements, the burst margin requirements for implementation in the operational assessment at the next and subsequent outages shall be increased by the percentage reduction in burst pressure found for the mixed mode indication. The requirement to reduce the burst pressure to less than 4000 psi is applied to identify mixed mode effects potentially impacting satisfaction of the burst margin requirements. The reduction for short throughwall cracks may exceed 10%, but the burst pressures are very high such that mixed mode corrections do not challenge satisfaction of burst margin requirements. If the existing mixed mode burst test database is not adequate to assess the indication, the indication should be simulated for additional burst testing as part of the 120 day report without affecting startup. All mixed mode evaluations and potential corrective actions are to be documented in the 120 day report (see Section 7.12).

The following conditional requirements apply to potentially adjust SLB leak rates for mixed mode effects:

- For condition monitoring of an axial indication with predicted leakage interacting (null point separation requirements not satisfied) with a circumferential crack that has >50% average depth, the condition monitoring leak rate (95/50 confidence) for the axial indication shall be increased by a factor of L_F based upon the mixed mode leakage methods of Section 6.6. The leakage factor, L_F, is 1.7 for circumferential average depths ≤ 80% and 10 for average depths > 80%. In addition, the operational assessment for the total PWSCC SLB leak rate for each SG must be increased by the leak rate multiplier, $M_L = 1 + (L_F-1)f$, of Section 6.6 (f = fraction of detected axial PWSCC indications found to be interacting). The adjustment for the operational assessment leakage should be made for all subsequent operational assessments.
- The operational assessment SLB leak rate must be adjusted if a previously +Point inspected (i.e., inspected in the last inspection) TSP intersection is found to have a circumferential indication with an average depth > 80% after accounting for NDE uncertainty. When required, the total PWSCC operational assessment SLB leak rate for each SG must be increased by the leak rate multiplier, $M_L = 1 + 9f$, of Section 6.6 (f = fraction of detected axial PWSCC indications found to be interacting). This requirement applies only to previously +Point inspected TSP intersections since the potential increase in risk due to mixed mode indications as a result of applying the PWSCC ARC exists only for intersections leaving an axial indication in service, which requires a +Point inspection. The adjustment for the operational assessment leakage should be made for all subsequent operational assessments.
- The adjusted axial PWSCC SLB leak rates are to be included in comparisons of predicted total leakage with allowable leakage limits.

7.9.6 Condition Monitoring Considerations

The condition monitoring analyses required for mixed mode indications are that all circumferential cracks are to be sized per the NDE analysis techniques described in Section 4.10, and if a mixed mode indication is found, the indication shall be evaluated as described in Section 7.9.5 above. These requirements are applied to provide a continuing supporting basis for the low probability of a mixed mode impact challenging structural and leakage integrity. Section 7.9.5 also describes the corrective actions to be taken if a significant mixed mode indication is found in the condition monitoring analyses.

7.9.7 Operational Assessment Considerations

Unless the mixed mode threshold criteria described in Section 7.9.5 are exceeded, no mixed mode considerations are applied for the operational assessment. Section 7.9.5 describes the corrective actions to be taken for the operational assessment if a significant mixed mode indication is found in the condition monitoring analyses.

7.9.8 Analysis of Diablo Canyon Mixed Mode Indications

Five mixed mode indications have been detected at DCPP, and NDE measurements are shown in Figures 7-7 to 7-11. For R12C25, R22C46 and R11C19, the estimated separation distances are greater than the 0.25 inch (all ≥ 0.35 inch based upon line-by-line sizing) separation requirement for circumferential crack depths ≤ 80%. More than two null points with an RPC pitch of about 0.025" were detected for these PWSCC indications with the 80 mil coil, so they are treated as non-interacting mixed mode flaws. No further evaluation for interacting mixed mode burst and leakage acceptance criteria are required for these flaws.

For R14C12, the C-scan for the PWSCC indications is shown in Figures 7-12, and the lissajous displays are shown in Figures 7-13. A return to null for three null points can be seen in Figure 7-13 for which independent line by line sizing of the indications led to a separation distance estimate of 0.28 inch (Figure 7-10). Thus, the R14C12 indication is "non-interacting" based on the presence of at least two null points (RPC pitch is about 0.025") in the pancake coil response, and a detailed mixed mode evaluation is not required. Given that the circumferential indication is shallow (circumferential average crack depth of 49%, 58% corrected for NDE uncertainty) and less than 80%, R14C12 would satisfy burst margins even if conservatively treated as an interacting mixed mode indication.

For R21C33, the C-scan is shown in Figure 7-14 and the lissajous display is shown in Figure 7-15. Figure 7-15 shows that the 80 mil pancake coil does not have a null point for R21C33. Based on line to line sizing of this indication, the separation distance is estimated at about 0.06 inch (Figure 7-9) for these shallow indications. Since R21C33 does not show a null point response between the axial and circumferential indications, R21C33 is treated as an "interacting" mixed mode indication and requires further evaluation based on the burst test data of Section 5.4. Per Section 5.7, this indication would have no mixed mode interaction effects causing a reduction in burst pressure below burst margin requirements since both the axial and circumferential indications are too shallow for a significant reduction in burst pressure even for intersecting axial and circumferential indications since the ligament tearing pressure for the axial indication exceeds the throughwall burst pressure. The average depth of the axial indication is 26%. Because the circ crack length is greater than the maximum length of 0.25 inch, the average depth of the circumferential crack is defined as the average depth over the 0.25 inch closest to the axial indication, i.e., 39.8 % (deepest 0.25" segment), or 53 % including NDE uncertainty, which is much less than the 80% threshold value. The total circumferential crack length average depth is 27.8%. In addition, due to the short 0.16 inch axial indication, the burst pressure would exceed burst requirements even if it was assumed that both indications were throughwall and intersecting.

7.10 Tube Removal Requirements for ARC Applications

The following define the requirements for pulling tubes in association with implementation of the alternate repair criteria of this report for axial PWSCC at dented TSP intersections.

- Plants shall pull a tube prior to or subsequent to implementing the PWSCC ARC to support +Point sizing of the indication and crack morphology consistent with the PWSCC database. PG&E has removed five intersections containing axial PWSCC indications, and all are representative of the types of indications to which the ARC will be applied. Four intersections are included in the data set used in the Plus Point qualification. Therefore, further tube removals are not required at DCPP Units 1 and 2 to support ARC application.
- When a tube pull is required to support +Point sizing, the tube selected for removal shall have a high probability of leaking in order to contribute to the leak rate database. The requirements for a tube removal to enhance the likelihood of finding a leaker are given below. The tube pull may be performed in the cycle following ARC implementation or later as necessary to obtain an indication satisfying the requirements for removal. No TSP intersection above the potentially leaking intersection should be removed due to the increased likelihood of damage to the desired intersection.
- The destructive exam for the removed tube shall include, as a minimum, a leak test at operating temperature, a burst test, fractography to obtain the depth profile of the burst crack and a second major crack if present and one or more transverse metallographic sections (cross sections of the tube) to characterize secondary cracking if present. If the tube section removed to obtain the potential leaking section includes a lower TSP with a PWSCC indication, this second intersection shall also be destructively examined.

Freespan indications that are predicted to leak at 95/50 confidence are required to be in situ tested as described in Section 7.8. If the indication leaks in an in situ test, the indication satisfies the requirements for tube removal. Selection of an indication within the TSP with a high probability of leaking can also be obtained from the condition monitoring evaluation. The single indication condition monitoring leakage analyses is performed for all indications predicted to leak in the operational assessment as described in Section 7.8. The Monte Carlo analyses provide a distribution of leak rates for the indication to permit selection of a leak rate at a specified probability of occurrence. To obtain a reasonable likelihood that the indication will leak, the indication selected for removal should be predicted to have a leak rate ≥ 0.01 gpm at 50% probability for the Monte Carlo leak rate distribution. For a 0.01 gpm calculated nominal leak rate, the ligament tearing breakthrough length would be predicted to be about 0.2 inch. The objective for a reasonable breakthrough length of at least 0.2 inch provides a better test of the leakage model than smaller leak rates for which local or specific depth points in the NDE profile may dominate the analysis. The use of the 50% probability value establishes a reasonable likelihood that the indication will leak in contrast to the 95% leak rate, which only assures a 5% likelihood of leakage since lower probability values could be zero or near zero.

In summary, the leakage based requirements that must be satisfied to pull a tube, when a tube pull is required to support +Point sizing, are:

1. The indication is found to leak in an in situ test, or

2. The indication has a predicted leak rate ≥ 0.01 gpm at 50% probability from the Monte Carlo leak rate distribution performed as part of the condition monitoring assessment

The above leakage based requirements apply as generic ARC requirements when plant specific tube pulls are required to support axial PWSCC sizing. As noted above, DCPP has four indications included in the ARC +Point qualification, and no further tube removals are required for the DCPP ARC.

7.11 Risk Assessment

NRC draft Regulatory Guide DG-1074 requires that a risk assessment be performed to support an ARC submittal. This section provides this risk assessment for the depth based repair limits of this report. The depth based repair limits are conservatively established to provide deterministic margins against burst under normal operation and accident conditions. Burst margins of $3\Delta P_{NO}$ are satisfied at 95% confidence levels for freespan indications and margins of $1.4\Delta P_{SLB}$ are satisfied at 95% confidence for indications within the TSP. Indications within the TSP inherently satisfy the $3\Delta P_{NO}$ burst margin since the presence of the TSP prevents rupture under normal operation and accident conditions with the postulated exception of a SLB event. The presence of the TSP would also prevent rupture of indications within the TSP under severe accident conditions such as a Station Blackout. As noted in Section 7.5.3, the maximum depth repair limit for freespan indications is 40%, which is consistent with the current Technical Specifications and deterministically satisfies the $3\Delta P_{NO}$ burst requirement with additional margin. Freespan indications are required to satisfy the $3\Delta P_{NO}$ burst margin for condition monitoring assessments. It is therefore concluded that the proposed depth based repair limits provide the same risk for rupture under severe accident conditions as current Technical Specifications which have been considered to be acceptable.

The 40% maximum depth repair limit for freespan indications provides a very low likelihood of freespan leakage under design basis or severe accident conditions. In addition, it is required that the total leakage from all freespan indications including all degradation mechanisms must be less than 1 gpm at SLB conditions. The number of indications left in service for any one operating cycle is expected to be a few hundred or less and not numbers measured in the thousands. The modest population of indications left in service support a negligible freespan leakage potential under design basis conditions. Leakage from indications inside the TSP is limited by the constraint of the TSP even under severe accident conditions and leakage behavior in a severe accident would be similar to that found acceptable for axial ODSCC at TSP intersections. Leakage tests for dented TSP intersections show very low or no leakage for throughwall indications inside the TSP. In addition, the constraint provided by the dented TSP intersection reduces leak rates even for throughwall indications extending outside the TSP. Even under severe accident conditions, the potential for significant leakage would be expected to be small and not significantly different than for other degradation mechanisms repaired to 40% depth limits but with less well-defined growth rates and NDE uncertainties. It is concluded that application of the depth based repair limits of this report result in negligible differences from current 40% repair limits in risk of a tube rupture or large leakage event under design basis or severe accident conditions.

7.12 NRC Reporting Requirements

In the event that condition monitoring requirements as discussed in Section 7.7 are not satisfied, the results shall be reported to the NRC in accordance with NEI 97-06 and time frames specified in 10 CFR 50.72/73.

The results of the condition monitoring assessment and the operational assessment performed to define indications requiring repair shall be reported to the NRC within 120 days following the return to service from the inservice inspection. The report shall include:

- Tabulations of indications found in the inspection, indications repaired and indications left in service under the ARC
- Growth rate distributions for indications found in the inspection and the growth rate distributions used to establish the tube repair limits
- +Point confirmation rates for bobbin detected indications when bobbin is relied upon for detection of axial PWSCC in ≤ 2.0 volt dents
- Performance evaluation of the operational assessment methodology for predicting flaw distributions as a function of flaw size.
- Evaluation results of number and size of previously reported versus new PWSCC indications found in the inspection, and the potential need to account for new indications in the operational assessment burst evaluation.
- For condition monitoring, an evaluation of any indications that satisfy burst margin requirements based upon application of the Westinghouse burst pressure correlation, but do not satisfy burst margin requirements based upon the combined ANL ligament tearing and throughwall burst model.
- Identification of mixed mode (axial PWSCC and circumferential) indications found in the inspection and an evaluation of the mixed mode indications for potential impact on the axial indication burst pressures or leakage as described in Section 7.9.
- Any corrective actions found necessary in the event that condition monitoring requirements are not met. Examples of potential corrective actions are described below.

Conditional corrective actions for mixed mode indications are described in Section 7.9.5. Conditional corrective actions for larger than expected axial indications would include the following:

Condition Monitoring Burst Probability > 10^{-2}

As described in Section 7.8 and Figure 7-5, if any indication is found by condition monitoring analyses to have a total length burst pressure less than the burst margin requirement, a total SG condition monitoring assessment for burst probability shall be performed applying a POD of 1.0 since only detected indications potentially require a corrective action. If the resulting SLB burst probability is $> 10^{-2}$, NRC reporting is required. In addition to these Section 7.8 requirements, the following conditional requirements are applied:

- A total SG Monte Carlo operational assessment burst probability analysis is required for the next operating cycle using a POD of 0.6. The largest growth rate distribution per the guidelines of Section 7.5.5 is to be used for the operational assessment. The potential need for including additional margin in the growth rate distribution should be assessed. The projected EOC SLB burst probability analysis must be completed prior to return to power and the resulting burst probability for axial PWSCC indications is required to be $\leq 10^{-2}$. If necessary, additional indications are to be repaired prior to return to power until the burst probability requirement is satisfied.

As described in Section 7.8 and Figure 7-5, if any free span crack length is found by in situ testing to have a burst pressure less that $3\Delta P_{NO}$, NRC reporting is required and a corrective action plan is required. In addition to these Section 7.8 requirements, the following conditional requirements are applied:

- Preliminary corrective actions must be implemented for the operational assessment prior to restart in order to reduce the potential for a reoccurrence of this issue. If the cause is identified to be larger than predicted growth rates, the larger growth rates should be included in the analysis, as required by Section 7.5.5, and the potential need for including additional margin in the growth rate distribution should be assessed. The preliminary corrective actions to be implemented for the operational assessment are to be reported to the NRC prior to restart. Final corrective actions are to be included in the 120 day report.

Condition Monitoring SLB Leak Rates Exceed Allowable Limits

Section 7.8 and Figure 7-6 define the SLB leak rate analysis requirements for constrained and freespan leakage. The results of the PWSCC analyses are added to the leakage from other constrained mechanisms or freespan mechanisms and compared to the acceptance limits. If either the total constrained or total freespan leakage limit is exceeded, condition monitoring leakage limits are not satisfied and the results must be reported to the NRC. If the PWSCC leakage exceeds the prior cycle projected leakage and is a significant contributor (in comparison with contributions from other mechanisms) to not satisfying the leakage limits, a corrective action program must be initiated to identify the PWSCC causative factors for exceeding the leakage limits. Details of all corrective actions taken are to be documented in the 120 day report. In addition to these Section 7.8 requirements, the following conditional requirements are applied:

- Preliminary corrective actions must be implemented for the operational assessment prior to restart in order to reduce the potential for a reoccurrence of this issue. If the cause is identified to be larger than predicted growth rates, the larger growth rates should be included in the analysis, as required by Section 7.5.5, and the potential need for including additional margin in the growth rate distribution should be assessed. The preliminary corrective actions taken to enhance confidence in the leakage projections for the next cycle are to be reported to the NRC prior to return to power. Final corrective actions are to be included in the 120 day report. This effort parallels that described above for burst pressure considerations.

New Axial PWSCC Indications

New indications are not included in the burst pressure operational assessment on the basis that undetected axial PWSCC indications are not expected to grow to sizes that would challenge structural integrity at the end of the operating cycle. This expectation is based upon the adequacy of bobbin detection in ≤ 2.0 volt dents and the +Point inspection of larger than 2.0 volt dents as described in Section 7.6. A new indication is defined as an axial PWSCC indication not reported at the prior inspection, and therefore not included in the operational assessment. The acceptance criterion for new indications is that the condition monitoring burst pressure (evaluated at 95/50 confidence) must exceed the $1.4\Delta P_{SLB}$ burst margin requirement. If this criterion is not satisfied, the following conditional requirement is applied:

- A total SG Monte Carlo operational assessment for burst probability is required for all SGs based on applying a POD = 0.6. The Monte Carlo assessment is required for all SGs because new indications are not confined to any one SG. This POD value is sufficiently low to account for new indications below detectable levels as well as undetected indications at the prior inspection. (Note: This total SG Monte Carlo analysis is described for leakage in Section 7.7 and Figure 7-4, which also define the acceptance requirements for SLB leakage.) The burst probability analysis must be completed prior to return to power and the burst probability for axial PWSCC indications must be $\leq 1x10^{-2}$. If necessary, additional PWSCC indications must be repaired to satisfy the burst probability requirement prior to return to power. Corrective actions included in the 120 day report should define methods for including new indications in future operational assessments.

Since the POD of 0.6 is included in the required SG Monte Carlo operational assessment when any single indications are found to predict leakage, the leakage calculation includes allowances for new indications and no additional leakage analysis requirements are needed prior to restart. However, if new indication leakage is the principal contributor to not satisfying condition monitoring leakage requirements, the corrective actions included in the 120 day report should define the need for improved methods for including new indications in future operational assessments.

Underpredictions of Inspection Results for Indications Left in Service

As noted in the above reporting requirements, an evaluation of the operational assessment methodology is required for predicting flaw distributions as a function of flaw size. This section addresses requirements for corrective actions when the single indication operational assessment predictions significantly underestimate the SLB burst pressures or leak rates when compared to the results calculated from the condition monitoring assessment based on inspection results. The conditional requirements for significant under predictions of burst and leakage are described below for documentation in the 120 day report and implementation in the next operating cycles.

- When comparing single indication projected leak and burst data with that obtained for the same indication from the inspection results, additional evaluations are to be performed and included in the 120 day report if: 1) the condition monitoring single indication burst pressure is < 6000 psi and more than 500 psi less than the projection obtained using the same burst model; or 2) the condition monitoring single indication leak rate is more than 0.2 gpm larger than the projected SLB leak rate. Any resulting corrective actions are targeted for implementation at the inspection following issuance of the 120 day report. The differences between projected and measured profile results of 500 psi for burst or 0.2 gpm are intended to define significant differences justifying further evaluation. Similarly, if the measured profile burst pressure is > 6000 psi, the indication is very small and differences between prediction and measured can be expected and are insignificant for small indications. In most cases, significant under predictions for the projections are due to increases in growth rates compared to that used for the projections. Growth rates are to be evaluated as the potential causative factor for the discrepancy between projections and measurements. If the under prediction is not attributable to underestimates of growth in the projections, additional evaluations shall be performed to identify the causative factor and the evaluation shall be included in the 120 day report. If the under prediction is attributable to underestimates of growth in the projections, the 120 day report should provide a corrected growth rate distribution to better predict the next EOC conditions. At the end of the next cycle, the measured growth rate distribution is to be compared with the corrected growth rate distribution that was predicted in the 120 day report. If the 90th percentile measured growth is greater than the 90th percentile predicted growth value, which indicates at least two successive cycles of increasing growth rates, the measured growth rate distribution for the just completed cycle is to be increased by a factor of 1.1 or more and applied in the operational assessment for repair decisions to enhance conservatism for the subsequent operating cycle.

7.13 ARC Summary

A summary of this section is provided in Section 2 of this report.

Table 7-1. Estimated Probability for Occurrence of a Mixed Mode Indication Leading to a Significant Reduction in the Axial Indication Burst Pressure

Quantity	Value	Comments
Number of PWSCC axial indications plugged and in service	(210p + 111 <40%) + (104p + 34 <40%) = 459	Total number of axial ind. to date plugged (p) and <40% max depth left in service. Values for (Unit 1) + (Unit 2).
Number of circumferential indications	(11 ID + 7 OD) + (38 ID + 7 OD) = 63	
Number of mixed mode indications (i.e., axial and circ at same TSP intersection)	1 + 4 = 5	
Number of circ indications without a null point separation	1 + 0 = 1	
Number of circ indications within separation distance and >80% average depth	0 + 0 = 0	Single circ within separation distance was shallow (25% avg. depth) as was the axial indication (26% avg. depth, 0.16" long).
Probability per axial ind. of a circ crack close enough to interact	1/459 = 0.0022	One circ crack found within separation distance
Conditional probability that interacting axial crack is near burst margin such that mixed mode effects could reduce burst pressure below the burst margin requirement	≈0.05	Conservative estimate assuming 1 in 20 axial indications will have burst pressure near burst margin at EOC.
Conditional probability that interacting circ is deep enough to affect axial burst pressure.	1/63 = 0.016	None of the circ indications found to date was sufficiently deep (>80% avg. depth) to affect axial burst pressure.
Conditional probability that deep intersecting circ cuts axial at the end of the deeper section of the axial crack in order to significantly affect the axial crack burst pressure	≈0.1	Estimated value. Circ must cut axial near edge of burst effective length for a significant burst reduction. Shallow tails of axial ind. reduce likelihood of circ interaction affecting axial burst pressure.
Estimated probability per axial indication of a mixed mode burst pressure reduction. **Assumes free span indications at SLB conditions.**	$\approx 2 \times 10^{-7}$	Negligible probability of a mixed mode effect on burst pressure.
Probability that TSPs will displace in a SLB event given dented TSP intersections	< 0.001	Analyses show that forces required to displace the TSP at a dent are much higher than SLB loads on the TSP.
Best estimate probability of a mixed mode burst pressure reduction per axial indication	$\approx 2 \times 10^{-10}$	
Estimated probability per cycle of a mixed mode burst pressure reduction	$\approx 8 \times 10^{-5}$ without locked TSPs to $\approx 8 \times 10^{-8}$ with locked TSPs	Negligible probability per cycle of a mixed mode burst pressure reduction conservatively assuming 400 axial PWSCC indications are left in service.

Figure 7-1. Preparation for Outage: Establish Operating Parameters, Growth Rates and Inspection Plan

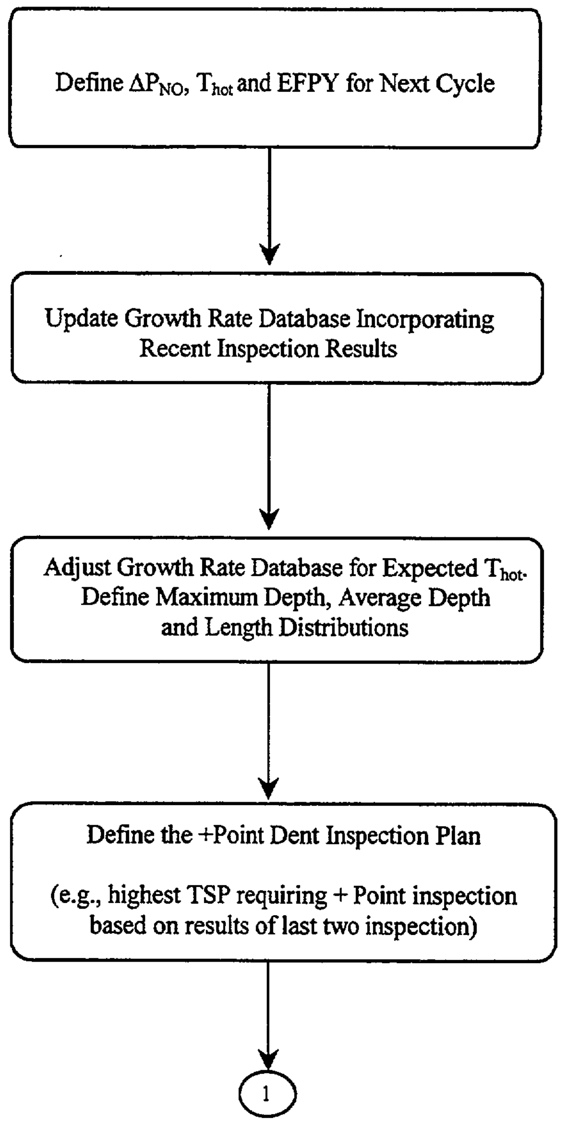

Figure 7-2. ARC Implementation: Inspection and Evaluations for Exclusion Zones and Maximum Depth Outside the TSP

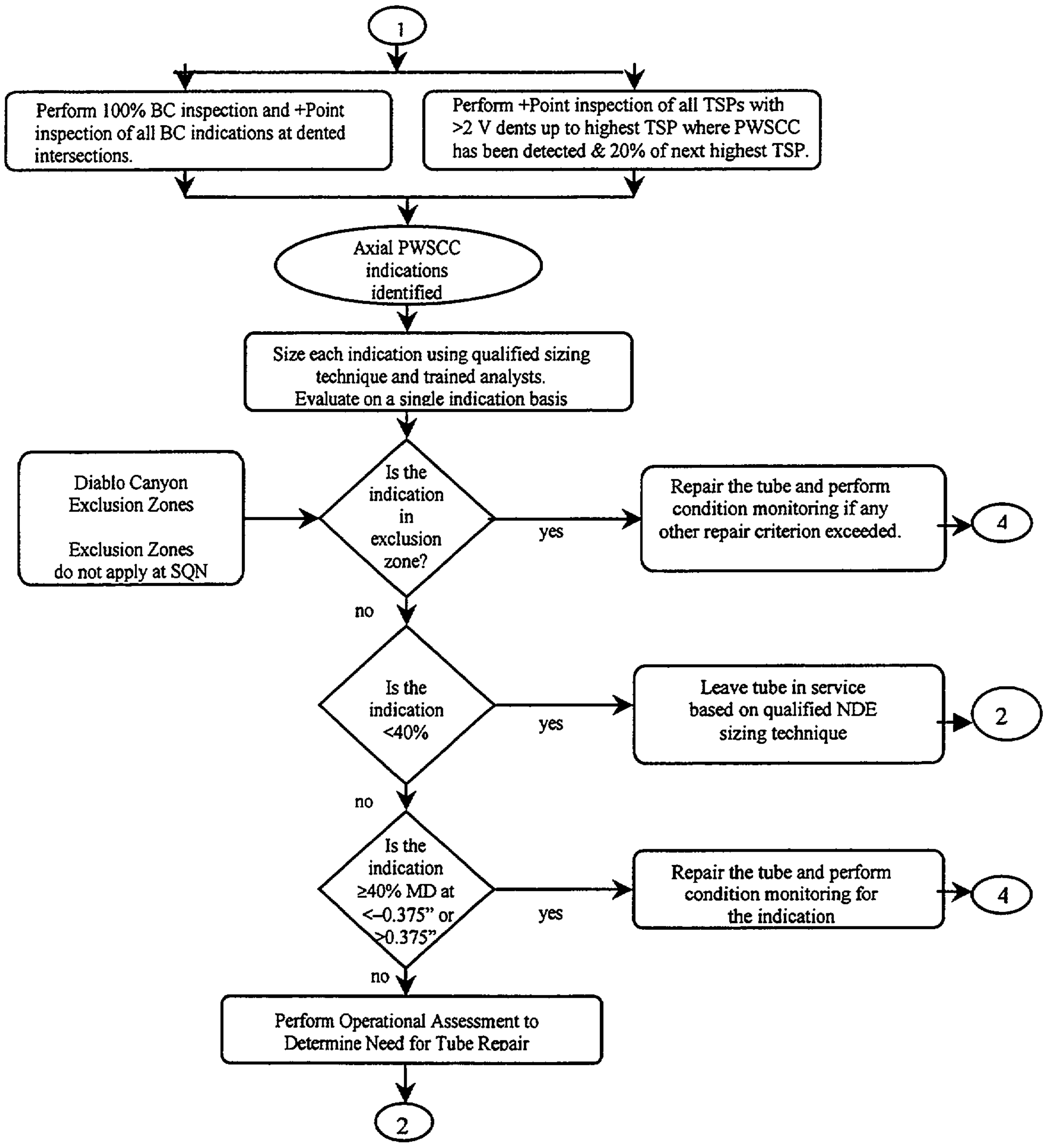

Figure 7-3. Burst Pressure Operational Assessment Repair Decision

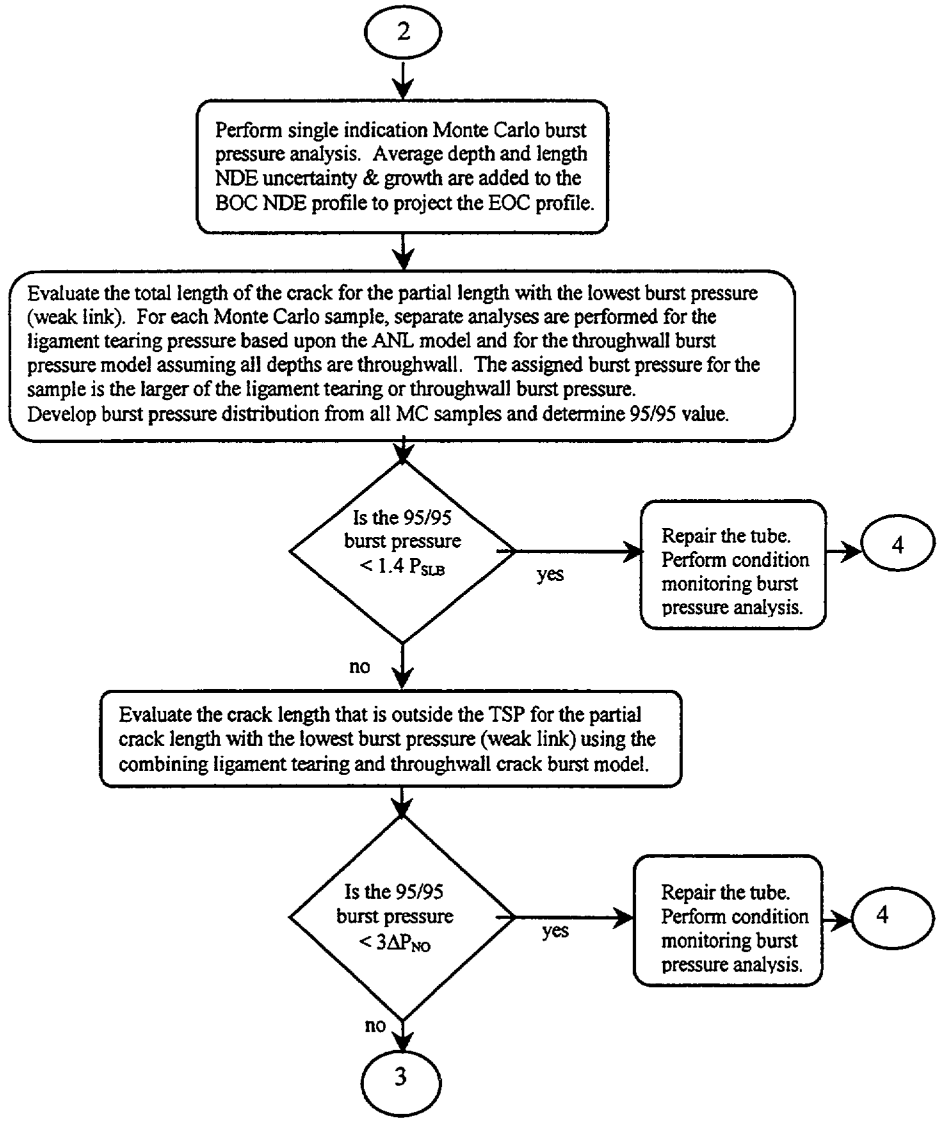

Figure 7-4. SLB Leak Rate Operational Assessment. Repair Decision

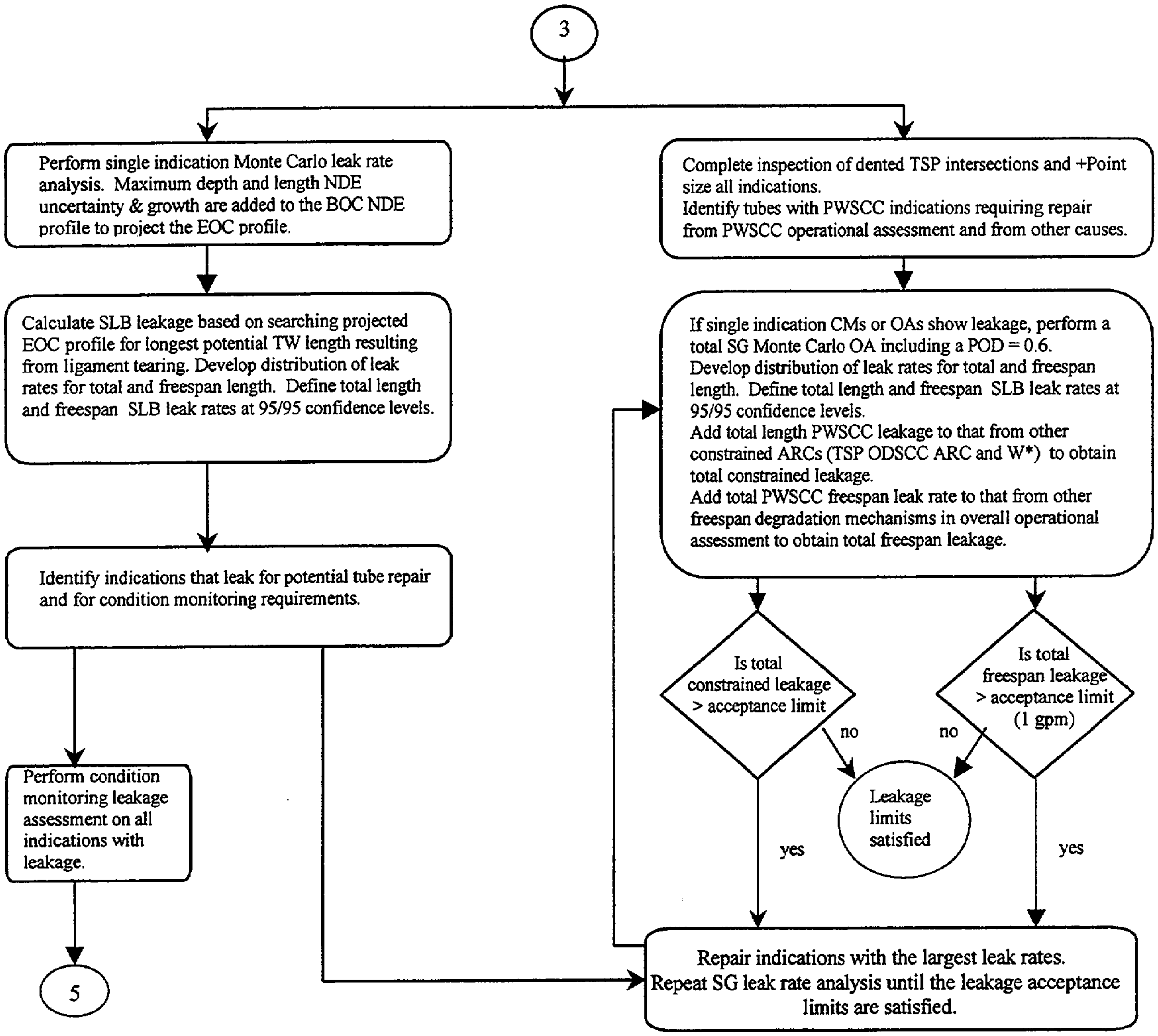

Figure 7-5. Condition Monitoring Burst Pressure Assessment
(only required for indications taken out of service)

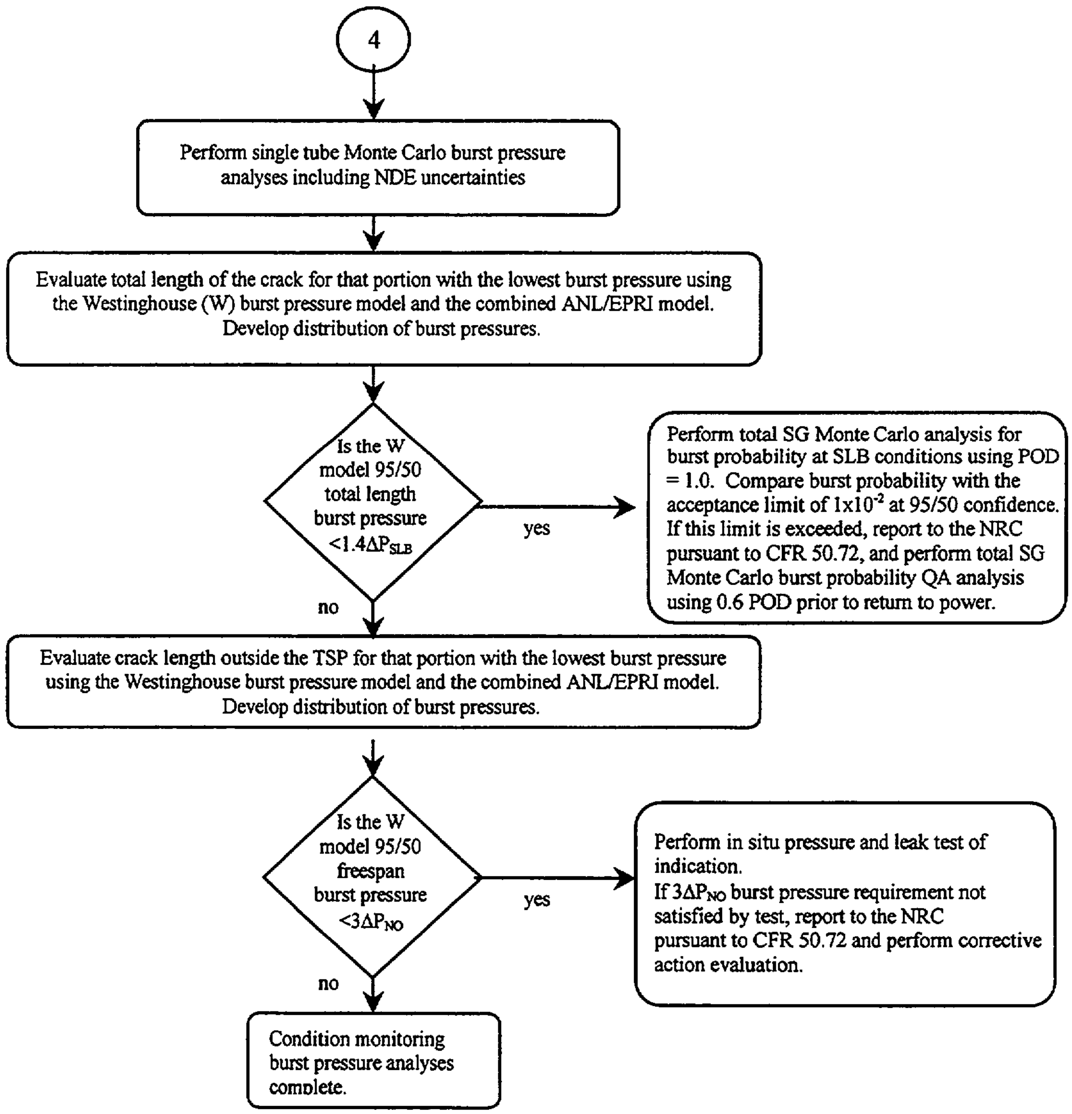

Figure 7-6. Condition Monitoring SLB Leakage Assessment

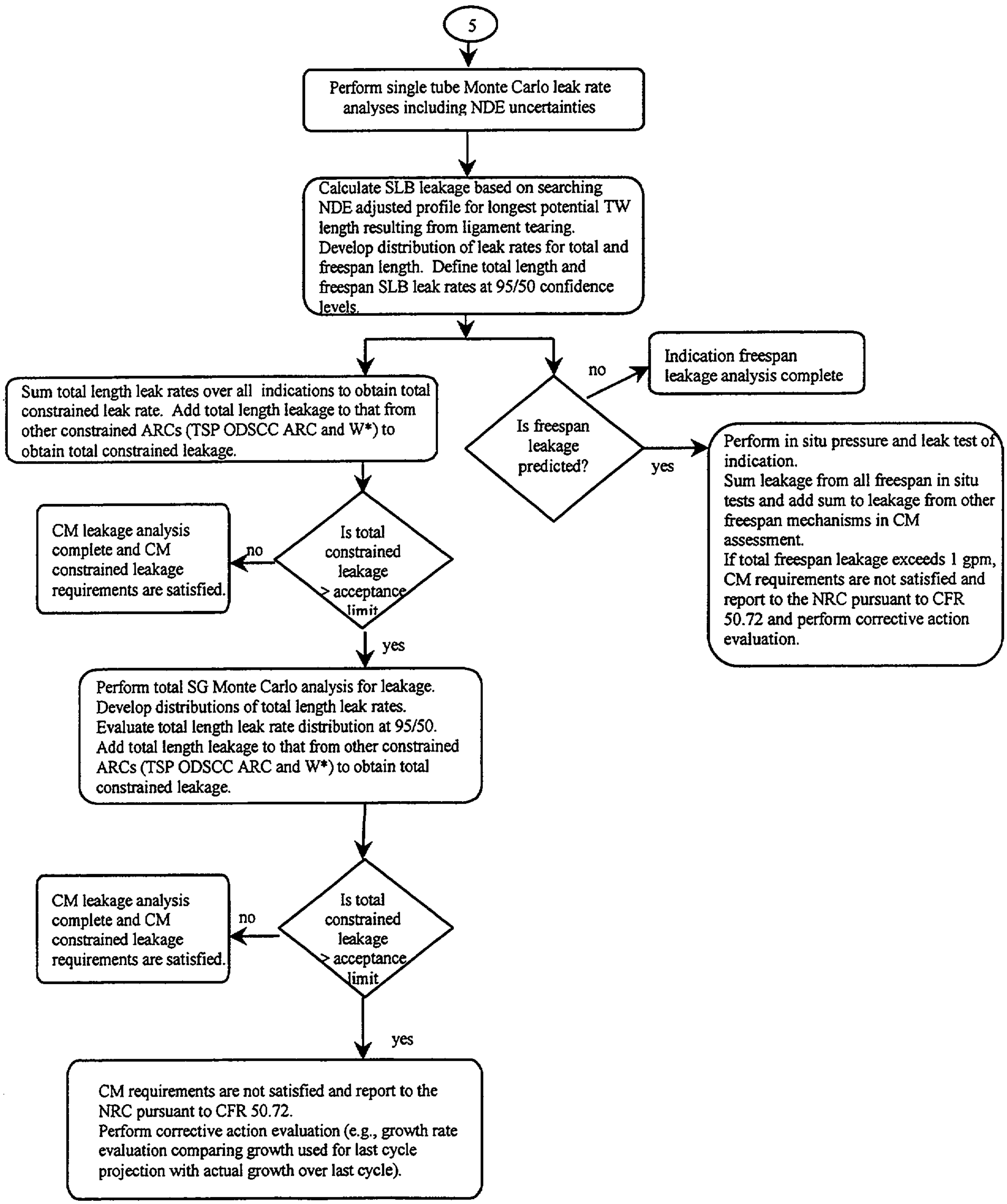

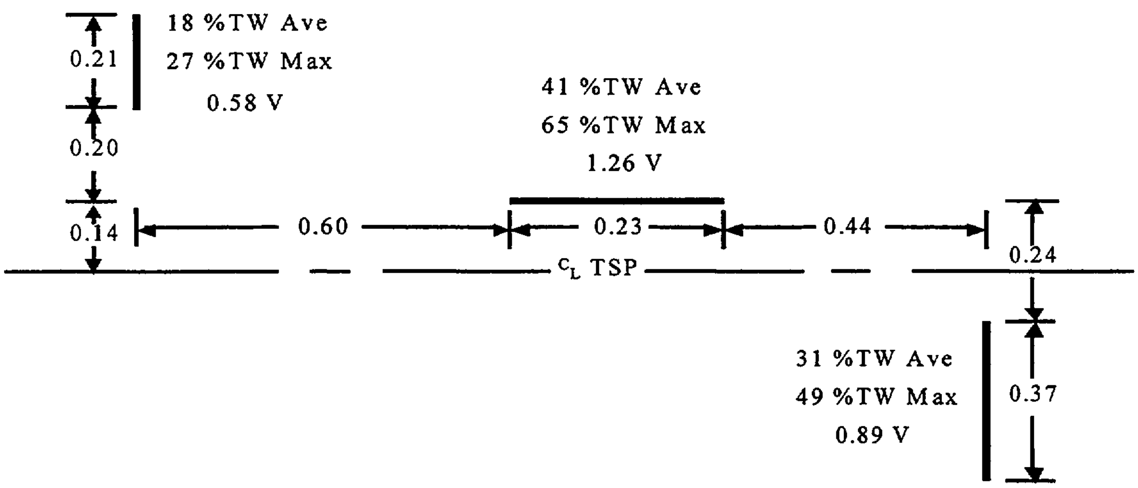

Figure 7-7. Geometry of Combined Axial and Circumferential Cracks Detected at 2R7, SG 22, R12C25 at 01H TSP Intersection

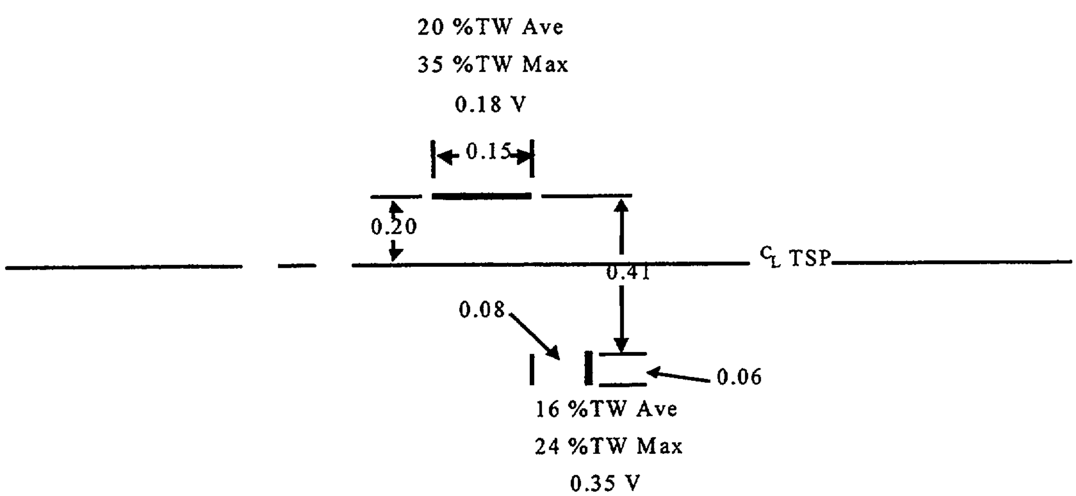

Figure 7-8. Geometry of Combined Axial and Circumferential Cracks Detected at 2R9, SG 22, R22C46 at 01H TSP Intersection

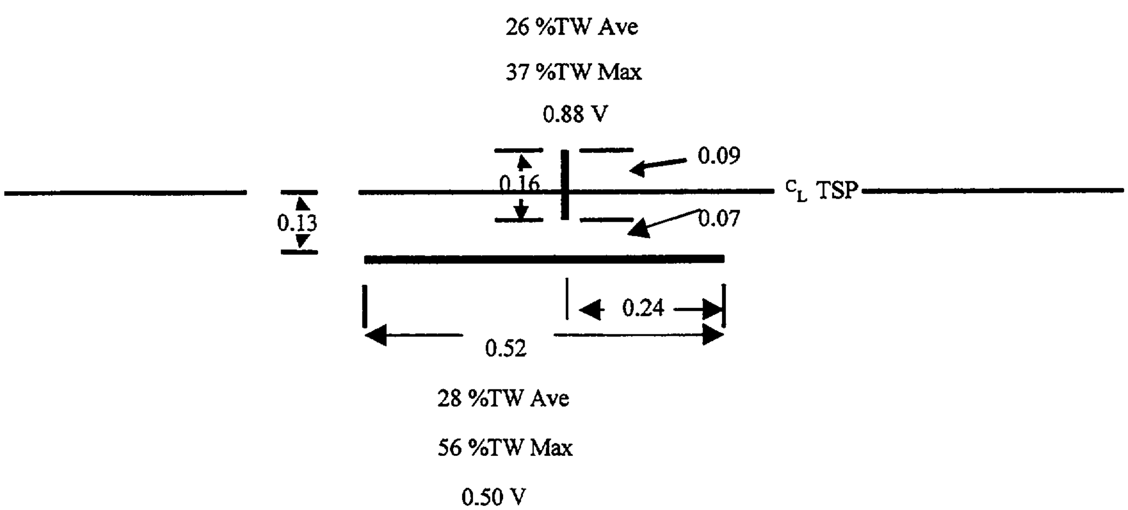

Figure 7-9. Geometry of Combined Axial and Circumferential Cracks Detected at 1R9, SG 12, R21C33 at 03H TSP Intersection

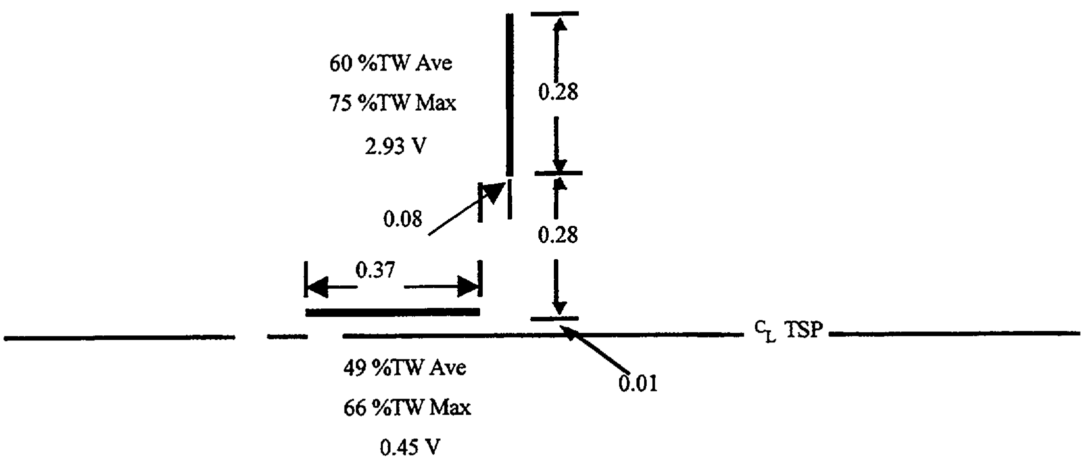

Figure 7-10. Geometry of Combined Axial and Circumferential Cracks Detected at 2R7, SG 22, R14C12 at 01H TSP Intersection

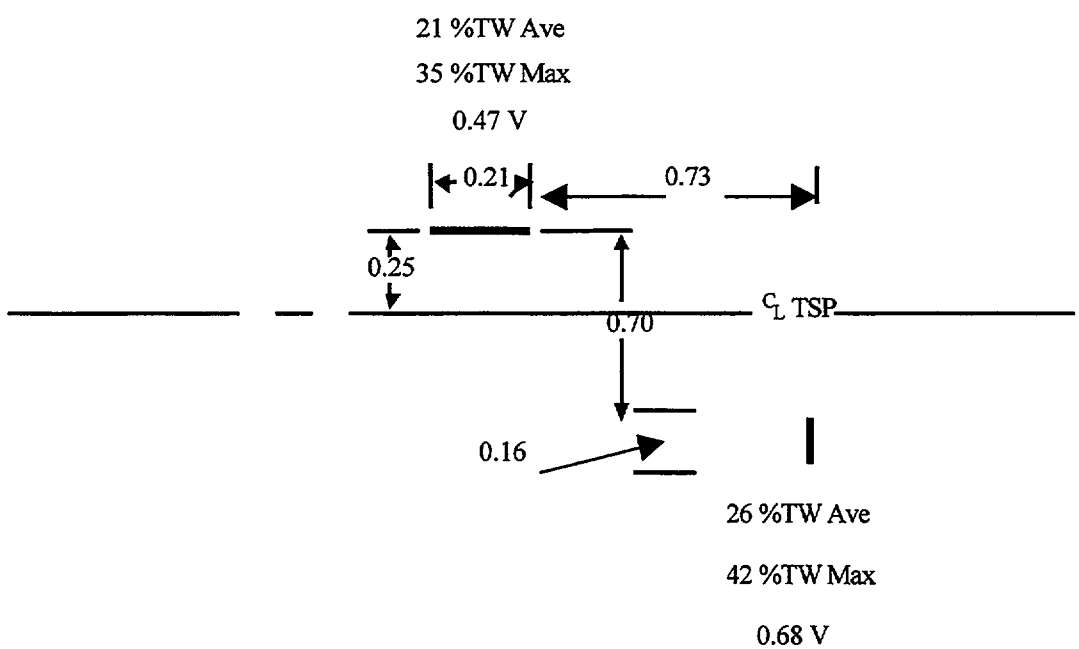

Figure 7-11. Geometry of Combined Axial and Circumferential Cracks Detected at 2R10, SG 22, R11C19 at 01H TSP Intersection

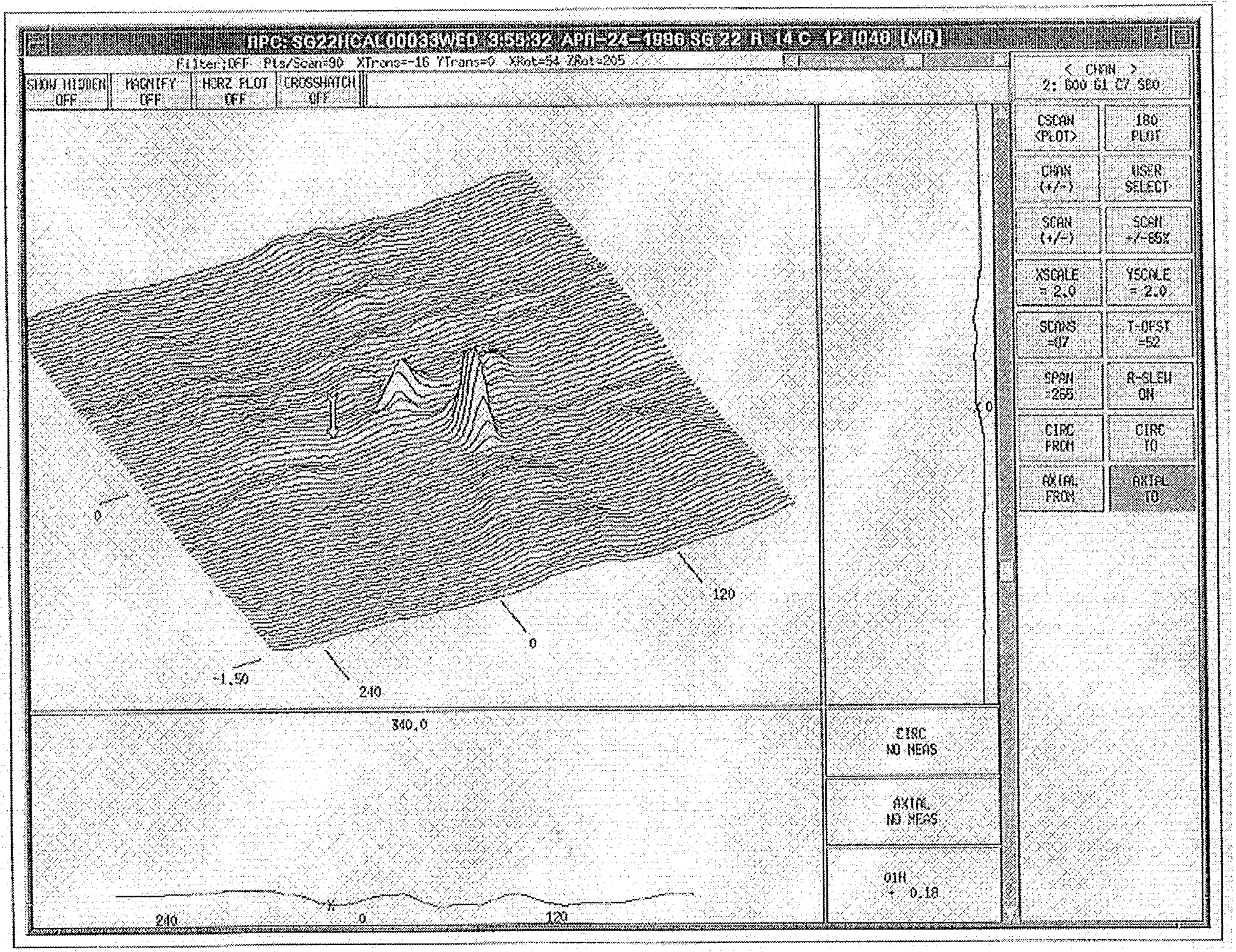

Figure 7-12
C-scan Projection for SG22 R14C12 at 1H TSP Intersection

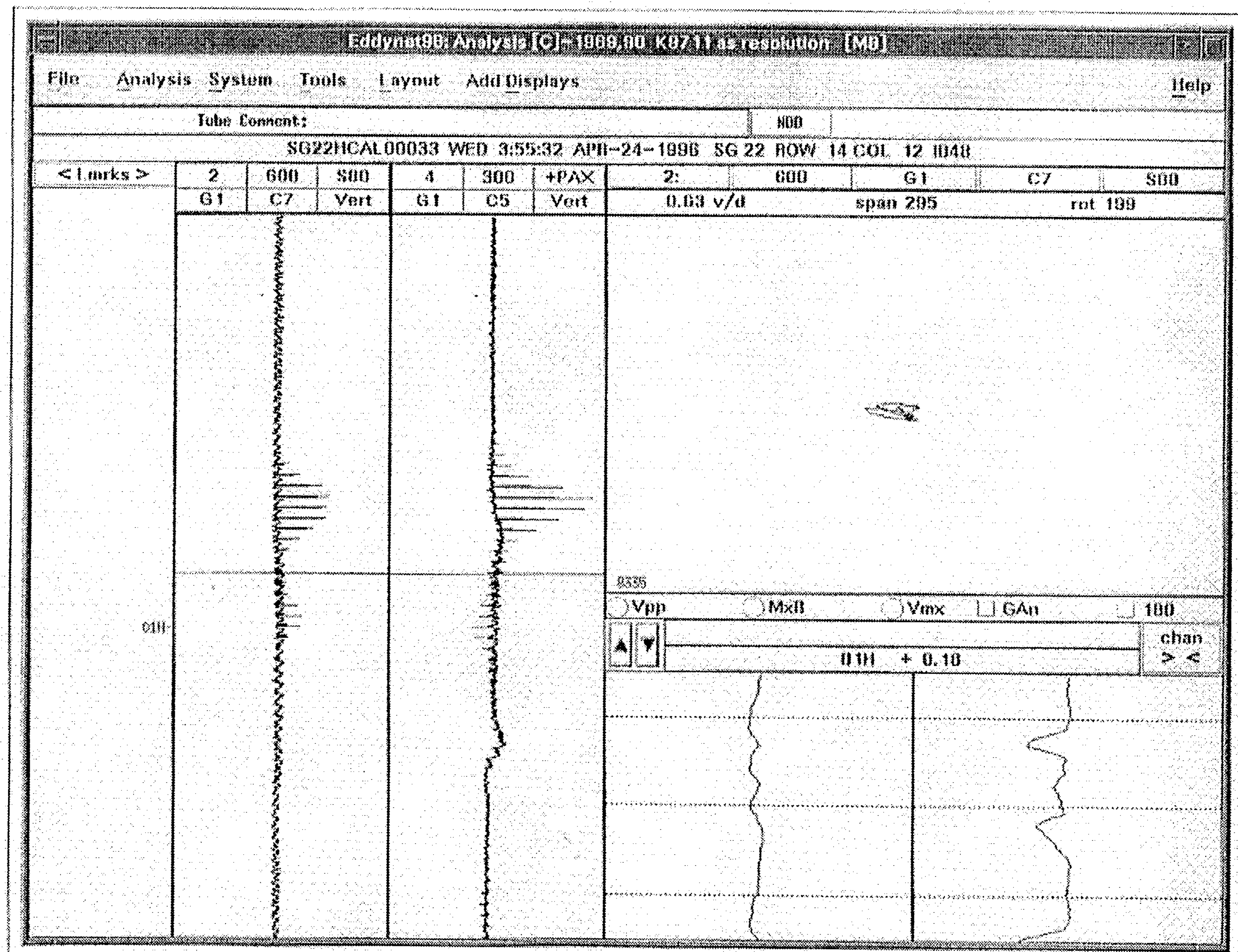

Figure 7-13
Lissajous Figure Display for SG22 R14C12 at 1H TSP Intersection

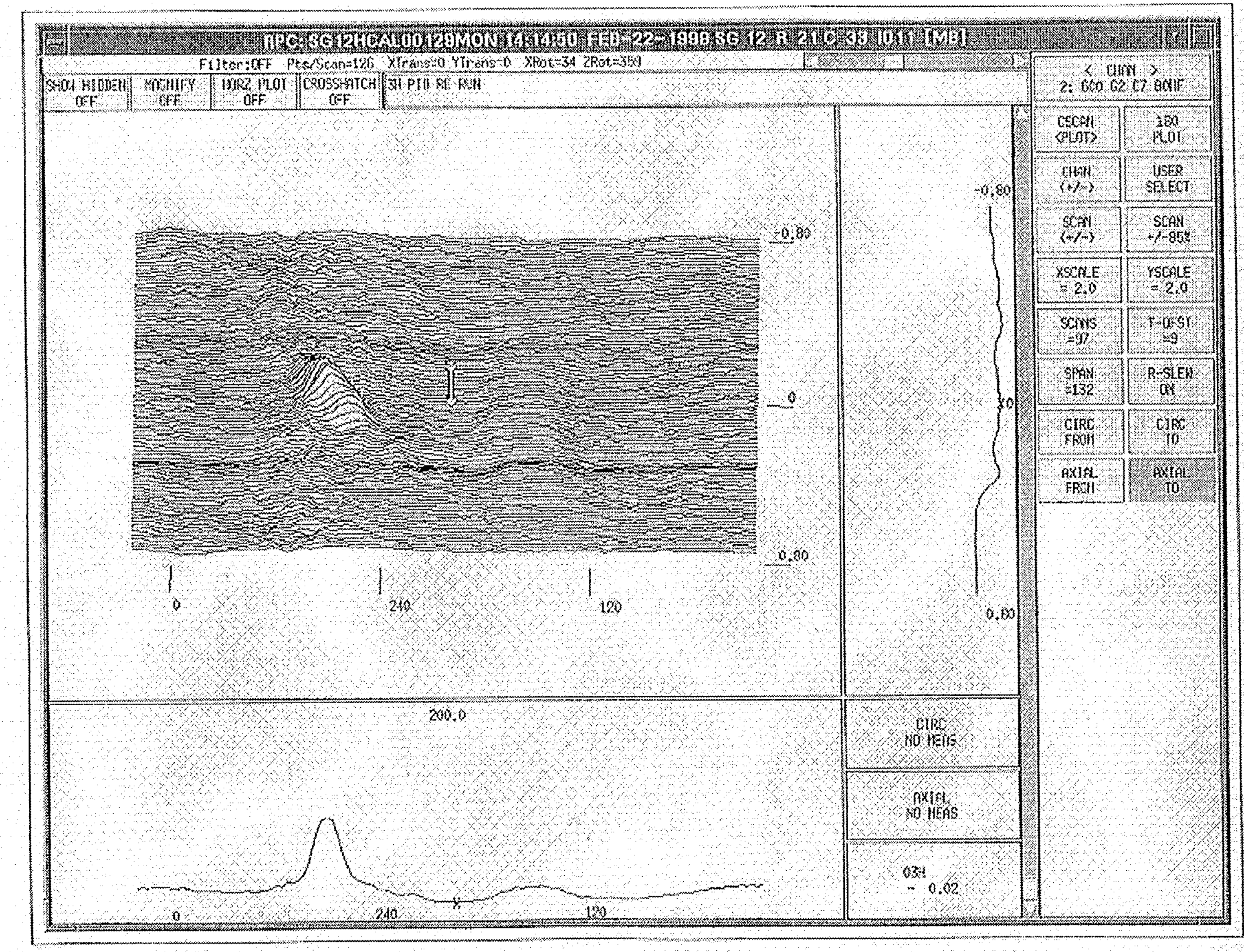

Figure 7-14
C-scan Projection for SG22 R21C33 at 3H TSP Intersection

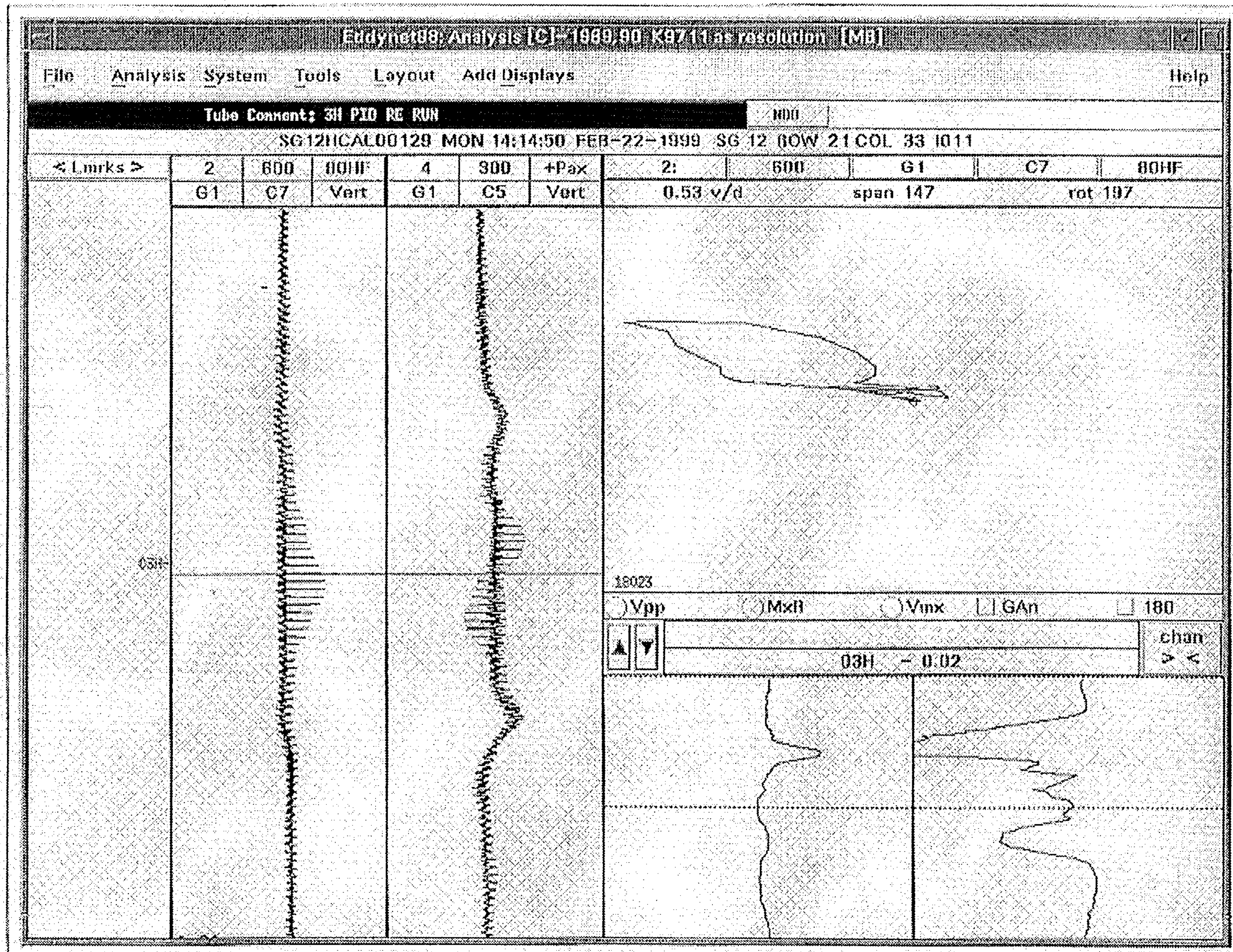

Figure 7-15
Lissajous Figure Display for SG22 R21C33 at 3H TSP Intersection

8.0 REFERENCES

8-1. SG-99-01-004, "NDE Qualification of Bobbin Detection and + Point Detection/Sizing for Axial PWSCC at Dented TSP Intersections", Westinghouse Electric Company, February 1999.

8-2. NRC/NEI Meeting of July 6, 2000, SG Burst Pressure Testing

8-3. EPRI Report, TR-107569-V1R5, "PWR Steam Generator Examination Guidelines: Revision 5 Volume 1: Requirements", September 1997.

8-4. SG-97-007, "Qualification of Rotating Coil Depth Sizing for Axial PWSCC at Dented TSP Intersections," Westinghouse Electric Corporation, December 1997.

8-5. NEI 97-06, "Steam Generator Program Guidelines," Nuclear Energy Institute, December 1997.

8-6. Draft Regulatory Guide 1.121, "Bases for Plugging Degraded PWR Steam Generator Tubes," September 1981.

8-7. Draft DG-1074, "Draft Regulatory Guide DG-1074 Steam Generator Tube Integrity", March 1998.

8-8. PG&E letter DCL-98-025 dated February 25, 1998, in response to the NRC RAI dated December 2, 1997.

8-9. EPRI NP-7480-L, Volume 1, Revision 2, and Volume 2, Revision 1, "Steam Generator Tubing Outside Diameter Stress Corrosion Cracking at Tube Support Plates – Database for Alternate Repair Limits," EPRI (August 1996).

8-10. WCAP-14277, Revision 1, "SLB Leak Rate and Tube Burst Probability Analysis Methods for ODSCC at TSP Intersections," Westinghouse Electric Company (December 1996).

8-11. Kunin, B., "A New Type of Extreme Value Distributions," *Engineering Fracture Mechanics*, Vol. 58, Nos. 5-6, pp. 557-570 (1997).

8-12. Kunin, Boris I., "An Extension of the List of Extreme Value Distributions," Submitted to *Advances in Applied Probability* (August 1998).

8-13. SG-95-03-010, "Burst Pressure Correlation for Steam Generator Tubes with Throughwall Axial Cracks," Westinghouse Electric Corporation for the Electric Power Research Institute (February, 1995). *Also EPRI TR-105505 (October 1998).*

8-14. WCAP-7832A, "Evaluation of Steam Generator Tube, Tubesheet, and Divider Plate Under Combined LOCA Plus SSE Conditions", April 1978 (Westinghouse Proprietary).

8-15. Cochet, B., and Flesch, B., "Crack Stability Criteria in Steam Generator Tubes," Transaction of the 9th International Conference on Structural Mechanics in Reactor Technology, Volume D, the American Association for Structural Mechanics in Reactor Technology, pp. 413-419 (1987).

8-16. Flesch, B., and Cochet, B., "Leak-Before-Break in Steam Generator Tubes," International Journal of Pressure Vessels and Piping, Vol. 43, pp. 165-179 (1990).

8-17. EPRI NP-4690-SR, "Evaluation of Flaws in Austenitic Steel Piping," Electric Power Research Institute, Palo Alto, CA (July 1986). Also in The Journal of Pressure Vessel Technology, Transactions of the ASME, Vol. 108 (August 1986).

8-18. BMI-1908, "Investigation of the Initiation and Extent of Ductile Pipe Rupture," Eiber, R. J., Maxey, W. A., Duffy, A. R., and Atterbury, T. J., Battelle Columbus Laboratories (June 1971).

8-19. EPRI Report NP-6864-L-Rev. 2, "PWR Steam Generator Tube Repair Limits: Technical Support Document for Expansion Zone PWSCC in Roll Transitions – Rev. 2", Draft Report, August 1993.

8-20. Streeter, "Fluid Mechanics," McGraw Hill, 1958.

8-21. ARL 64-174, "The Stresses in a Cylindrical Shell Containing an Axial Crack," E. Folias, Aerospace Research Laboratories (1964).

8-22. Henry, R. E., "The Two-phase Critical Discharge of Initially Saturated or Subcooled Liquid," Nuclear Science and Engineering, 41,336-342 (1970).

8-23. Henry, R. E., "The Two Phase Critical Flow of One-Component Mixtures in Nozzles, Orifices and Short Tubes," Journal of Heat Transfer, May 1971.

8-24. V. E. Schrock, et. al., "A Computational Model for Critical Flow through Intergranular Stress Corrosion Cracks, NUREG/CR-5133, November 1988.

8-25. Tada, Paris, & Irwin, The Stress Analysis for Cracks Handbook, Paris Productions and Del Research Corp., 1985.

8-26. J. A. Begley & J. L. Houtman, Inconel Alloy 600 Tubing Material Burst and Strength Properties, WCAP-12522, January 1990.

8-27. Erdogan, F., "Ductile Failure Theories for Pressurized Pipes and Containers," International Journal of Pressure Vessels & Piping, Vol. 4 (1976).

8-28. Majumdar, Saurin, "Predictions of Structural Integrity of Steam Generator Tubes Under Normal Operating, Accident, and Severe Accident Conditions," 24th Water Reactor Safety Meeting, October 21-26, 1996, Bethesda, MD (September 1996).

8-29. PG&E Letter DCL-97-034 to USNRC, "License Amendment Request 97-03, Voltage Based Alternate Steam Generator Tube Repair Limit for Outside Diameter Stress Corrosion Cracking at Tube Support Plate Intersections" (February 26, 1997).

8-30. Personal communications on the *ANL Ligament Tearing Model*, W. Shack, Argonne National Laboratory, and R. Keating, Westinghouse (February 15, 2000).

8-31. EPRI TR-109136, "Crack Growth and Microstructural Characterization of Nickel Alloy PWR Vessel Head Penetration Materials", EPRI, Palo Alto, CA

8-32. EPRI TR-107621-R1, "Steam Generator Integrity Assessment Guidelines: Revision 1", Final Report, March 2000

8-33. WCAP-15579, "Burst Pressure Data for Steam Generator Tubes with Combined Axial and Circumferential Cracks", Westinghouse Proprietary Class 2, Westinghouse Electric Company LLC, August, 2000.

8-34. EPRI Report TR-107620-R1, Rev. 1, "Steam Generator In Situ Pressure Test Guidelines", EPRI Palo Alto CA, June, 1999.

8-35. EMECH-0738-SR-1, "Evaluation of Circumferential Cracking at TSP Intersections at Sequoyah Unit 1", E-Mech Technology Inc., Begley, J. A., Begley, C. J., and Peck, M. G., August 2000.

8-36. McMeeking, R. M., "Finite Deformation Analysis of Crack-Tip Opening in Elastic-Plastic Materials and Implications for Fracture", Journal Mech. Phys Solids, 1977, Vol. 25, page 357, Pergamon Press, Great Britain

8-37. EPRI Report TR-107197-P1, "Depth Based Structural Analysis Methods for SG Circumferential Indications", November, 1997

8-38 WCAP-15573, Revision 0, "Depth Based SG Tube Repair Criteria for Axial PWSCC at Dented TSP Intersections - Alternate Burst Correlation", Westinghouse Electric Company LLC, February 2001

8-39 TVA Letter to NRC, Docket No. 50-327, "Sequoyah Nuclear Plant (SQN) - Special Report on Steam Generator (SG) Activities Completed During the Unit 1 Cycle 10 (U1C10) Refueling Outage", October 6, 2000

8-40 Framatome ANP Reports 51-5009352-01 Volume 1 and 51-5011201-00 2, "Tube Destructive Examination Results for Flaw Extents (Volume-1)", "Tube E-Slv Destructive Examination Results (Volume-2)", September, 2001

8-41 ABB CE Report A-PENG-TR-009, Rev. 0, "Circumferential Cracks for Entergy", October 1995

APPENDIX A

NDE Performance Test – Bobbin and + Point Detection Results

Table A-1: Bobbin Flaws with Destructive Exam Data for NDE Performance Test

Table A-2: +Point Flaws with Destructive Exam Data and NDE Performance Test +Point Results

Table A-3: False Call Rates for Detection of PWSCC in Dented TSP Intersections

Table A-4: Bobbin False Call Rates (Dents < 5 Volts)

Table A-5: +Point False Call Rates for NDD Intersections (All Dents)

Table A-1

Bobbin Flaws with Destructive Exam Data for NDE Performance Test

LAB SAMPLES					NEW	New	New		Max.	Resolution 1			Resolution 2			Reso	Analyst A1	Analys B1	Analyst A2	Analyst B2
Optical	Reel	Row	Column	Location	REEL	Row	Column	Indication	Depth	Dent V	Flaw V	Call	Dent V	Flaw V	Call	POD	Call	Call	Call	Call
ECLab	2	1	9	2H	459	1	7	DDI	84%		4.29	DSI		4.29	DSI	1.00	DSI	DSI	DSI	DSI
LAB	556	D-0	9	1H	1126	12	10	DDI	100%		12.82	DSI		12.82	DSI	1.00	DSI	DSI	DSI	DSI
ECLab	14	1	12	3H	296	9	13	DDI	16%	1.4		DNT	1.23	0.17	DDI	0.50	DDI	DNT	DNT	DDI
ECLab	2	1	11	4H	227	17	13	DDI	94%		2.3	DSI	2.49	2.44*	DDI	1.00	DSI	DSI	DSI	DSI
ECLab	2	1	2	3H	1068	5	16	DDI	22%	2.16	0.37	DDI	2.16	0.38	DDI	1.00	DDI	DNT	DNT	DDI
ECLab	2	1	6	5H	780	33	16	DDI	78%	1.06	0.7	DDI	1.05	0.73	DDI	1.00	DDI	DDI	DDI	DDI
ECLab	323	1	4	4H	558	17	19	DDI	15%	6.29		DNT	6.29	0.17	DDI	0.50	DDI	DDI	DNT	DDI
LAB	556	D-0	8	1H	1123	18	22	DDI	100%		1.35	DSI		8.25*	DSI	1.00	DSI	DSI	DSI	DSI
ECLab	2	1	9	3H	86	25	28	DDI	85%		2.32	DSI		1.91*	DSI	1.00	DSI	DSI	DSI	DDI
ECLab	2	1	1	4H	113	29	28	DDI	54%	1.84	2.53	DDI	1.84	2.53*	DDI	1.00	DDI	NDD	DSI	DDI
PGE-SAG	225	12	32	1H	936	37	28	DDI	89%	1.21	3.58*	DDI	1.21	3.58	DDI	1.00	DDI	DSI	DDI	DSI
ECLab	2	1	2	4H	750	33	31	DDI	48%	1.3		DNT	1.3	0.21	DDI	0.50	DDI	DNT	DDI	DDI
ECLab	2	1	6	1H	949	5	34	DDI	84%	1.05	1.68	DDI		1.68*	DSI	1.00	DDI	DDI	DSI	DSI
ECLab	14	1	7	1H	839	5	37	DDI	30%	4.55	0.66	DDI	4.24	0.66	DDI	1.00	DDI	DDI	DDI	DDI
ECLab	14	1	7	3H	65	29	37	DDI	34%	3.7	0.89	DDI	3.7	0.78	DDI	1.00	DDI	DDI	DDI	DDI
ECLab	33	1	3	3H	436	5	40	DDI	29%	6.17		DNT	6.17		DNT	0.00	DDI	DDI	DNT	DNT
ECLab	2	1	8	2H	778	21	40	DDI	46%	0.93	0.88	DDI	0.92	0.87	DDI	1.00	DDI	DDI	DSI	DDI
ECLab	2	1	6	3H	487	1	43	DDI	67%		0.8	DSI		0.79	DSI	1.00	DSI	DSI	DSI	DDI
ECLab	2	1	10	4H	841	9	46	DDI	82%	0.89	1.5*	DDI	1.01	0.92*	DDI	1.00	DDI	DDI	DDI	DSI
ECLab	14	1	12	2H	241	13	46	DDI	23%	1.54		DNT	1.54		DNT	0.00	DDI	DNT	DNT	DDI
ECLab	2	1	10	3H	107	25	46	DDI	96%	0.74	1.24	DDI	0.74	1.44*	DDI	1.00	DDI	DDI	DSI	DDI
ECLab	2	1	9	4H	288	37	46	DDI	70%	1.2	1.49*	DDI	1.2	1.47*	DDI	1.00	DDI	DDI	DSI	DDI
LAB	556	D-0	7	1H	239	35	47	DDI	100%		11.65	DSI		11.65	DSI	1.00	DSI	DSI	DSI	DSI
LAB	556	D-0	10	1H	1115	9	51	DDI	100%		2.35	DSI		3.58*	DSI	1.00	NDD	DSI	DSI	DSI
ECLab	14	1	12	4H	694	29	52	DDI	26%	1.18		DNT	1.18	0.12	DDI	0.50	DDI	DNT	DDI	NDD
ECLab	2	1	9	1H	758	45	52	DDI	39%		0.63*	DSI		1.74*	DSI	1.00	DDI	DDI	DDI	DDI
ECLab	2	1	11	2H	293	21	55	DDI	97%	0.78	2.15*	DDI	0.78	2.01*	DDI	1.00	DDI	DDI	DSI	DDI
ECLab	2	1	6	2H	394	29	58	DDI	74%	1.84	2.05*	DDI	1.84	2.05*	DDI	1.00	DDI	DDI	DSI	DDI
ECLab	2	1	2	5H	47	45	58	DDI	36%	2.88	1.61	DDI	2.88	1.66	DDI	1.00	DDI	DDI	DNT	DDI
ECLab	2	1	2	1H	6	41	61	DDI	33%	3.83	2.39	DDI	3.63	2.39	DDI	1.00	DDI	DDI	DNT	DDI
ECLab	2	1	8	1H	812	5	64	DDI	52%		0.91	DSI		0.91	DSI	1.00	DSI	DSI	DSI	DSI
ECLab	2	1	11	3H	724	21	67	DDI	89%		2.79*	DSI		2.96*	DSI	1.00	DSI	DSI	DSI	DSI
ECLab	2	1	6	4H	748	13	70	DDI	64%	1.12	0.68*	DDI	1.12	0.58*	DDI	1.00	DDI	DDI	DDI	DDI
PGE-SAG	225	21	43	1H	509	21	70	DDI	91%	3.89	3.83	DDI	3.84	3.69*	DDI	1.00	DDI	DDI	DDI	DDI
ECLab	33	1	3	4H	889	25	70	DDI	8%	5.22		DNT	5.22		DNT	0.00	DNT	DDI	DNT	DNT
ECLab	2	1	8	3H	1011	33	70	DDI	44%		0.72	DSI		0.72	DSI	1.00	DDI	DSI	DSI	DDI
ECLab	223	1	5	1H	583	1	76	DDI	40%	2.28	0.6	DDI	2.28	0.6	DDI	1.00	DDI	DNT	DDI	DDI
ECLab	2	1	9	5H	1086	21	76	DDI	75%	0.93	1.15	DDI		1.2	DSI	1.00	DDI	DSI	DSI	DSI
PGE-SAG	225	10	22	2H	570	37	76	DDI	23%	2.39	0.52	DDI	2.39	0.33	DDI	1.00	DDI	DDI	DDI	DDI
ECLab	14	1	13	3H	200	33	79	DDI	37%	0.93	0.4	DDI	0.68	0.28	DDI	1.00	DDI	DNT	DDI	DDI
LAB	556	D-0	11	1H	1118	20	80	DDI	100%		14.42	DSI		14.42	DSI	1.00	DSI	DSI	DSI	DSI
ECLab	2	1	1	3H	1024	1	82	DDI	48%	2.78	3.22*	DDI	2.78	2.35*	DDI	1.00	DDI	DDI	DDI	DDI

POD:	All Flaws	N=42			0.73			0.84		0.87	0.7	0.7	0.84
	>/= 30%	N=39			0.8			0.86		0.9	0.71	0.77	0.86
	>/=34%	N=32			0.88			0.93		0.88	0.76	0.88	0.93

Table A-2

Bobbin Flaws with Destructive Exam Data for NDE Performance Test																	
LAB SAMPLES					NEW	New	New		Maximum	Resolution R1		Resolution R2		Analyst A1	Analyst B1	Analyst A2	Analyst B2
Optical	Reel	Row	Column	Location	REEL	Row	Column	Indication	Depth	Flaw V	Call	Flaw V	Call	Flaw V	Flaw V	Flaw V	Flaw V
ECLab	1	1	10	3H-1	416	9	7	MAI	96.2%	4.6	SAI	20.57	SAI	1.58	4.6	20.57	25.7
ECLab	1	1	10	3H-2	416	9	7	MAI	38.0%	1.31	SAI	7.77	SAI	0.38	1.31	7.77	7.24
ECLab	9	1	12	4H	417	13	7	SAI	26.3%	0.47	SAI	0.44	SAI	0.47	0.47	0.44	0.42
ECLab	1	1	11	4H-1	806	21	13	MAI	95.3%	3.28	SAI	13.21	SAI	3.28	3.28	5.75	7.36
ECLab	1	1	11	4H-2	806	21	13	MAI	44.0%	0.6	SAI	2.16	SAI	0.6	0.66	1.66	1.68
PGE	127	10	22	2H	709	23	15	SAI	23.2%	0.6	SAI	0.56	SAI	0.6	0.6	0.56	0.56
ECLab	1	1	11	3H	972	13	16	MAI	89.3%	3.17	SAI	3.09	MAI	3.17	3.09	3.09	1.12
ECLab	1	1	6	3H	776	29	16	SAI	67.3%	1.93	SAI	1.91	SAI	1.93	1.91	1.91	6.2
LAB	506	D-0	11	1H-1	1121	5	18	MAI	100.0%	7.66	SAI	7.21	SAI	7.66	7.66	7.21	7.65
LAB	506	D-0	11	1H-2	1121	5	18	MAI	90.3%	5.37	SAI	5.37	SAI	5.37	5.37	5.37	5.24
ECLab	1	1	9	2H-1	1109	9	19	MAI	84.1%	3.87	SAI	3.81	SAI	3.87	3.87	3.81	7.86
ECLab	1	1	9	2H-2	1109	9	19	MAI	46.3%	0.67	SAI	0.66	SAI	0.67	0.65	0.66	1.44
ECLab	1	1	2	5H	1110	6	24	SAI	35.5%	0.69	SAI	0.69	SAI		0.69	0.69	0.58
ECLab	1	1	2	4H	1101	21	28	SAI	47.6%	1.26	SAI	1.22	SAI	1.26	1.26	1.22	3.13
LAB	506	D-0	8	1H-1	1117	39	28	MAI	99.6%	7.8	SAI	6.64	SAI	7.8	7.4	6.64	7.41
LAB	506	D-0	8	1H-2	1117	39	28	MAI	99.7%	4.74	SAI	5.37	SAI	4.74	6.04	5.37	4.74
ECLab	1	1	9	5H-1	420	6	31	MAI	74.6%	5.37	SAI	8.31	SAI	5.37	5.37	8.31	5.37
ECLab	1	1	9	5H-2	420	6	31	MAI	26.7%		NDD	1.31	SAI			1.31	
ECLab	1	1	9	3H-1	837	21	31	MAI	84.6%	2.44	SAI	2.44	SAI	2.44	2.44	2.44	4.95
ECLab	1	1	9	3H-2	837	21	31	MAI	54.1%	0.93	SAI	0.81	SAI	0.93	0.93	0.81	1.67
ECLab	1	1	1	3H	393	37	31	SAI	47.9%	7.04	SAI	2.42	SAI	2.42	7.04	2.42	2.42
ECLab	9	1	12	2H	1043	13	34	SAI	34.0%	0.42	SAI	0.4	SAI	0.42	0.42	0.4	
ECLab	9	1	12	3H	929	29	34	SAI	16.0%		NDD	1.69	SAI			1.69	
ECLab	9	1	7	3H	898	33	34	SAI	34.4%	0.89	SAI	0.85	SAI		0.89	0.85	0.85
ECLab	9	1	7	1H	1078	9	37	SAI	77.9%	1.29	SAI	1.14	SAI	0.81	1.29	1.14	1.14
PGE	127	21	43	1H-1	947	19	38	MAI	90.5%	3.45	SAI	3.48	SAI	3.45	3.43	3.48	3.47
PGE	127	21	43	1H-2	947	19	38	MAI	45.5%	1.4	SAI	1.13	SAI	1.4	1.44	1.13	1.31
ECLab	1	1	6	1H	962	25	40	SAI	83.7%	2.41	SAI	2.41	SAI	2.41	2.41	2.41	0.99
PGE	127	12	32	1H	418	43	40	SAI	88.9%	3.71	SAI	3.71	SAI	3.71	3.71	3.71	3.68
ECLab	17	1	5	1H	545	5	43	SAI	30.0%		NDD	0.48	SAI			0.48	0.46
ECLab	1	1	1	4H	761	17	43	SAI	54.3%	2.14	SAI	2.14	SAI	2.14	2.15	2.14	1.11
LAB	506	D-0	10	1H-1	1114	30	45	MAI	100.0%	6.65	SAI	6.27	SAI	6.44	6.55	6.27	6.27
LAB	506	D-0	10	1H-2	1114	30	45	MAI	90.9%	4.93	SAI	5.08	SAI	5.08	4.93	5.08	4.61
ECLab	1	1	6	5H	301	25	52	SAI	77.9%	1.24	SAI	1.24	SAI	1.24	0.82	1.24	1.27
ECLab	17	1	3	3H	814	37	52	SAI	29.1%	0.81	SAI		NDD		0.81	1.00	
ECLab	1	1	9	4H-1	979	13	55	MAI	70.2%	1.69	SAI	1.61	SAI	1.69	1.69	1.61	3.79
ECLab	1	1	9	4H-2	979	13	55	MAI	23.1%		NDD		NDD				
ECLab	1	1	6	2H	581	17	58	SAI	73.7%	2.47	SAI	2.36	SAI	2.47	2.47	2.36	0.97
ECLab	17	1	3	4H	503	33	58	SAI	7.7%	0.4	SAI		NDD		0.4		
LAB	506	D-0	7	1H-1	1122	6	64	MAI	99.8%	6.73	SAI	6.73	SAI	6.73	6,73	6.73	6.32
LAB	506	D-0	7	1H-2	1122	6	64	MAI	89.7%	4.93	SAI	3.94	SAI	4.93	4.94	3.94	4.83
ECLab	1	1	8	3H	196	9	64	SAI	44.2%	1.4	SAI	1.36	SAI	1.4	0.77	1.36	1.25
ECLab	1	1	8	1H	207	41	64	SAI	52.2%	5.95	SAI	1.14	SAI	1.25	5.95	1.14	0.74
LAB	506	D-0	9	1H-1	362	2	66	MAI	99.5%	10.67	SAI	10.42	SAI	10.67	10.69	10.42	8.81
LAB	506	D-0	9	1H-2	362	2	66	MAI	99.4%	4.74	SAI	4.53	SAI	4.74	4.49	4.53	4.48
ECLab	1	1	2	3H	682	29	67	SAI	33.4%	0.47	SAI	2.82	SAI	0.47	0.47	2.82	0.38
ECLab	1	1	9	1H-1	773	5	73	SAI	38.8%	0.92	SAI	2.3	SAI	0.92	0.92	0.92	2.3
ECLab	1	1	9	1H-2	773	5	73	SAI	25.4%	0.4	SAI	0.7	SAI	0.39	0.4	0.37	0.7
ECLab	17	1	4	4H	275	21	73	SAI	15.0%	0.93	SAI	0.62	SAI		0.93	0.62	0.93
ECLab	1	1	6	4H	651	21	79	SAI	64.3%	1.46	SAI	1.42	SAI	1.46	1.46	1.42	0.86
ECLab	1	1	10	4H	1105	25	79	MAI	81.8%	1.41	SAI	1.37	SAI	1.41	1.41	1.37	4.39
ECLab	1	1	8	2H	233	1	85	SAI	45.8%	1.38	SAI	1.34	SAI	1.38	1.34	1.34	1.12
ECLab	9	1	13	3H	1026	13	85	SAI	37.3%	0.7	SAI	0.54	SAI	0.7	0.67	0.54	3.31
ECLab	1	1	2	1H	1027	21	85	SAI	33.4%	0.66	SAI	0.6	SAI		0.66	0.6	0.91
ECLab	1	1	11	2H-1	449	1	91	MAI	96.8%	3.09	SAI	6.33	SAI	3.09	3.09	2.88	6.33
ECLab	1	1	11	2H-2	449	1	91	MAI	32.8%		NDD		NDD			0.2	

Where Flaw V is blank, no flaw was reported; these represent "misses".

POD:	All (>7.7%)	N=56	0.84		0.86	0.71	0.84	0.9	0.79
	>/= 20%	N=53	0.85		0.87	0.76	0.83	0.92	0.85
	>/= 30%	N=47	0.89		0.91	0.81	0.86	0.95	0.89

Table A-3

False Call Rates for Detection of PWSCC in Dented TSP Intersections

Bobbin Probes: ETSS #96012
PlusPoint Probe: ETSS #96703

Probe	# NDDs	False Calls	False Call Rate
Bobbin (Dents < 5V)			
Team 1 Phase 1b	124	90	72.6%
Team 2 Phase 1b	124	113	91.1%
Bobbin (All Dents)			
Team 1 Phase 1b	150	100	66.7%
Team 2 Phase 1b	150	129	86.0%
+Point (All dents)			
Team 1	143	1	0.7%
Team 2	143	2	1.4%

Table A-4

Bobbin Flaws with Destructive Exam Data for NDE Performance Test														
	Old	Old	Old	Old	New	New	New		Team 1			Team 2		
Optical	Reel	Row	Col	Loc	REEL	Row	Col	Dent V	R1 Call	PRI-1	SEC-1	R2 Call	PRI-2	SEC-2
STCLab	212	0	7	4H	811	9	3	2.37	DDI	x	x	DDI	X	X
STCLab	202	0	6	2H	987	5	4	2.28	DDI	x	x	DDI	X	X
STCLab	202	0	4	1H	657	17	7	2.71		x	x	DDI	X	X
STCLab	202	0	4	2H	297	21	7	1.96			x	DDI	X	
STCLab	202	0	1	1H	139	5	10	3.27		x		DDI		X
STCLab	215	0	13	3H	291	13	10	1.41	DDI	x	x	DDI	X	X
STCLab	212	0	5	5H	115	5	12	1.96	DDI	x	x	DDI	X	X
STCLab	206	0	8	3H	1107	1	16	1.93	DDI	x	x	DDI	X	X
STCLab	215	0	13	2H	12	17	16	2.05	DDI	x	x	DDI		X
STCLab	212	0	1	3H	856	30	17	3.13		x	x	DDI	X	X
STCLab	212	0	3	4H	413	7	19	2.06		x		DDI		X
STCLab	202	0	6	4H	278	29	19	2.6	DDI	x	x	DDI	X	X
STCLab	212	0	3	3H	332	30	19	2.47		x		DDI		X
STCLab	206	0	10	5H	519	5	22	1.76	DDI	x	x	DDI	X	X
STCLab	206	0	8	2H	45	21	22	1.79	DDI	x	x	DDI	X	X
STCLab	206	0	8	4H	73	29	22	2.46	DDI	x	x	DDI	X	X
STCLab	206	0	10	3H	114	33	22	1.54	DDI	x	x	DDI	X	X
STCLab	206	0	11	3H	574	37	22	1.58	DDI	x	x	DDI	X	X
3	213	17	25	2H	777	5	23	3.62	DDI	x	x	DDI	X	X
STCLab	212	0	6	5H	28	26	24	2.36	DDI	x	x	DDI	X	X
STCLab	212	0	5	4H	989	32	24	3.1	DDI	x	x	DDI	X	X
STCLab	206	0	11	2H	652	9	25	1.77	DDI	x	x	DDI	X	X
STCLab	206	0	8	5H	993	17	25	2.01	DDI	x	x	DDI	X	X
STCLab	202	0	1	5H	938	37	25	2.58			x	DDI	X	X
STCLab	212	0	4	1H	816	18	27	3.46		x	x	DDI		X
STCLab	215	0	12	2H	941	5	28	1.36	DDI	x	x	DDI	X	X
STCLab	212	0	6	2H	404	32	29	2.26	DDI	x	x	DDI	X	X
STCLab	206	0	9	3H	415	1	31	1.47	DDI	x	x	DDI	X	X
STCLab	202	0	2	4H	39	5	31	2.19		x				
STCLab	202	0	3	1H	950	9	31	1.85	DDI	x	x	DDI		X
STCLab	202	0	3	4H	530	13	31	2.06		x				X
STCLab	206	0	10	2H	572	25	31	1.81	DDI	x	x	DDI	X	X
STCLab	212	0	5	2H	60	8	32	2.71	DDI	x	x	DDI	X	X
STCLab	212	0	1	4H	41	44	33	2.78	DDI	x	x	DDI	X	X
STCLab	206	0	10	4H	1029	1	34	1.99	DDI	x	x	DDI	X	X
STCLab	202	0	7	4H	4	9	34	2.37	DDI	x	x	DDI	X	X
STCLab	202	0	5	3H	80	21	34	2.7	DDI	x	x	DDI	X	X
STCLab	212	0	2	4H	348	42	34	2.19		x		DDI	X	X
STCLab	212	0	6	1H	953	36	35	2.42	DDI	x	x	DDI	X	X
STCLab	206	0	10	1H	259	25	37	1.73	DDI	x	x	DDI	X	X
STCLab	212	0	6	4H	559	35	37	2.8	DDI	x	x	DDI	X	X
STCLab	202	0	1	2H	1104	1	40	2.86		x	x	DDI		X
STCLab	215	0	12	3H	504	13	40	1.45	DDI	x	x	DDI	X	X
STCLab	202	0	3	3H	521	33	40	2.47		x		DDI		X
STCLab	202	0	3	2H	678	21	43	2.53		x	x	DDI		
STCLab	212	0	4	4H	985	23	43	2.58			x	DDI	X	X
STCLab	212	0	7	2H	815	34	43	2.57	DDI	x	x	DDI	X	X
STCLab	202	0	5	2H	110	37	43	2.71	DDI	x	x	DDI	X	X
STCLab	212	0	5	3H	160	14	44	2.7	DDI	x	x	DDI	X	X
STCLab	212	0	1	2H	172	28	44	2.86			x	DDI		X
STCLab	212	0	3	1H	662	8	45	1.85	DDI	x	x	DDI	X	X
STCLab	202	0	6	3H	372	17	46	2.67	DDI	x	x	DDI	X	X
3	213	19	24	2H	1037	25	47	4.94	DDI	x	x	DDI	X	X
STCLab	212	0	3	2H	336	3	49	2.53		x		DDI		X
STCLab	206	0	9	4H	769	5	49	1.44	DDI	x	x	DDI	X	X
STCLab	202	0	2	3H	232	29	49	2.64		x		DDI		X
STCLab	202	0	7	5H	442	33	49	2.64	DDI	x	x	DDI	X	X
STCLab	215	0	13	5H	564	37	49	1.77	DDI	x	x	DDI	X	X
STCLab	206	0	9	1H	218	5	52	1.61	DDI	x	x	DDI	X	X
STCLab	212	0	2	2H	739	6	52	2.47			x	DDI		X
STCLab	202	0	6	5H	481	13	52	2.38	DDI	x	x	DDI	X	X
STCLab	215	0	12	5H	680	41	52	1.54	DDI	x	x	DDI	X	X
2	212	20	23	2H	148	41	53	2.2	DDI	x	x	DDI	X	X
STCLab	212	0	1	5H	851	3	54	2.58	DDI	x	x	DDI	X	X

Table A-4

	Old	Old	Old	Old	New	New	New		Team 1			Team 2		
Optical	Reel	Row	Col	Loc	REEL	Row	Col	Dent V	R1 Call	PRI-1	SEC-1	R2 Call	PRI-2	SEC-2
STCLab	202	0	7	2H	1023	17	55	2.57	DDI	x	x	DDI	X	X
STCLab	202	0	2	1H	908	25	55	4.59			x	DDI		X
STCLab	215	0	12	4H	607	33	55	1.54	DDI	x	x	DDI	X	X
STCLab	215	0	12	1H	584	37	58	1.75	DDI	x	x	DDI	X	X
STCLab	202	0	5	5H	266	41	58	1.93	DDI	x	x	DDI	X	X
STCLab	212	0	7	5H	130	28	59	2.64	DDI	x	x	DDI	X	X
STCLab	212	0	1	1H	756	37	60	3.27		x	x	DDI	X	X
STCLab	212	0	6	3H	585	36	61	2.67	DDI		x	DDI	X	X
STCLab	206	0	11	4H	166	1	64	2.35	DDI	x	x	DDI	X	X
STCLab	202	0	6	1H	526	21	64	2.42	DDI	x	x	DDI	X	X
STCLab	202	0	5	4H	792	25	64	3.1	DDI	x	x	DDI	X	X
STCLab	206	0	8	1H	696	9	67	1.67	DDI	x	x	DDI	X	X
STCLab	202	0	2	2H	1048	13	67	2.47	·	x	x	DDI		X
STCLab	202	0	2	5H	1052	17	67	2.76		x	x	DDI		X
STCLab	206	0	9	5H	981	33	67	1.56	DDI	x	x	DDI	X	X
STCLab	215	0	13	1H	997	41	67	1.73	DDI	x	x	DDI	X	X
STCLab	212	0	5	1H	9	1	72	2.87	DDI	x	x	DDI	X	X
STCLab	206	0	11	1H	744	37	73	1.58	DDI	x	x	DDI	X	X
STCLab	202	0	1	4H	679	13	76	2.76	DDI	x	x	DDI	X	X
3	213	23	25	1H	646	9	77	3.37						
3	214	13	28	1H	356	13	77	3.64	DDI	x	x	DDI	X	X
STCLab	212	0	2	5H	567	26	81	2.73			x	DDI		X
STCLab	212	0	4	5H	140	27	81	2.55	DDI	x				
STCLab	202	0	4	4H	925	5	82	2.58		x	x	DDI		X
STCLab	202	0	4	5H	598	29	82	2.55						
STCLab	215	0	13	4H	1065	25	85	1.53	DDI	x	x	DDI	X	X
STCLab	206	0	9	2H	189	5	88	1.5	DDI	x	x	DDI	X	X
STCLab	202	0	5	1H	894	21	88	2.87	DDI	x	x	DDI	X	X
STCLab	212	0	2	3H	540	4	90	2.64		x	x	DDI		X
STCLab	212	0	4	2H	725	18	90	2.01		x	x	DDI	X	X
STCLab	206	0	11	5H	887	9	91	1.73	DDI	x	x	DDI	X	X
TVA	30	14	7	4H	631	14	7	3.07	DDI	x	x		X	
TVA	30	18	8	4H	195	18	8	3.22	DDI	x		DDI	X	X
TVA	30	6	14	4H	494	6	14	2.32	DDI	x				
TVA	32	9	14	2H	395	9	14	1.04	DDI	x		DDI	X	X
TVA	32	5	15	3H	407	5	15	2.32		x	x	DDI	X	X
2	212	8	20	2H	718	8	20	4.18		x	x	DDI	X	
2	212	20	20	2H	203	20	20	2.58	DDI	x	x	DDI	X	X
2	212	23	20	2H	386	23	20	3.35	DDI	x	x	DDI	X	X
2	212	21	21	1H	978	21	21	3.14	DDI	x	x	DDI	X	X
PGE-4/97	28	27	21	5H	552	27	21	3.14	DDI	x	x	DDI	X	X
2	212	28	21	1H	852	28	21	3.53	DDI	x	x	DDI	X	X
2	212	20	22	2H	20	20	22	2.91	DDI	x		DDI	X	X
PGE-4/97	28	36	22	7H	79	36	22	1.47	DDI	x	x	DDI	X	X
2	212	7	23	2H	707	7	23	2.92	DDI	x	x	DDI	X	X
PGE-4/97	28	38	23	7H	628	38	23	2	DDI		x	DDI	X	X
PGE-4/97	27	10	24	1H	619	10	24	2.07	DDI	x	x		X	X
PGE-4/97	27	17	24	1H	692	17	24	2.47	DDI	x	x	DDI	X	
PGE-4/97	27	22	24	2H	1035	22	24	0.57	DDI	x	x	DDI	X	
PGE-4/97	28	27	24	2H	14	27	24	1.28	DDI	x	x	DDI	X	X
3	213	23	25	3H	446	23	25	3.5	DDI	x	x	DDI	X	X
3	213	27	25	2H	579	27	25	3.31	DDI	x	x	DDI	X	X
3	213	28	25	2H	220	28	25	2.83	DDI	x	x	DDI	X	X
3	213	35	26	2H	836	35	26	2.88	DDI	x	x	DDI	X	X
3	213	11	27	2H	473	11	27	2.8	DDI	x	x	DDI	X	X
3	213	16	27	1H	833	16	27	3.46	DDI	x	x	DDI	X	X
3	213	24	27	1H	573	24	27	3.69						
3	214	7	28	2H	888	7	28	2.79		x				
3	214	19	29	2H	5	19	29	3.44	DSI	x		DDI	X	X
3	214	26	30	1H	614	26	30	2.61					X	
FALSE CALL RATE=# False calls/ # NDD Grading Units =									72.6%	89.5%	83.9%	91.1%	78.2%	88.7%

Table A-5

Bobbin Flaws with Destructive Exam Data for NDE Performance Test

AB SAMPLES		Bold=Training REEL			NEW	New	New	Resolution R1		Analyst A1	Analyst B1	Resolution R2		Analyst A2	Analyst B2
Optical	Reel	Row	Column	Location	REEL	Row	Column	Flaw V	Call	Flaw V	Flaw V	Flaw V	Call	Flaw V	Flaw V
STCLab	201	0	2	2H	1007	1	1								
STCLab	201	0	4	4H	286	1	4								
STCLab	207	0	9	4H	137	9	10								
STCLab	213	0	12	5H	821	25	10								
2 -1R8	28	1	4	3H	238	25	11								
STCLab	201	0	5	5H	131	1	13								
STCLab	213	0	13	5H	77	29	13								
STCLab	211	0	5	1H	597	16	14								
STCLab	211	0	4	4H	180	25	15								
STCLab	211	0	7	4H	354	29	15								
STCLab	207	0	8	4H	346	25	16								
STCLab	211	0	2	4H	15	20	17								
2 -1R8	28	14	4	1H	456	33	17								
STCLab	201	0	3	5H	1069	37	19								
17	93	16	59	3H	274	5	20								
STCLab	211	0	5	2H	171	8	21								
STCLab	211	0	1	2H	706	18	21								
STCLab	211	0	3	5H	98	22	21								
STCLab	207	0	9	2H	1019	1	22								
STCLab	201	0	1	3H	452	9	22								
STCLab	213	0	12	2H	563	13	22								
STCLab	207	0	8	2H	68	25	22					0.16	SAI	0.16	
2 -1R8	28	12	3	1H	96	17	23							0.06	
STCLab	211	0	3	3H	671	18	23								
STCLab	201	0	3	4H	911	13	25								
STCLab	201	0	1	5H	85	25	25								
STCLab	211	0	6	4H	484	14	26								
STCLab	211	0	6	3H	159	27	28								
STCLab	207	0	11	1H	94	41	28							0.13	
STCLab	201	0	5	3H	206	17	31								
17	97	10	67	2H	650	25	32								
2 -1R8	29	22	47	4H	982	33	32								
STCLab	201	0	1	2H	445	17	34								
STCLab	213	0	12	3H	150	25	34								
STCLab	213	0	12	4H	67	37	34							0.13	
2 -1R8	29	22	47	1H	538	13	35								
17	93	9	64	3H	823	17	35							0.55	
STCLab	211	0	7	5H	895	4	36								
STCLab	211	0	4	3H	54	17	36								
STCLab	213	0	12	1H	187	21	37								
STCLab	201	0	2	3H	358	37	37								
15	80	9	85	1H	164	21	38			0.12					
STCLab	211	0	3	2H	971	34	39								
STCLab	201	0	2	4H	328	37	40								
STCLab	201	0	4	5H	374	45	40							0.27	
2 -1R8	28	15	3	1H	267	33	41								
15	80	6	78	1H	901	37	41								
PGE	127	10	22	1H	467	46	41								
STCLab	211	0	3	1H	176	15	42								
STCLab	211	0	3	4H	320	8	43							0.31	
STCLab	207	0	9	5H	666	33	43								
STCLab	201	0	7	3H	461	45	43								
STCLab	211	0	2	3H	527	8	44								
2 -1R8	26	8	2	1H	48	29	44								
STCLab	201	0	7	2H	517	1	46							0.28	
STCLab	201	0	5	1H	501	5	46								
STCLab	201	0	1	4H	711	33	46								
STCLab	207	0	8	1H	512	45	46								
STCLab	201	0	2	5H	368	9	49								
STCLab	201	0	6	4H	710	17	49					0.35	SAI	0.35	
STCLab	207	0	11	5H	435	25	49								0.22
STCLab	211	0	5	4H	158	31	49								
STCLab	201	0	3	1H	251	41	49								
STCLab	201	0	2	1H	548	45	49								
STCLab	211	0	2	5H	144	15	50								
16	90	9	73	1H	942	17	50								
STCLab	207	0	8	5H	1096	1	52								
STCLab	207	0	10	1H	897	9	52								
STCLab	201	0	4	2H	904	5	55							0.24	
STCLab	201	0	7	4H	193	9	55								
STCLab	211	0	4	5H	1083	14	55							0.31	
STCLab	201	0	7	1H	647	41	55								
15	80	8	85	1H	994	17	56								
17	93	16	59	1H	1095	45	56								
STCLab	211	0	5	3H	921	22	57								
STCLab	211	0	1	1H	330	33	57								
STCLab	207	0	10	3H	371	13	58								

Table A-5

Bobbin Flaws with Destructive Exam Data for NDE Performance Test															
LAB SAMPLES		Bold=Training REEL			NEW	New	New	Resolution R1		Analyst A1	Analyst B1	Resolution R2		Analyst A2	Analyst B2
Optical	Reel	Row	Column	Location	REEL	Row	Column	Flaw V	Call	Flaw V	Flaw V	Flaw V	Call	Flaw V	Flaw V
STCLab	207	0	9	3H	129	25	58								
STCLab	211	0	5	5H	419	39	58								
STCLab	211	0	1	5H	1085	40	60								
STCLab	213	0	13	4H	868	5	61								
STCLab	201	0	7	5H	1073	17	61								
STCLab	213	0	13	3H	793	21	61								
STCLab	201	0	1	1H	322	25	61								
STCLab	207	0	11	4H	33	33	61								
STCLab	211	0	4	1H	95	44	62								
STCLab	211	0	2	2H	980	29	63								
STCLab	211	0	2	1H	163	3	64								
STCLab	201	0	6	1H	854	37	64								
STCLab	211	0	1	3H	818	42	64								
STCLab	201	0	4	1H	794	37	67								
STCLab	207	0	10	5H	226	1	70								
STCLab	213	0	13	2H	560	9	70								
STCLab	211	0	1	4H	713	19	70								
17	93	5	61	2H	422	5	71								
2 -1R8	26	6	2	1H	963	21	71								
STCLab	211	0	6	2H	257	38	72								
STCLab	201	0	5	2H	134	1	73								
STCLab	201	0	3	3H	1079	25	73								
STCLab	211	0	6	1H	81	26	75								
STCLab	211	0	7	3H	759	30	75							0.54	
STCLab	211	0	7	1H	132	10	76								
STCLab	213	0	13	1H	636	25	76								
STCLab	207	0	8	3H	932	33	76								
STCLab	201	0	5	4H	300	5	79								
STCLab	207	0	11	3H	104	9	79								
STCLab	201	0	6	5H	736	17	79								
STCLab	211	0	6	5H	365	28	79								
STCLab	211	0	7	2H	327	27	80								
STCLab	201	0	6	2H	55	17	82								
STCLab	201	0	6	3H	529	9	85								
STCLab	207	0	10	2H	141	17	85								
STCLab	207	0	11	2H	863	1	88							0.27	
STCLab	201	0	3	2H	399	9	88							0.14	
STCLab	207	0	9	1H	190	13	91								
STCLab	211	0	4	2H	242	1	93								
STCLab	201	0	4	3H	252	1	94								
STCLab	207	0	10	4H	890	5	94								
2 -1R8	28	4	1	1H	475										
2 -1R8	28	5	1	1H	18										
2 -1R8	26	6	2	2H	1108										
2 -1R8	26	7	2	1H	726										
2 -1R8	26	9	2	1H	197										
2 -1R8	26	4	3	3H	642										
2 -1R8	26	12	3	1H	635										
2 -1R8	28	14	3	1H	689										
2 -1R8	28	10	4	3H	253										
2 -1R8	29	23	47	1H	827										
2 -1R8	29	24	47	1H	613										
17	98	7	48	1H	913										
17	98	20	54	3H	88										
17	98	27	64	1H	235										
17	97	8	67	3H	820										
17	97	9	68	2H	674										
17	97	18	68	1H	586			0.24	SAI		0.24				
16	90	7	72	3H	268					0.17					
15	80	5	84	1H	443									0.11	
15	80	8	84	1H	273										
15	80	12	86	1H	880										
15	80	6	88	1H	590										
15	80	18	88	1H	547										
15	80	12	92	1H	891										
15	80	7	93	1H	528										
						NDD Gading Units = 143									
		FALSE CALL RATE=# False calls/ # NDD Grading Units =							0.7%	1.4%	0.7%		1.4%	10.5%	0.7%

Appendix B

Depth Profiling of Circumferential PWSCC and ODSCC[1]

Note 1: Section 3 (independent technical review) of the attached NDE guidelines was not applied for testing of NDE analysts to develop NDE sizing uncertainties for circumferential cracks. Independent technical review (ITR) is applied for field inspections.

Depth Profiling of Circumferential PWSCC and ODSCC

1. The sizing techniques described below in Section 2 are generally consistent with the sizing techniques of EPRI ETSS # 20510.1 for circumferential PWSCC and ETSS # 20409.1 for circumferential ODSCC. Sizing analysts who have completed site specific training and testing are qualified to perform sizing or independent technical review (ITR) of sizing results.

2. Circumferential PWSCC and ODSCC depth profiling shall be performed as follows:

   2.1 All phase angle measurements shall be made volts peak to peak using the entrance leg. If the crack indication is influenced by dent or tube ovalization to such an extent that the exit leg does not retrace the entrance leg, then two measurements shall be taken, i.e., both entrance and exit legs. The circumferential positions for the two measurements should be the same position or as close as possible to the same position, and should not exceed half of the smallest spacing between independent circumferential positions. Software for processing the circumferential profiles will automatically average the two measurements.

   2.2 Depth profiling shall be performed using 300kHz +Point data.
   2.2.1 In the main window, set the 40% ID circ EDM to 15 degrees. Set the span to 5 divisions.
   2.2.2 In the Ax Liz window, set the 100% circ EDM to 20.00 volts.
   2.2.3 In the Ax Liz window, establish a phase angle curve using the as built ID and OD circ EDM notches. If the OD circ EDM notches are not available, use the default OD curve.

   2.3 Verify the axial scale is correct. At each tube support plate, set the distance between the lower half ramp and upper half ramp to 0.75".

   2.4 Verify the scan direction is correct, i.e., push vs. pull.

   2.5 In the User Selectables, set the increments to 10 degrees or less.
   2.5.1 Find the first hit of the crack in the Ax Liz window.
   2.5.2 Click the arrow button backwards once. Enter 0.00 volts, 0 degrees and 0 percent at that circumferential position into the report.
   2.5.3 Click the arrow button forward to the first hit and enter the percent through-wall depth at that circumferential position into the report.
   2.5.4 Continue the incremental depth measurements around the tube circumference until all hits have been entered.
   2.5.5 Click the arrow button forward past the last hit of the crack. Enter 0.00 volts, 0 degrees, and 0 percent at that circumferential position into the report.

   2.6 All flaw like hits shall be entered into the report even though the flaw signal may read 0% depth. Software for processing the circumferential profiles will use voltage ratios to assign depths at 0% depth locations based upon maximum voltage and the voltage at the 0% depth location.

2.7 Volts and depths within 5% of the maximum volts are important to processing of low voltage profiles and should be carefully established.

2.8 Successive entries of zero volts and zero percent depth between the extreme zero end points of a profile will be processed as the end of one crack and the start of another crack. Entries of a single zero volt and zero percent depth point between the extreme zero end points of a profile will be processed as a ligament within the major crack and not as an end point between cracks.

2.9 Crack sizing should be performed for each and every crack if there are multiple cracks. Two successive zero volt and zero depth points should be entered for multiple cracks with these points representing the end of one crack and the start of the second crack. Extreme care should be exercised to correctly follow the particular crack being sized.

2.10 Inherent field spread about the eddy current coil may cause a phase shift from ID to OD flaw plane. Also the field spread may cause a small amplitude signal to read unusually high % through-wall. Nevertheless they should be reported as is.

2.11 C-scan graphics are required.

3. Independent Technical Review

3.1 ITR is required to ensure that crack sizing has been performed correctly.

3.2 If crack sizing was performed by a primary sizing analyst, ITR should be performed by a secondary sizing analyst and vice versa. The Lead Analyst or PG&E Level III Analyst may function as ITR.

3.3 The ITR should check the following as a minimum:

1) Phase rotation

2) Volts scale

3) Axial scale

4) Scan direction

5) Calibration curve

6) Sample incremental % through-wall depths

7) The % through-wall depth at the maximum signal amplitude

8) The first and last hits of the crack

3.4 If the ITR agrees with the sizing results, concurrence should be documented on the sizing report.

3.5 If the ITR does not agree with the sizing results, the ITR and sizing analyst should discuss the discrepancies and resolve them. If the discrepancies cannot be resolved, the Lead Analyst or PG&E Level III should be involved.

4. Computerized processing of the depth profiles requires electronic transmittal of the depth profiles with some formatting restrictions. Entries for the first profile should start in line 3 (entries in line 1 and line 2 are not processed). A blank line is required between each tube or support location. Multiple cracks at the same support location should be separated by zero entries, as described in Section 2, and not by a blank line. There is no need to enter crack1, crack 2, etc.

Appendix C

Data Exclusion Criteria for Axial PWSCC at Dented TSP Intersections

Data Exclusion Criteria for Axial PWSCC at Dented TSP Intersections

1.0 OBJECTIVE

This section addresses criteria for excluding data from databases used to qualify/quantify NDE analyses and/or to develop burst and leak rate correlations. Data exclusion criteria were developed by EPRI for application to the ARC for ODSCC at TSP intersections under NRC Generic Letter 95-05. The exclusion criteria defined herein are similar to the EPRI ODSCC criteria but are specific to axial PWSCC at dented TSP intersections. The use of crack depth profiles from destructive examinations is a specific application that requires an extension of the EPRI exclusion criteria.

The objective of the data exclusion criteria is to eliminate from databases, test or measurement data that that are unacceptable or inadequate due to errors in obtaining the data or the data are inappropriate for the application. The general categories identified for data exclusion are:

1. Invalid or Inadequate Test
2. Morphology Related Criteria
3. Test Measurement Error
4. Destructive Exam Crack Depth Profile Related Criteria

Categories 1 to 3 are the same broad groups used for the EPRI exclusion criteria (EPRI Report NP-7480-L, Volume 1, Rev. 2) for ODSCC and the criteria are the same or adapted to PWSCC. Category 4 is added specifically for programs utilizing detailed destructive exam information such as crack depth profiles for NDE qualification or ARC applications. The exclusion criteria are developed in Section 2. Section 3 applies the criteria to identify indications excluded from the database.

2.0 DATA EXCLUSION CRITERIA

NRC guidelines for acceptance of data used for ARC applications are based on accepting all data that do not satisfy criteria for exclusion from the database. The NRC's general criteria for exclusion of data from a database are:

- Data is associated with an invalid test.
- Data is associated with atypical degradation based on morphology criteria which are defined rigorously and applied to all data, and which can be unambiguously applied by an independent observer.
- Exclusion of data results in conservatism associated with application of the affected correlation.

This section defines the specific data exclusion criteria for application to axial PWSCC at dented TSP intersections.

Criterion 1: Invalid or Inadequate Test

1a: Unacceptable NDE Data Collection: This condition applies to specimens for which NDE data was not obtained with acceptable data acquisition techniques or probes, specimens that have been damaged for reasons other than the corrosion process and specimens exhibiting extraneous eddy current signal effects (e.g. proximity to a test article weld or tube mark). This criterion results in the data point being excluded from NDE qualification programs and any ARC correlations based on NDE data.

1b: Inadequate or Inappropriate Burst Test: This condition applies to specimens that did not attain a true burst condition (e.g., caused by leakage in the burst test), a test fixture malfunction with inability to retest and specimens tested for other purposes (with a constraint such as a TSP when free span test is required). Specimens satisfying this criterion are excluded from use in an ARC burst correlation or burst test database for which it is assumed that TSPs displace in a SLB event. Specimens tested with a TSP and achieving an acceptable burst condition for the length of PWSCC outside the TSP may be used in burst correlations based on no SLB TSP displacement.

1c: Inadequate Leak Test: This condition applies to unacceptable leak tests such as insufficient test loop flow capacity to reach the specimen's leak rate for SLB conditions and a test fixture malfunction with inability to retest. Specimens satisfying this criterion are excluded from use in ARC leak rate correlations or leak test database.

1d: Tube Damage from Tube Pull Forces: This condition applies to crack distortion or damage such as excessive ligament tearing as indicated by increased post-pull NDE flaw measurements such as voltage or length and post-pull leak rates much higher than indicated by plant data. For application of this criterion, it must be demonstrated that the damage from the tube pulling operations such as ligament tearing are greater than expected at SLB conditions. Specimens satisfying this criterion are excluded from use in ARC leak rate correlations or leak test database and possibly from use in burst correlations.

1e: Unavailable Test Information: This condition applies to specimens for which complete testing such as leak, burst and fractography have not been performed. For example, a leak test may not have been performed and the fractography is not performed or not conclusive relative to including the specimen in a probability of leak database. This criterion is most applicable to excluding data from the probability of leak correlation when the test information is inadequate to draw a conclusion on whether the specimen would leak at SLB conditions.

Criterion 2: Morphology Related Criteria

2a: Crack Morphology Atypical of Axial PWSCC at Dented TSP: This condition applies to crack morphologies, particularly laboratory specimens, that have crack morphologies that are not characteristic of axial PWSCC at dented TSP intersections as found by pulled tube examinations. The required, pulled tube morphology is that of very narrow bands (such as having < 25° circumferential extent) of axial PWSCC that may be within or extending outside the TSP. Specimens with broad bands of cracks or multiple initiation sites extending more than about 25° as a single band are excluded by this criterion. This criterion excludes the data point from all NDE qualification efforts and any ARC databases or correlations.

Criterion 3: Probable Test Error in Leakage Measurement

No criteria except that under Criterion 1 are applied to exclude data from the database for the leak rate correlation.

Criterion 4: Destructive Exam Data Crack Depth Profile Related Criteria

4a: Incomplete Crack Length/Depth Profile: This condition applies when the length versus depth profile provided from the destructive examination is less than the length of significant cracking. Verification of cracking beyond the length profiled, such as photographs, must be obtained to support exclusion per this criterion. When indications are opened by bending rather than by a burst test, the length to be opened requires some judgment and the full extent of significant cracking may not be depth profiled as part of the tube exam. This criterion excludes the data point from all NDE sizing qualification efforts including NDE uncertainty estimates and from burst correlations with an NDE parameter. The indication may be used for NDE detection such as POD or a leak rate correlation with maximum depth if the available data is adequate to define the maximum depth.

4b: Incomplete Depth Profile: This condition applies when the crack is opened by bending or other techniques (e.g., radial grinding) than burst and it can be demonstrated that either the complete depth profile or the structurally or leakage limiting crack may not have been obtained. To apply this criterion, it must be demonstrated by destructive examination data, such as metallography, that the complete depth profile has not been defined or that the microcracks or macrocracks parallel to the crack opened by bending have depths or lengths exceeding the opened crack. An example of this criterion application could be depth profiles obtained from radial grinds, but the initial grind may have been too deep to define shallow depths. In this example, the crack length and maximum depth are defined but the average crack depth is not obtained. This criterion does not apply to a crack opened by a valid burst test which opens the structurally limiting crack. This criterion excludes the data point from NDE depth sizing qualification efforts for the data not obtained and from burst correlations with destructive exam data or a NDE parameter. The indication may be used for NDE detection such as POD or a leak rate correlation with maximum depth if the available data is adequate to define the maximum depth. If the total crack length is obtained, the indication may be used for NDE length sizing qualification.

4c: Selective Length Adjustments to Destructive Exam Crack Depth Profiles: This condition applies when the crack depth profile from destructive examination includes shallow cracking at the ends of the crack and the depths at the tails are much less than the more dominant or maximum crack depths. Under this criterion, only the shallow tails are excluded from the crack length and average depth of the crack used for qualification of NDE sizing techniques or potential burst pressure correlations. To apply this criterion, the depths of the tails excluded from the crack length must be less than 40% maximum depth, and the average depth over the length cutoff must be less than 15%. This selective length adjustment of the depth profiles is necessary to ensure that the shallow tails of cracks, which have no tube integrity implications, do not significantly impact NDE sizing uncertainty estimates.

3.0 APPLICATION TO CURRENT DATABASE

The available pulled tube and laboratory specimen indications were evaluated against the PWSCC Data Exclusion Criteria defined in Section 2. Specimens affected by application of the criteria are identified in Table C-1. Pending determination of the parameters to be correlated with burst pressure for ARC applications, a burst test data point may have potential applications in a correlation with destructive exam depth (BvD in Table C-1) and/or an NDE parameter (BvNDE). Indications P8 to P10, which were burst with a TSP and part of the crack length extending outside the TSP, are acceptable for NDE qualification, but are limited for burst correlations only under the assumption that TSPs do not displace in a SLB event. A number of specimens were pressure tested to open the cracks for destructive exam fractography of the pressurized crack opening and were not intended to be qualified burst tests. The second crack for these specimens, as identified in Table C-1, was opened after prior pressurization to burst the larger crack. Criterion 1b applies for exclusion of these data from the burst pressure correlation. In some cases, the pressurization tests resulted in burst of the indication away from the flaw such as in welded extensions to the test specimen. Since the resulting burst pressures cannot be associated with the flaw, the tests are not considered acceptable and are also excluded from the burst correlation database per Criterion 1b. Two specimens, 9-5H and 10-3H, had reported burst pressures in excess of 11 ksi (near that of undegraded tubing), and the destructive exam reported flaws exceeding 57% averaged depth over lengths greater than 0.63 inch. It would be physically impossible for flaws of this size to have burst pressures >11 ksi. Therefore, these two specimens are considered to have an unacceptable burst test. Acceptable applications for the specimen after applying the exclusion criteria are identified in the 4th column of Table C-1.

Application of Criterion 4c leads to exclusion of shallow points at the tail of a crack from the destructive exam profile and average depth used for NDE comparisons and potentially in burst evaluations. Figures C-1 to C-19 show the points excluded from the destructive exam profile for the specimens indicated in Table C-1.

Table C-1
Evaluation of Axial PWSCC Data Against Data Exclusion Criteria
Database Status – 2/00

Specimen	Basis for Excluding Indications	Exclusion Category	Remaining Data App.(1)
Plant W-1 R21C64	Field data obtained with pancake coil. NDE qualification based on + Point coil	1a	M, BvD
P8, crack 1 P9, crack 1 P10, crack 1	Indication burst with presence of TSP. Application to burst correlations limited to assumption that TSP does not displace in a SLB event.	1b	NDE, burst only for length outside TSP
Crack 2 for 9-3H, 9-4H, 9-5H, 10-3H, 11-3H	Specimen was initially burst to open crack 1. Crack 2 was cut from tube and weld into another tube section in order to pressurize the crack to open the crack for NDE fractography	1b	NDE
2-3H, 3-3H, 4-4H, 5-1H, 12-2H	Specimens burst away from flaw, typically at a weld joint or attachment to tube. Specimen lower bound burst pressure is not appropriate for use in a burst correlation.	1b	NDE
9-5H, 10-3H	Reported burst pressures were >11 ksi for indications >0.63" and 57% average depth. It is physically impossible for these large indications to correspond to the reported burst pressures, and the indications are excluded from the burst correlation.	1b	NDE
P13, cracks 1 to 3	Crack morphology of wide bands of microcracks is atypical of pulled tube PWSCC morphology	2a	None
5-1H	Complete depth profile not defined. Depth profile from radial grinding obtained at too large of depth steps to define profile. Length obtained and max. depth reasonably estimated.	4b	NDE-POD, Max. Depth, Length
9-1H, crack 2	Total crack length of significant depth was not opened by bending in destructive exam and data not valid for NDE sizing qualification. Indication can be use for NDE detection or POD as maximum depth defined.	4a	NDE-POD, Max. Depth
9-4H, crack 2	Complete depth profile not defined. Depth profile from radial grinding obtained at too large of depth steps to define profile. Length obtained and max. depth reasonably estimated.	4b	NDE-POD, Max. Depth, Length
1-3H	Shallow tails (0.05", 0.05") of crack with depths ≤ 14% excluded from crack length as avg. depth < 15% & max. depth < 40%.	4c	NDE, BvD, BvNDE
2-1H	Shallow tails (0.03", 0.11") of crack with depths ≤ 10% excluded from crack length as avg. depth < 15% & max. depth < 40%.	4c	NDE, BvD, BvNDE
2-3H	Long shallow tails (0.089", 0.212") of crack with max. depth dominantly < 9% and average depths ≤ 6% excluded from crack length as avg. depth < 15% & max. depth < 40%.	4c	NDE, BvD, BvNDE
2-4H	Shallow tails (0.11", 0.09") of crack with depths ≤ 13% excluded from crack length as avg. depth < 15% & max. depth < 40%.	4c	NDE, BvD, BvNDE
2-5H	Shallow tail (0.08") of crack with depths < 13% excluded from crack length as avg. depth < 15% & max. depth < 40%. Extensive length of crack <20% depth retained in profile.	4c	NDE, BvD, BvNDE
6-2H	Shallow tail (0.04") of crack with depths < 14% excluded from crack length as avg. depth < 15% & max. depth < 40%.	4c	NDE, BvD, BvNDE
7-1H	Shallow tail (0.19") of crack with depths ranging from 1% to 24% with an average depth < 8% excluded as avg. depth < 15% & max. depth < 40%.	4c	NDE, BvD, BvNDE
7-3H	Shallow tails (0.07", 0.35") of crack with depths ≤ 13% excluded from crack length as avg. depth < 15% & max. depth < 40%.	4c	NDE, BvD, BvNDE

Specimen	Basis for Excluding Indications	Exclusion Category	Remaining Data App.[1]
8-2H	Shallow tails (0.05", 0.04") of crack with depths < 15% excluded from crack length as avg. depth < 15% & max. depth < 40%.	4c	NDE, BvD, BvNDE
9-2H, crack 2	Shallow tail (0.05") of crack with depths < 6% excluded from crack length as avg. depth < 15% & max. depth < 40%.	4c	NDE, BvD, BvNDE
9-3H, crack 1	Shallow tail (0.03") of crack with depths < 15% excluded from crack length as avg. depth < 15% & max. depth < 40%.	4c	NDE, BvD, BvNDE
9-3H, crack 2	Shallow tail (0.11") of crack with depths ranging from 1% to 26% with an average depth <8% excluded as avg. depth < 15% & max. depth < 40%.	4c	NDE, BvD, BvNDE
9-5H, crack 1	Shallow tails (0.05", 0.02") of crack with depths < 19% excluded from crack length as avg. depth < 15% & max. depth < 40%.	4c	NDE, BvD, BvNDE
11-3H, crack 1	Shallow tail (0.04") of crack with depths ≤ 10% excluded from crack length as avg. depth < 15% & max. depth < 40%.	4c	NDE, BvD, BvNDE
11-3H, crack 2	Long shallow tails (0.17", 0.26") of multiple microcracks (3 and 2 microcracks, respectively) with average depths ≤ 12% and 10% excluded from crack length avg. depth < 15% & max. depth < 40%.	4c	NDE, BvD, BvNDE
11-4H, crack 1	Shallow tail (0.04") of crack with depths < 23% excluded from crack length as avg. depth < 15% & max. depth < 40%.	4c	NDE, BvD, BvNDE
12-4H	Shallow tails (0.08", 0.09") of crack with depths < 5% excluded from crack length as avg. depth < 15% & max. depth < 40%.	4c	NDE, BvD, BvNDE
P9, crack 2	Shallow tail (0.09") of 3 microcracks with maximum depths 24%, 33% and 17% excluded from crack length as avg. depth < 15% & max. depth < 40%. The 33% max. depth microcrack is farther in the tail than the 17% microcrack.	4c	NDE, BvD, BvNDE
P10, crack 2	Shallow tail (0.06") of crack with depths < 28% excluded from crack length as avg. depth < 15% & max. depth < 40%.	4c	NDE, BvD, BvNDE

Notes:
1. NDE = used in NDE qualification, BvD = used in burst pressure correlations with destructive exam depth, BvNDE = used in burst pressure correlations with NDE data, L = used in leak rate database, M = used to characterize pulled tube PWSCC morphology.

Figure C-1
Sample 1, TSP 3H - Crack 1
Mid-Range +Point, 300 kHz
Recommended Destructive Exam and Destructive Exam Excluded by 4C Criterion

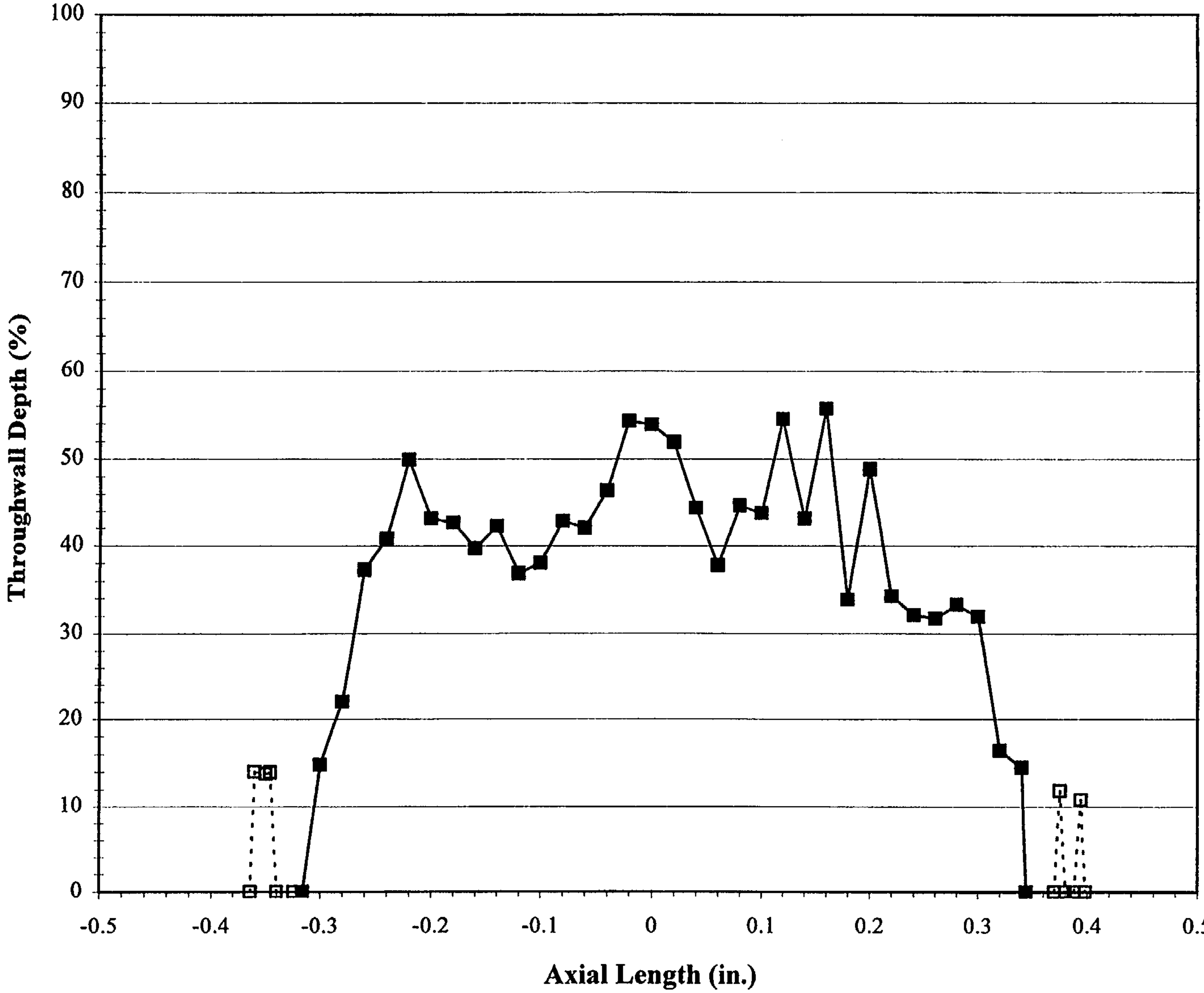

	Reported DE	Rec. DE
Max. Depth (%)	00.0	00.0
Max. Depth w/o RA(%)	55.7	55.7
Length (in.)	0.762	0.66
Avg. Depth (%)	34.43	39.18

Figure C-2
Sample 2, TSP 1H - Crack 1
Mid-Range +Point, 300 kHz
Recommended Destructive Exam and Destructive Exam Excluded by 4C Criterion

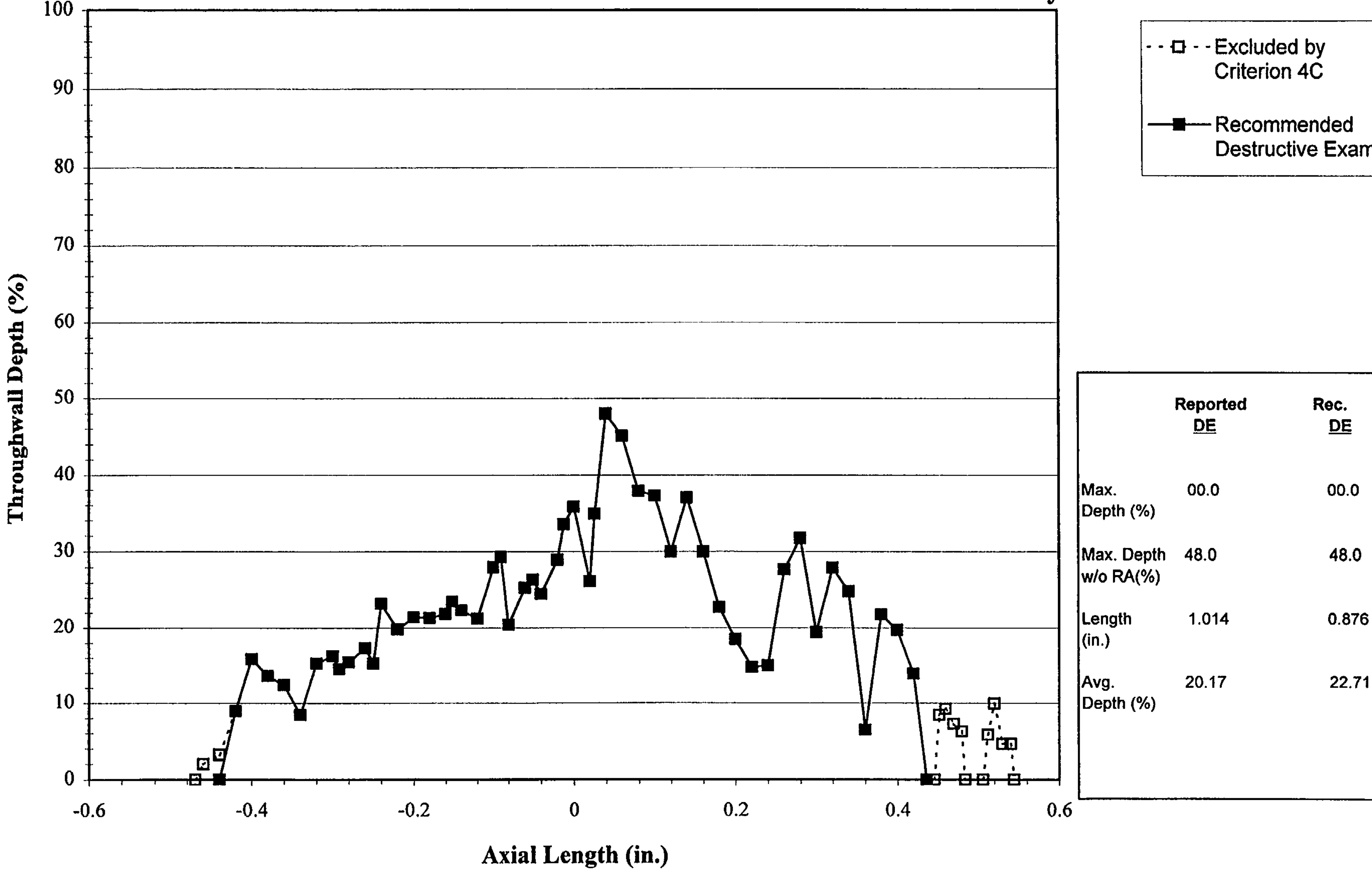

	Reported DE	Rec. DE
Max. Depth (%)	00.0	00.0
Max. Depth w/o RA(%)	48.0	48.0
Length (in.)	1.014	0.876
Avg. Depth (%)	20.17	22.71

Figure C-3
Sample 2, TSP 3H - Crack 1
Mid-Range +Point, 300 kHz
Recommended Destructive Exam and Destructive Exam Excluded by 4C Criterion

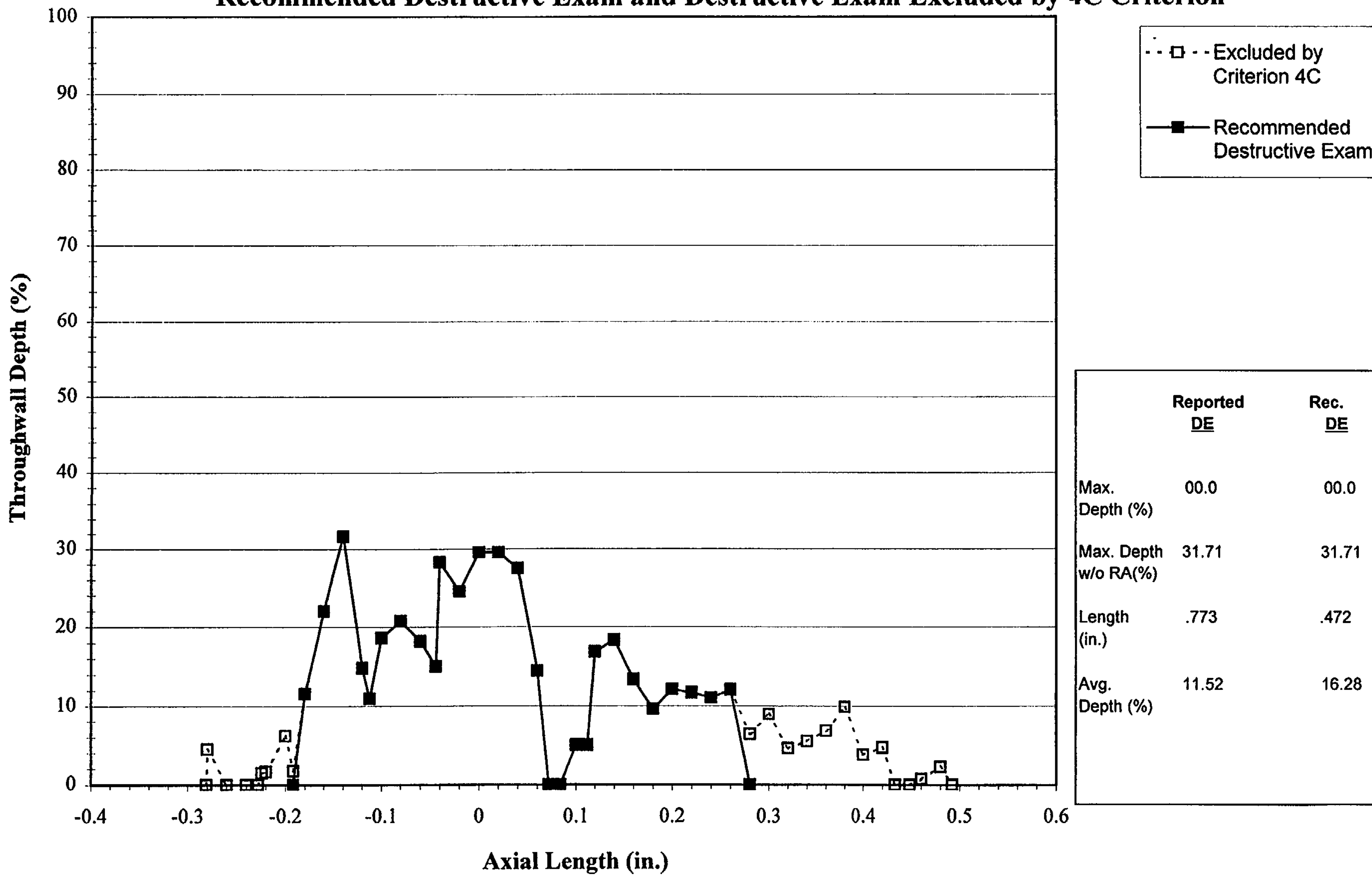

	Reported DE	Rec. DE
Max. Depth (%)	00.0	00.0
Max. Depth w/o RA(%)	31.71	31.71
Length (in.)	.773	.472
Avg. Depth (%)	11.52	16.28

Figure C-4
Sample 2, TSP 4H - Crack 1
Mid-Range +Point, 300 kHz
Recommended Destructive Exam and Destructive Exam Excluded by 4C Criterion

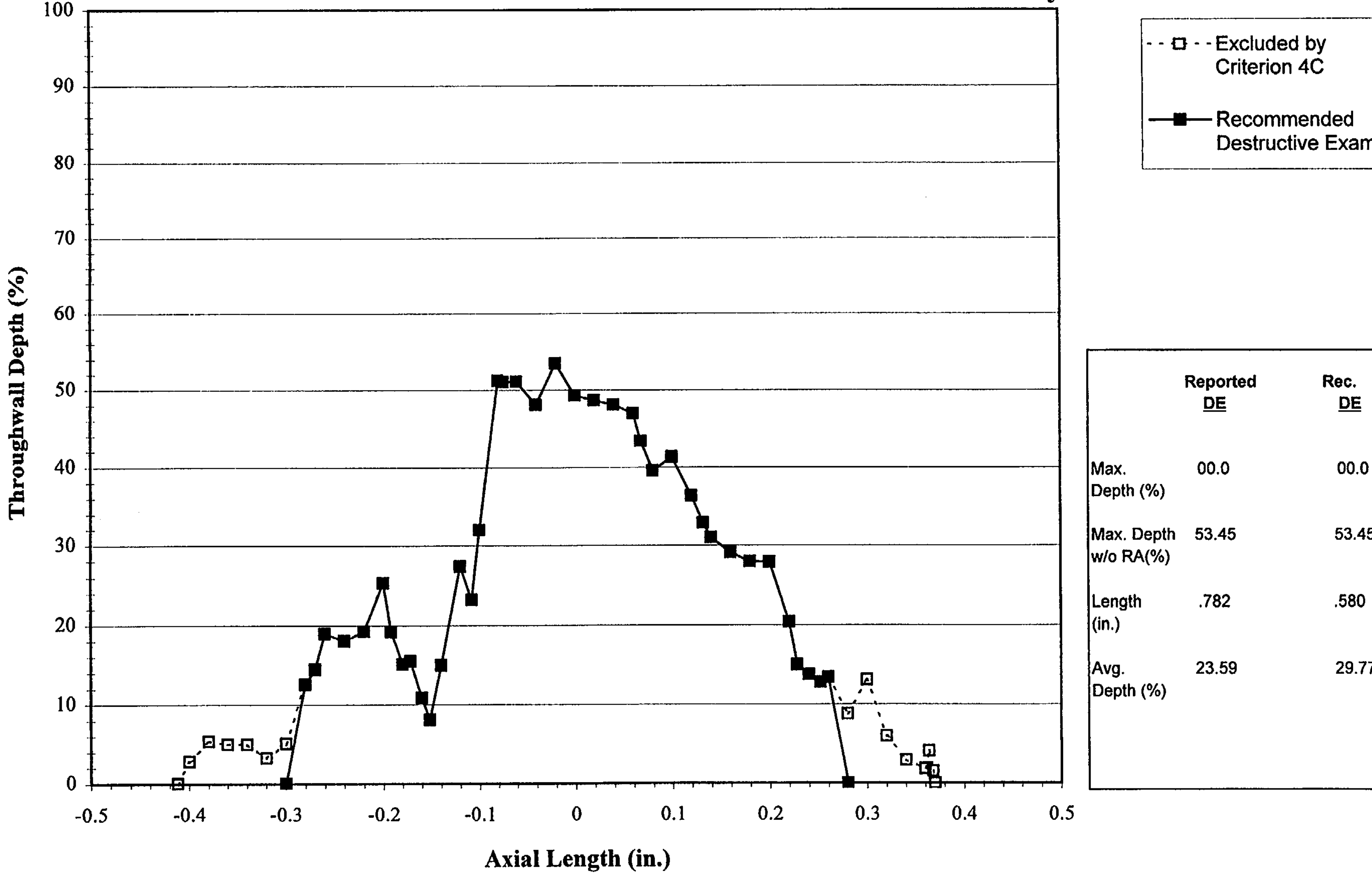

	Reported DE	Rec. DE
Max. Depth (%)	00.0	00.0
Max. Depth w/o RA(%)	53.45	53.45
Length (in.)	.782	.580
Avg. Depth (%)	23.59	29.77

Figure C-5
Sample 2, TSP 5H
Depth vs. Axial Length
Recommended Destructive Exam and Destructive Exam Excluded by 4C Criterion

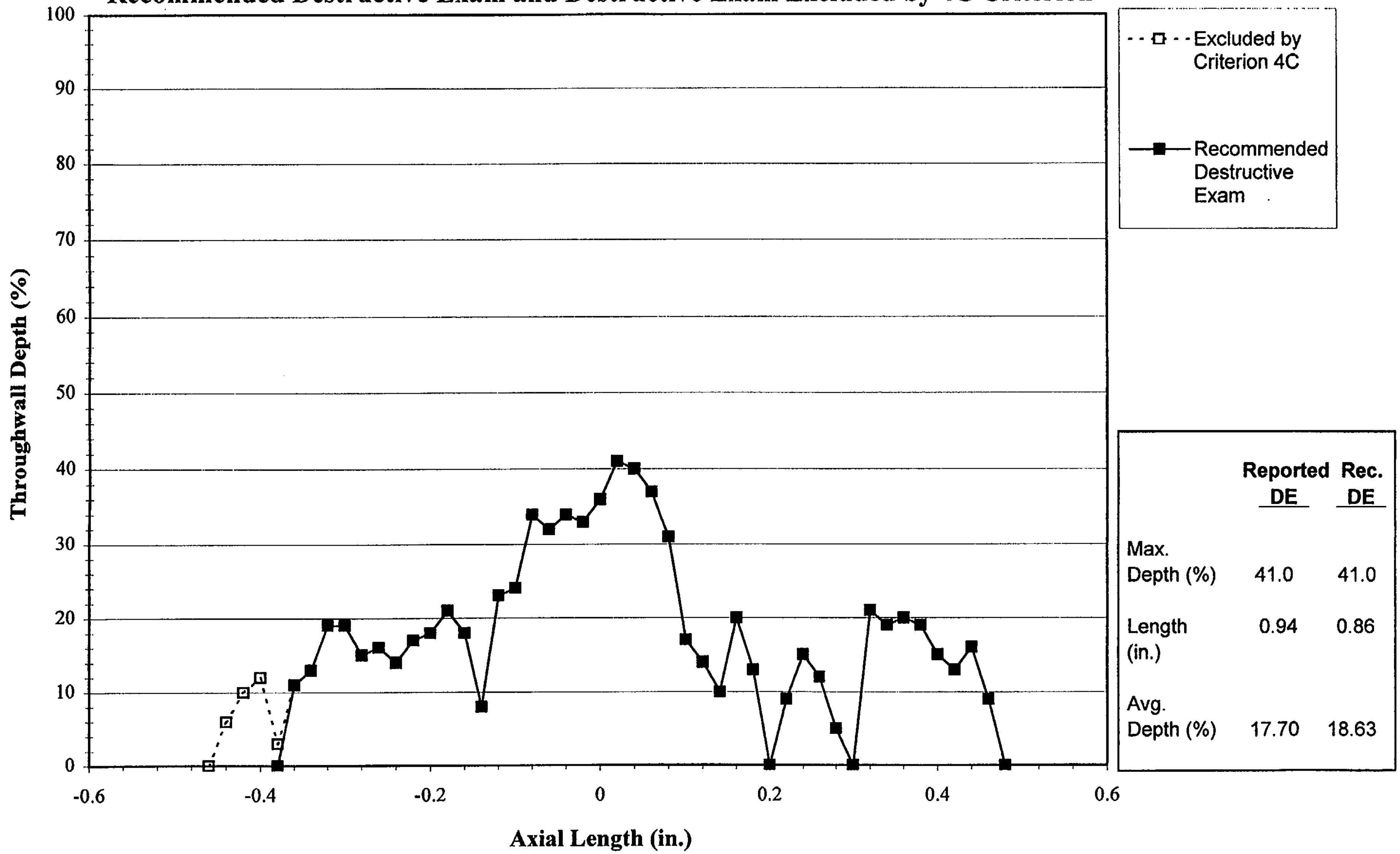

Figure C-6
Sample 6, TSP 2H - Crack 1
Mid-Range +Point, 300 kHz
Recommended Destructive Exam and Destructive Exam Excluded by 4C Criterion

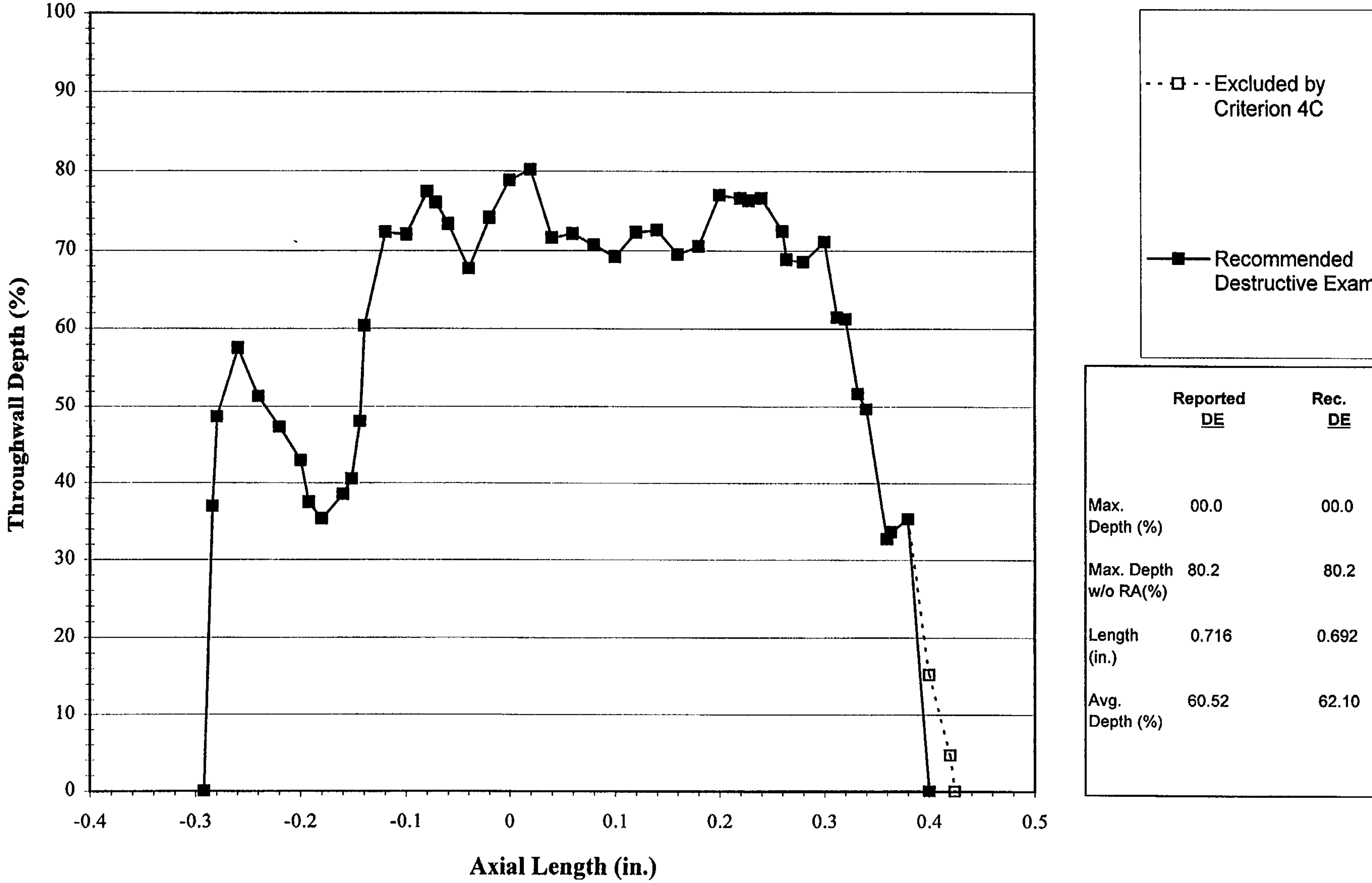

	Reported DE	Rec. DE
Max. Depth (%)	00.0	00.0
Max. Depth w/o RA(%)	80.2	80.2
Length (in.)	0.716	0.692
Avg. Depth (%)	60.52	62.10

Figure C-7
Sample 7, TSP 1H - Crack 1
Mid-Range +Point, 300 kHz
Recommended Destructive Exam and Destructive Exam Excluded by 4C Criterion

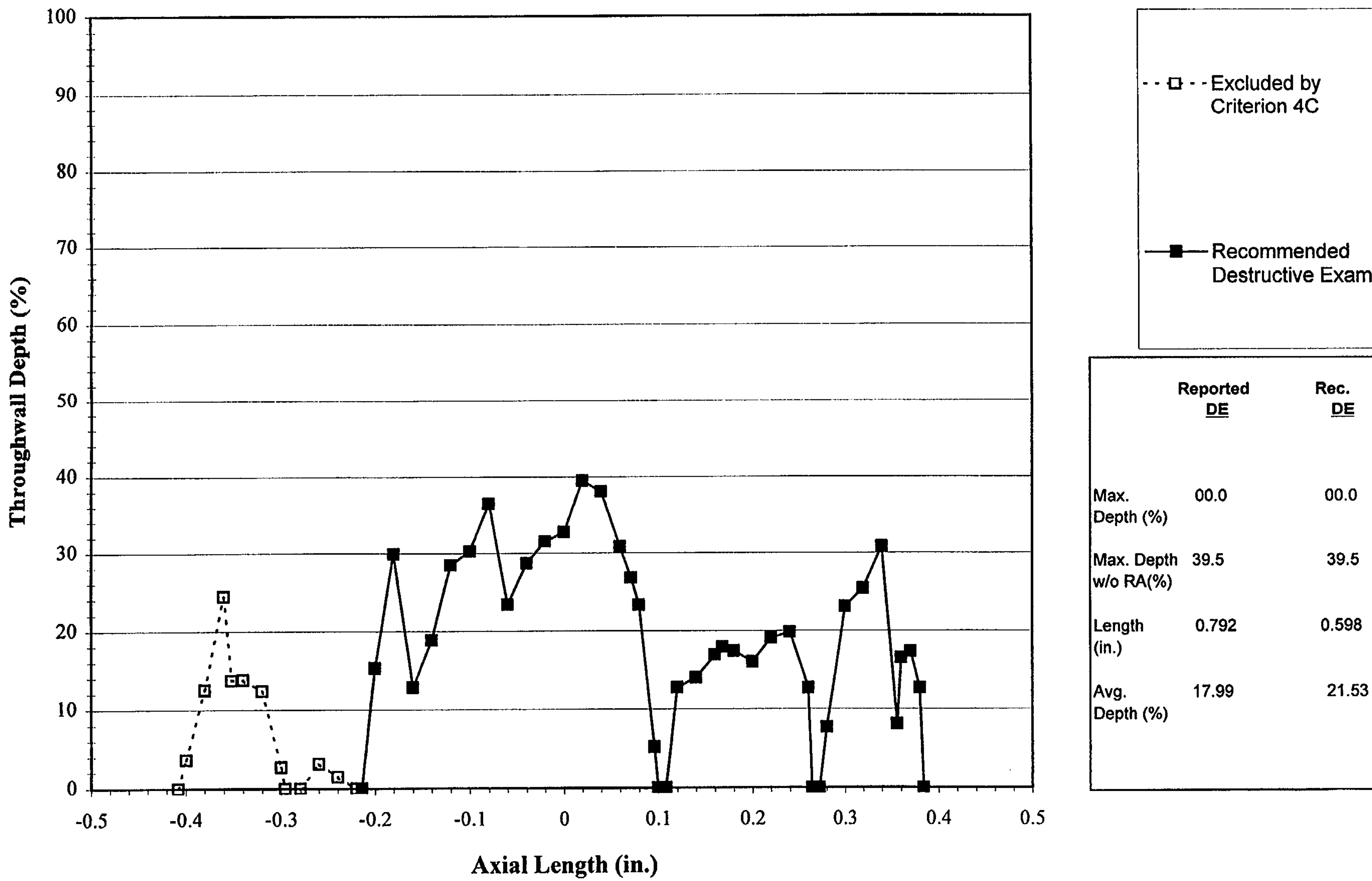

	Reported DE	Rec. DE
Max. Depth (%)	00.0	00.0
Max. Depth w/o RA(%)	39.5	39.5
Length (in.)	0.792	0.598
Avg. Depth (%)	17.99	21.53

Figure C-8
Sample 7, TSP 3H - Crack 1
Mid-Range +Point, 300 kHz
Recommended Destructive Exam and Destructive Exam Excluded by 4C Criterion

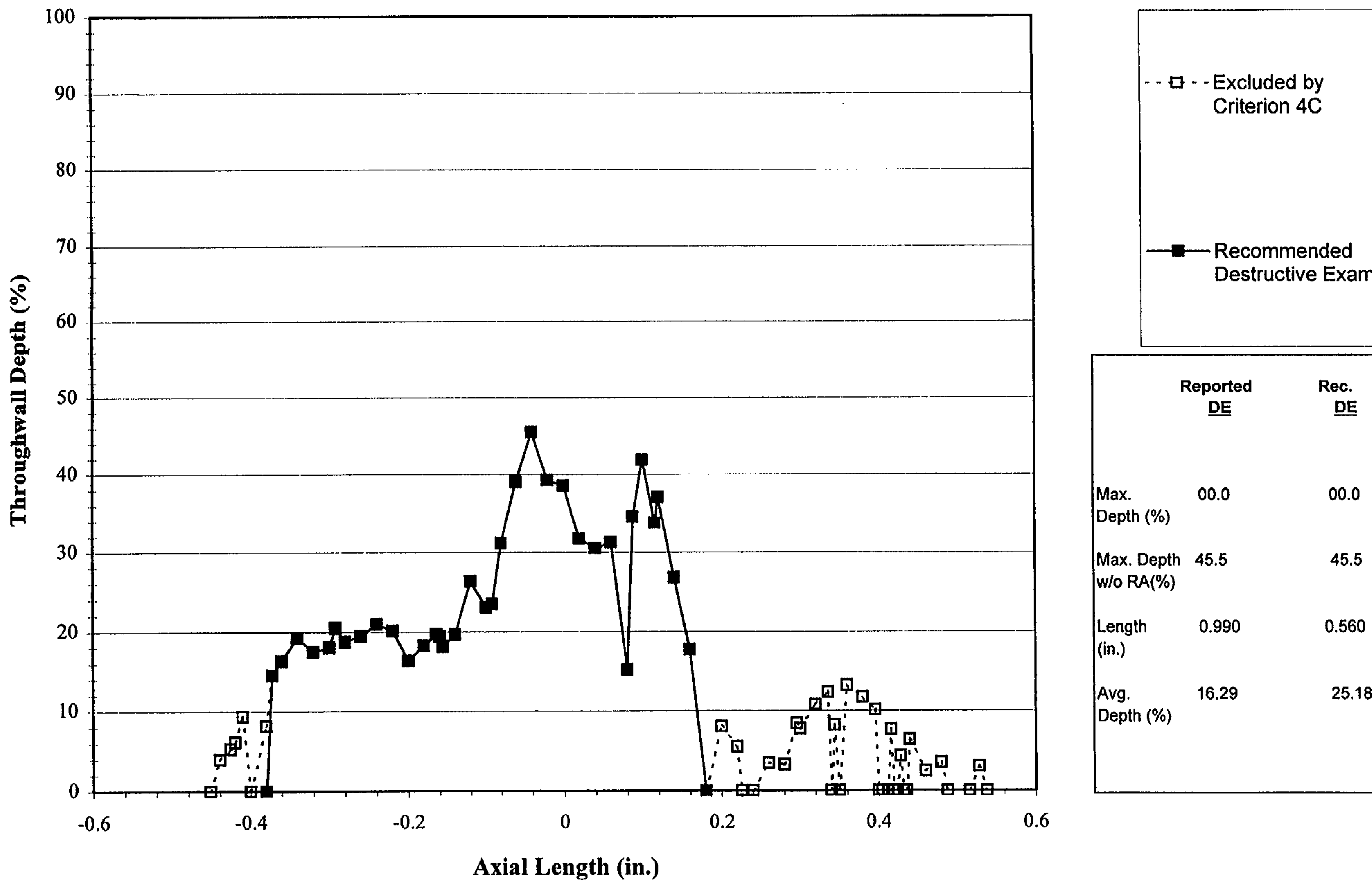

	Reported DE	Rec. DE
Max. Depth (%)	00.0	00.0
Max. Depth w/o RA(%)	45.5	45.5
Length (in.)	0.990	0.560
Avg. Depth (%)	16.29	25.18

Figure C-9
Sample 8, TSP 2H - Crack 1
Mid-Range +Point, 300 kHz
Recommended Destructive Exam and Destructive Exam Excluded by 4C Criterion

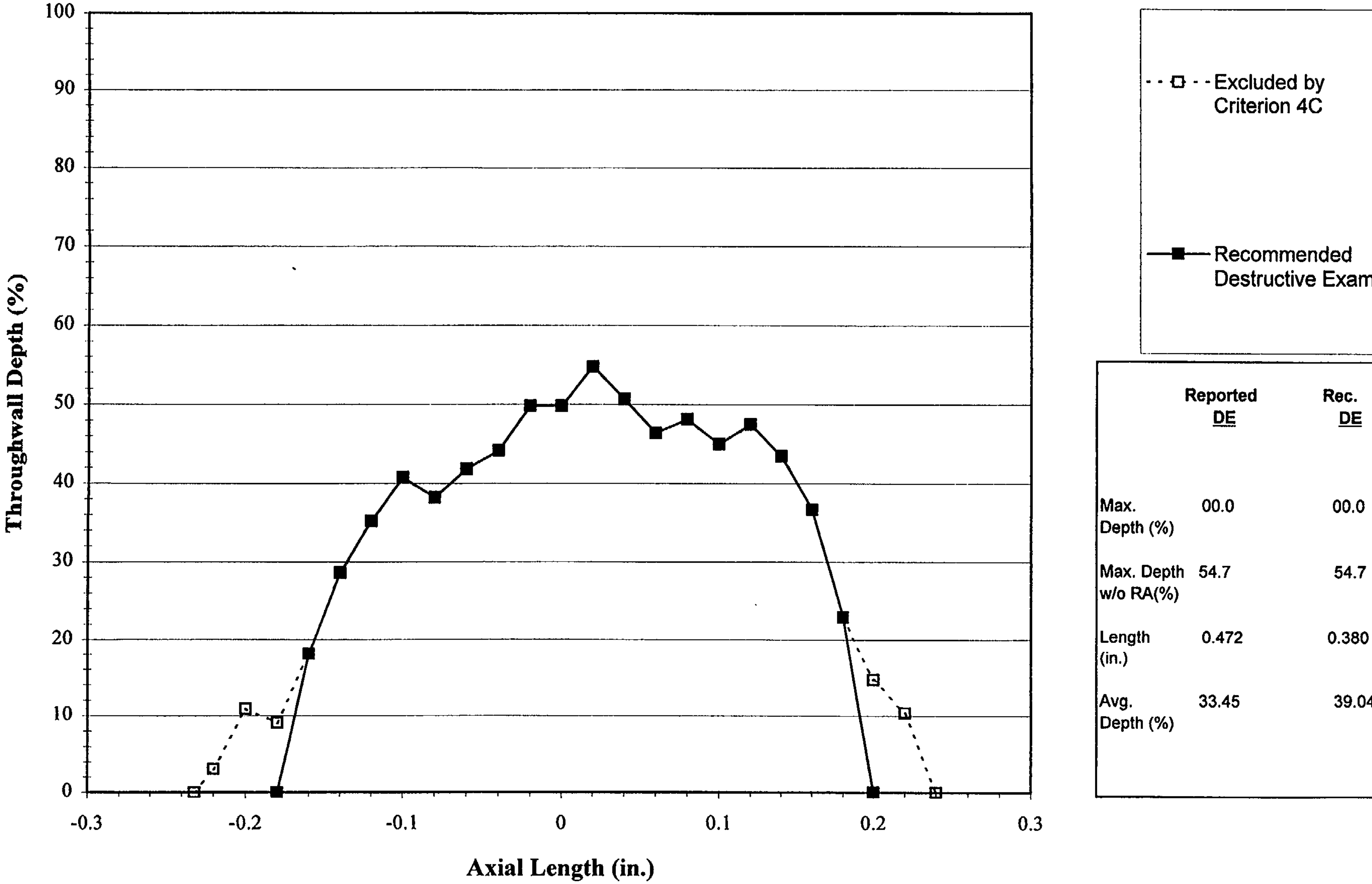

	Reported DE	Rec. DE
Max. Depth (%)	00.0	00.0
Max. Depth w/o RA(%)	54.7	54.7
Length (in.)	0.472	0.380
Avg. Depth (%)	33.45	39.04

Figure C-10
Sample 9, TSP 2H - Crack 2
Depth vs. Axial Length
Recommended Destructive Exam and Destructive Exam Excluded by 4C Criterion

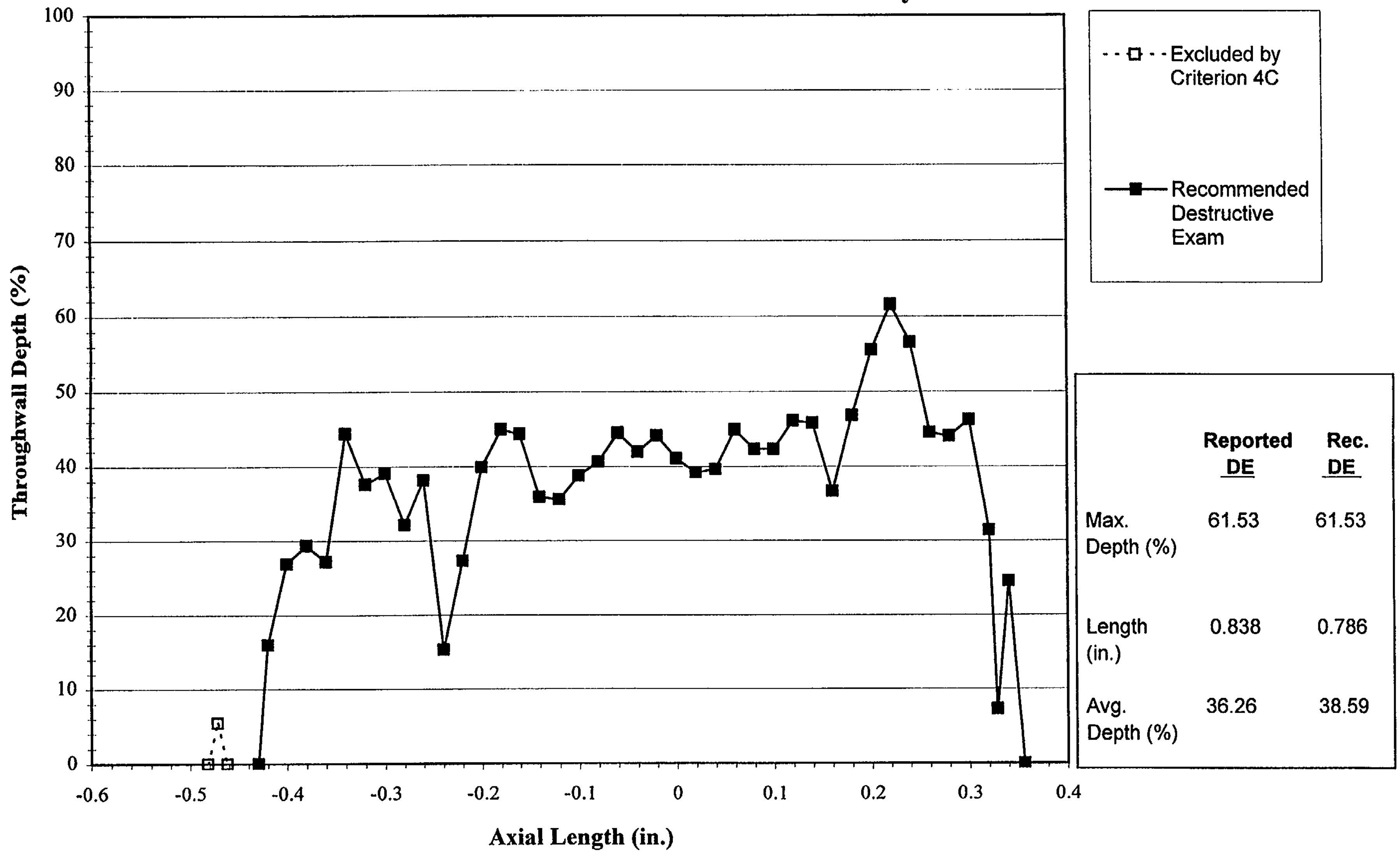

Figure C-11
Sample 9, TSP 3H - Crack 1
Depth vs. Axial Length
Recommended Destructive Exam and Destructive Exam Excluded by 4C Criterion

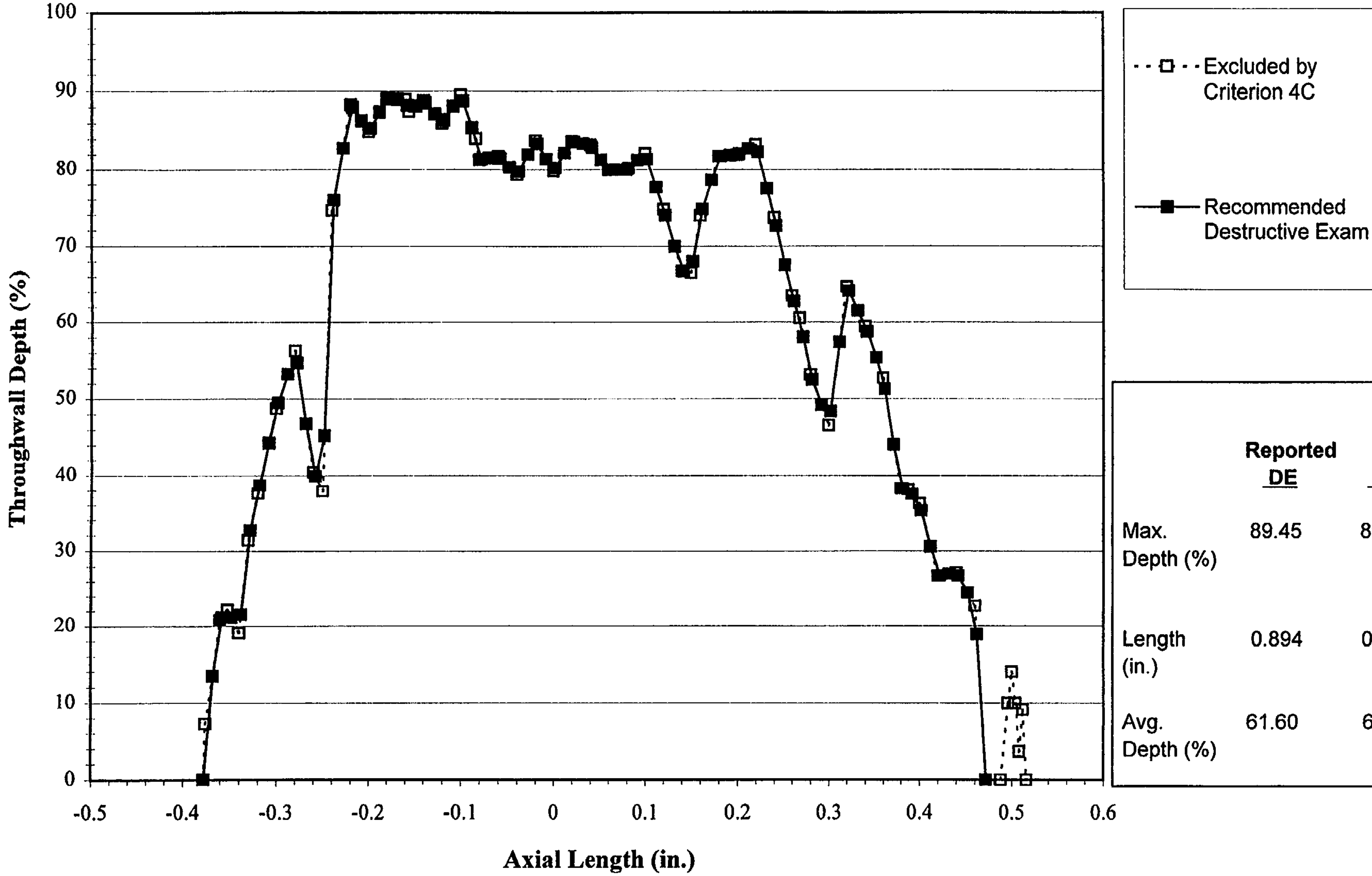

	Reported DE	Rec. DE
Max. Depth (%)	89.45	89.01
Length (in.)	0.894	0.850
Avg. Depth (%)	61.60	64.49

Figure C-12
Sample 9, TSP 3H - Crack 2
Depth vs. Axial Length
Recommended Destructive Exam and Destructive Exam Excluded by 4C Criterion

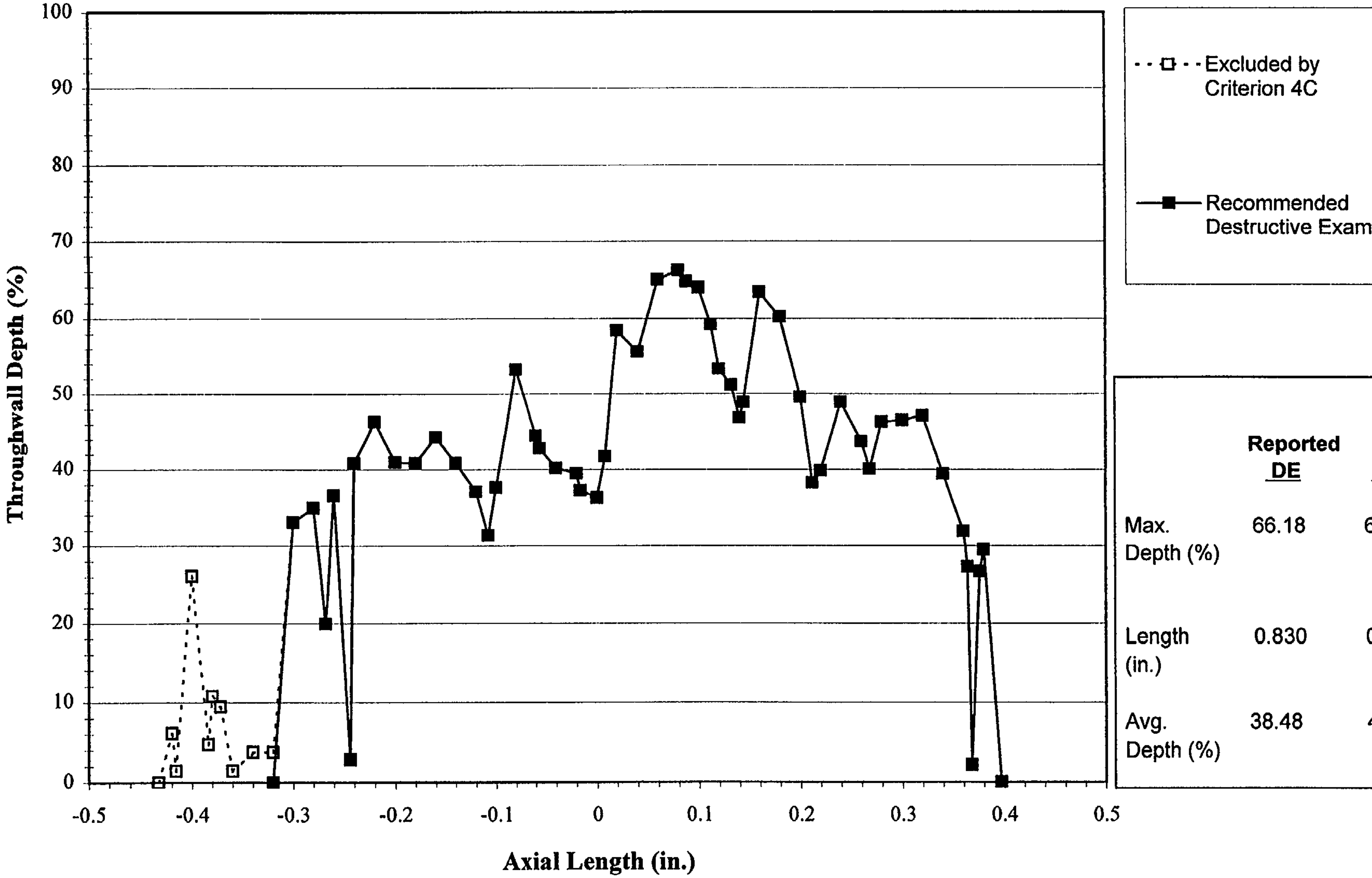

	Reported DE	Rec. DE
Max. Depth (%)	66.18	66.18
Length (in.)	0.830	0.717
Avg. Depth (%)	38.48	43.34

Figure C-13
Sample 9, TSP 5H - Crack 1
Depth vs. Axial Length
Recommended Destructive Exam and Destructive Exam Excluded by 4C Criterion

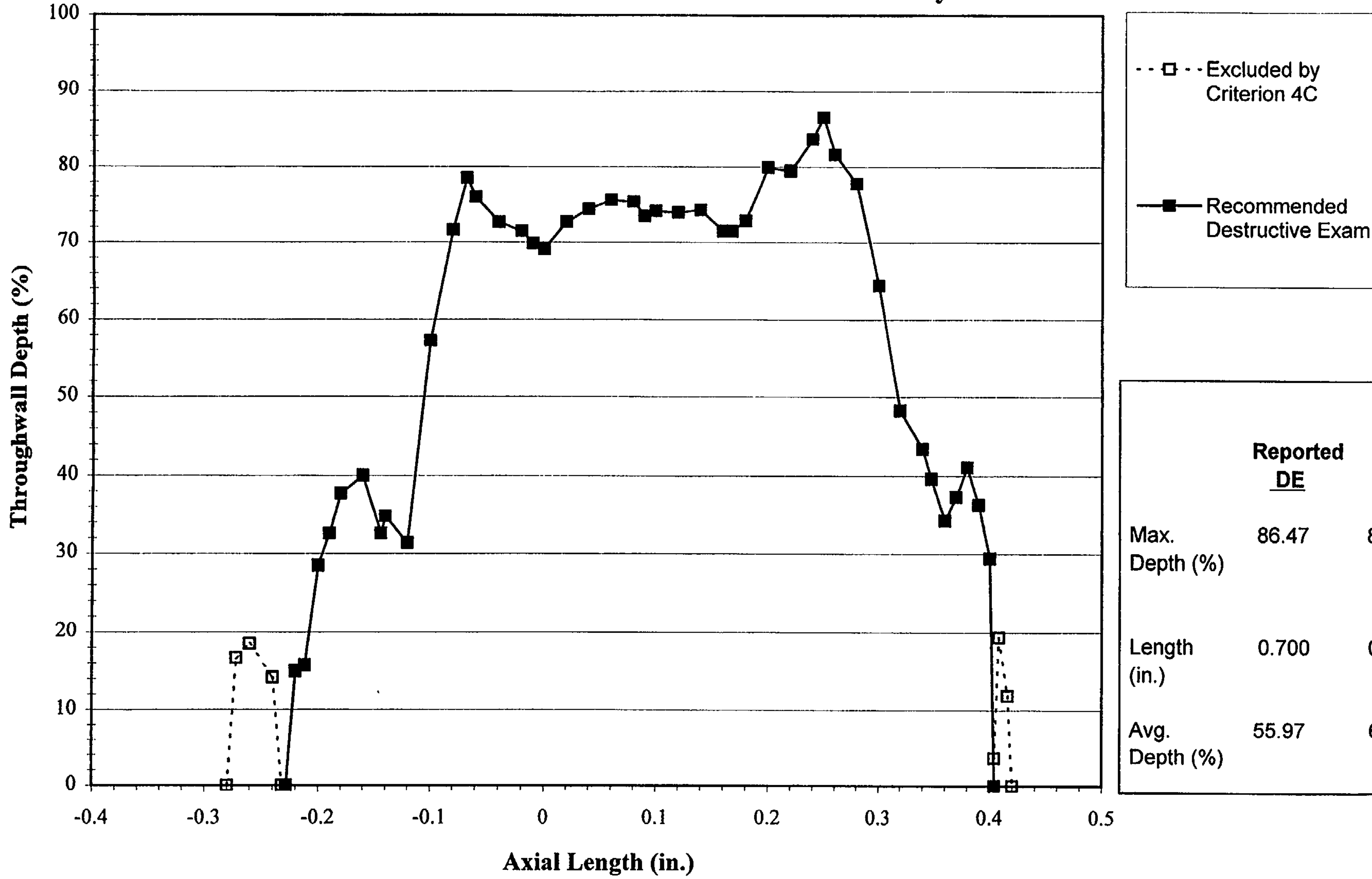

	Reported DE	Rec. DE
Max. Depth (%)	86.47	86.47
Length (in.)	0.700	0.632
Avg. Depth (%)	55.97	60.62

Figure C-14
Sample 11, TSP 3H - Crack 1
Depth vs. Axial Length
Recommended Destructive Exam and Destructive Exam Excluded by 4C Criterion

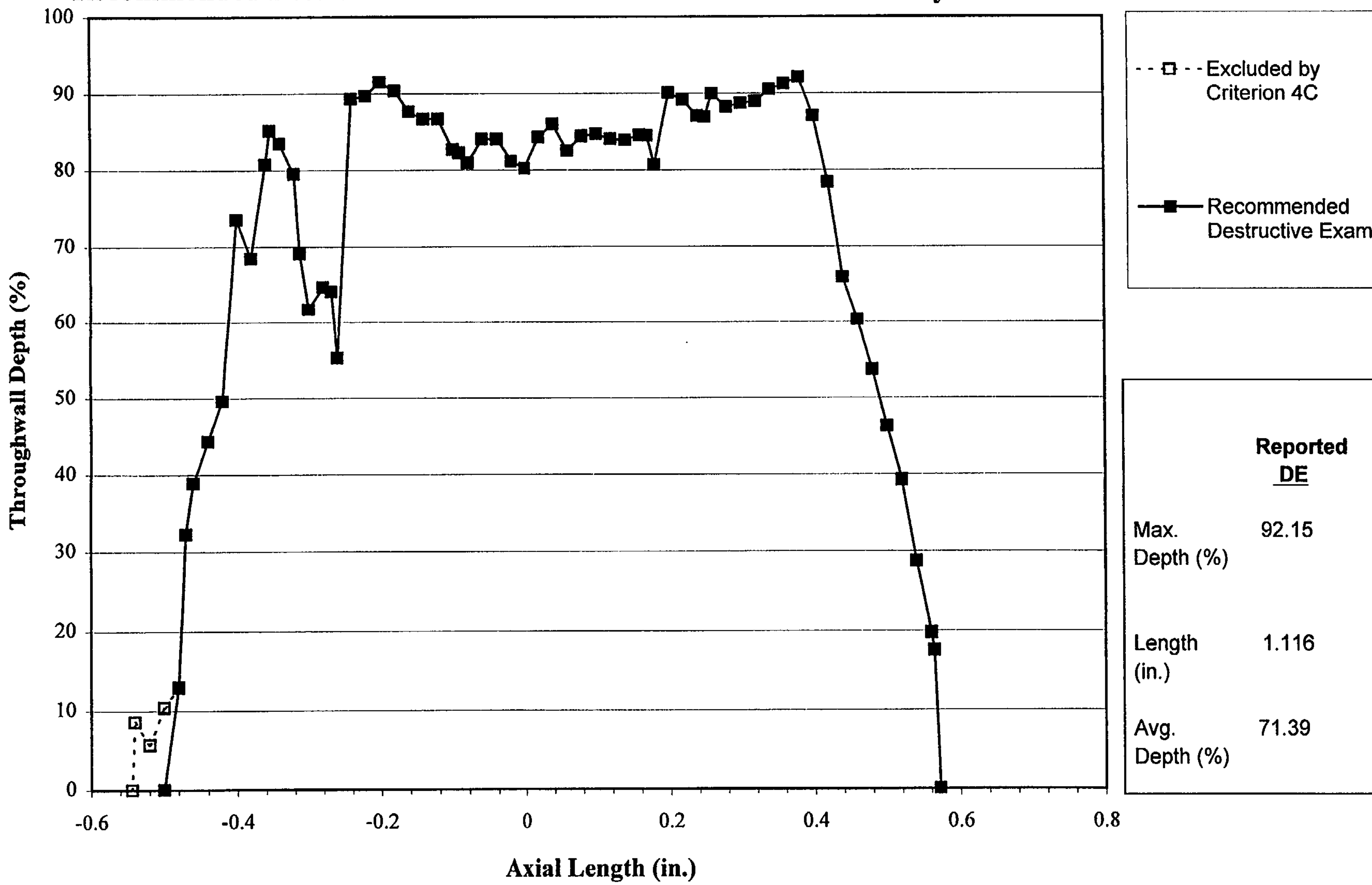

	Reported DE	Rec. DE
Max. Depth (%)	92.15	92.15
Length (in.)	1.116	1.072
Avg. Depth (%)	71.39	73.93

Figure C-15
Sample 11, TSP 3H - Crack 2
Depth vs. Axial Length
Recommended Destructive Exam and Destructive Exam Excluded by 4C Criterion

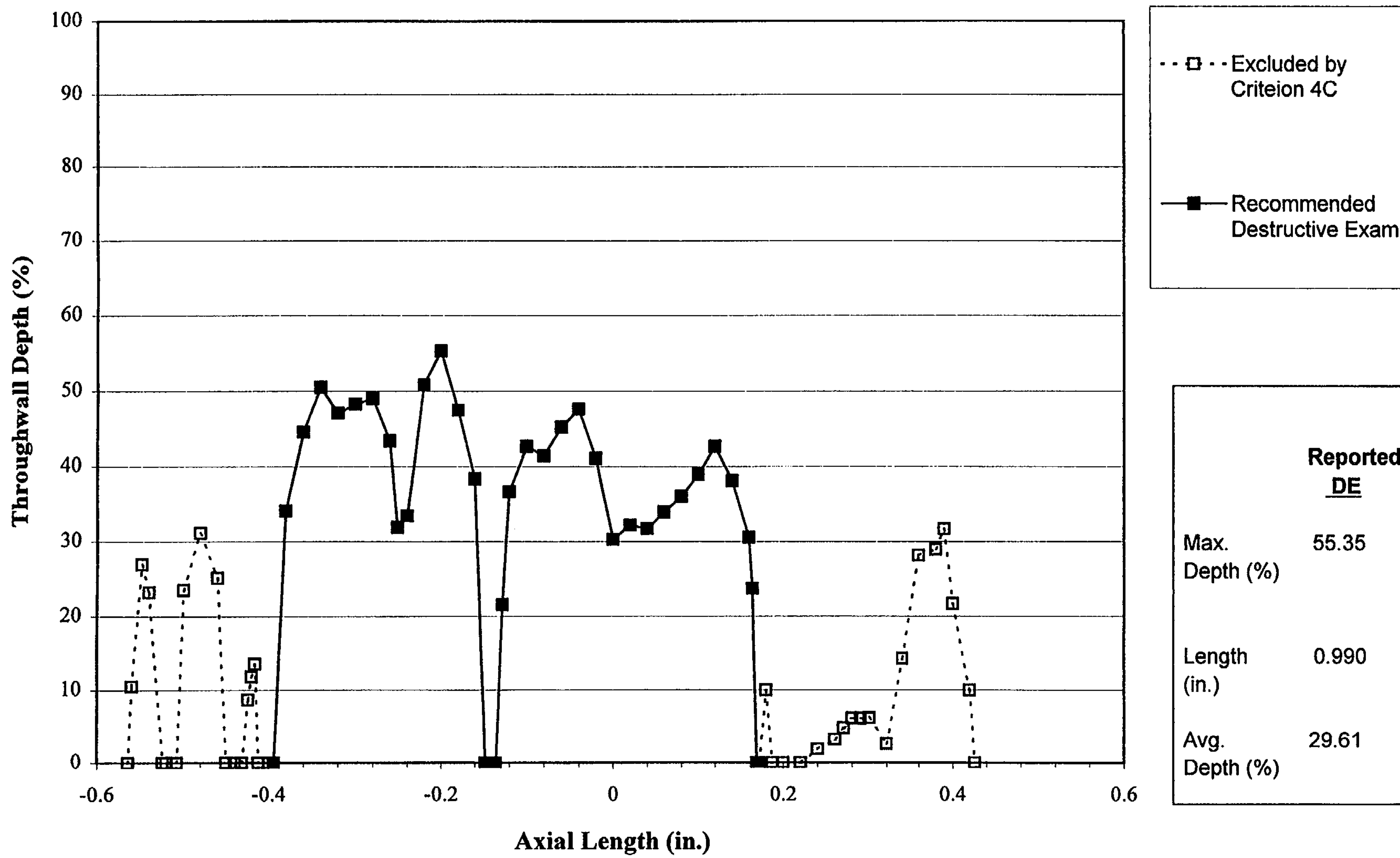

	Reported DE	Rec. DE
Max. Depth (%)	55.35	55.35
Length (in.)	0.990	0.563
Avg. Depth (%)	29.61	38.56

Figure C-16
Sample 11, TSP 4H - Crack 1
Depth vs. Axial Length
Recommended Destructive Exam and Destructive Exam Excluded by 4C Criterion

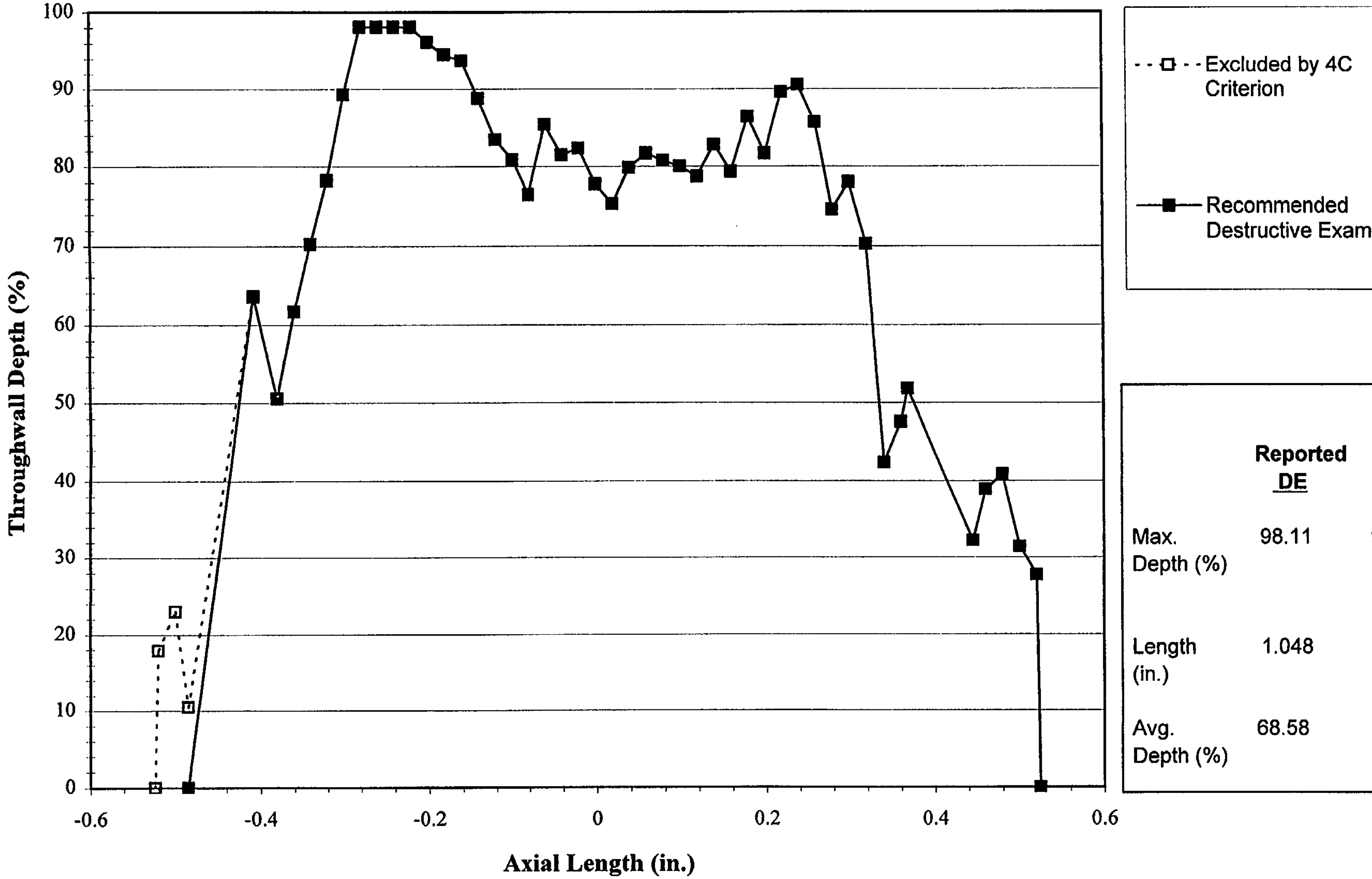

	Reported DE	Rec. DE
Max. Depth (%)	98.11	98.11
Length (in.)	1.048	1.009
Avg. Depth (%)	68.58	70.14

Figure C-17
Sample 12, TSP 4H
Depth vs. Axial Length
Recommended Destructive Exam and Destructive Exam Excluded by 4C Criterion

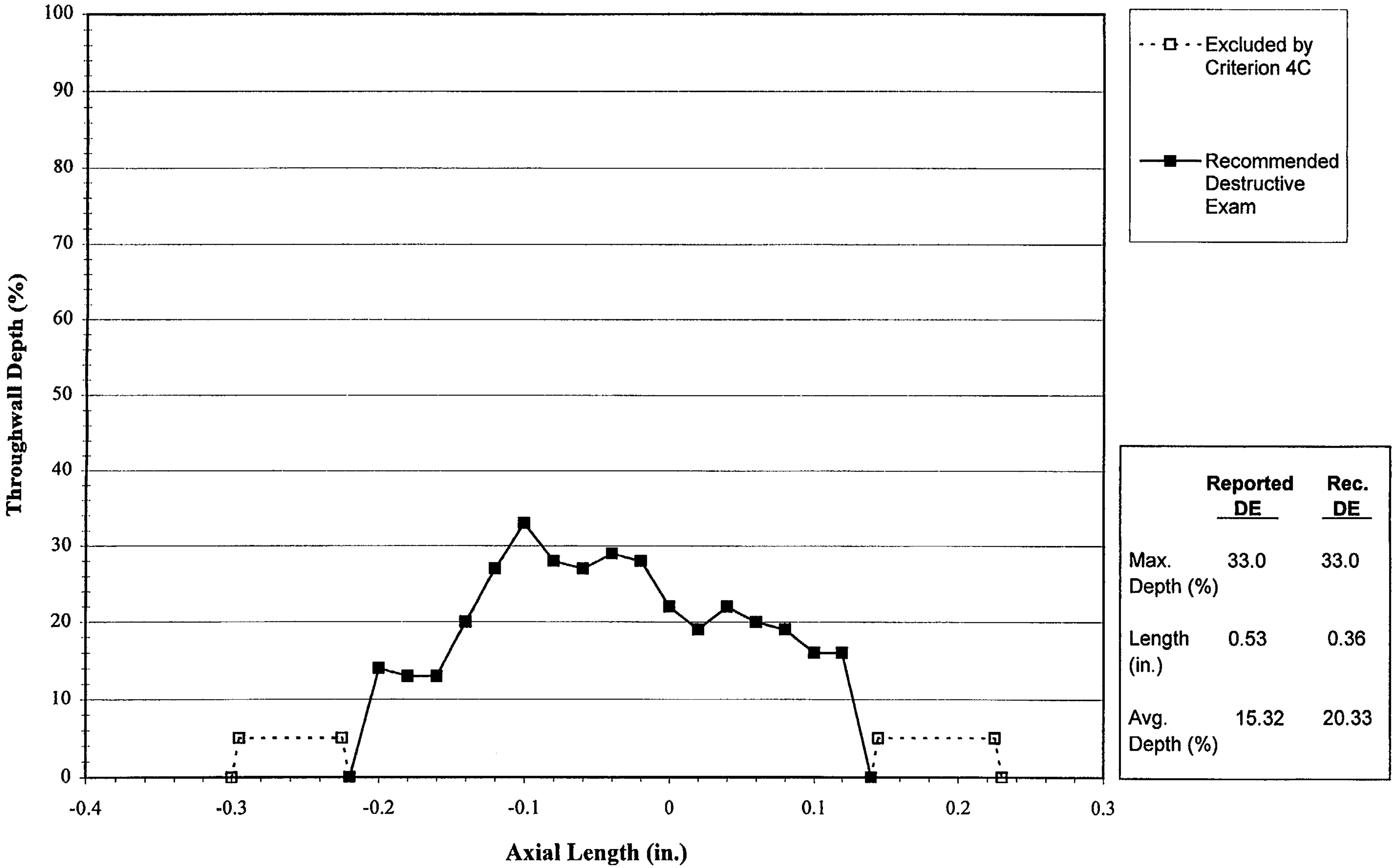

Figure C-18
Sample P9 - Crack 2
Depth vs. Axial Length
Recommended Destructive Exam and Destructive Exam Excluded by 4C Criterion

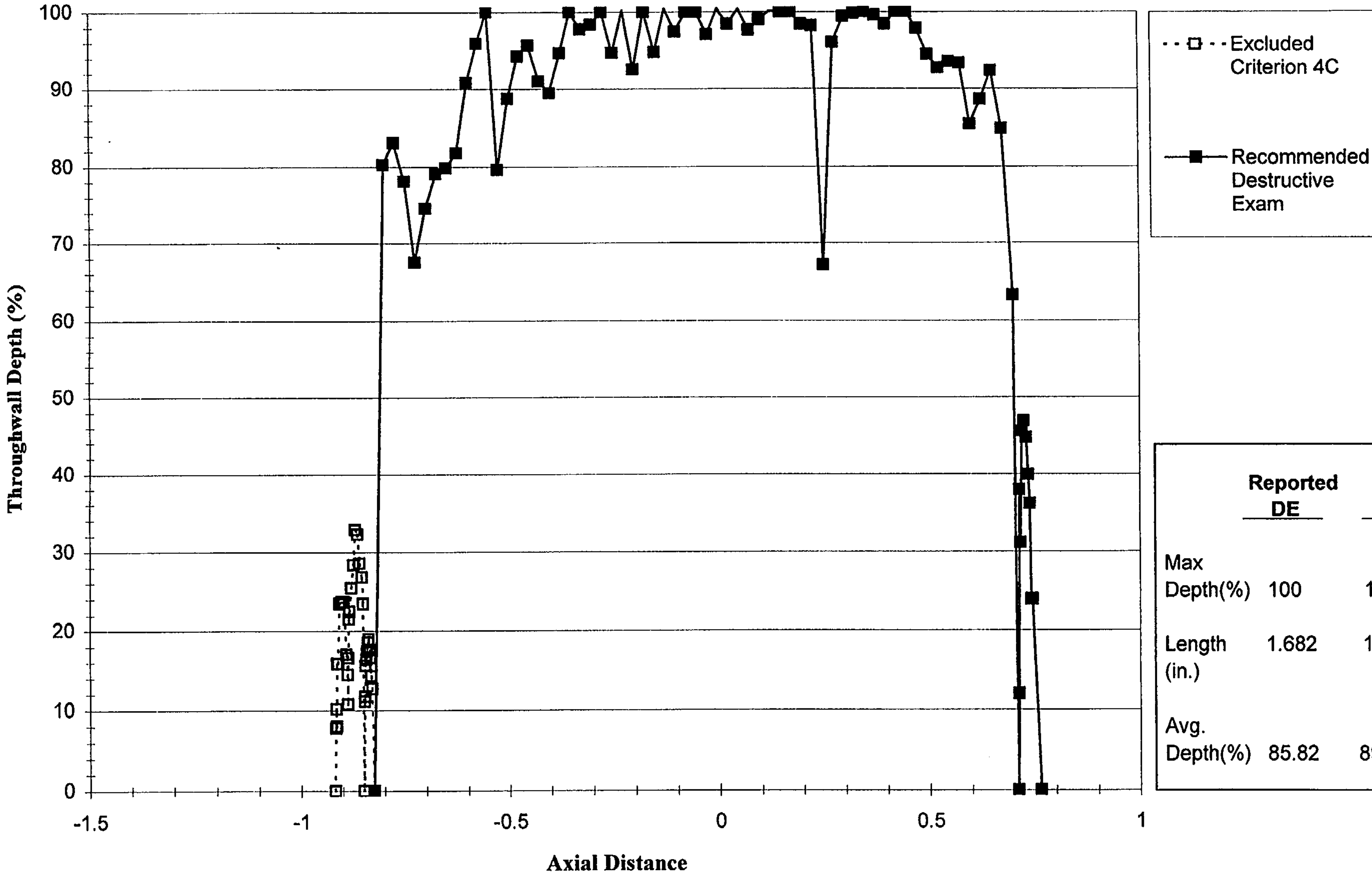

	Reported DE	Rec. DE
Max Depth(%)	100	100
Length (in.)	1.682	1.589
Avg. Depth(%)	85.82	89.64

Figure C-19
Sample P10 - Crack 2
Depth vs. Axial Length
Recommended Destructive Exam and Destructive Exam Excluded by 4C Criterion

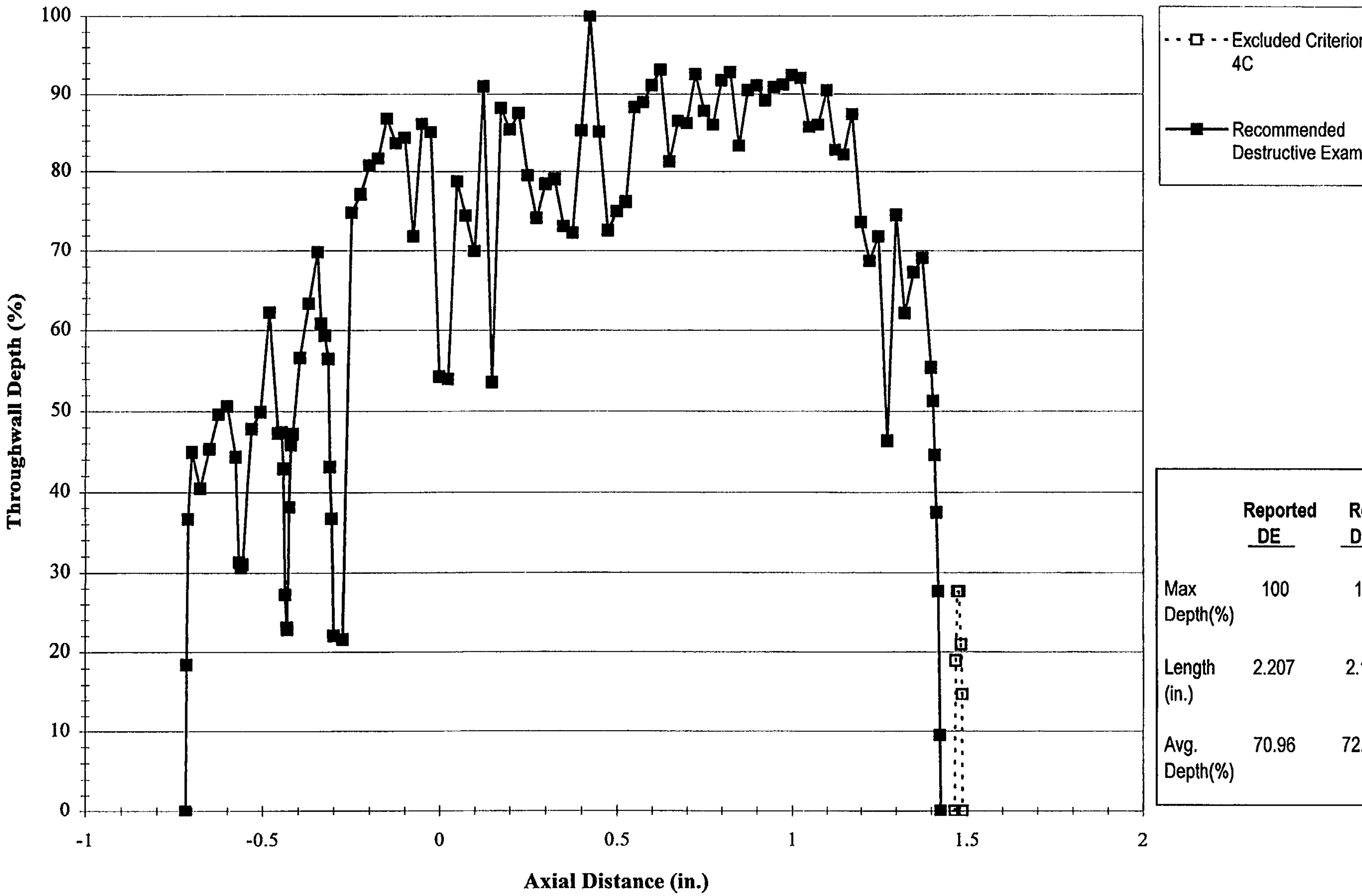

	Reported DE	Rec. DE
Max Depth(%)	100	100
Length (in.)	2.207	2.146
Avg. Depth(%)	70.96	72.76

APPENDIX D

Plots of NDE Performance Test Analyses for +Point Coil Depth Profiles with Destructive Exam Data

PWSCC ARC Release 1.1

Figure D-1
Specimen R 1 - C 85 - 01H - Crack 1 - Year 1998
Comparison of Unadjusted, Adjusted, Burst and Voltage with Exam
NDE Depth vs. Axial Length

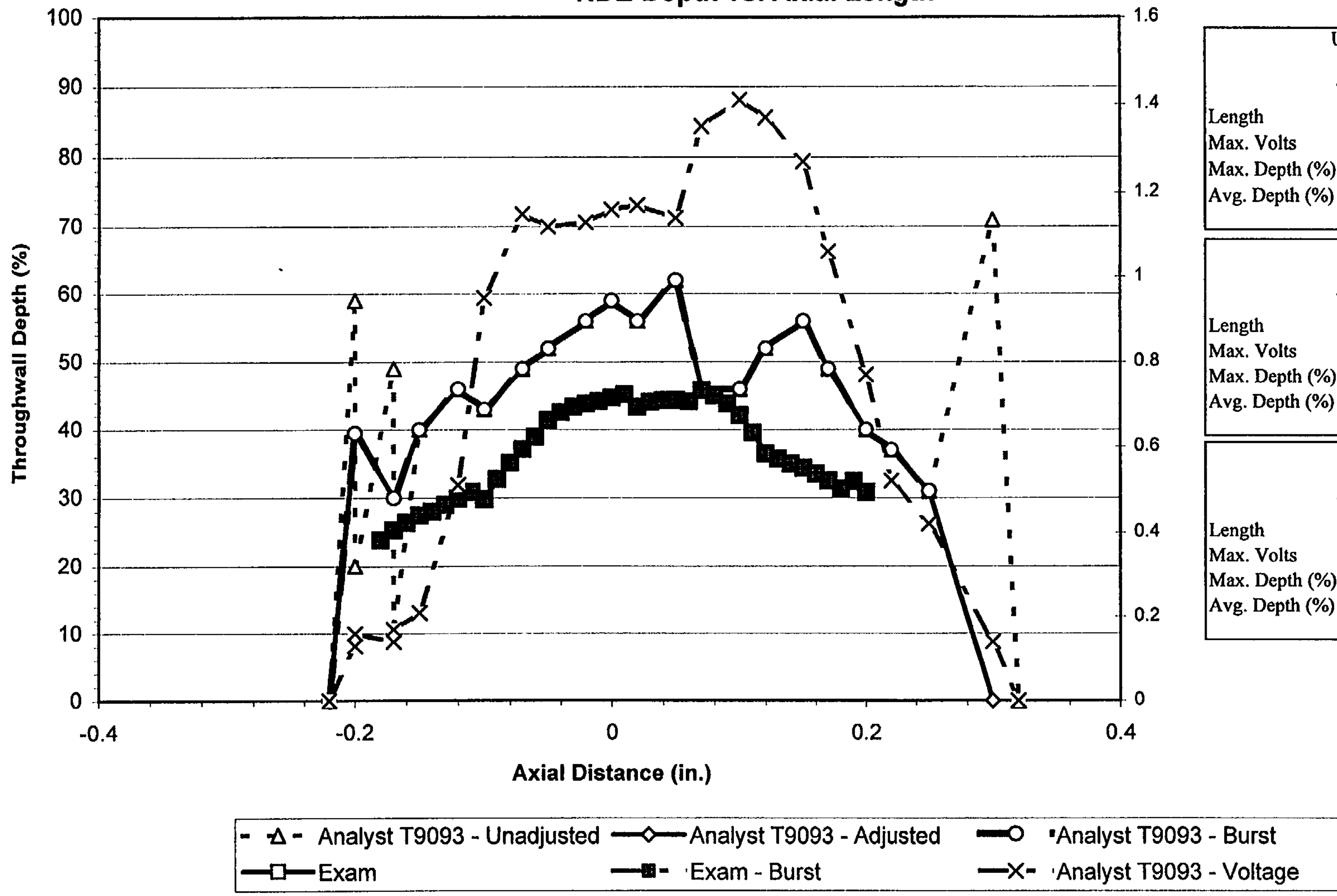

Unadjusted	T9093	Exam
Length	0.54	0.38
Max. Volts	1.41	
Max. Depth (%)	71.0	45.8
Avg. Depth (%)	46.1	37.1

Adjusted	T9093	Exam
Length	0.52	0.38
Max. Volts	1.41	
Max. Depth (%)	62.0	45.8
Avg. Depth (%)	43.1	37.1

Burst	T9093	Exam
Length	0.47	0.38
Max. Volts	1.41	
Max. Depth (%)	62.0	45.8
Avg. Depth (%)	46.0	37.1

PWSCC ARC Release 1.1

Figure D-2
Specimen R 1 - C 91 - 01H - Crack 1 - Year 1998
Comparison of Unadjusted, Adjusted, Burst and Voltage with Exam
NDE Depth vs. Axial Length

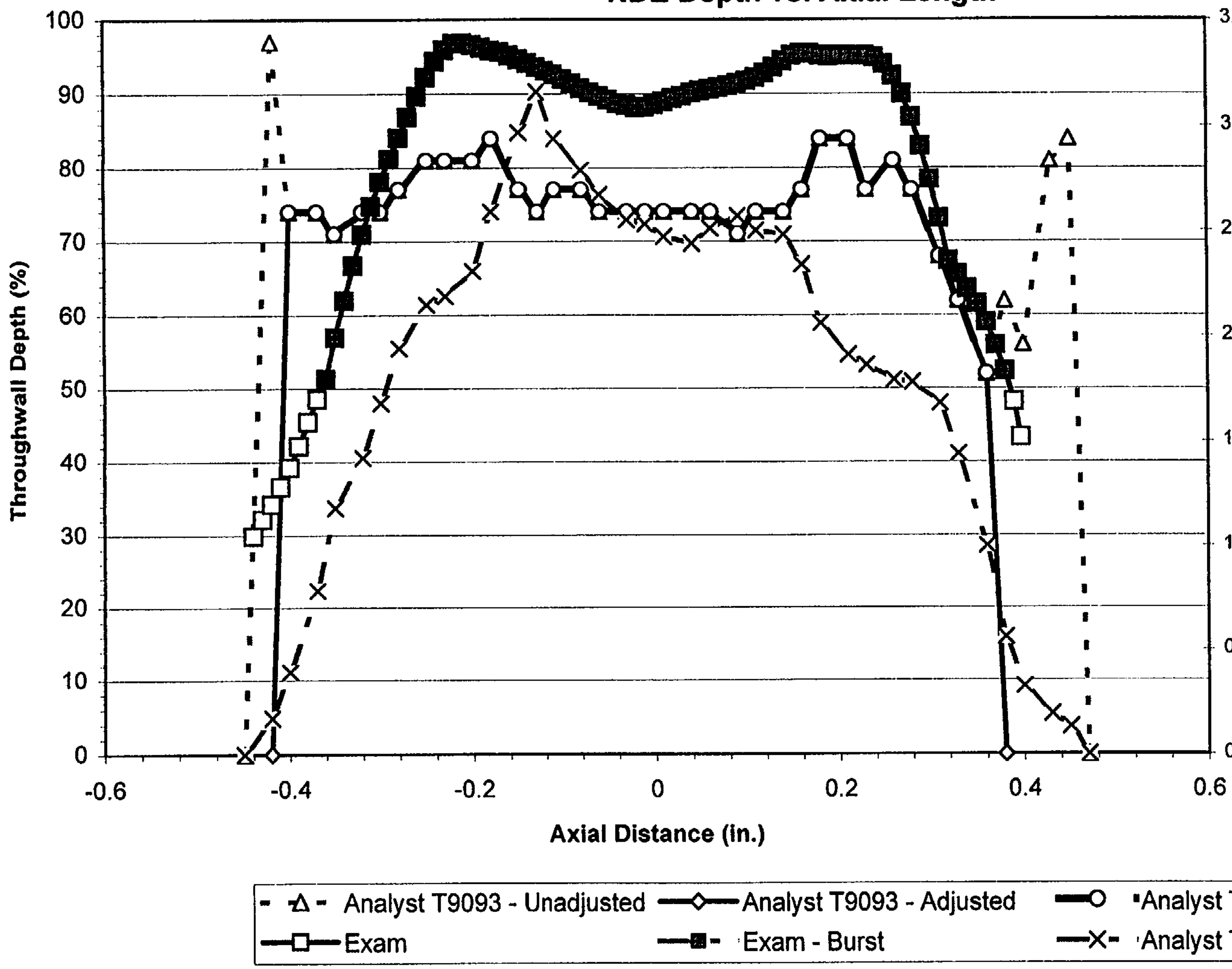

Unadjusted

	T9093	Exam
Length	0.92	0.84
Max. Volts	3.16	
Max. Depth (%)	97.0	96.8
Avg. Depth (%)	73.2	81.4

Adjusted

	T9093	Exam
Length	0.80	0.84
Max. Volts	3.16	
Max. Depth (%)	84.0	96.8
Avg. Depth (%)	73.2	81.4

Burst

	T9093	Exam
Length	0.76	0.74
Max. Volts	3.16	
Max. Depth (%)	84.0	96.8
Avg. Depth (%)	75.4	86.6

Figure D-3
Specimen R 1 - C 91 - 01H - Crack 2 - Year 1998
Comparison of Unadjusted, Adjusted, Burst and Voltage with Exam
NDE Depth vs. Axial Length

PWSCC ARC Release 1.1

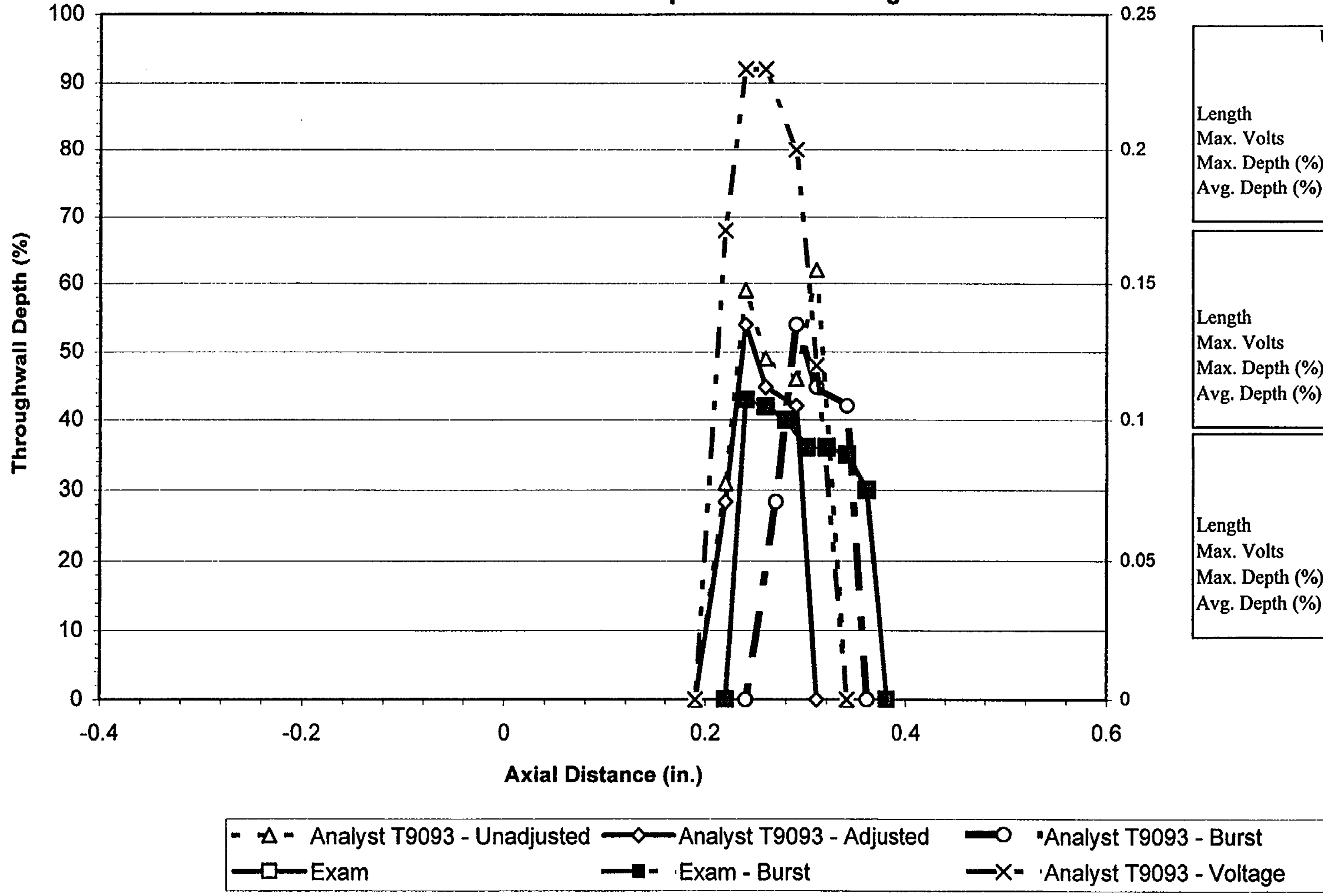

Unadjusted

	T9093	Exam
Length	0.15	0.16
Max. Volts	0.23	
Max. Depth (%)	62.0	43.0
Avg. Depth (%)	39.2	32.8

Adjusted

	T9093	Exam
Length	0.12	0.16
Max. Volts	0.23	
Max. Depth (%)	54.0	43.0
Avg. Depth (%)	33.0	32.8

Burst

	T9093	Exam
Length	0.12	0.16
Max. Volts	0.23	
Max. Depth (%)	54.0	43.0
Avg. Depth (%)	33.0	32.8

PWSCC ARC Release 1.1

Figure D-4
Specimen R 2 - C 66 - 01H - Crack 1 - Year 1998
Comparison of Unadjusted, Adjusted, Burst and Voltage with Exam
NDE Depth vs. Axial Length

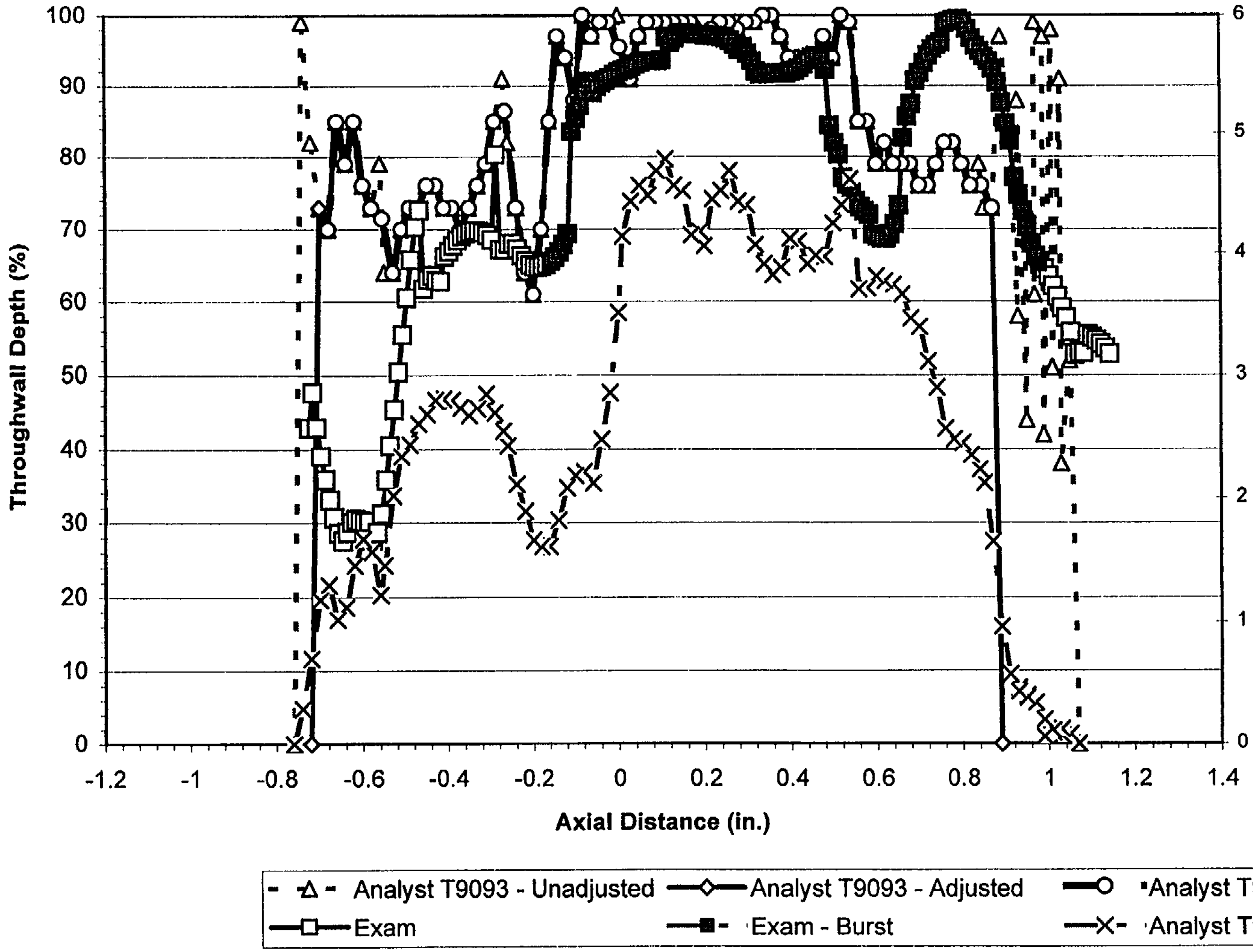

Unadjusted

	T9093	Exam
Length	1.83	1.87
Max. Volts	4.78	
Max. Depth (%)	100.0	99.5
Avg. Depth (%)	83.4	75.3

Adjusted

	T9093	Exam
Length	1.61	1.87
Max. Volts	4.78	
Max. Depth (%)	100.0	99.5
Avg. Depth (%)	84.4	75.3

Burst

	T9093	Exam
Length	1.55	1.14
Max. Volts	4.78	
Max. Depth (%)	100.0	99.5
Avg. Depth (%)	85.8	88.0

PWSCC ARC Release 1.1

Figure D-5
Specimen R 2 - C 66 - 01H - Crack 2 - Year 1998
Comparison of Unadjusted, Adjusted, Burst and Voltage with Exam
NDE Depth vs. Axial Length

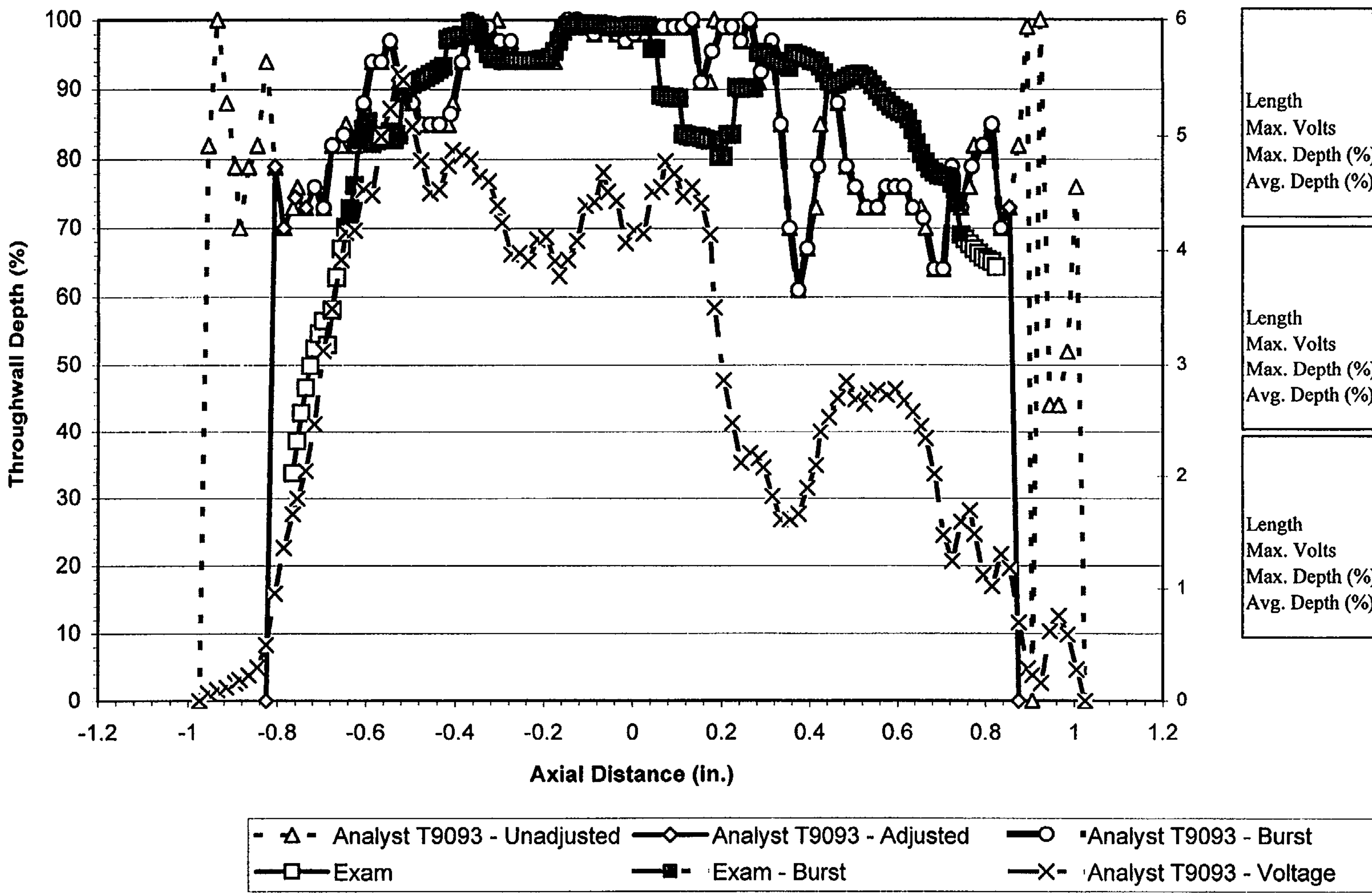

Unadjusted	T9093	Exam
Length	2.00	1.59
Max. Volts	5.54	
Max. Depth (%)	100.0	99.4
Avg. Depth (%)	84.0	86.6

Adjusted	T9093	Exam
Length	1.70	1.59
Max. Volts	5.51	
Max. Depth (%)	100.0	99.4
Avg. Depth (%)	85.8	86.6

Burst	T9093	Exam
Length	1.55	1.39
Max. Volts	5.51	
Max. Depth (%)	100.0	99.4
Avg. Depth (%)	87.9	90.6

PWSCC ARC Release 1.1

Figure D-6
Specimen R 5 - C 18 - 01H - Crack 1 - Year 1998
Comparison of Unadjusted, Adjusted, Burst and Voltage with Exam NDE Depth vs. Axial Length

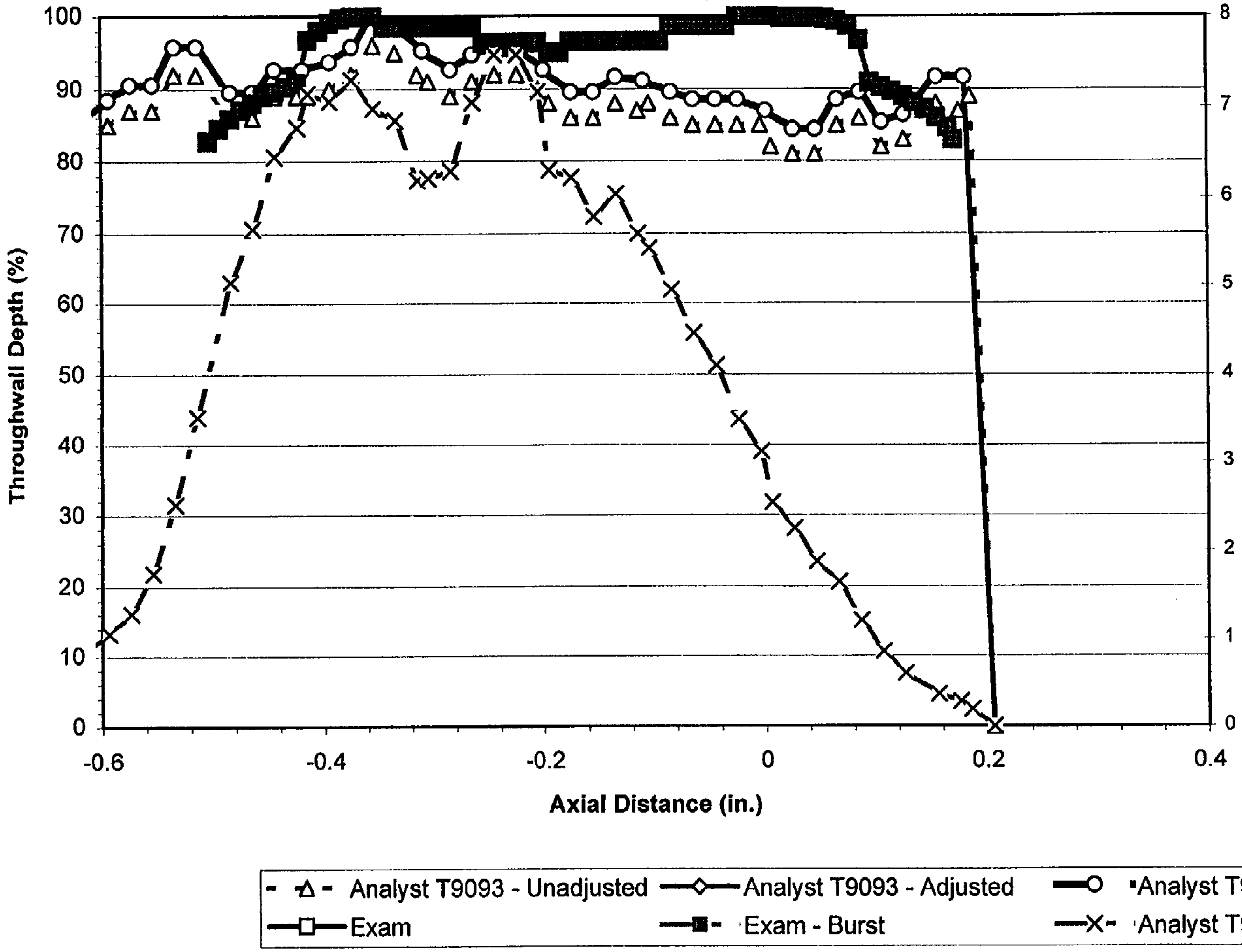

Unadjusted

	T9093	Exam
Length	0.93	0.68
Max. Volts	7.58	
Max. Depth (%)	96.0	100.0
Avg. Depth (%)	83.1	95.6

Adjusted

	T9093	Exam
Length	0.93	0.68
Max. Volts	7.58	
Max. Depth (%)	100.0	100.0
Avg. Depth (%)	86.3	95.6

Burst

	T9093	Exam
Length	0.86	0.68
Max. Volts	7.58	
Max. Depth (%)	100.0	100.0
Avg. Depth (%)	89.7	95.6

PWSCC ARC Release 1.1

Figure D-7
Specimen SG R 5 - C 18 - 01H - Crack 2 - Year 1998
Comparison of Unadjusted, Adjusted, Burst and Voltage with Exam
NDE Depth vs. Axial Length

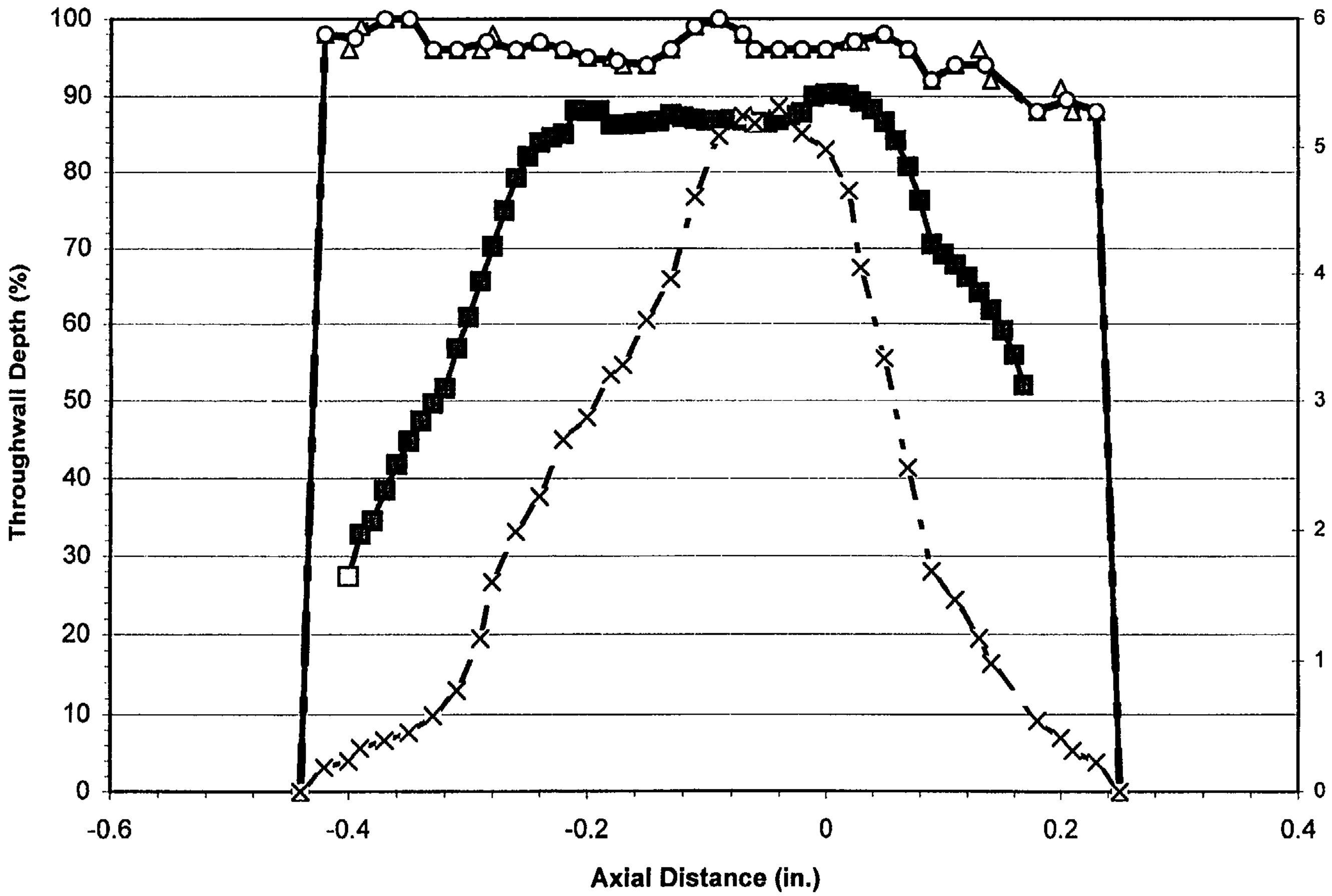

Unadjusted	T9093	Exam
Length	0.69	0.57
Max. Volts	5.32	
Max. Depth (%)	100.0	90.3
Avg. Depth (%)	92.7	74.6

Adjusted	T9093	Exam
Length	0.69	0.57
Max. Volts	5.32	
Max. Depth (%)	100.0	90.3
Avg. Depth (%)	92.7	74.6

Burst	T9093	Exam
Length	0.69	0.56
Max. Volts	5.32	
Max. Depth (%)	100.0	90.3
Avg. Depth (%)	92.7	75.4

PWSCC ARC Release 1.1

Figure D-8
Specimen SG R 6 - C 24 - 01H - Crack 1 - Year 1998
Comparison of Unadjusted, Adjusted, Burst and Voltage with Exam
NDE Depth vs. Axial Length

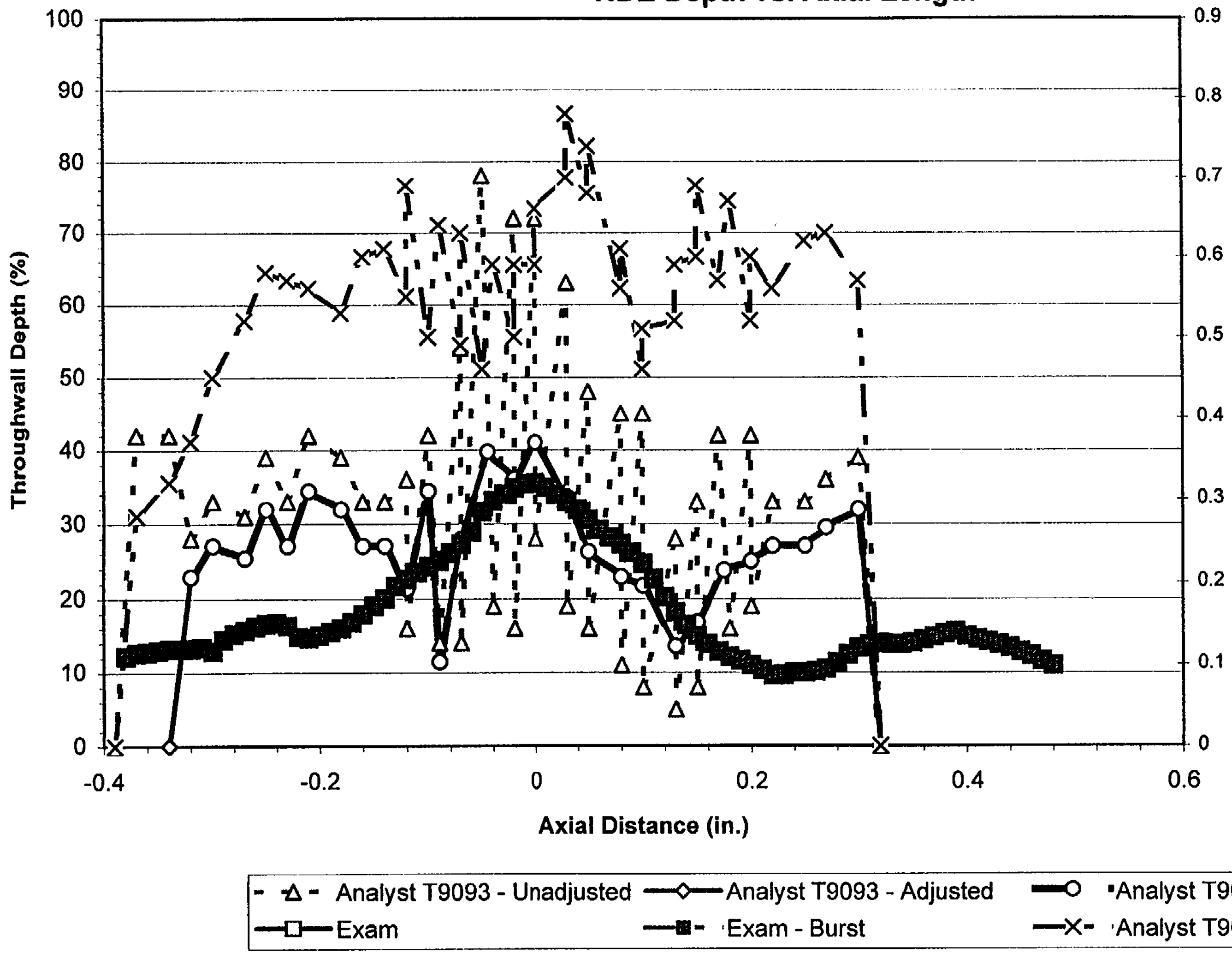

Unadjusted	T9093	Exam
Length	0.71	0.86
Max. Volts	0.78	
Max. Depth (%)	78.0	35.5
Avg. Depth (%)	33.4	18.3

Adjusted	T9093	Exam
Length	0.66	0.86
Max. Volts	0.74	
Max. Depth (%)	41.0	35.5
Avg. Depth (%)	26.7	18.3

Burst	T9093	Exam
Length	0.64	0.86
Max. Volts	0.74	
Max. Depth (%)	41.0	35.5
Avg. Depth (%)	27.2	18.3

PWSCC ARC Release 1.1

Figure D-9
Specimen R 6 - C 31 - 01H - Crack 1 - Year 1998
Comparison of Unadjusted, Adjusted, Burst and Voltage with Exam
NDE Depth vs. Axial Length

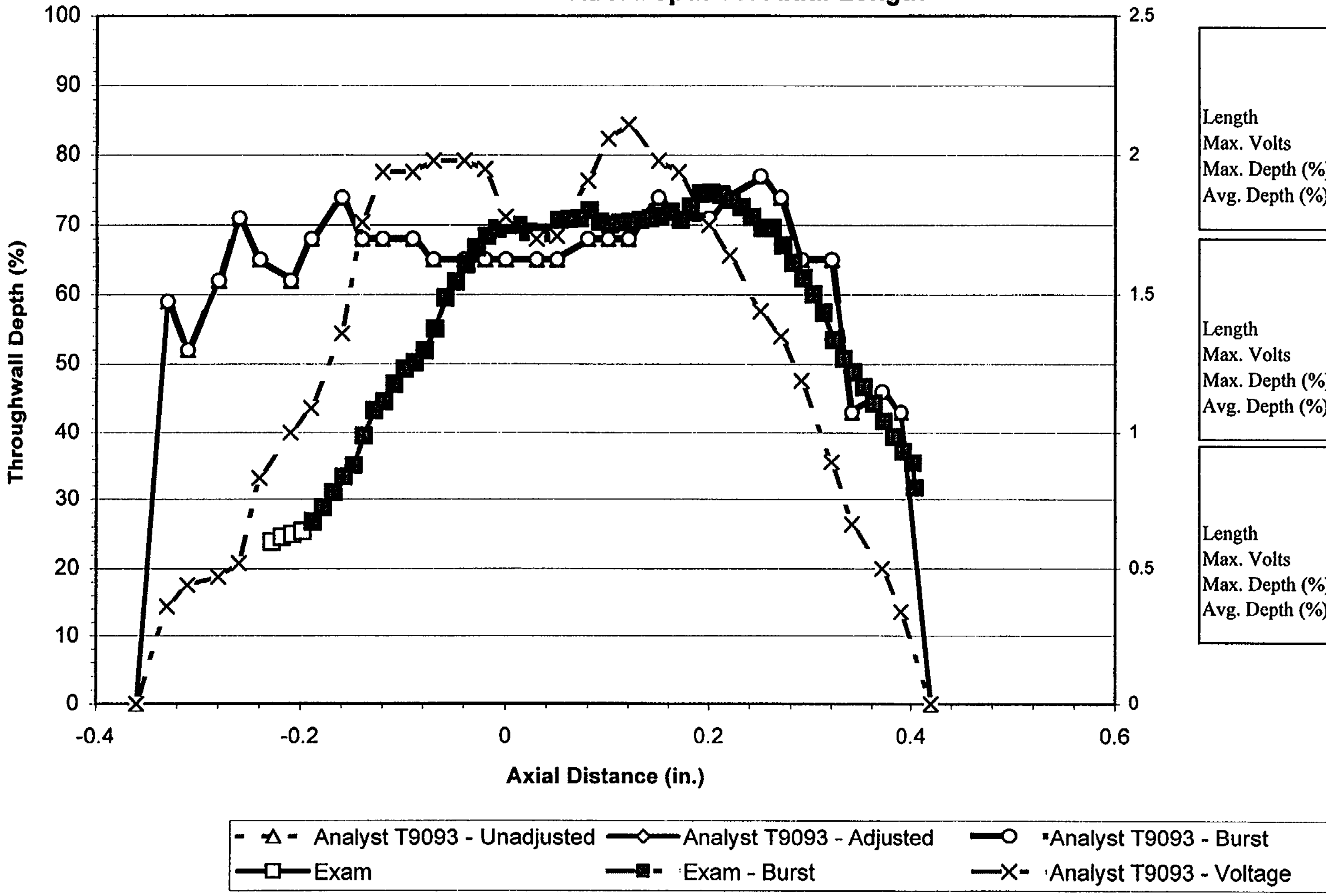

Unadjusted	T9093	Exam
Length	0.78	0.63
Max. Volts	2.11	
Max. Depth (%)	77.0	74.6
Avg. Depth (%)	62.3	57.5

Adjusted	T9093	Exam
Length	0.78	0.63
Max. Volts	2.11	
Max. Depth (%)	77.0	74.6
Avg. Depth (%)	62.3	57.5

Burst	T9093	Exam
Length	0.72	0.59
Max. Volts	2.11	
Max. Depth (%)	77.0	74.6
Avg. Depth (%)	65.4	59.7

PWSCC ARC Release 1.1

Figure D-10
Specimen R 6 - C 31 - 01H - Crack 2 - Year 1998
Comparison of Unadjusted, Adjusted, Burst and Voltage with Exam
NDE Depth vs. Axial Length

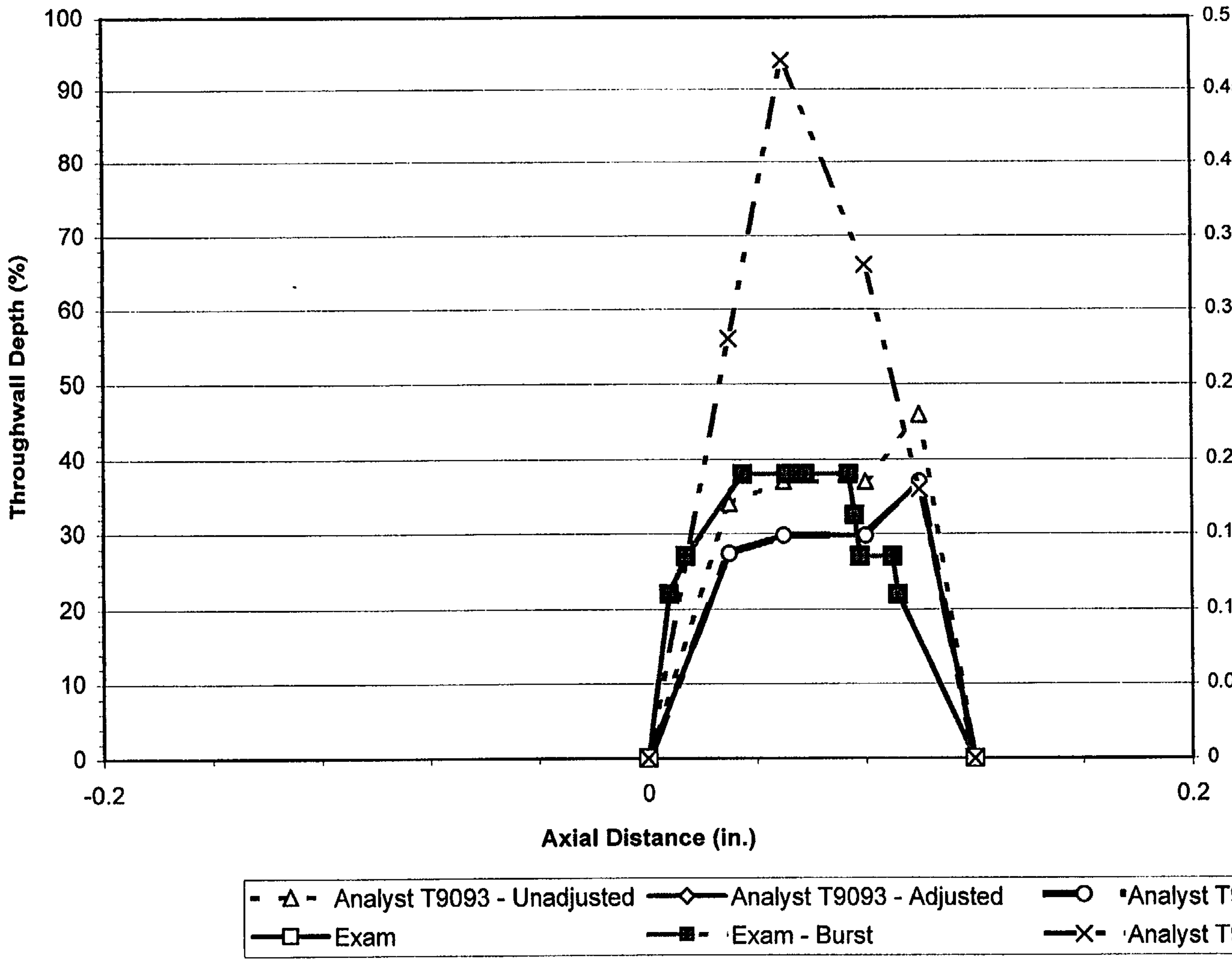

Unadjusted

	T9093	Exam
Length	0.12	0.12
Max. Volts	0.47	
Max. Depth (%)	46.0	38.0
Avg. Depth (%)	30.2	26.8

Adjusted

	T9093	Exam
Length	0.12	0.12
Max. Volts	0.47	
Max. Depth (%)	37.0	38.0
Avg. Depth (%)	24.3	26.8

Burst

	T9093	Exam
Length	0.12	0.12
Max. Volts	0.47	
Max. Depth (%)	37.0	38.0
Avg. Depth (%)	24.3	26.8

PWSCC ARC Release 1.1

Figure D-11
Specimen R 6 - C 64 - 01H - Crack 1 - Year 1998
Comparison of Unadjusted, Adjusted, Burst and Voltage with Exam
NDE Depth vs. Axial Length

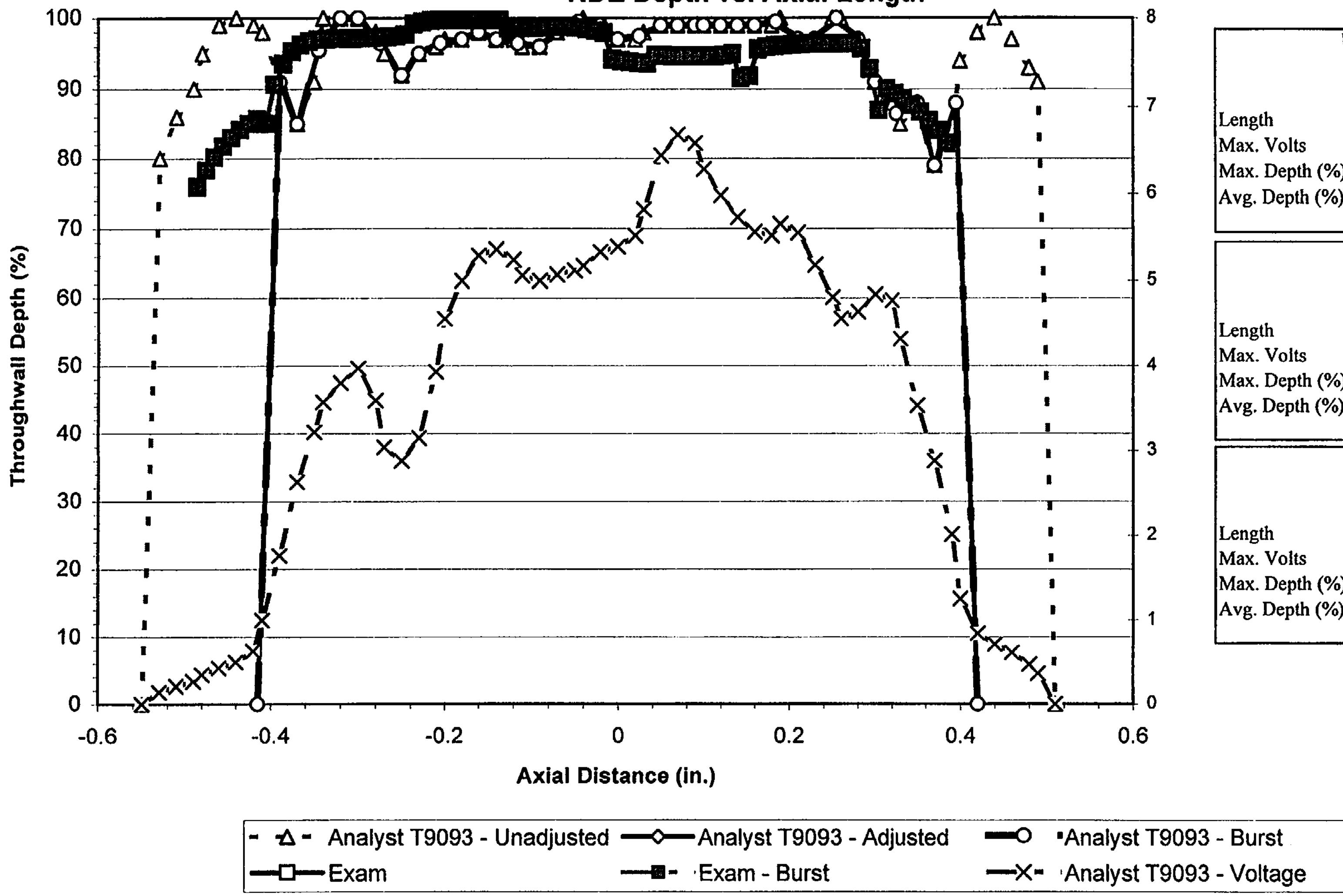

Unadjusted	T9093	Exam
Length	1.06	0.87
Max. Volts	6.68	
Max. Depth (%)	100.0	99.8
Avg. Depth (%)	93.5	94.3

Adjusted	T9093	Exam
Length	0.83	0.87
Max. Volts	6.68	
Max. Depth (%)	100.0	99.8
Avg. Depth (%)	92.7	94.3

Burst	T9093	Exam
Length	0.83	0.87
Max. Volts	6.68	
Max. Depth (%)	100.0	99.8
Avg. Depth (%)	92.7	94.3

PWSCC ARC Release 1.1

Figure D-12
Specimen R 6 - C 64 - 01H - Crack 2 - Year 1998
Comparison of Unadjusted, Adjusted, Burst and Voltage with Exam
NDE Depth vs. Axial Length

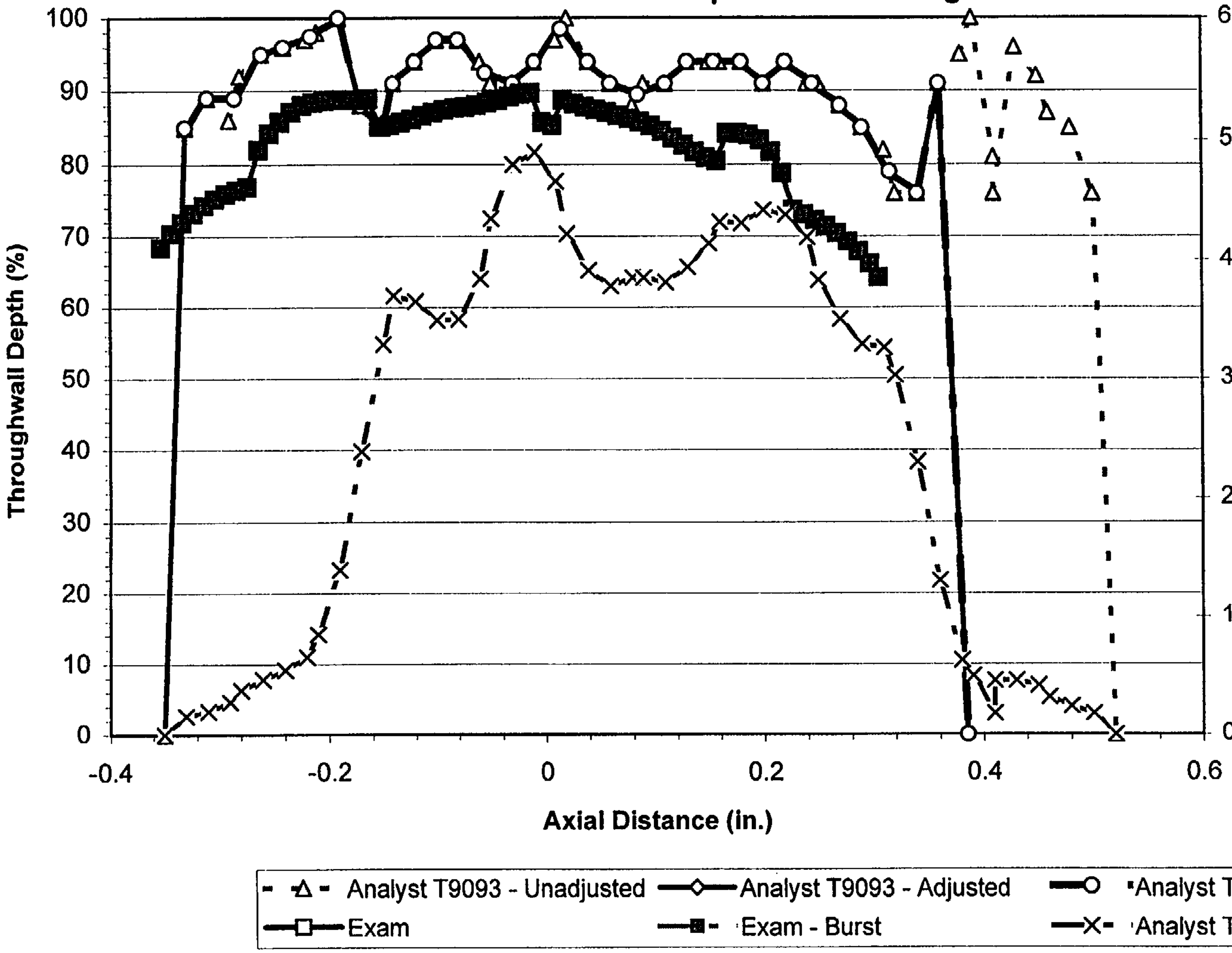

Unadjusted

	T9093	Exam
Length	0.87	0.66
Max. Volts	4.90	
Max. Depth (%)	100.0	89.7
Avg. Depth (%)	88.7	82.5

Adjusted

	T9093	Exam
Length	0.74	0.66
Max. Volts	4.90	
Max. Depth (%)	100.0	89.7
Avg. Depth (%)	88.6	82.5

Burst

	T9093	Exam
Length	0.72	0.66
Max. Volts	4.90	
Max. Depth (%)	100.0	89.7
Avg. Depth (%)	89.9	82.5

Figure D-13
Specimen R 9 - C 7 - 01H - Crack 1 - Year 1998
Comparison of Unadjusted, Adjusted, Burst and Voltage with Exam
NDE Depth vs. Axial Length

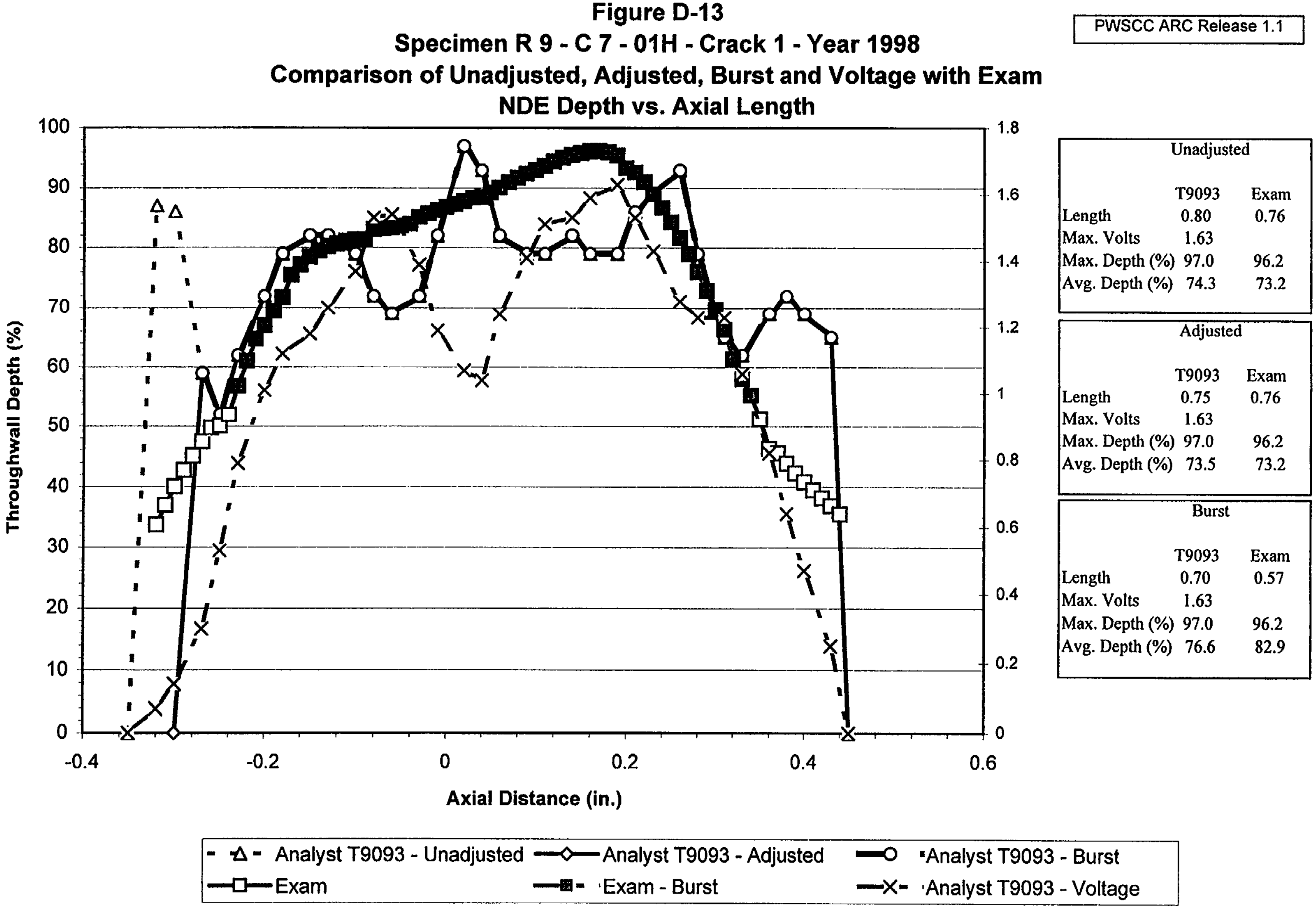

PWSCC ARC Release 1.1

Figure D-14
Specimen R 9 - C 7 - 01H - Crack 2 - Year 1998
Comparison of Unadjusted, Adjusted, Burst and Voltage with Exam
NDE Depth vs. Axial Length

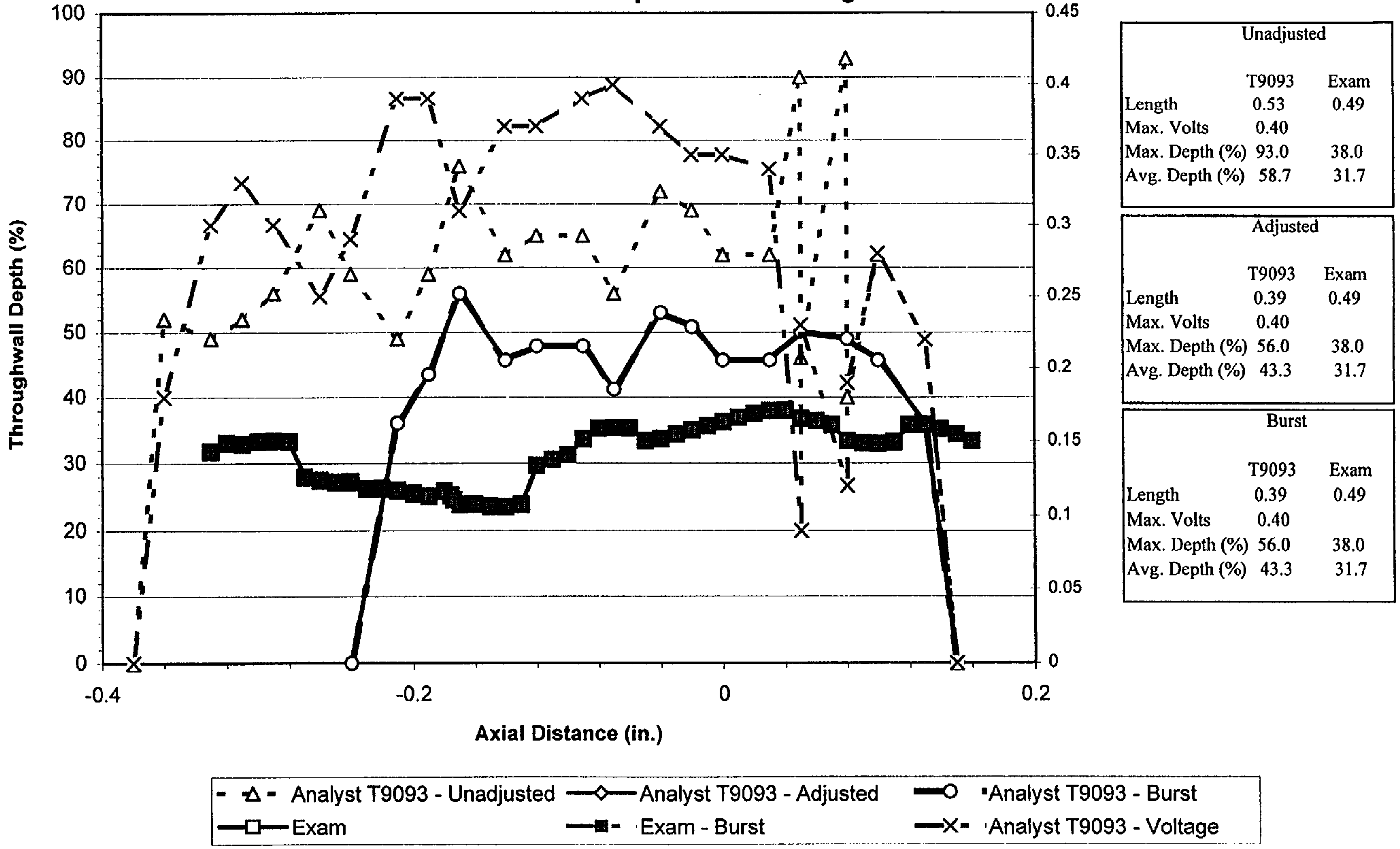

PWSCC ARC Release 1.1

Figure D-15
Specimen R 9 - C 19 - 01H - Crack 1 - Year 1998
Comparison of Unadjusted, Adjusted, Burst and Voltage with Exam
NDE Depth vs. Axial Length

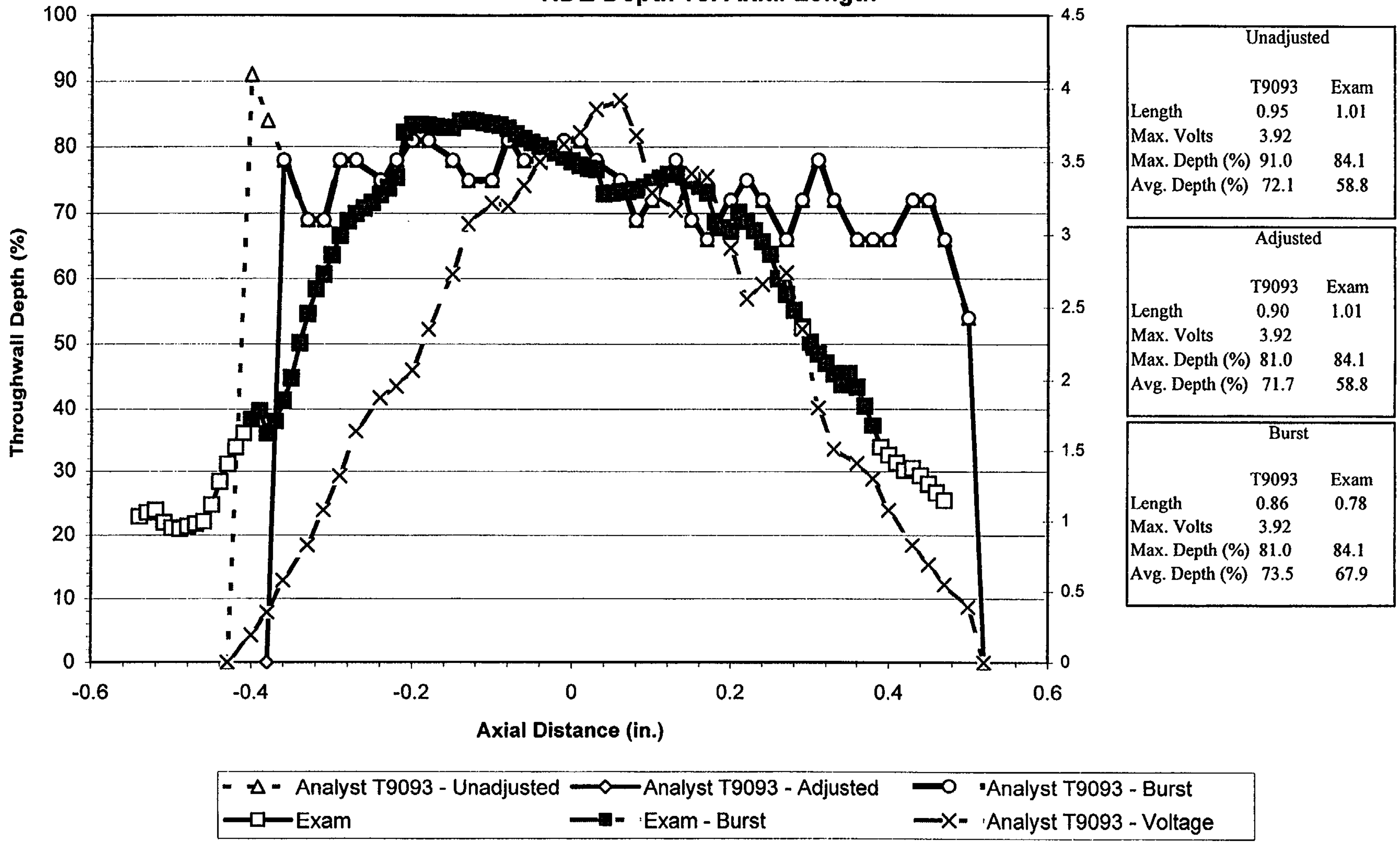

PWSCC ARC Release 1.1

Figure D-16
Specimen R 9 - C 19 - 01H - Crack 2 - Year 1998
Comparison of Unadjusted, Adjusted, Burst and Voltage with Exam
NDE Depth vs. Axial Length

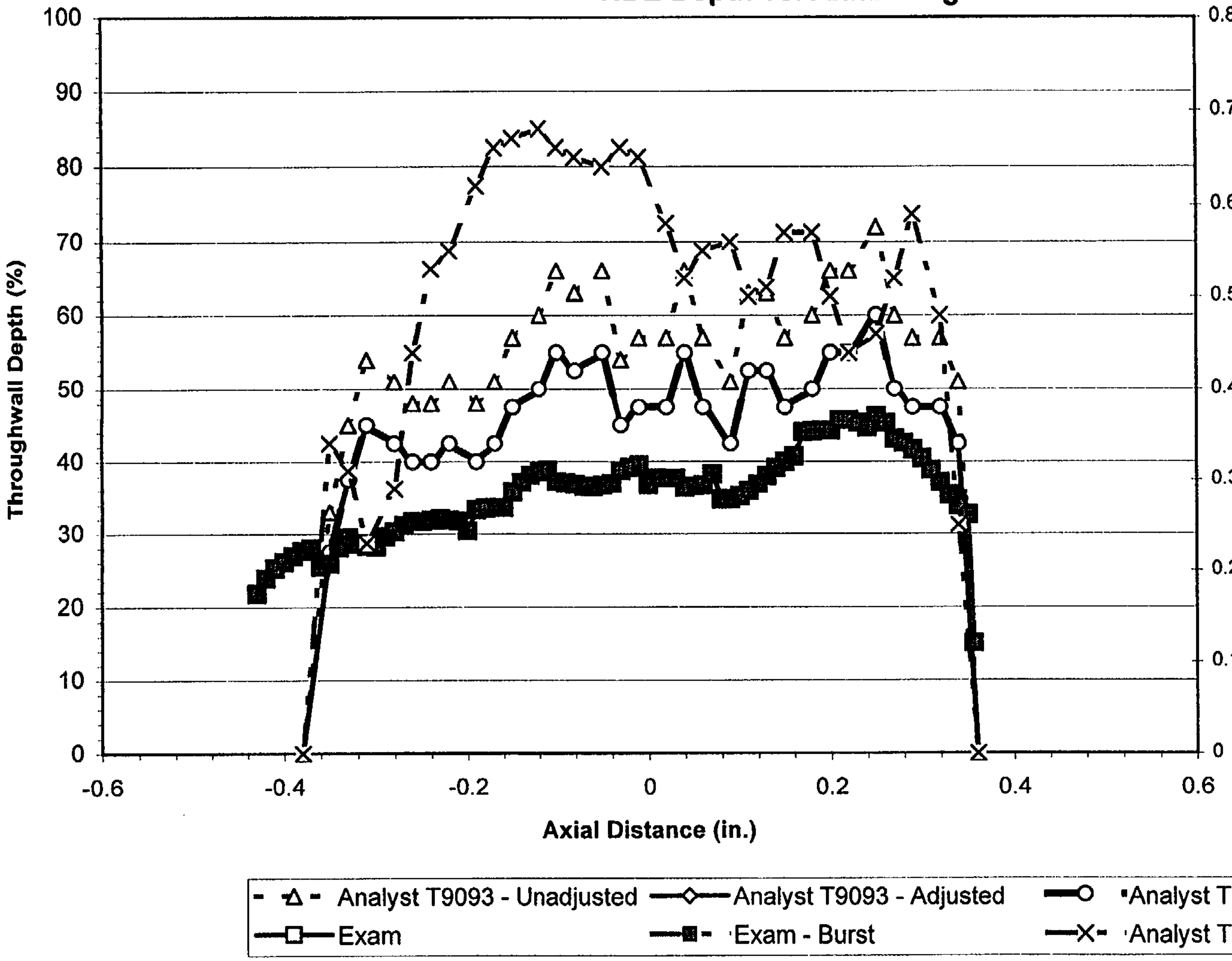

Unadjusted	T9093	Exam
Length	0.74	0.79
Max. Volts	0.68	
Max. Depth (%)	72.0	46.3
Avg. Depth (%)	54.7	35.6

Adjusted	T9093	Exam
Length	0.74	0.79
Max. Volts	0.68	
Max. Depth (%)	60.0	46.3
Avg. Depth (%)	45.6	35.6

Burst	T9093	Exam
Length	0.69	0.79
Max. Volts	0.68	
Max. Depth (%)	60.0	46.3
Avg. Depth (%)	47.7	35.6

PWSCC ARC Release 1.1

Figure D-17
Specimen R 9 - C 37 - 01H - Crack 1 - Year 1998
Comparison of Unadjusted, Adjusted, Burst and Voltage with Exam
NDE Depth vs. Axial Length

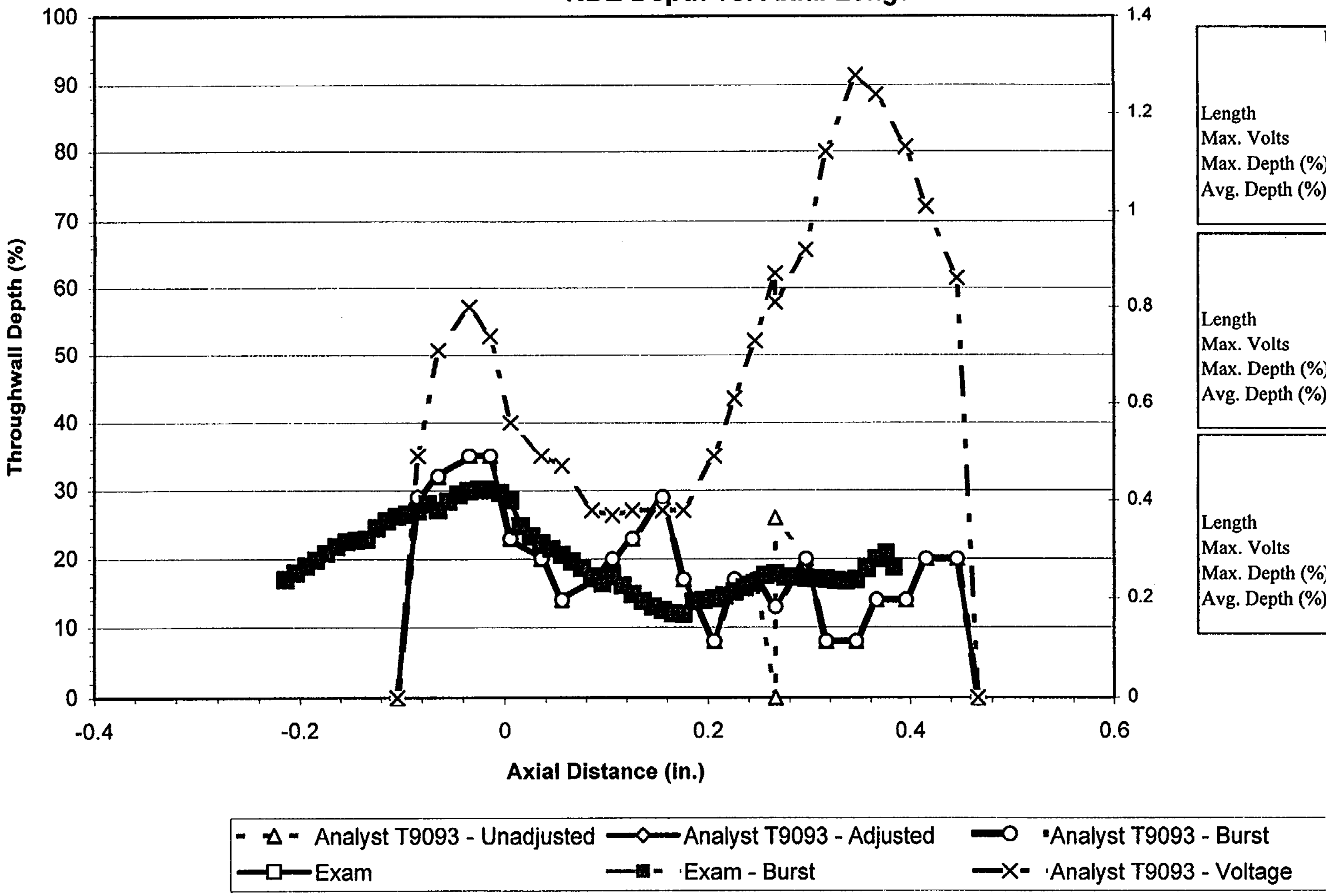

Unadjusted

	T9093	Exam
Length	0.57	0.60
Max. Volts	1.28	
Max. Depth (%)	35.0	30.1
Avg. Depth (%)	18.9	20.1

Adjusted

	T9093	Exam
Length	0.57	0.60
Max. Volts	1.28	
Max. Depth (%)	35.0	30.1
Avg. Depth (%)	18.8	20.1

Burst

	T9093	Exam
Length	0.57	0.60
Max. Volts	1.28	
Max. Depth (%)	35.0	30.1
Avg. Depth (%)	18.8	20.1

PWSCC ARC Release 1.1

Figure D-18
Specimen R 9 - C 64 - 01H - Crack 1 - Year 1998
Comparison of Unadjusted, Adjusted, Burst and Voltage with Exam NDE Depth vs. Axial Length

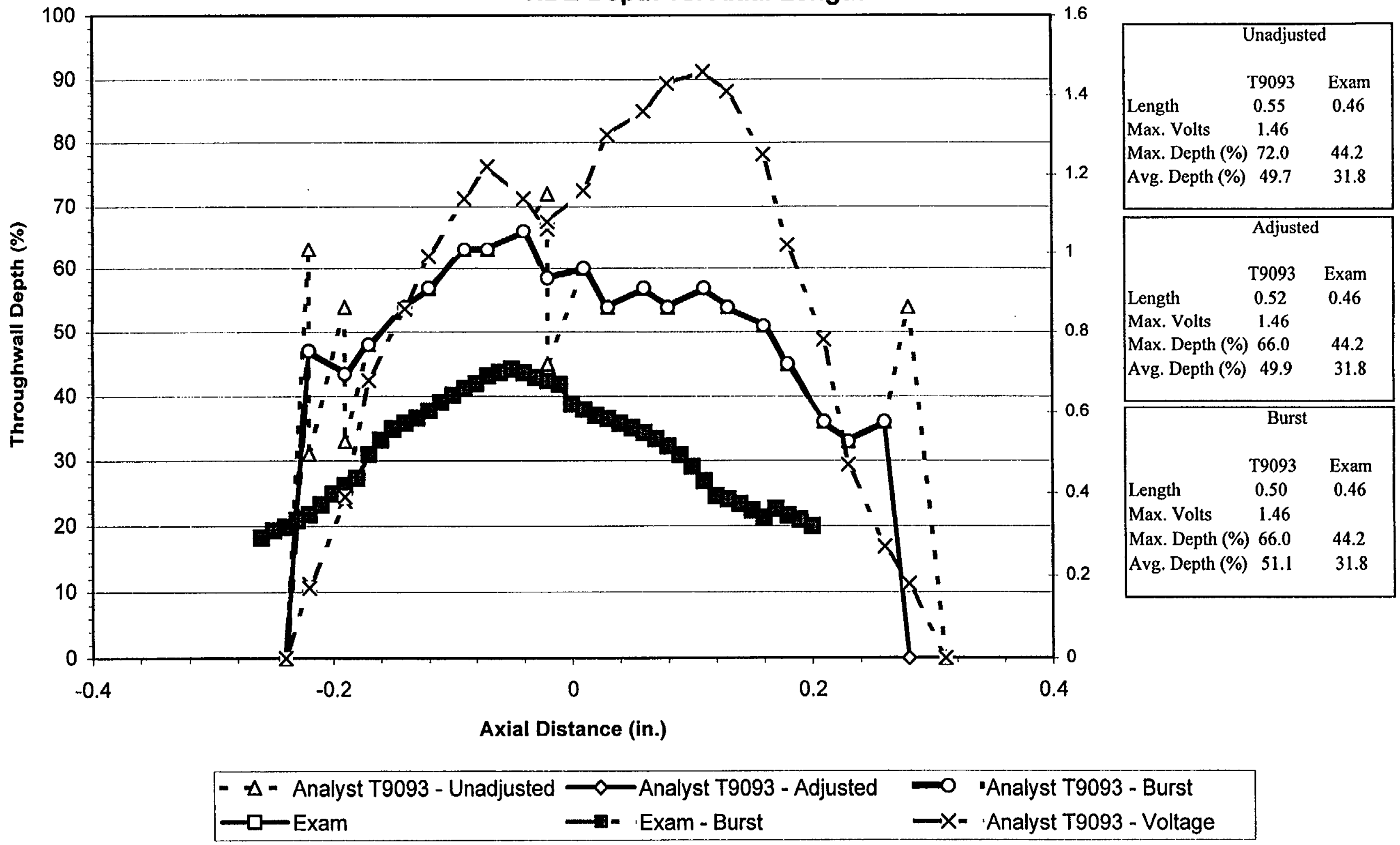

PWSCC ARC Release 1.1

Figure D-19
Specimen R 13 - C 7 - 01H - Crack 1 - Year 1998
Comparison of Unadjusted, Adjusted, Burst and Voltage with Exam
NDE Depth vs. Axial Length

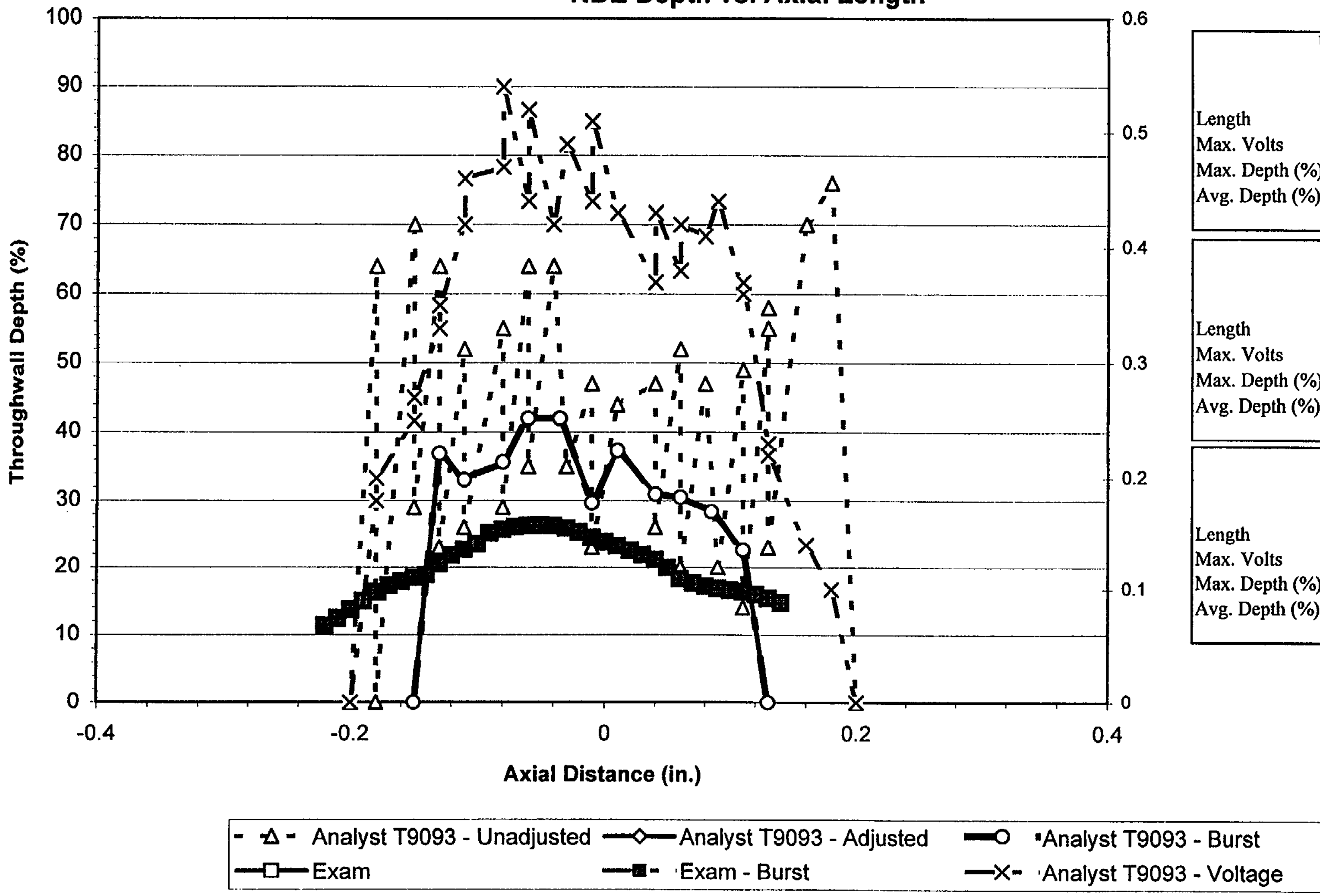

Unadjusted	T9093	Exam
Length	0.40	0.36
Max. Volts	0.54	
Max. Depth (%)	76.0	26.3
Avg. Depth (%)	40.5	20.2

Adjusted	T9093	Exam
Length	0.28	0.36
Max. Volts	0.51	
Max. Depth (%)	42.0	26.3
Avg. Depth (%)	31.2	20.2

Burst	T9093	Exam
Length	0.28	0.36
Max. Volts	0.51	
Max. Depth (%)	42.0	26.3
Avg. Depth (%)	31.2	20.2

PWSCC ARC Release 1.1

Figure D-20
Specimen R 13 - C 16 - 01H - Crack 1 - Year 1998
Comparison of Unadjusted, Adjusted, Burst and Voltage with Exam
NDE Depth vs. Axial Length

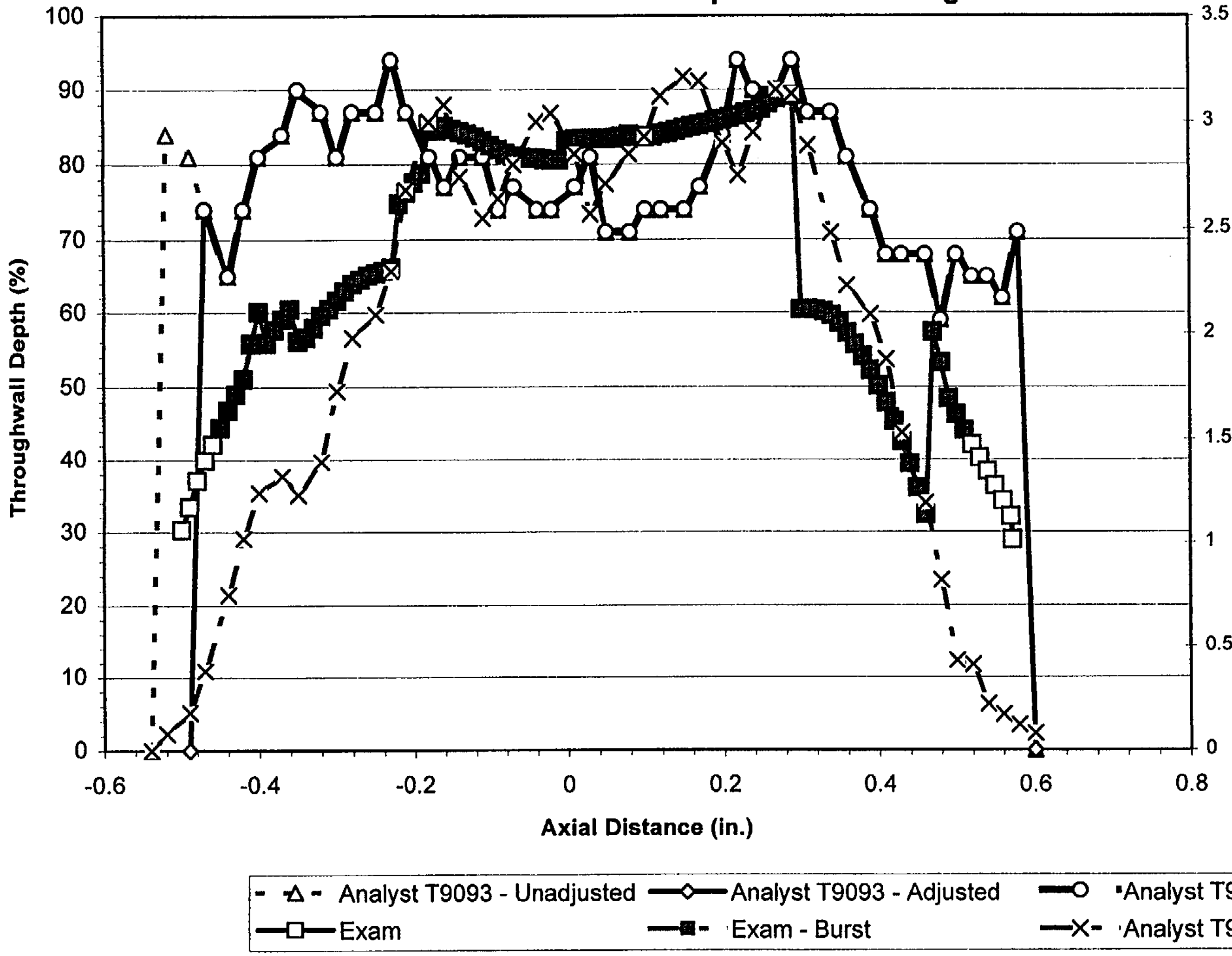

Unadjusted	T9093	Exam
Length	1.14	1.07
Max. Volts	3.21	
Max. Depth (%)	94.0	89.3
Avg. Depth (%)	76.9	67.2

Adjusted	T9093	Exam
Length	1.09	1.07
Max. Volts	3.21	
Max. Depth (%)	94.0	89.3
Avg. Depth (%)	76.7	67.2

Burst	T9093	Exam
Length	1.05	0.96
Max. Volts	3.21	
Max. Depth (%)	94.0	89.3
Avg. Depth (%)	78.2	70.6

PWSCC ARC Release 1.1

Figure D-21
Specimen R 13 - C 16 - 01H - Crack 2 - Year 1998
Comparison of Unadjusted, Adjusted, Burst and Voltage with Exam
NDE Depth vs. Axial Length

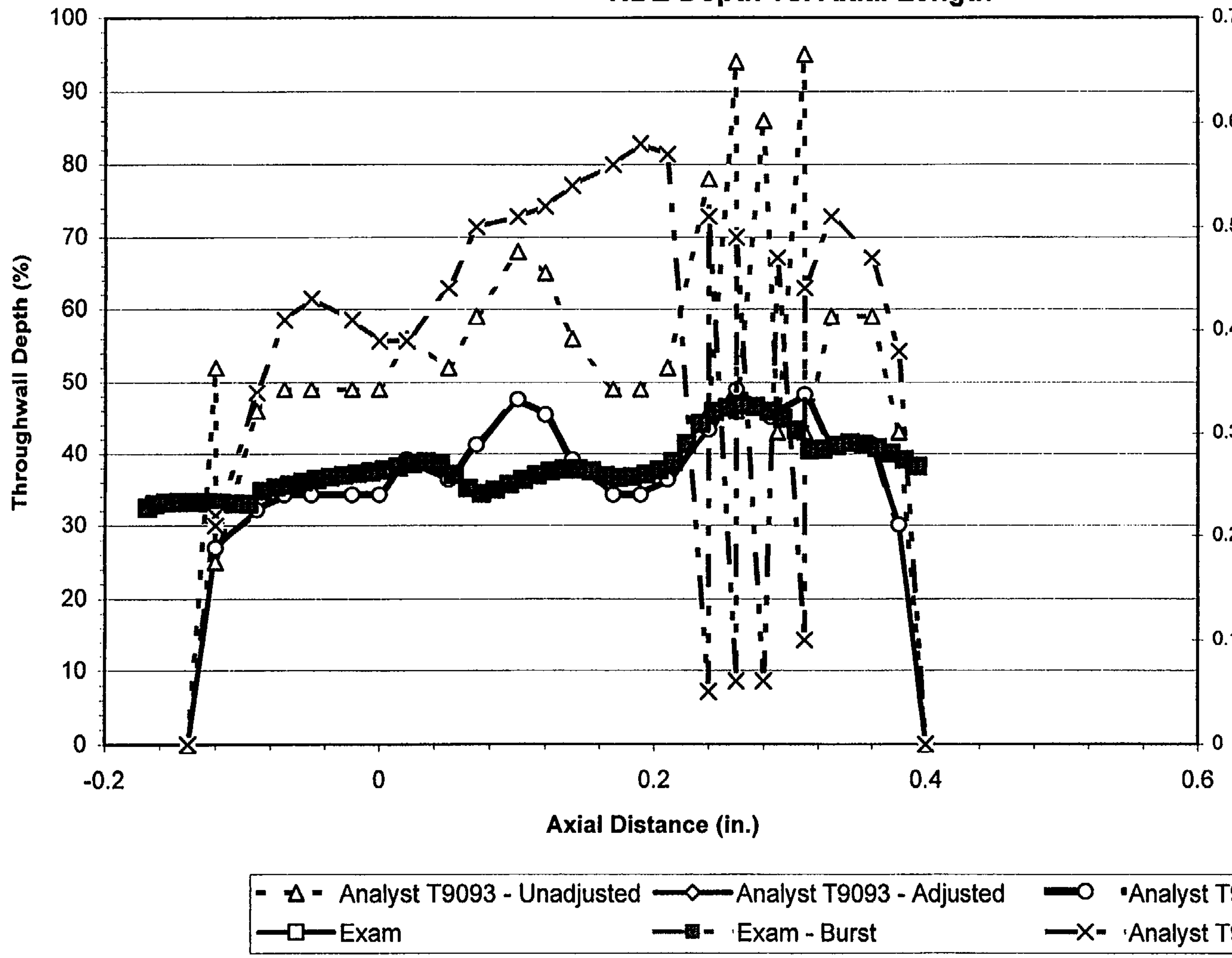

Unadjusted	T9093	Exam
Length	0.54	0.56
Max. Volts	0.58	
Max. Depth (%)	95.0	46.7
Avg. Depth (%)	53.1	38.2

Adjusted	T9093	Exam
Length	0.54	0.56
Max. Volts	0.58	
Max. Depth (%)	49.0	46.7
Avg. Depth (%)	37.2	38.2

Burst	T9093	Exam
Length	0.50	0.56
Max. Volts	0.58	
Max. Depth (%)	49.0	46.7
Avg. Depth (%)	39.0	38.2

PWSCC ARC Release 1.1

Figure D-22
Specimen R 13 - C 34 - 01H - Crack 1 - Year 1998
Comparison of Unadjusted, Adjusted, Burst and Voltage with Exam
NDE Depth vs. Axial Length

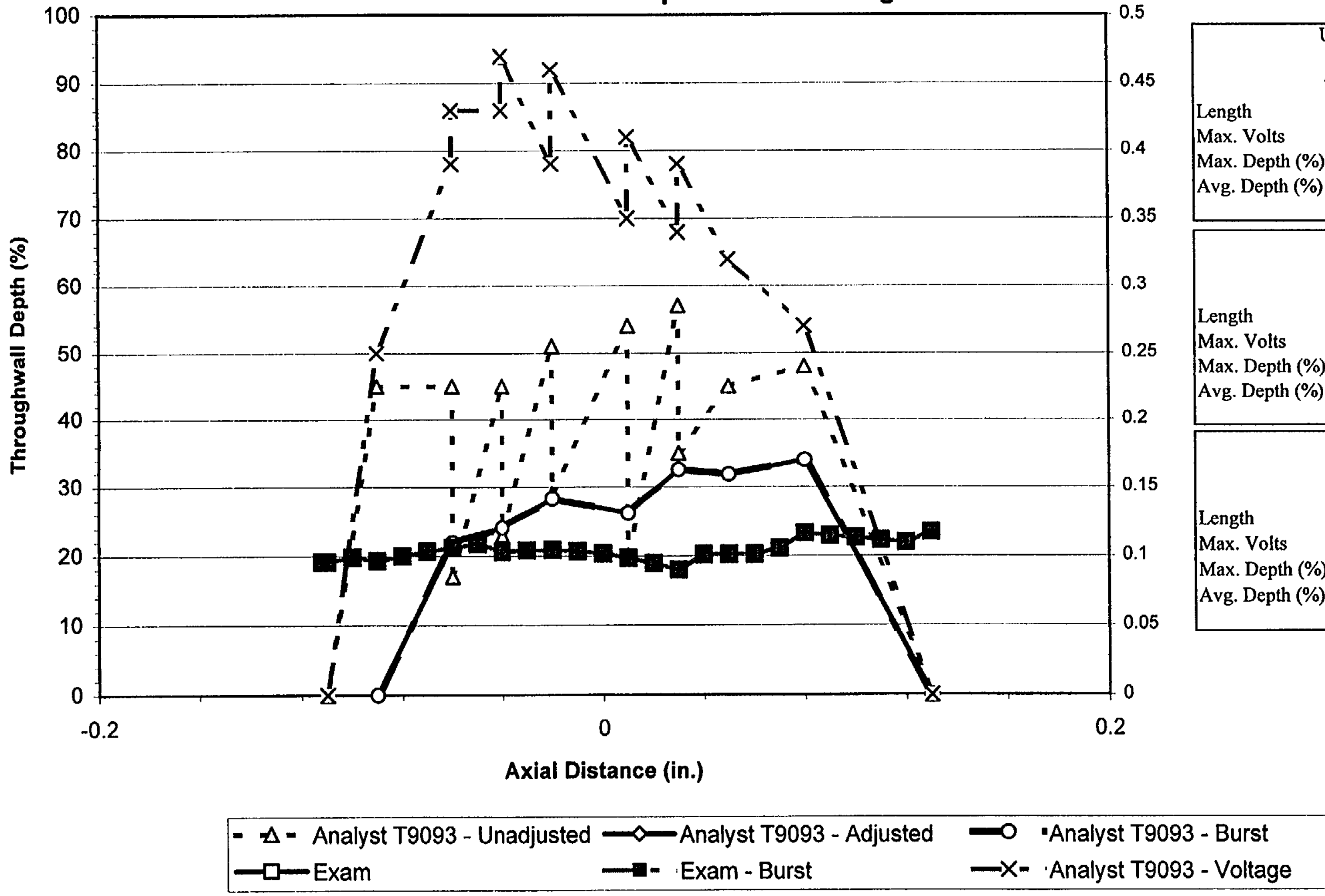

Unadjusted	T9093	Exam
Length	0.24	0.24
Max. Volts	0.47	
Max. Depth (%)	57.0	23.4
Avg. Depth (%)	34.9	20.7

Adjusted	T9093	Exam
Length	0.22	0.24
Max. Volts	0.45	
Max. Depth (%)	34.0	23.4
Avg. Depth (%)	23.6	20.7

Burst	T9093	Exam
Length	0.22	0.24
Max. Volts	0.45	
Max. Depth (%)	34.0	23.4
Avg. Depth (%)	23.6	20.7

PWSCC ARC Release 1.1

Figure D-23
Specimen R 13 - C 59 - 01H - Crack 1 - Year 1998
Comparison of Unadjusted, Adjusted, Burst and Voltage with Exam
NDE Depth vs. Axial Length

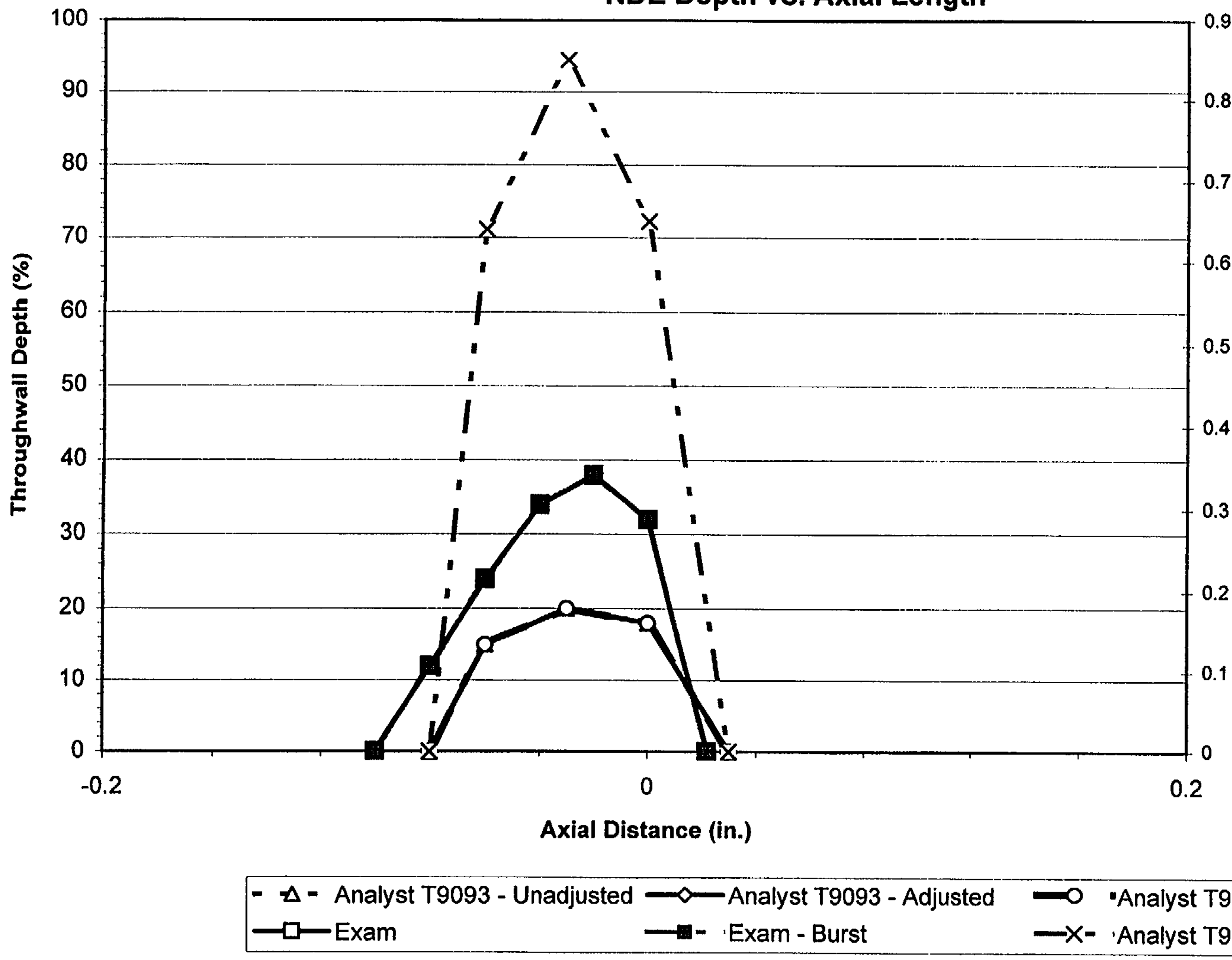

Unadjusted

	T9093	Exam
Length	0.11	0.12
Max. Volts	0.85	
Max. Depth (%)	20.0	38.0
Avg. Depth (%)	13.8	23.2

Adjusted

	T9093	Exam
Length	0.11	0.12
Max. Volts	0.85	
Max. Depth (%)	20.0	38.0
Avg. Depth (%)	13.8	23.2

Burst

	T9093	Exam
Length	0.11	0.12
Max. Volts	0.85	
Max. Depth (%)	20.0	38.0
Avg. Depth (%)	13.8	23.2

PWSCC ARC Release 1.1

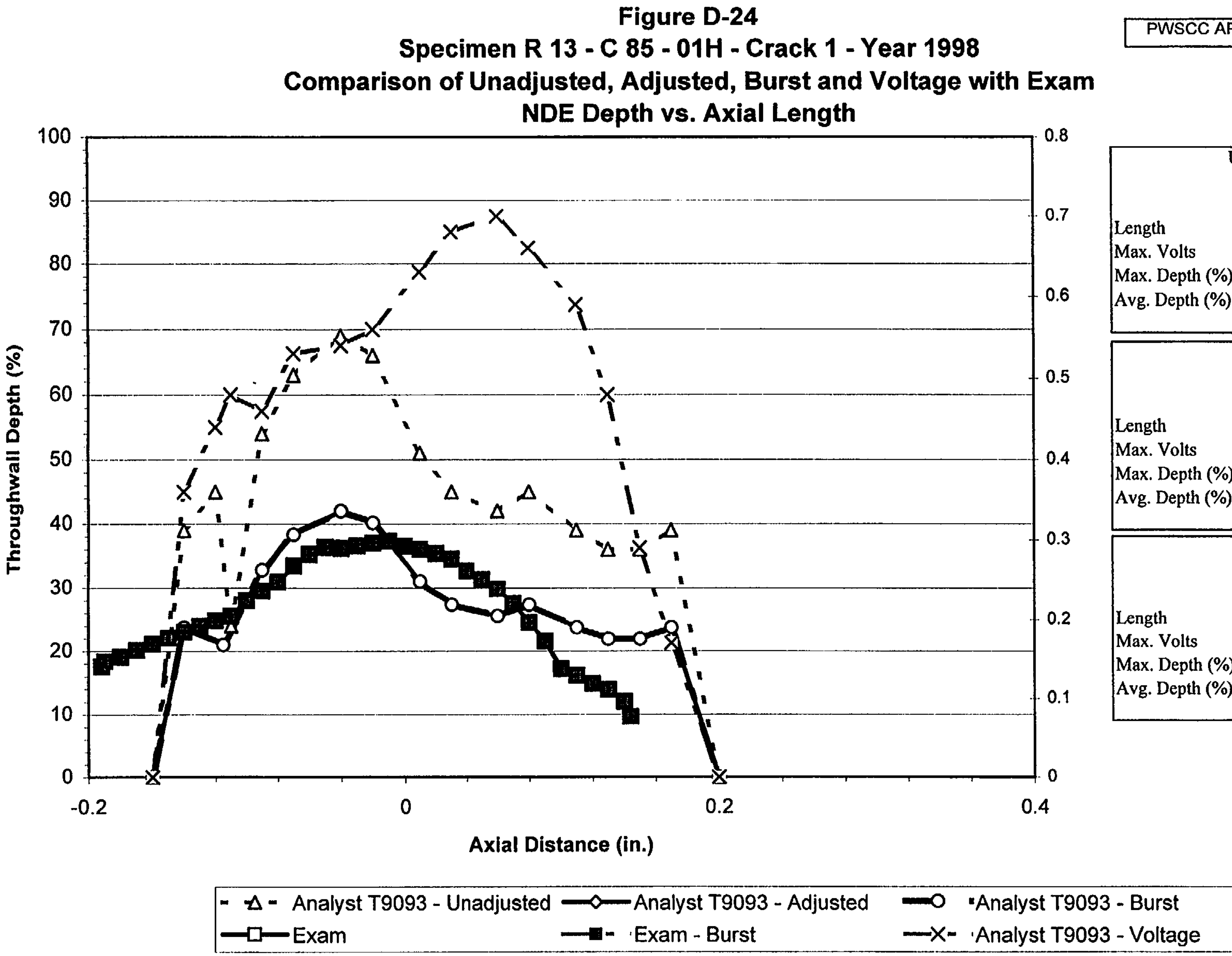

Unadjusted	T9093	Exam
Length	0.36	0.34
Max. Volts	0.70	
Max. Depth (%)	69.0	37.3
Avg. Depth (%)	43.9	27.3

Adjusted	T9093	Exam
Length	0.36	0.34
Max. Volts	0.70	
Max. Depth (%)	42.0	37.3
Avg. Depth (%)	26.8	27.3

Burst	T9093	Exam
Length	0.36	0.34
Max. Volts	0.70	
Max. Depth (%)	42.0	37.3
Avg. Depth (%)	26.8	27.3

Figure D-25
Specimen R 17 - C 43 - 01H - Crack 1 - Year 1998
Comparison of Unadjusted, Adjusted, Burst and Voltage with Exam NDE Depth vs. Axial Length

PWSCC ARC Release 1.1

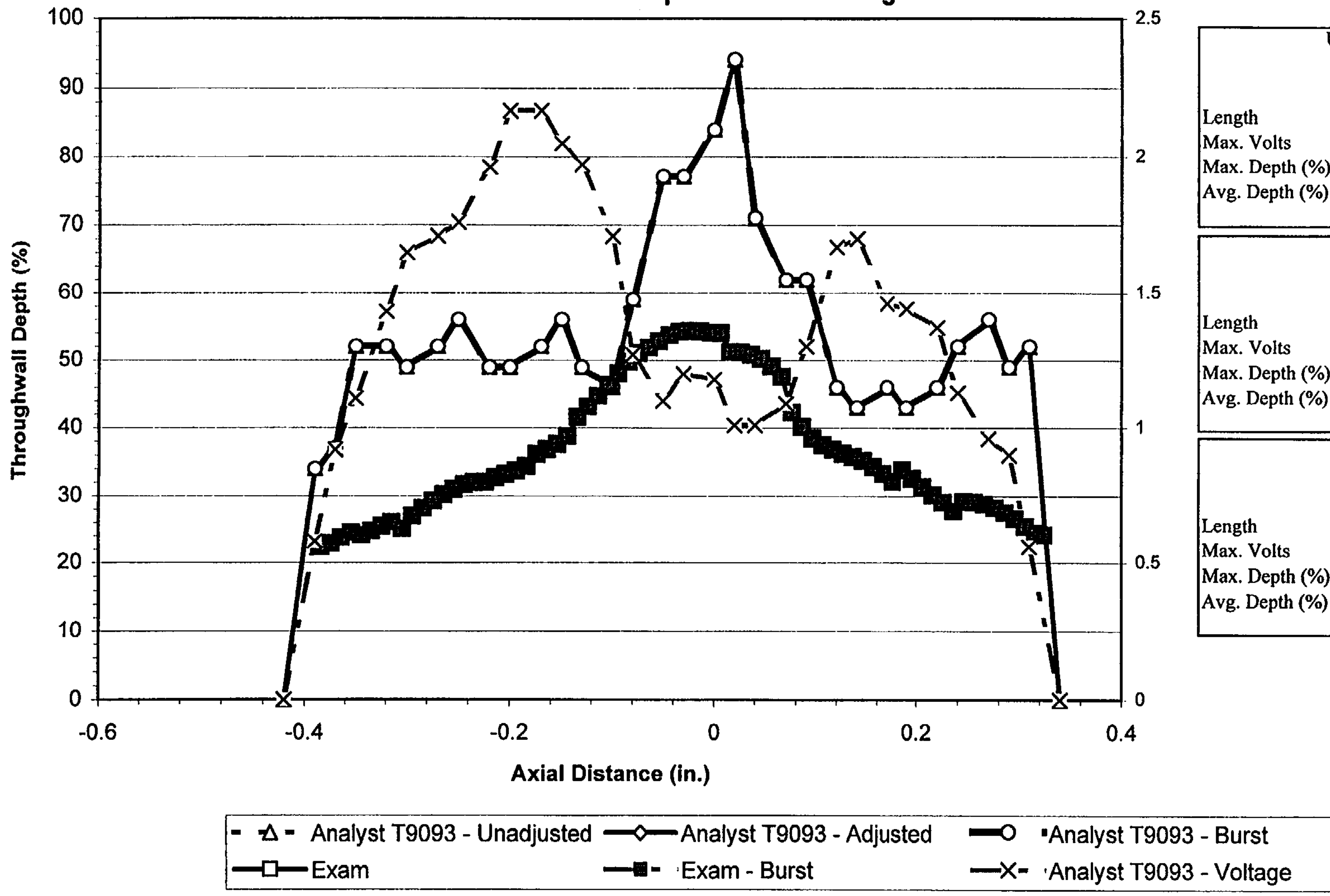

Unadjusted	T9093	Exam
Length	0.76	0.71
Max. Volts	2.17	
Max. Depth (%)	94.0	54.3
Avg. Depth (%)	52.8	36.7

Adjusted	T9093	Exam
Length	0.76	0.71
Max. Volts	2.17	
Max. Depth (%)	94.0	54.3
Avg. Depth (%)	52.8	36.7

Burst	T9093	Exam
Length	0.70	0.71
Max. Volts	2.17	
Max. Depth (%)	94.0	54.3
Avg. Depth (%)	55.5	36.7

Figure D-26
Specimen R 17 - C 58 - 01H - Crack 1 - Year 1998
Comparison of Unadjusted, Adjusted, Burst and Voltage with Exam
NDE Depth vs. Axial Length

PWSCC ARC Release 1.1

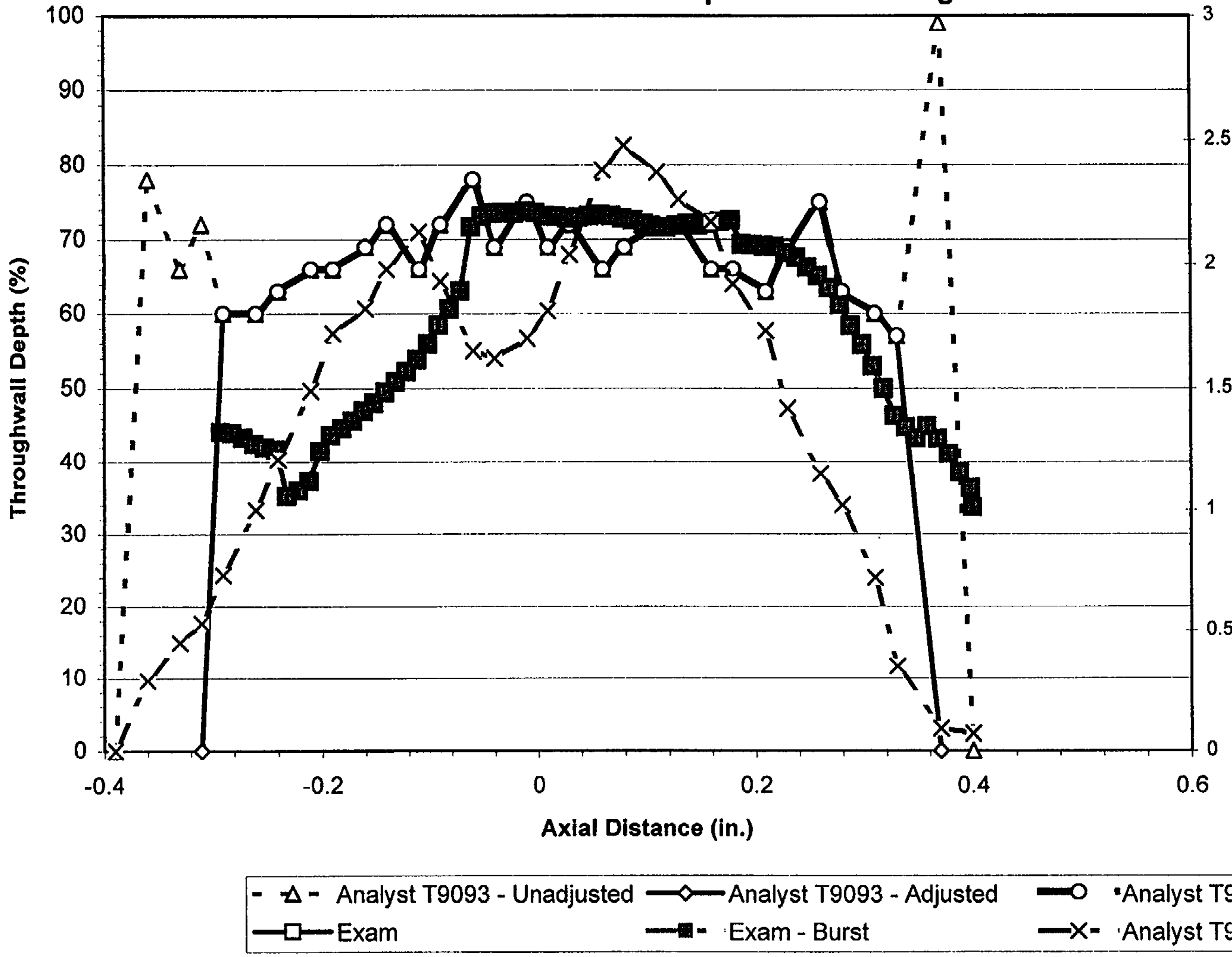

Unadjusted	T9093	Exam
Length	0.79	0.69
Max. Volts	2.48	
Max. Depth (%)	99.0	73.7
Avg. Depth (%)	66.7	59.1

Adjusted	T9093	Exam
Length	0.68	0.69
Max. Volts	2.48	
Max. Depth (%)	78.0	73.7
Avg. Depth (%)	64.4	59.1

Burst	T9093	Exam
Length	0.62	0.69
Max. Volts	2.48	
Max. Depth (%)	78.0	73.7
Avg. Depth (%)	67.9	59.1

PWSCC ARC Release 1.1

Figure D-27
Specimen R 19 - C 38 - 01H - Crack 1 - Year 1998
Comparison of Unadjusted, Adjusted, Burst and Voltage with Exam
NDE Depth vs. Axial Length

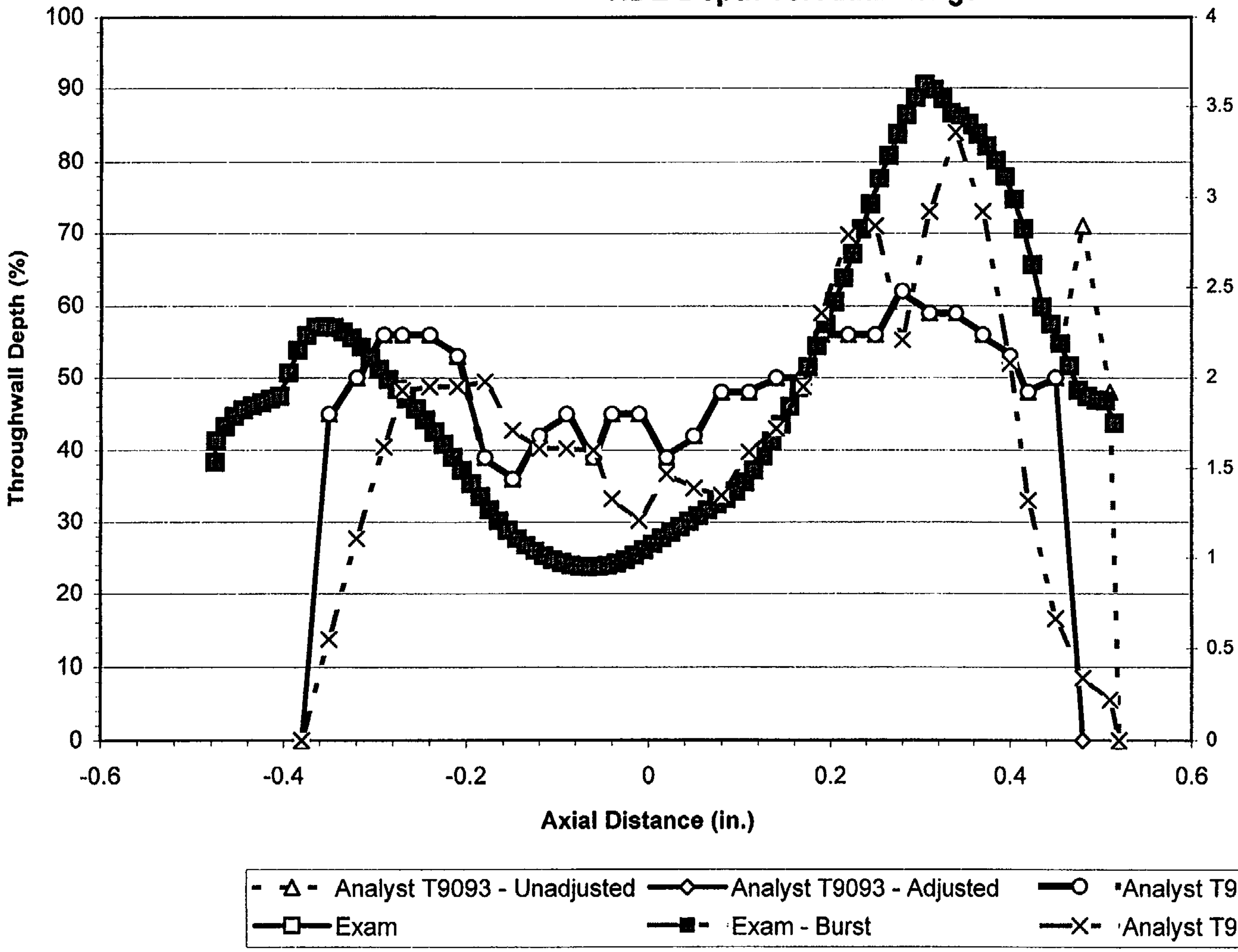

Unadjusted

	T9093	Exam
Length	0.90	0.99
Max. Volts	3.36	
Max. Depth (%)	71.0	90.5
Avg. Depth (%)	49.2	49.3

Adjusted

	T9093	Exam
Length	0.86	0.99
Max. Volts	3.36	
Max. Depth (%)	62.0	90.5
Avg. Depth (%)	47.9	49.3

Burst

	T9093	Exam
Length	0.80	0.99
Max. Volts	3.36	
Max. Depth (%)	62.0	90.5
Avg. Depth (%)	49.7	49.3

PWSCC ARC Release 1.1

Figure D-28
Specimen R 19 - C 38 - 01H - Crack 2 - Year 1998
Comparison of Unadjusted, Adjusted, Burst and Voltage with Exam
NDE Depth vs. Axial Length

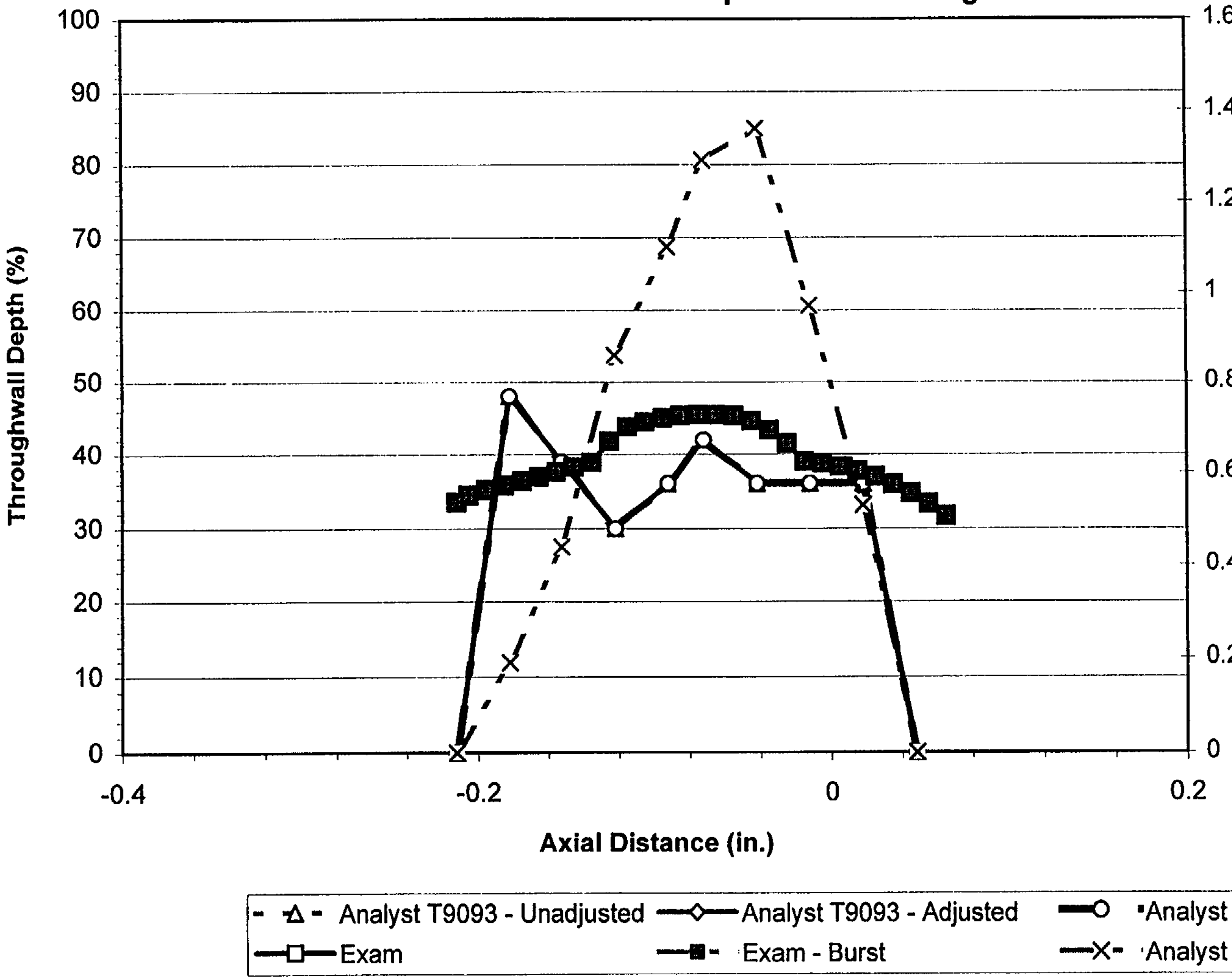

Unadjusted	T9093	Exam
Length	0.26	0.28
Max. Volts	1.36	
Max. Depth (%)	48.0	45.5
Avg. Depth (%)	33.5	39.6

Adjusted	T9093	Exam
Length	0.26	0.28
Max. Volts	1.36	
Max. Depth (%)	48.0	45.5
Avg. Depth (%)	33.5	39.6

Burst	T9093	Exam
Length	0.26	0.28
Max. Volts	1.36	
Max. Depth (%)	48.0	45.5
Avg. Depth (%)	33.5	39.6

PWSCC ARC Release 1.1

Figure D-29
Specimen R 21 - C 13 - 01H - Crack 1 - Year 1998
Comparison of Unadjusted, Adjusted, Burst and Voltage with Exam
NDE Depth vs. Axial Length

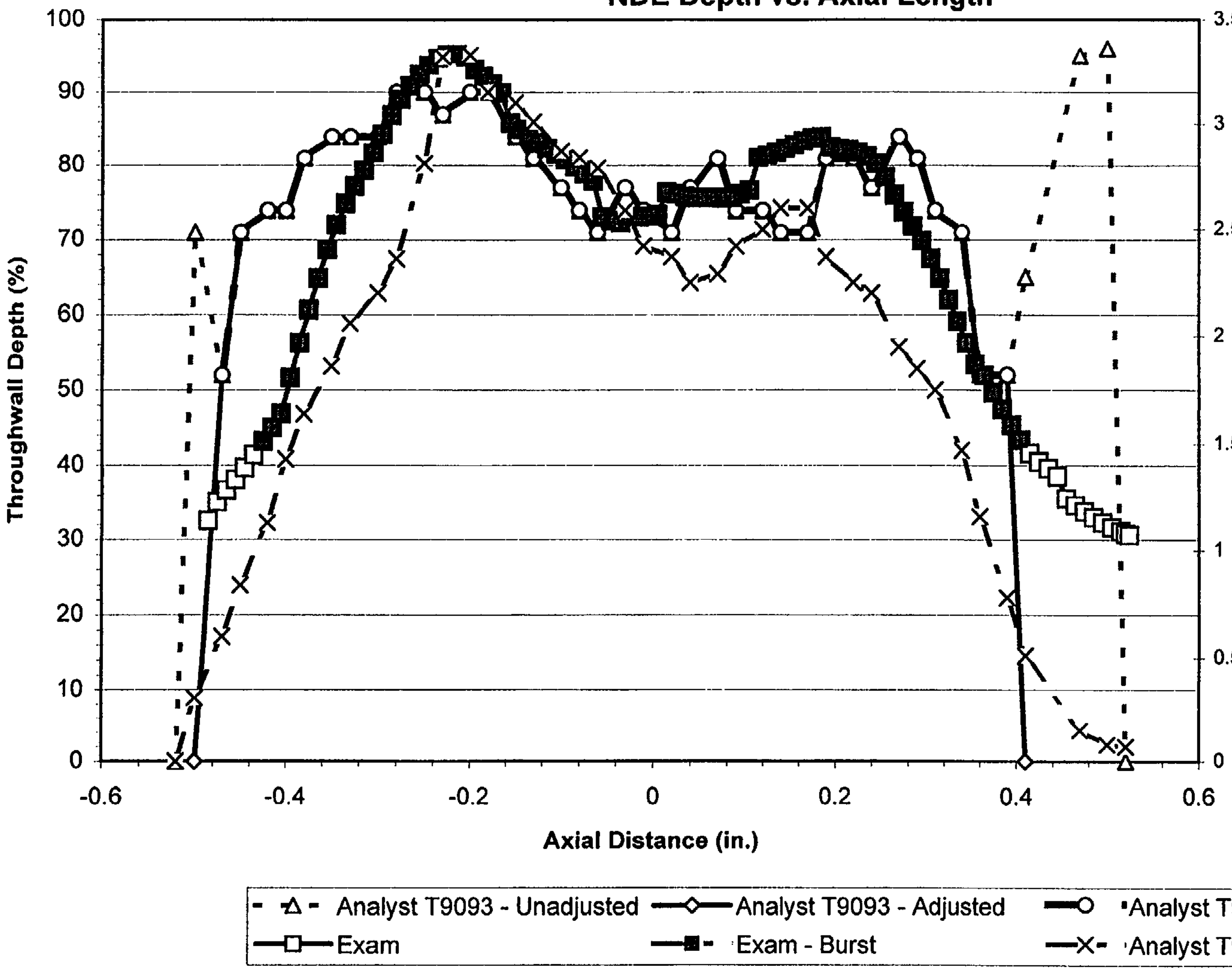

Unadjusted	T9093	Exam
Length	1.04	1.01
Max. Volts	3.33	
Max. Depth (%)	96.0	95.3
Avg. Depth (%)	75.9	68.7

Adjusted	T9093	Exam
Length	0.91	1.01
Max. Volts	3.33	
Max. Depth (%)	90.0	95.3
Avg. Depth (%)	74.6	68.7

Burst	T9093	Exam
Length	0.86	0.83
Max. Volts	3.33	
Max. Depth (%)	90.0	95.3
Avg. Depth (%)	77.4	75.6

PWSCC ARC Release 1.1

Figure D-30
Specimen R 21 - C 13 - 01H - Crack 2 - Year 1998
Comparison of Unadjusted, Adjusted, Burst and Voltage with Exam
NDE Depth vs. Axial Length

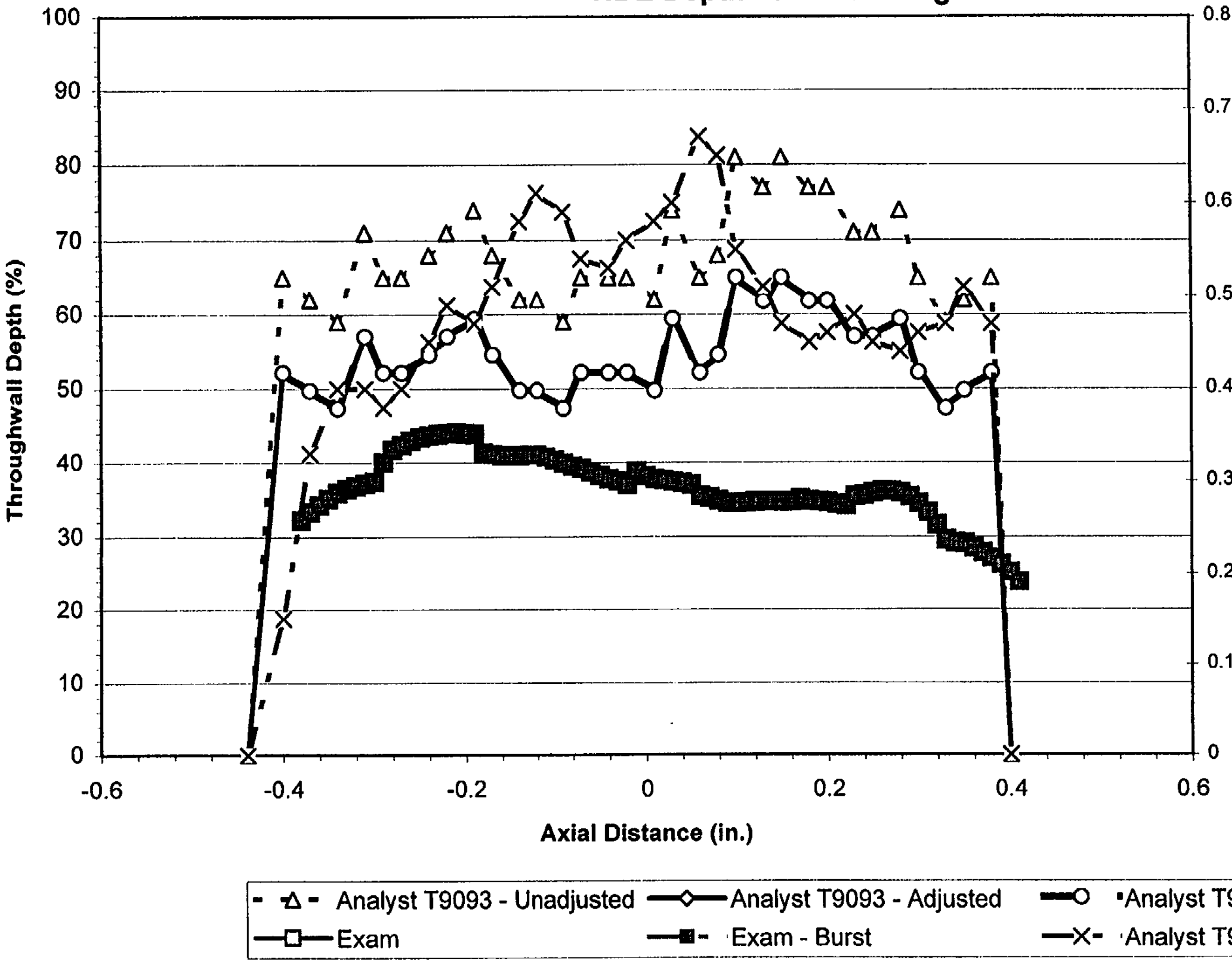

Unadjusted	T9093	Exam
Length	0.84	0.79
Max. Volts	0.67	
Max. Depth (%)	81.0	44.0
Avg. Depth (%)	65.4	36.6

Adjusted	T9093	Exam
Length	0.84	0.79
Max. Volts	0.67	
Max. Depth (%)	65.0	44.0
Avg. Depth (%)	52.5	36.6

Burst	T9093	Exam
Length	0.78	0.79
Max. Volts	0.67	
Max. Depth (%)	65.0	44.0
Avg. Depth (%)	54.5	36.6

PWSCC ARC Release 1.1

Figure D-31
Specimen R 21 - C 28 - 01H - Crack 1 - Year 1998
Comparison of Unadjusted, Adjusted, Burst and Voltage with Exam
NDE Depth vs. Axial Length

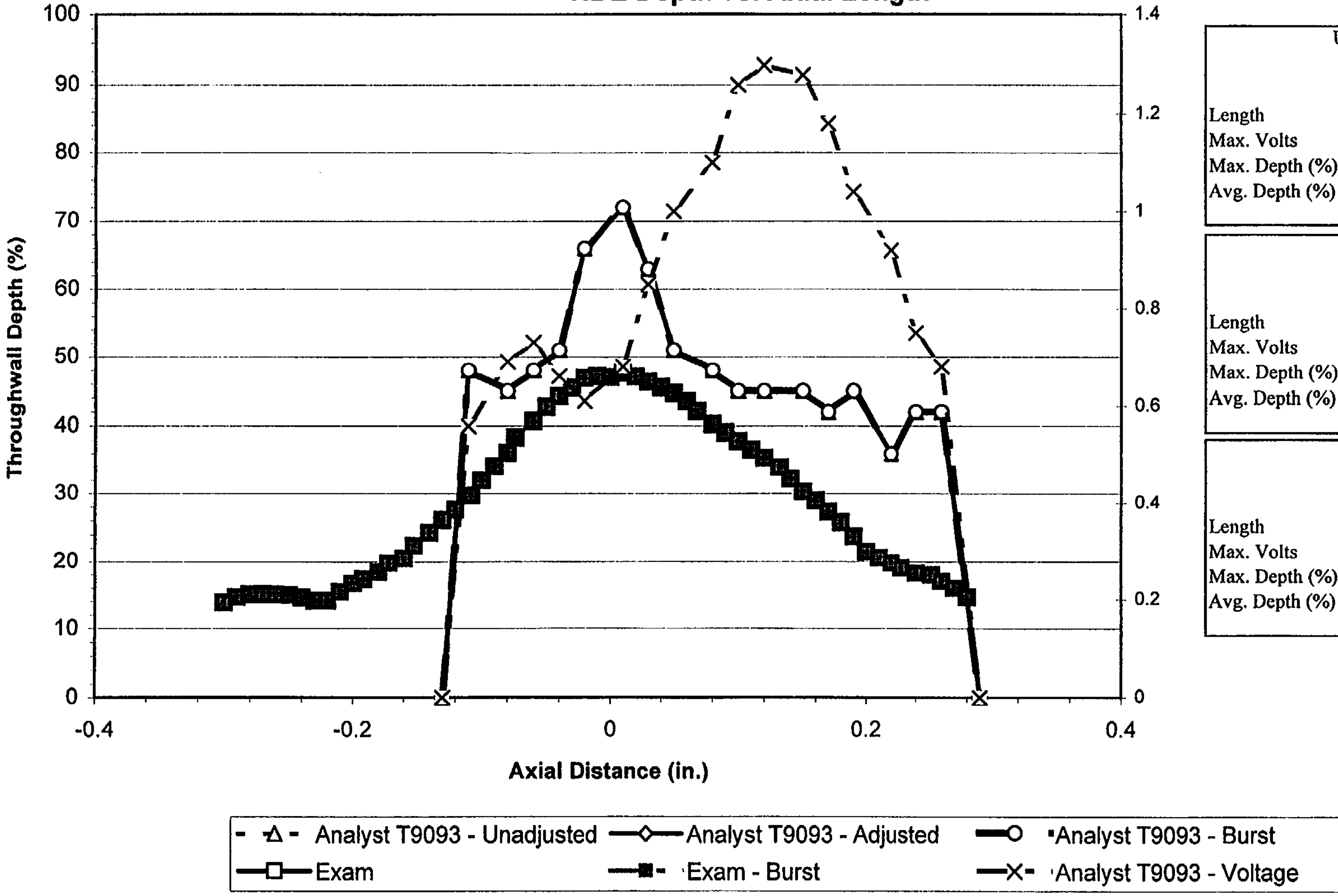

Unadjusted	T9093	Exam
Length	0.42	0.58
Max. Volts	1.30	
Max. Depth (%)	72.0	47.6
Avg. Depth (%)	46.2	29.0

Adjusted	T9093	Exam
Length	0.42	0.58
Max. Volts	1.30	
Max. Depth (%)	72.0	47.6
Avg. Depth (%)	46.2	29.0

Burst	T9093	Exam
Length	0.42	0.58
Max. Volts	1.30	
Max. Depth (%)	72.0	47.6
Avg. Depth (%)	46.2	29.0

PWSCC ARC Release 1.1

Figure D-32
Specimen R 21 - C 31 - 01H - Crack 1 - Year 1998
Comparison of Unadjusted, Adjusted, Burst and Voltage with Exam
NDE Depth vs. Axial Length

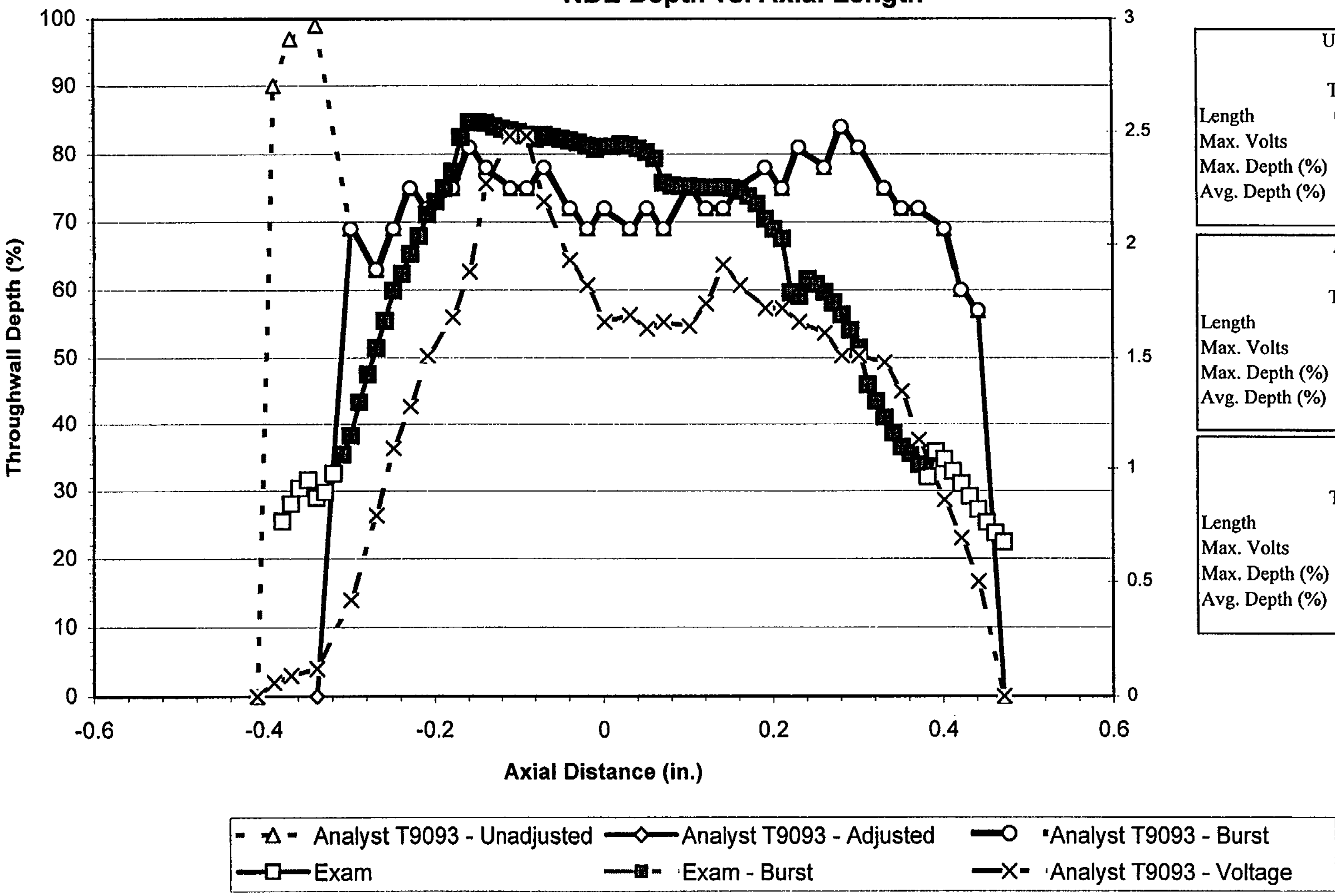

Unadjusted	T9093	Exam
Length	0.88	0.85
Max. Volts	2.48	
Max. Depth (%)	99.0	84.6
Avg. Depth (%)	73.0	60.9

Adjusted	T9093	Exam
Length	0.81	0.85
Max. Volts	2.48	
Max. Depth (%)	84.0	84.6
Avg. Depth (%)	69.8	60.9

Burst	T9093	Exam
Length	0.74	0.68
Max. Volts	2.48	
Max. Depth (%)	84.0	84.6
Avg. Depth (%)	73.4	68.6

PWSCC ARC Release 1.1

Figure D-33
Specimen R 21 - C 31 - 01H - Crack 2 - Year 1998
Comparison of Unadjusted, Adjusted, Burst and Voltage with Exam
NDE Depth vs. Axial Length

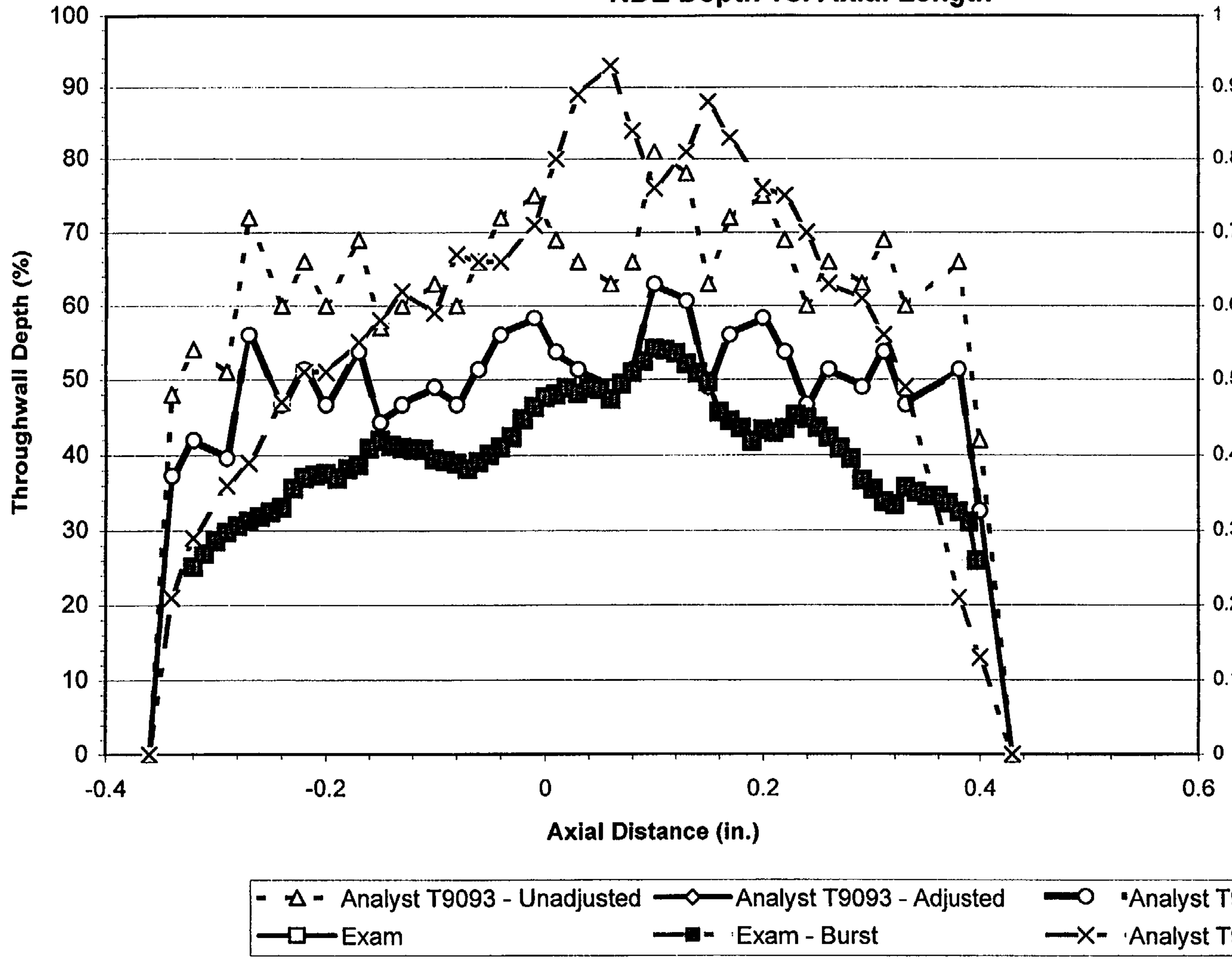

Unadjusted	T9093	Exam
Length	0.79	0.72
Max. Volts	0.93	
Max. Depth (%)	81.0	54.1
Avg. Depth (%)	62.4	40.7

Adjusted	T9093	Exam
Length	0.79	0.72
Max. Volts	0.93	
Max. Depth (%)	63.0	54.1
Avg. Depth (%)	48.6	40.7

Burst	T9093	Exam
Length	0.74	0.72
Max. Volts	0.93	
Max. Depth (%)	63.0	54.1
Avg. Depth (%)	50.7	40.7

PWSCC ARC Release 1.1

Figure D-34
Specimen R 21 - C 73 - 01H - Crack 1 - Year 1998
Comparison of Unadjusted, Adjusted, Burst and Voltage with Exam
NDE Depth vs. Axial Length

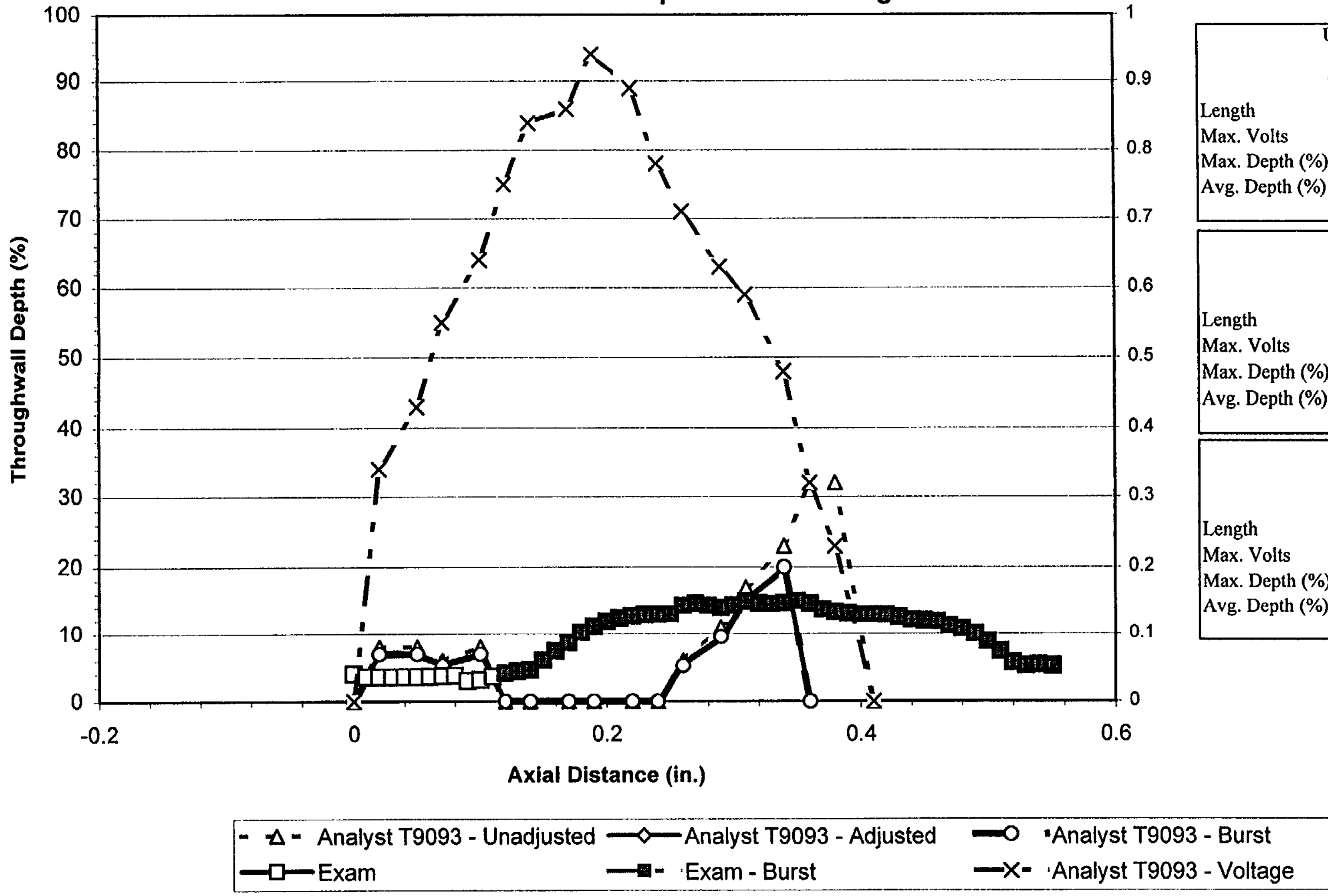

Unadjusted	T9093	Exam
Length	0.41	0.55
Max. Volts	0.94	
Max. Depth (%)	32.0	15.0
Avg. Depth (%)	8.8	9.6

Adjusted	T9093	Exam
Length	0.36	0.55
Max. Volts	0.94	
Max. Depth (%)	20.0	15.0
Avg. Depth (%)	5.3	9.6

Burst	T9093	Exam
Length	0.36	0.43
Max. Volts	0.94	
Max. Depth (%)	20.0	15.0
Avg. Depth (%)	5.3	11.2

PWSCC ARC Release 1.1

Figure D-35
Specimen R 21 - C 79 - 01H - Crack 1 - Year 1998
Comparison of Unadjusted, Adjusted, Burst and Voltage with Exam
NDE Depth vs. Axial Length

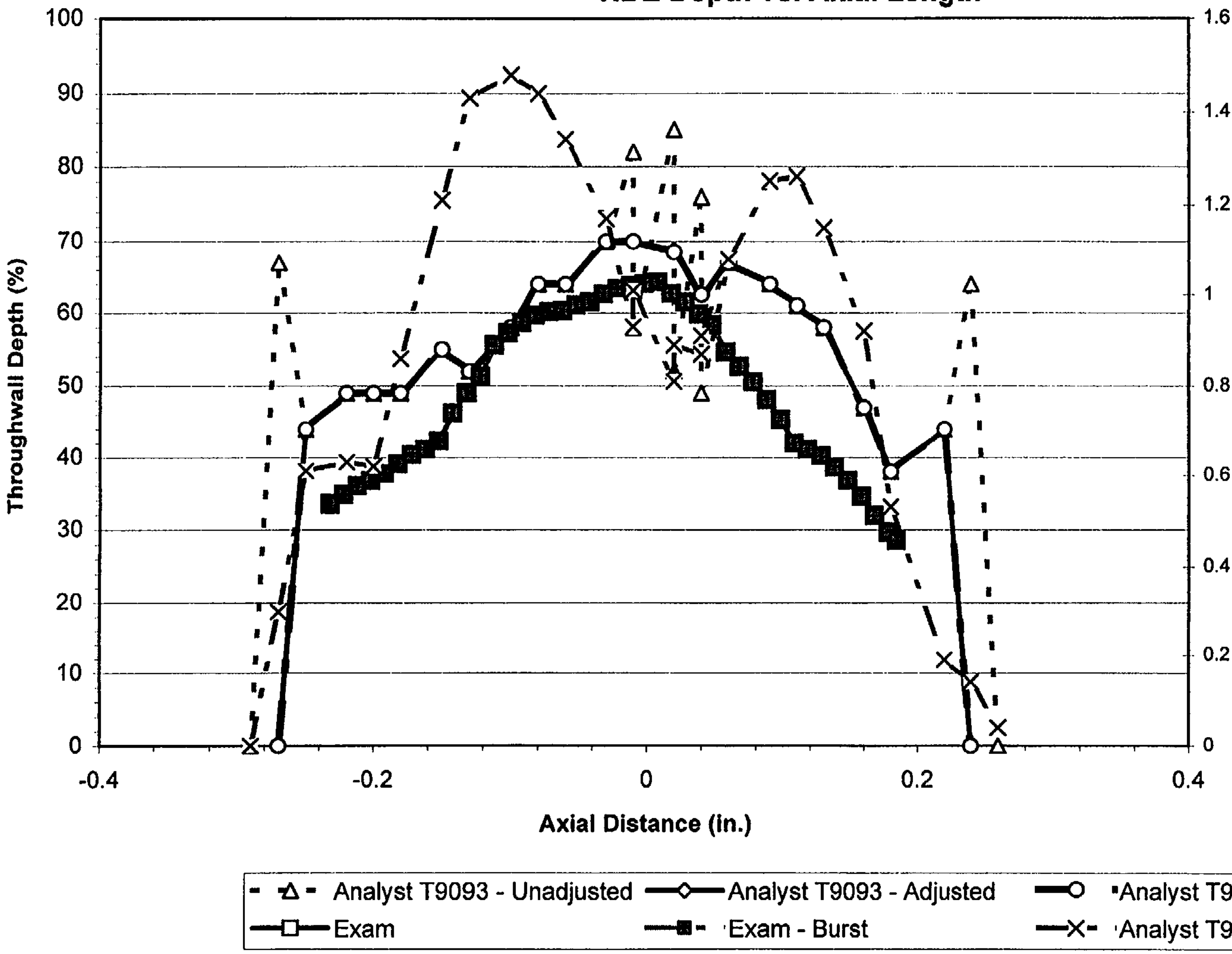

Unadjusted	T9093	Exam
Length	0.55	0.42
Max. Volts	1.48	
Max. Depth (%)	85.0	64.3
Avg. Depth (%)	54.9	49.4

Adjusted	T9093	Exam
Length	0.51	0.42
Max. Volts	1.48	
Max. Depth (%)	70.0	64.3
Avg. Depth (%)	54.1	49.4

Burst	T9093	Exam
Length	0.51	0.42
Max. Volts	1.48	
Max. Depth (%)	70.0	64.3
Avg. Depth (%)	54.1	49.4

PWSCC ARC Release 1.1

Figure D-36
Specimen R 21 - C 85 - 01H - Crack 1 - Year 1998
Comparison of Unadjusted, Adjusted, Burst and Voltage with Exam
NDE Depth vs. Axial Length

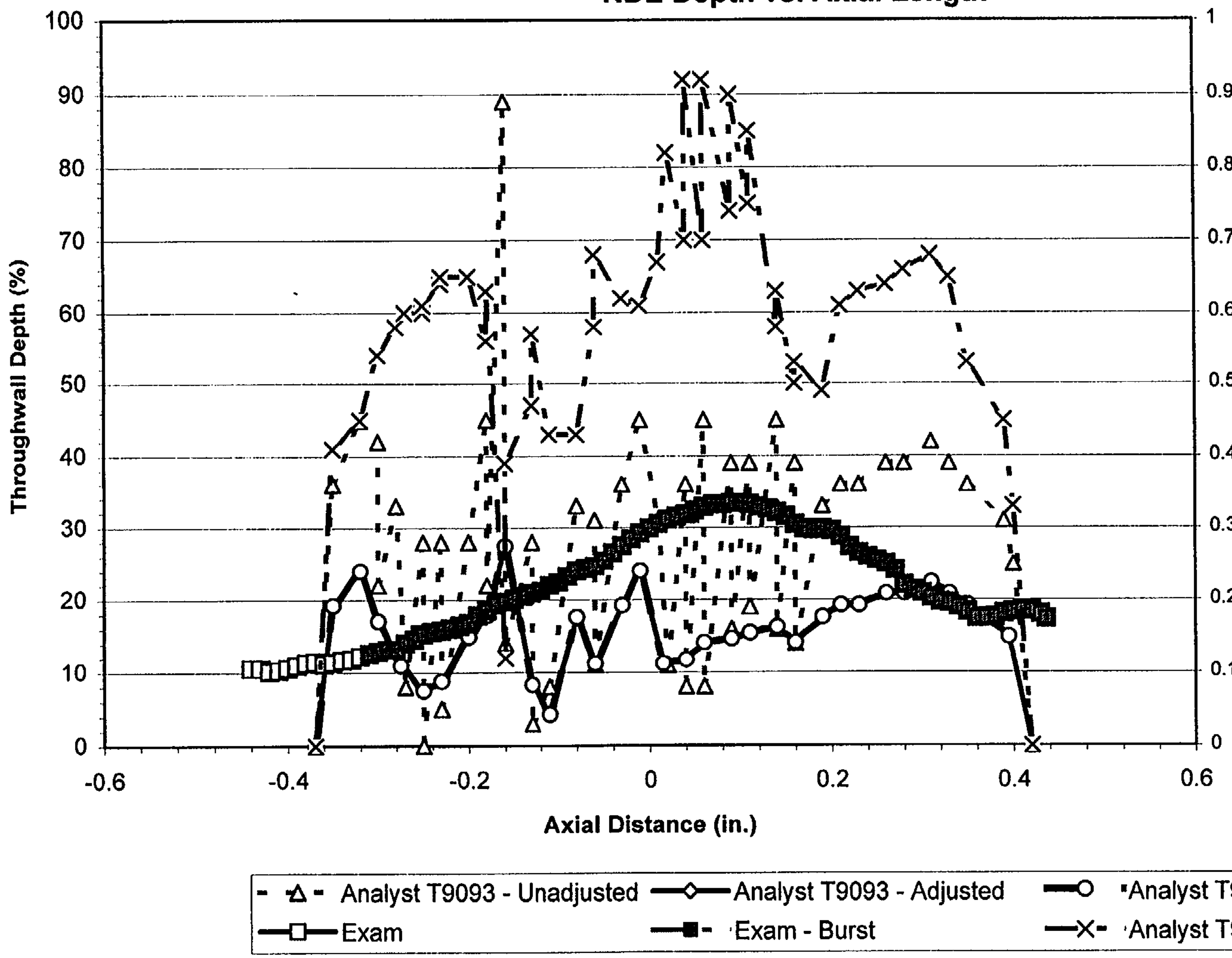

Unadjusted

	T9093	Exam
Length	0.79	0.88
Max. Volts	0.92	
Max. Depth (%)	89.0	33.4
Avg. Depth (%)	29.0	21.8

Adjusted

	T9093	Exam
Length	0.79	0.88
Max. Volts	0.82	
Max. Depth (%)	27.5	33.4
Avg. Depth (%)	15.8	21.8

Burst

	T9093	Exam
Length	0.77	0.75
Max. Volts	0.82	
Max. Depth (%)	27.5	33.4
Avg. Depth (%)	16.1	23.6

PWSCC ARC Release 1.1

Figure D-37
Specimen R 23 - C 15 - 01H - Crack 1 - Year 1998
Comparison of Unadjusted, Adjusted, Burst and Voltage with Exam
NDE Depth vs. Axial Length

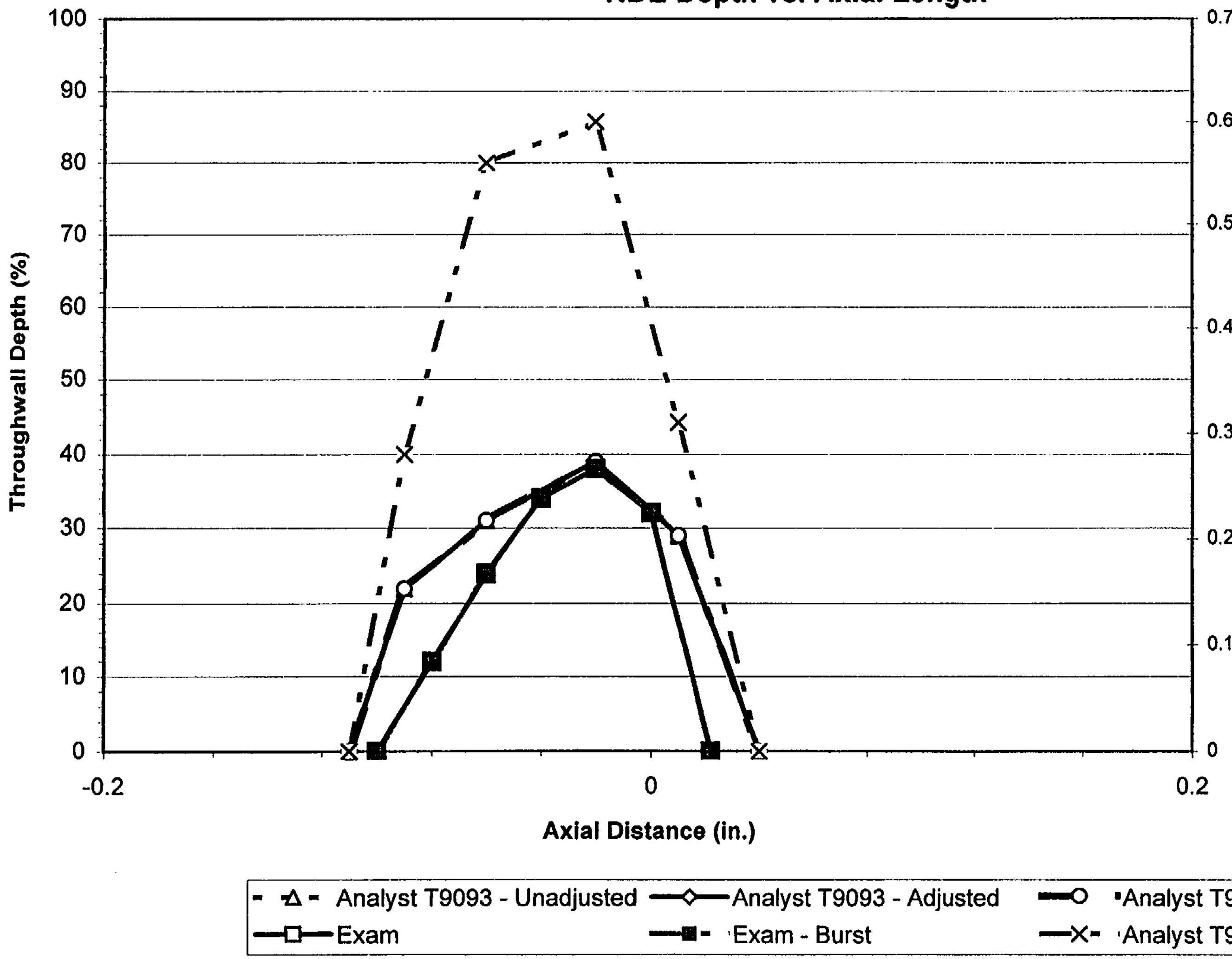

Unadjusted	T9093	Exam
Length	0.15	0.12
Max. Volts	0.60	
Max. Depth (%)	39.0	38.0
Avg. Depth (%)	25.8	23.2

Adjusted	T9093	Exam
Length	0.15	0.12
Max. Volts	0.60	
Max. Depth (%)	39.0	38.0
Avg. Depth (%)	25.8	23.2

Burst	T9093	Exam
Length	0.15	0.12
Max. Volts	0.60	
Max. Depth (%)	39.0	38.0
Avg. Depth (%)	25.8	23.2

PWSCC ARC Release 1.1

Figure D-38
Specimen R 25 - C 40 - 01H - Crack 1 - Year 1998
Comparison of Unadjusted, Adjusted, Burst and Voltage with Exam NDE Depth vs. Axial Length

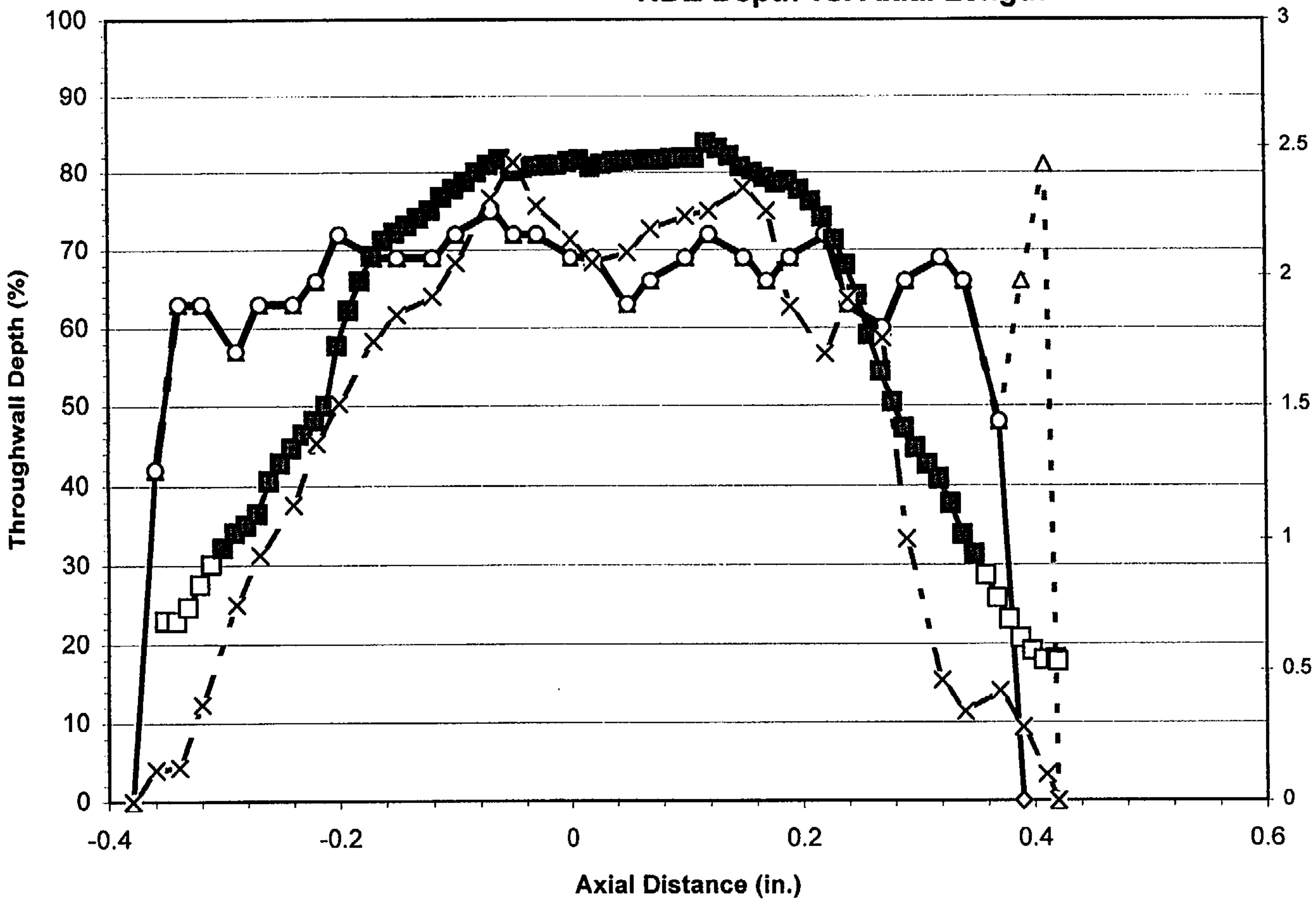

Unadjusted

	T9093	Exam
Length	0.80	0.77
Max. Volts	2.44	
Max. Depth (%)	81.0	83.7
Avg. Depth (%)	65.1	60.5

Adjusted

	T9093	Exam
Length	0.77	0.77
Max. Volts	2.44	
Max. Depth (%)	75.0	83.7
Avg. Depth (%)	64.3	60.5

Burst

	T9093	Exam
Length	0.73	0.65
Max. Volts	2.44	
Max. Depth (%)	75.0	83.7
Avg. Depth (%)	66.6	67.4

Analyst T9093 - Unadjusted
Analyst T9093 - Adjusted
Analyst T9093 - Burst
Exam
Exam - Burst
Analyst T9093 - Voltage

PWSCC ARC Release 1.1

Figure D-39
Specimen R 25 - C 52 - 01H - Crack 1 - Year 1998
Comparison of Unadjusted, Adjusted, Burst and Voltage with Exam
NDE Depth vs. Axial Length

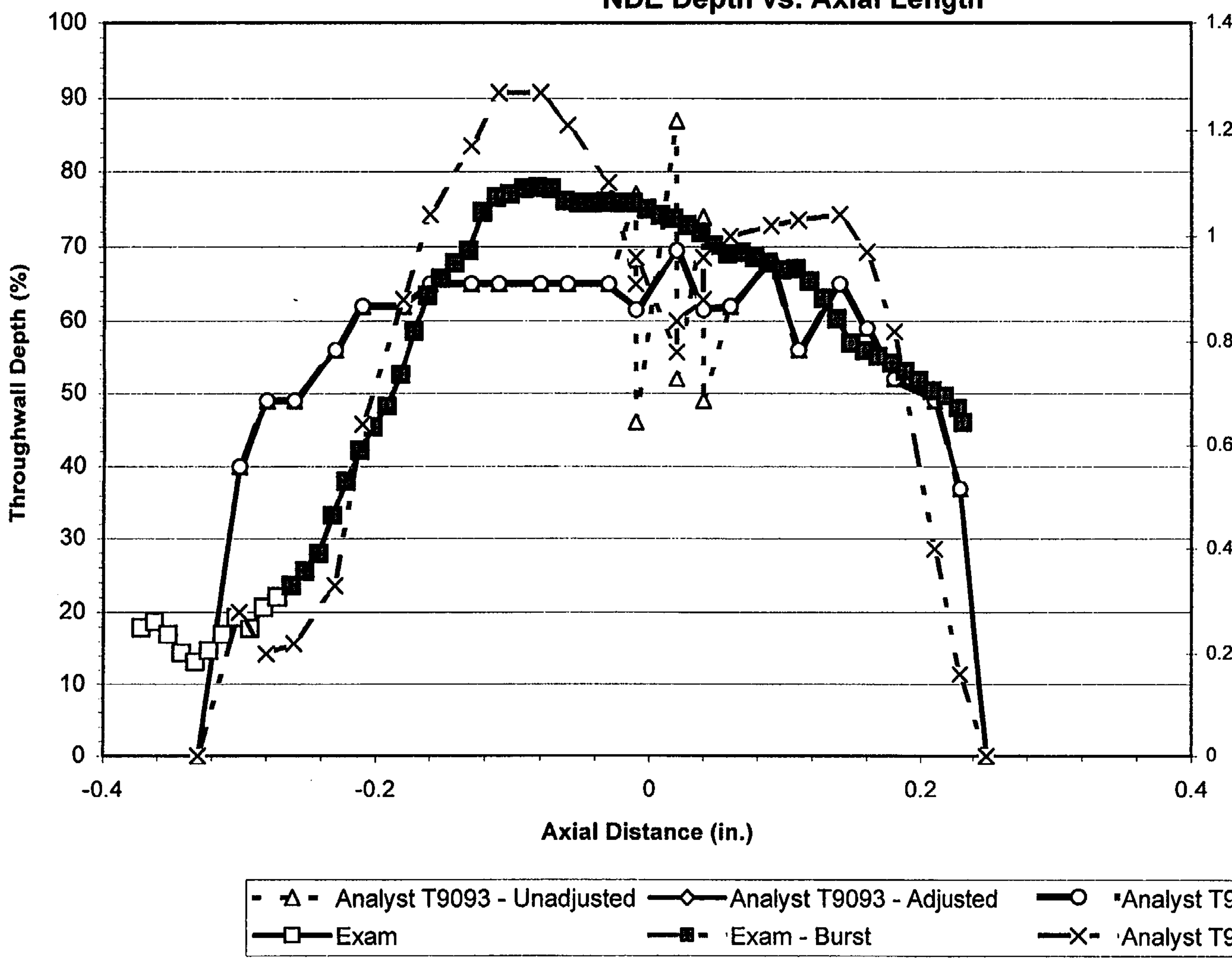

Unadjusted

	T9093	Exam
Length	0.58	0.60
Max. Volts	1.27	
Max. Depth (%)	87.0	77.9
Avg. Depth (%)	56.6	54.1

Adjusted

	T9093	Exam
Length	0.58	0.60
Max. Volts	1.27	
Max. Depth (%)	69.5	77.9
Avg. Depth (%)	56.3	54.1

Burst

	T9093	Exam
Length	0.53	0.49
Max. Volts	1.27	
Max. Depth (%)	69.5	77.9
Avg. Depth (%)	59.8	62.2

PWSCC ARC Release 1.1

Figure D-40
Specimen R 25 - C 79 - 01H - Crack 1 - Year 1998
Comparison of Unadjusted, Adjusted, Burst and Voltage with Exam
NDE Depth vs. Axial Length

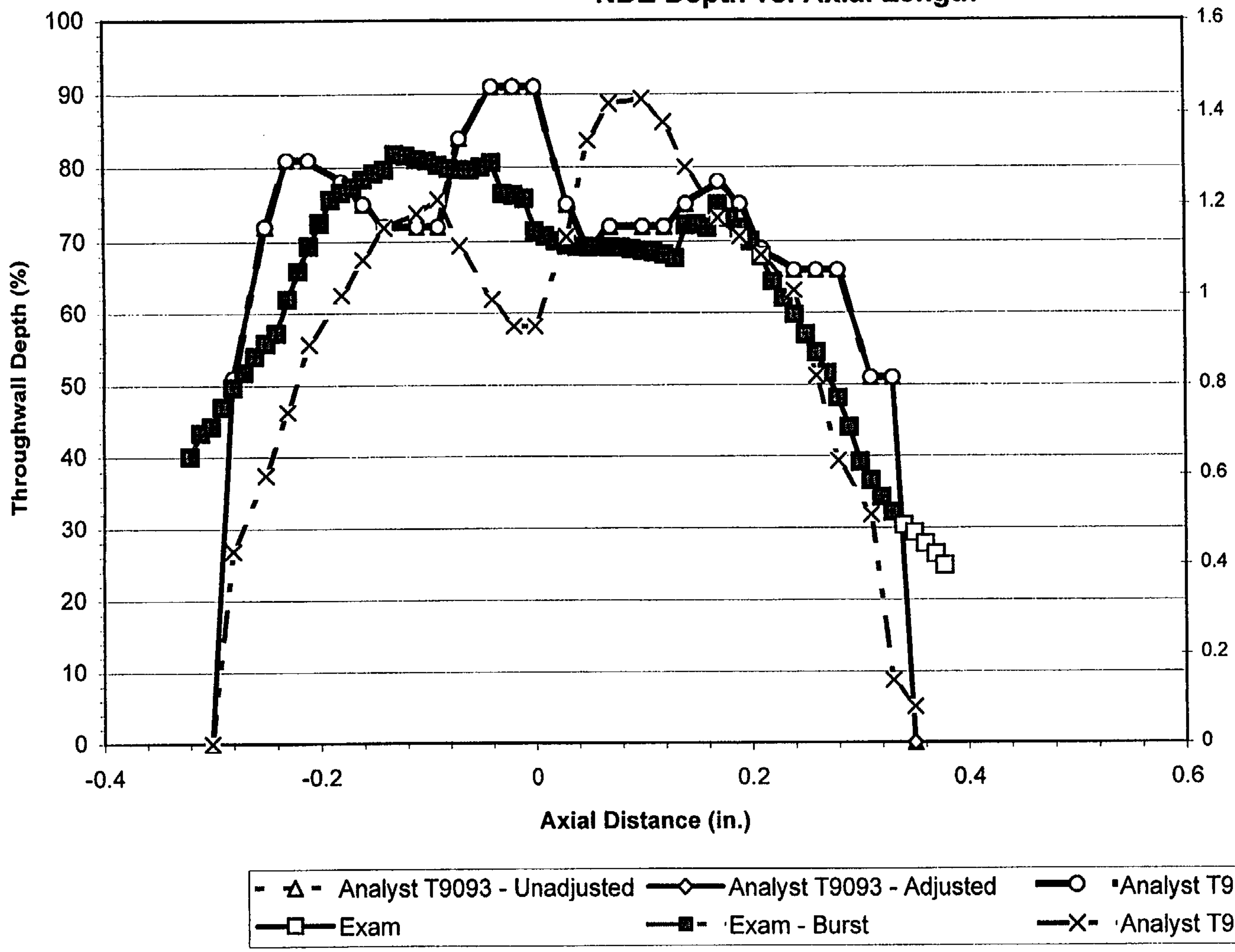

Unadjusted	T9093	Exam
Length	0.65	0.70
Max. Volts	1.43	
Max. Depth (%)	91.0	81.8
Avg. Depth (%)	70.7	63.6

Adjusted	T9093	Exam
Length	0.65	0.70
Max. Volts	1.43	
Max. Depth (%)	91.0	81.8
Avg. Depth (%)	70.7	63.6

Burst	T9093	Exam
Length	0.61	0.65
Max. Volts	1.43	
Max. Depth (%)	91.0	81.8
Avg. Depth (%)	73.6	66.2

PWSCC ARC Release 1.1

Figure D-41
Specimen R 27 - C 77 - 01H - Crack 1 - Year 1998
Comparison of Unadjusted, Adjusted, Burst and Voltage with Exam
NDE Depth vs. Axial Length

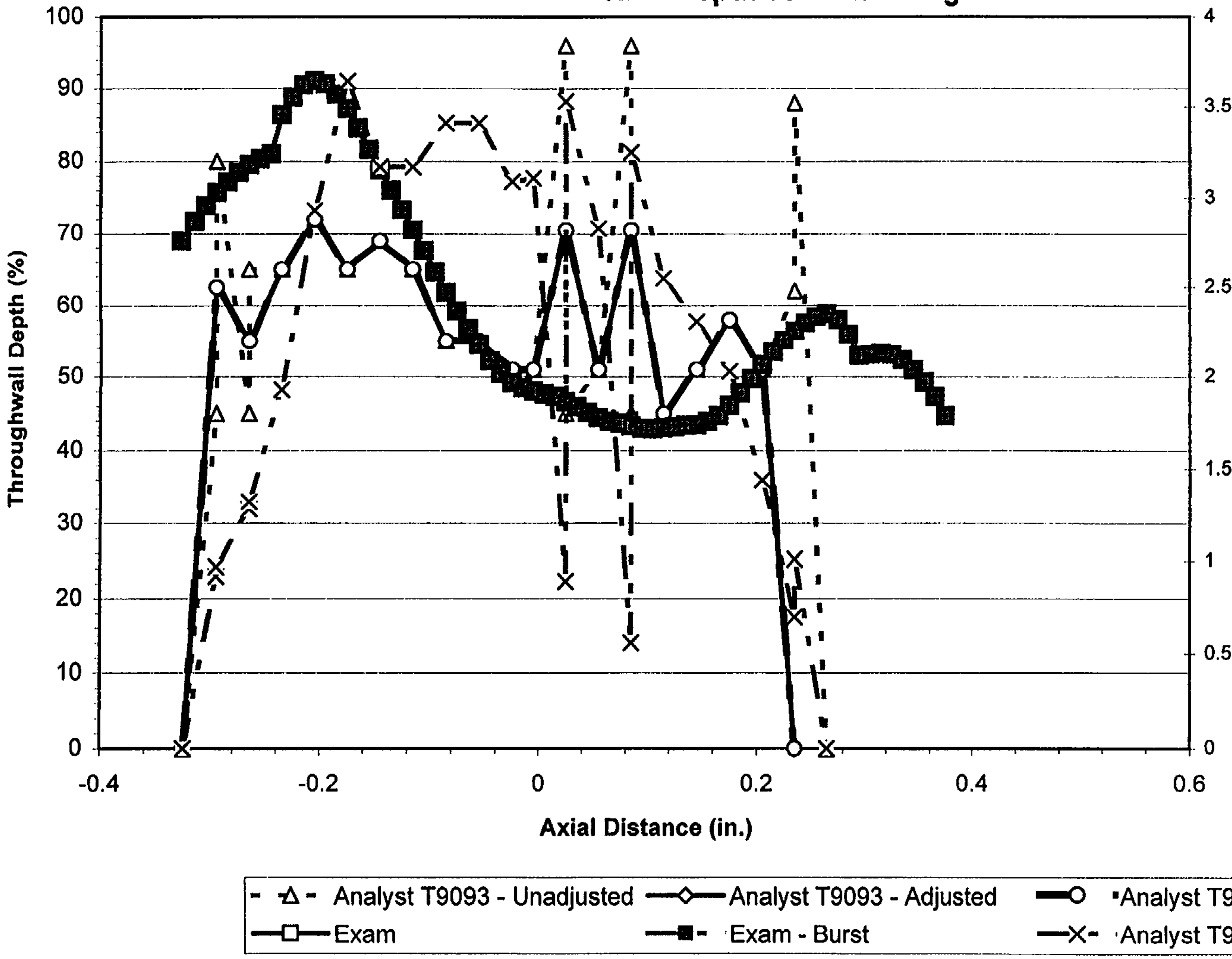

Unadjusted

	T9093	Exam
Length	0.59	0.70
Max. Volts	3.64	
Max. Depth (%)	96.0	91.1
Avg. Depth (%)	57.0	59.9

Adjusted

	T9093	Exam
Length	0.56	0.70
Max. Volts	3.64	
Max. Depth (%)	72.0	91.1
Avg. Depth (%)	56.0	59.9

Burst

	T9093	Exam
Length	0.56	0.70
Max. Volts	3.64	
Max. Depth (%)	72.0	91.1
Avg. Depth (%)	56.0	59.9

Figure D-42
Specimen R 29 - C 34 - 01H - Crack 1 - Year 1998
Comparison of Unadjusted, Adjusted, Burst and Voltage with Exam NDE Depth vs. Axial Length

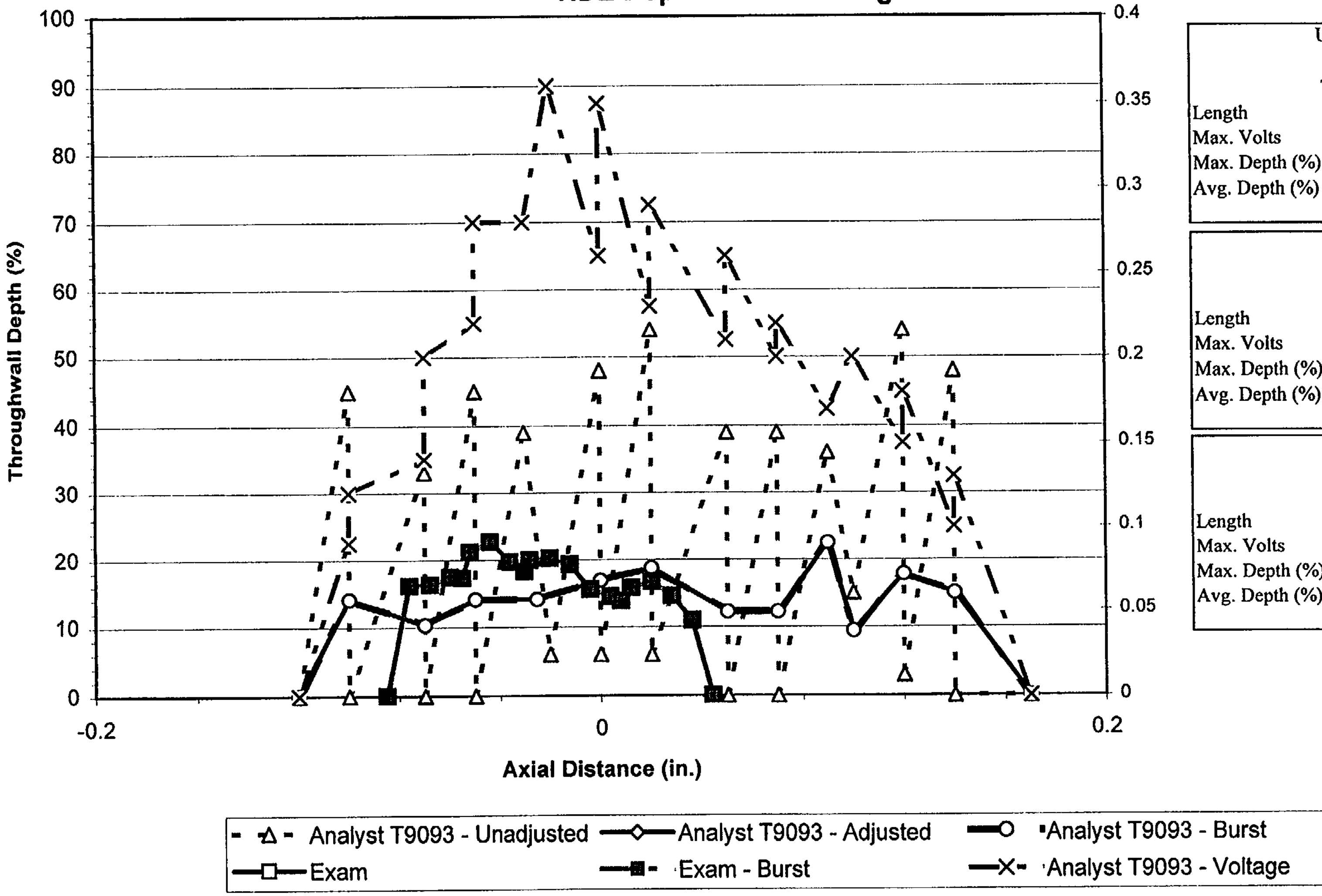

Unadjusted

	T9093	Exam
Length	0.29	0.13
Max. Volts	0.36	
Max. Depth (%)	54.0	22.7
Avg. Depth (%)	20.9	16.1

Adjusted

	T9093	Exam
Length	0.29	0.13
Max. Volts	0.32	
Max. Depth (%)	22.5	22.7
Avg. Depth (%)	13.4	16.1

Burst

	T9093	Exam
Length	0.29	0.13
Max. Volts	0.32	
Max. Depth (%)	22.5	22.7
Avg. Depth (%)	13.4	16.1

Figure D-43
Specimen R 29 - C 16 - 01H - Crack 1 - Year 1998
Comparison of Unadjusted, Adjusted, Burst and Voltage with Exam
NDE Depth vs. Axial Length

PWSCC ARC Release 1.1

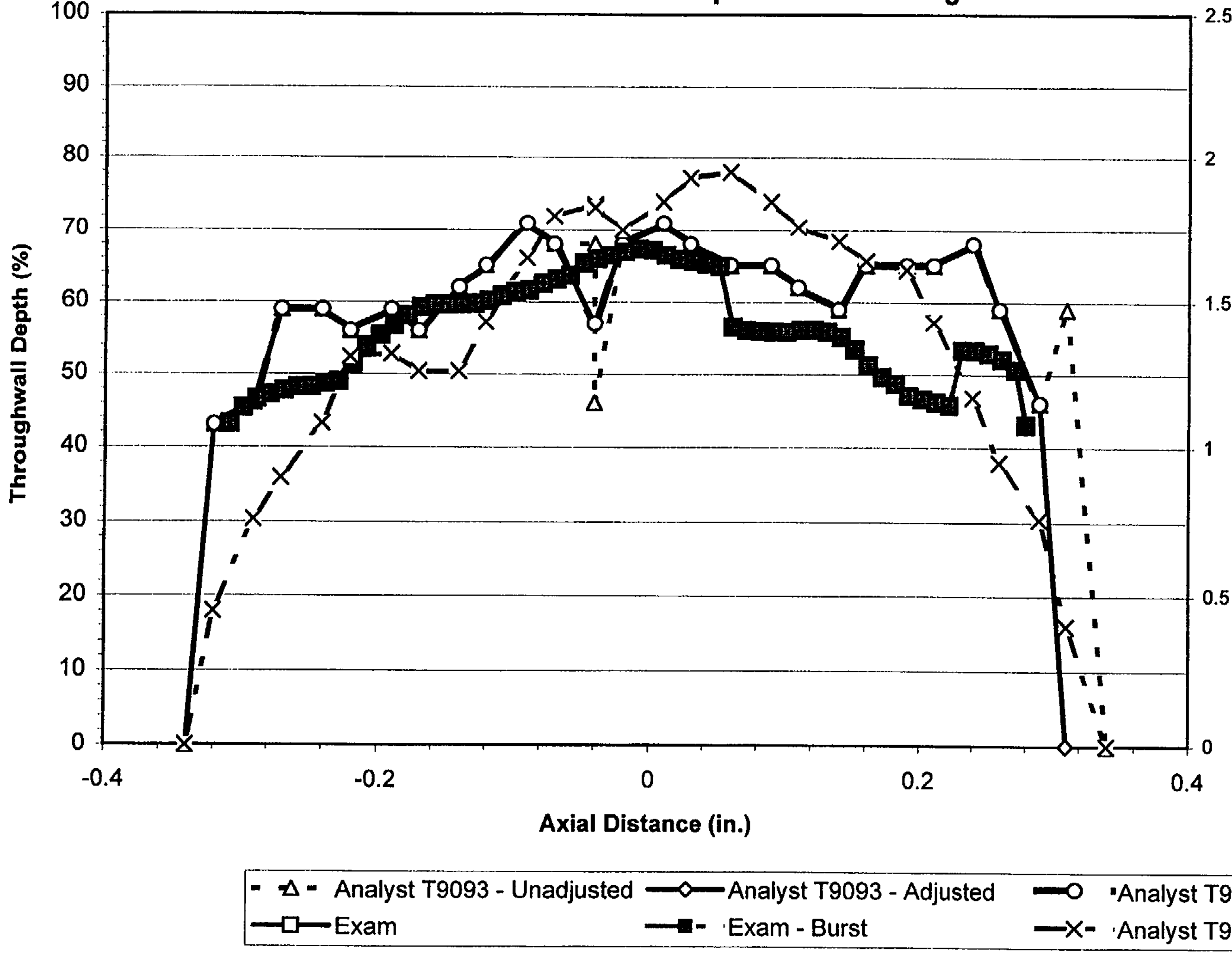

Unadjusted	T9093	Exam
Length	0.68	0.59
Max. Volts	1.95	
Max. Depth (%)	71.0	67.3
Avg. Depth (%)	58.7	56.1

Adjusted	T9093	Exam
Length	0.65	0.59
Max. Volts	1.95	
Max. Depth (%)	71.0	67.3
Avg. Depth (%)	59.2	56.1

Burst	T9093	Exam
Length	0.61	0.59
Max. Volts	1.95	
Max. Depth (%)	71.0	67.3
Avg. Depth (%)	61.7	56.1

PWSCC ARC Release 1.1

Figure D-44
Specimen R 29 - C 41 - 01H - Crack 1 - Year 1998
Comparison of Unadjusted, Adjusted, Burst and Voltage with Exam
NDE Depth vs. Axial Length

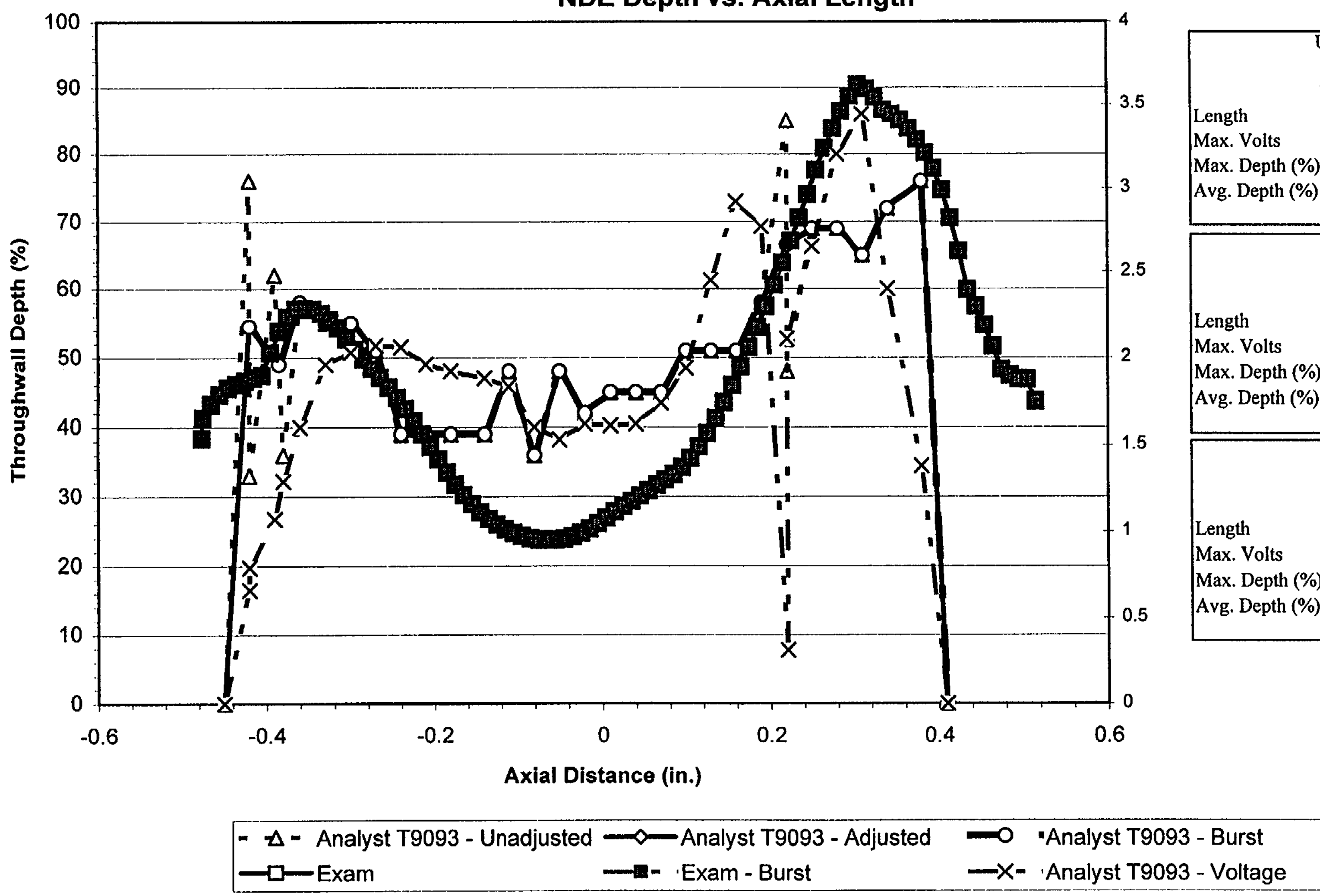

Unadjusted	T9093	Exam
Length	0.86	0.99
Max. Volts	3.44	
Max. Depth (%)	85.0	90.5
Avg. Depth (%)	50.7	49.3

Adjusted	T9093	Exam
Length	0.86	0.99
Max. Volts	3.44	
Max. Depth (%)	76.0	90.5
Avg. Depth (%)	50.7	49.3

Burst	T9093	Exam
Length	0.83	0.99
Max. Volts	3.44	
Max. Depth (%)	76.0	90.5
Avg. Depth (%)	51.5	49.3

PWSCC ARC Release 1.1

Figure D-45
Specimen R 29 - C 41 - 01H - Crack 2 - Year 1998
Comparison of Unadjusted, Adjusted, Burst and Voltage with Exam
NDE Depth vs. Axial Length

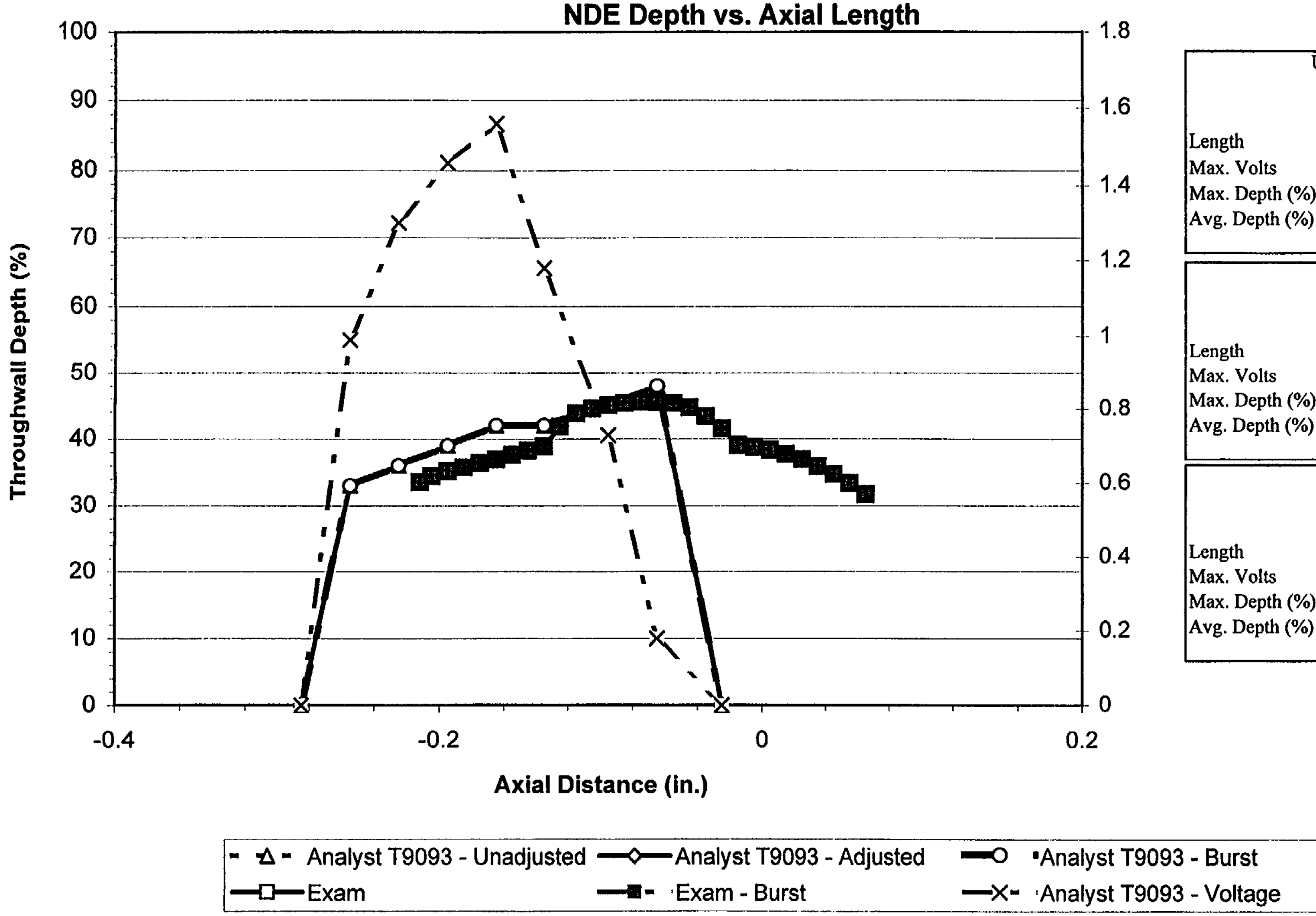

Unadjusted	T9093	Exam
Length	0.26	0.28
Max. Volts	1.56	
Max. Depth (%)	48.0	45.5
Avg. Depth (%)	35.5	39.6

Adjusted	T9093	Exam
Length	0.26	0.28
Max. Volts	1.56	
Max. Depth (%)	48.0	45.5
Avg. Depth (%)	35.5	39.6

Burst	T9093	Exam
Length	0.26	0.28
Max. Volts	1.56	
Max. Depth (%)	48.0	45.5
Avg. Depth (%)	35.5	39.6

PWSCC ARC Release 1.1

Figure D-46
Specimen R 29 - C 67 - 01H - Crack 1 - Year 1998
Comparison of Unadjusted, Adjusted, Burst and Voltage with Exam
NDE Depth vs. Axial Length

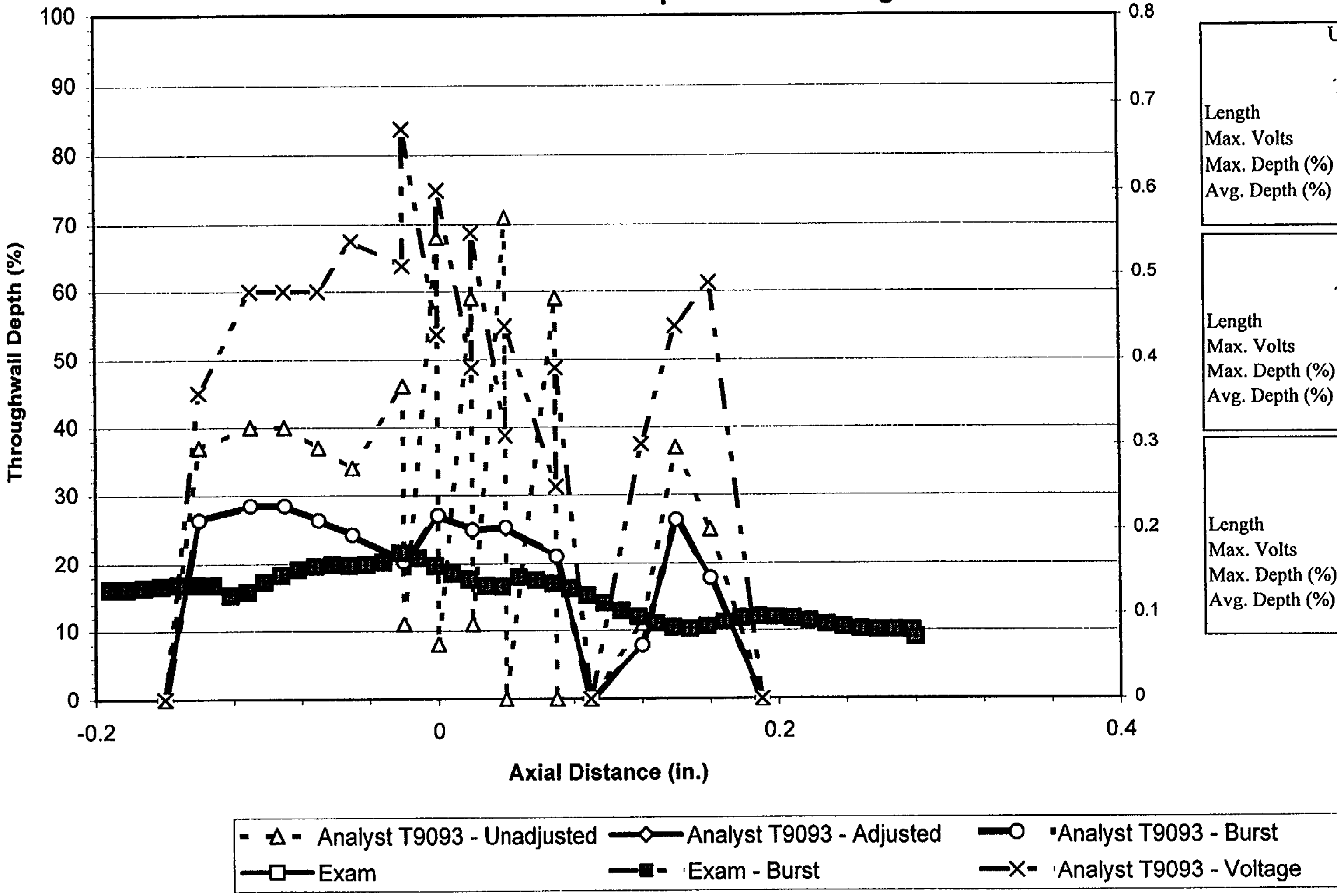

Unadjusted	T9093	Exam
Length	0.35	0.47
Max. Volts	0.67	
Max. Depth (%)	71.0	21.5
Avg. Depth (%)	28.0	15.2

Adjusted	T9093	Exam
Length	0.35	0.47
Max. Volts	0.59	
Max. Depth (%)	28.5	21.5
Avg. Depth (%)	19.9	15.2

Burst	T9093	Exam
Length	0.35	0.47
Max. Volts	0.59	
Max. Depth (%)	28.5	21.5
Avg. Depth (%)	19.9	15.2

PWSCC ARC Release 1.1

Figure D-47
Specimen R 30 - C 45 - 01H - Crack 1 - Year 1998
Comparison of Unadjusted, Adjusted, Burst and Voltage with Exam
NDE Depth vs. Axial Length

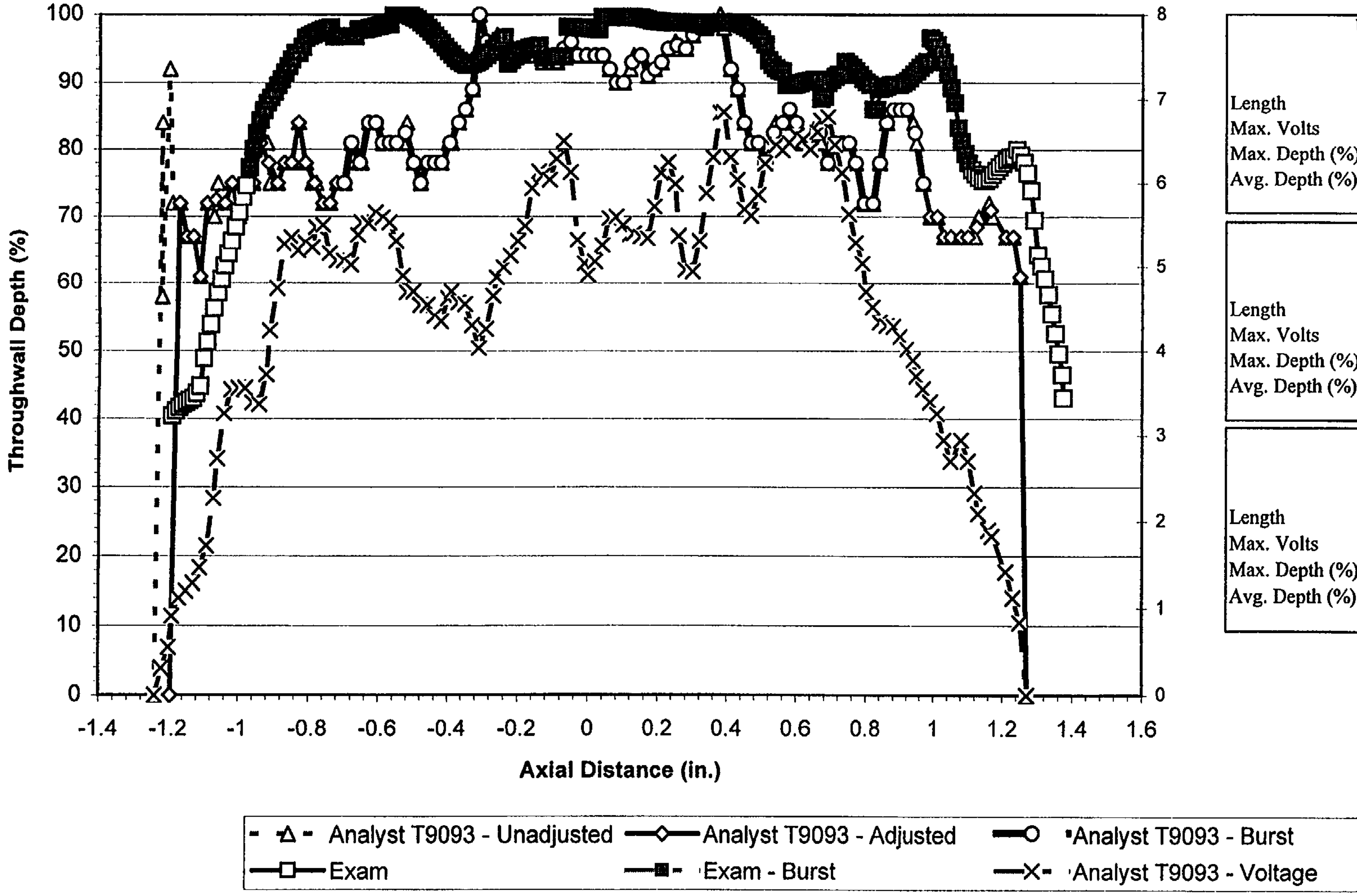

Unadjusted	T9093	Exam
Length	2.51	2.56
Max. Volts	6.85	
Max. Depth (%)	100.0	100.0
Avg. Depth (%)	81.5	88.7

Adjusted	T9093	Exam
Length	2.46	2.56
Max. Volts	6.84	
Max. Depth (%)	100.0	100.0
Avg. Depth (%)	81.5	88.7

Burst	T9093	Exam
Length	1.67	2.07
Max. Volts	6.84	
Max. Depth (%)	100.0	100.0
Avg. Depth (%)	87.1	94.6

PWSCC ARC Release 1.1

Figure D-48
Specimen R 30 - C 45 - 01H - Crack 2 - Year 1998
Comparison of Unadjusted, Adjusted, Burst and Voltage with Exam
NDE Depth vs. Axial Length

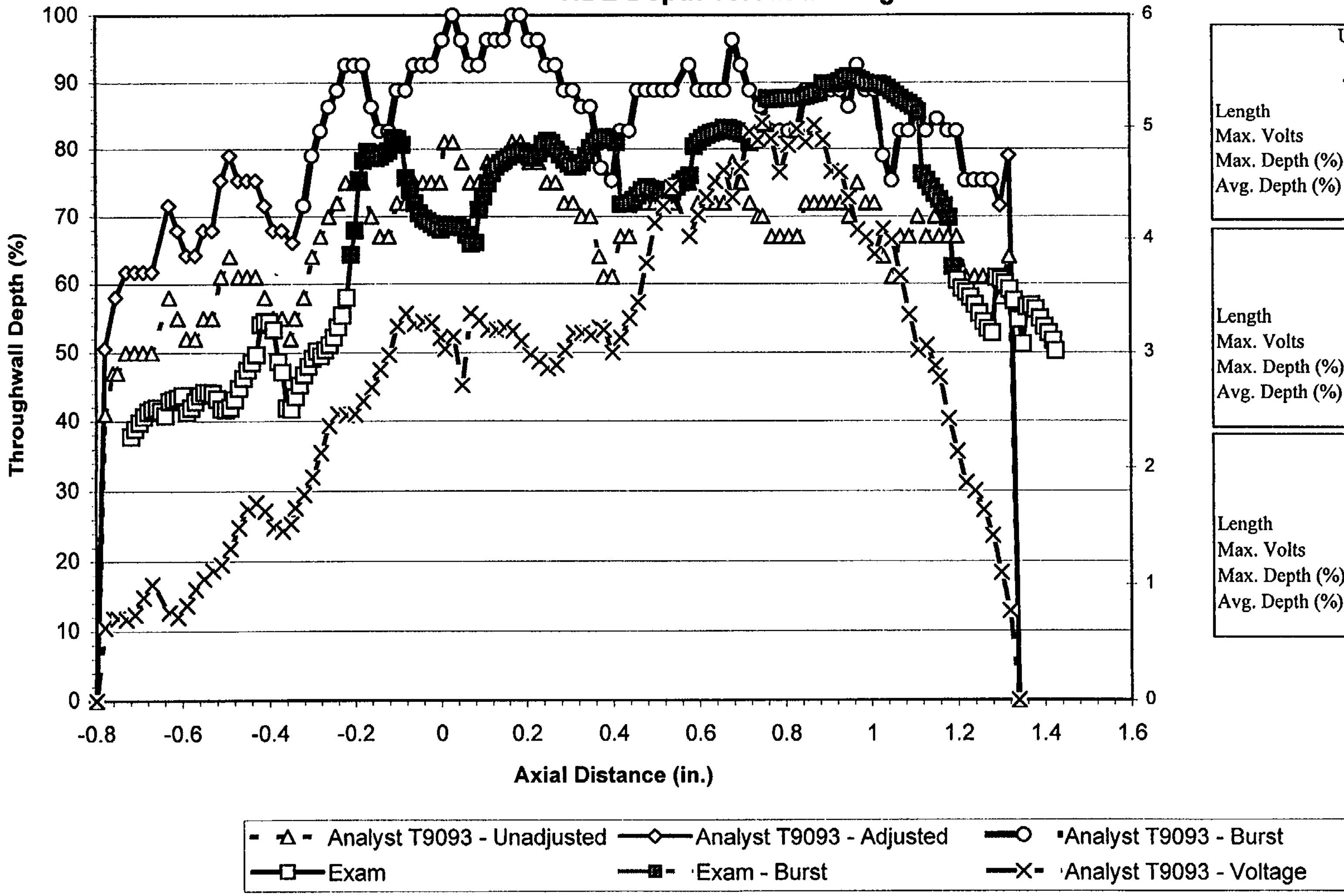

Unadjusted	T9093	Exam
Length	2.14	2.15
Max. Volts	5.04	
Max. Depth (%)	81.0	90.9
Avg. Depth (%)	66.5	69.0

Adjusted	T9093	Exam
Length	2.14	2.15
Max. Volts	5.02	
Max. Depth (%)	100.0	90.9
Avg. Depth (%)	82.2	69.0

Burst	T9093	Exam
Length	1.60	1.40
Max. Volts	5.02	
Max. Depth (%)	100.0	90.9
Avg. Depth (%)	87.8	79.5

PWSCC ARC Release 1.1

Figure D-49
Specimen R 33 - C 34 - 01H - Crack 1 - Year 1998
Comparison of Unadjusted, Adjusted, Burst and Voltage with Exam
NDE Depth vs. Axial Length

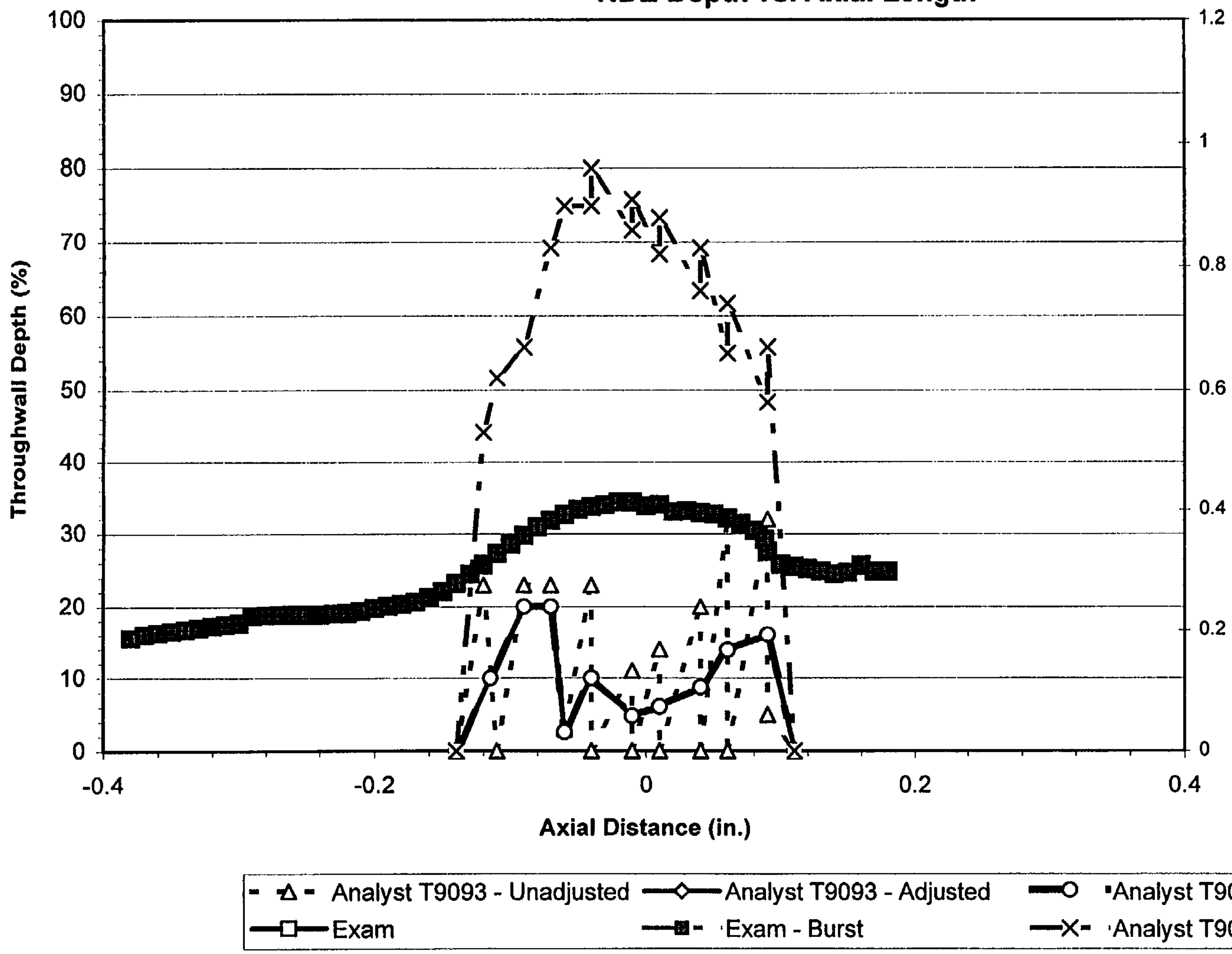

Unadjusted		
	T9093	Exam
Length	0.25	0.56
Max. Volts	0.96	
Max. Depth (%)	32.0	34.4
Avg. Depth (%)	11.6	24.9

Adjusted		
	T9093	Exam
Length	0.25	0.56
Max. Volts	0.93	
Max. Depth (%)	20.0	34.4
Avg. Depth (%)	10.1	24.9

Burst		
	T9093	Exam
Length	0.25	0.56
Max. Volts	0.93	
Max. Depth (%)	20.0	34.4
Avg. Depth (%)	10.1	24.9

PWSCC ARC Release 1.1

Figure D-50
Specimen R 33 - C 58 - 01H - Crack 1 - Year 1998
Comparison of Unadjusted, Adjusted, Burst and Voltage with Exam
NDE Depth vs. Axial Length

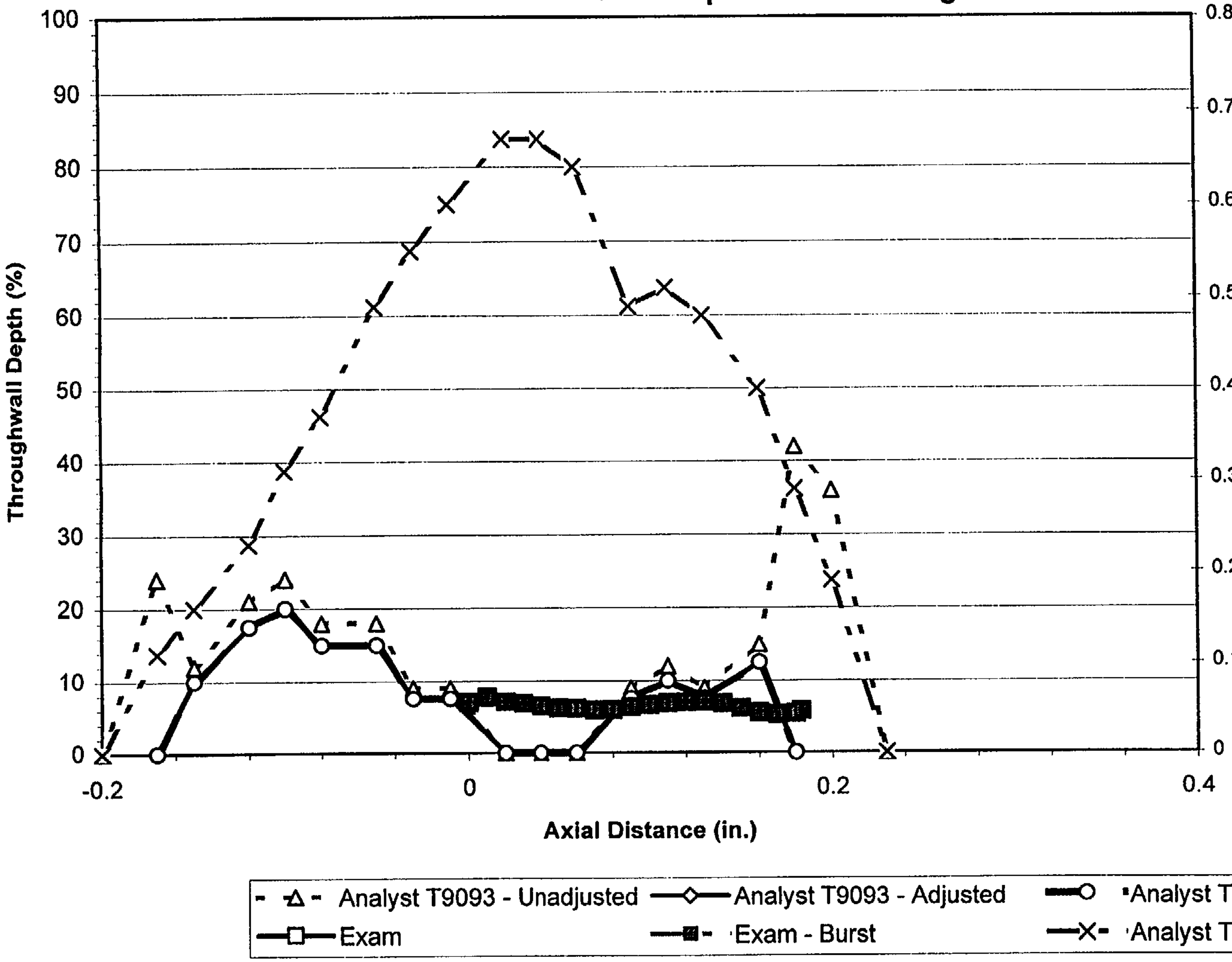

Unadjusted	T9093	Exam
Length	0.43	0.18
Max. Volts	0.67	
Max. Depth (%)	42.0	7.7
Avg. Depth (%)	14.0	6.4

Adjusted	T9093	Exam
Length	0.35	0.18
Max. Volts	0.67	
Max. Depth (%)	20.0	7.7
Avg. Depth (%)	8.7	6.4

Burst	T9093	Exam
Length	0.35	0.18
Max. Volts	0.67	
Max. Depth (%)	20.0	7.7
Avg. Depth (%)	8.7	6.4

PWSCC ARC Release 1.1

Figure D-51
Specimen R 37 - C 31 - 01H - Crack 1 - Year 1998
Comparison of Unadjusted, Adjusted, Burst and Voltage with Exam
NDE Depth vs. Axial Length

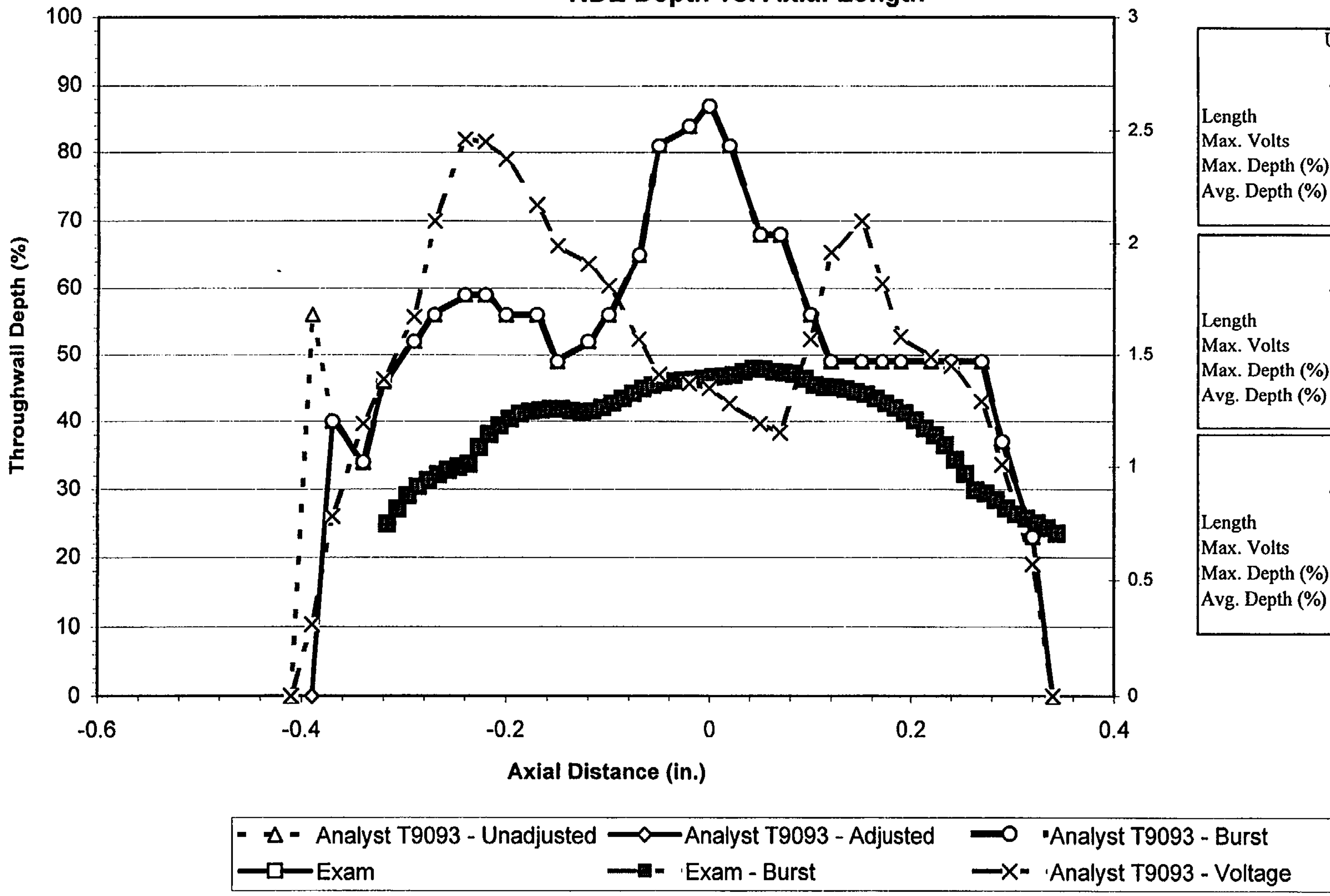

Unadjusted

	T9093	Exam
Length	0.75	0.66
Max. Volts	2.46	
Max. Depth (%)	87.0	47.9
Avg. Depth (%)	53.8	39.4

Adjusted

	T9093	Exam
Length	0.73	0.66
Max. Volts	2.46	
Max. Depth (%)	87.0	47.9
Avg. Depth (%)	53.7	39.4

Burst

	T9093	Exam
Length	0.69	0.66
Max. Volts	2.46	
Max. Depth (%)	87.0	47.9
Avg. Depth (%)	55.9	39.4

PWSCC ARC Release 1.1

Figure D-52
Specimen R 37 - C 52 - 01H - Crack 1 - Year 1998
Comparison of Unadjusted, Adjusted, Burst and Voltage with Exam
NDE Depth vs. Axial Length

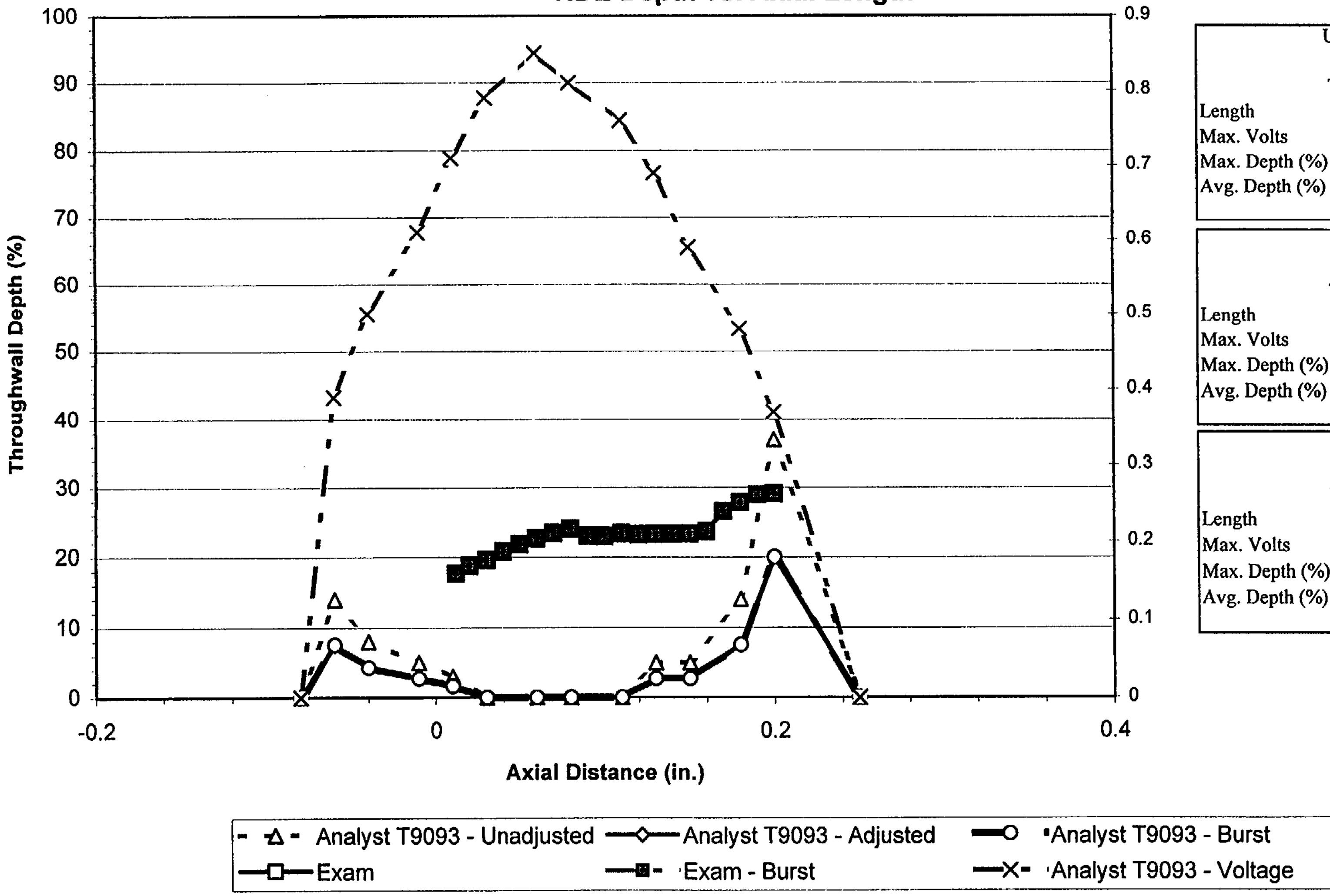

Unadjusted	T9093	Exam
Length	0.33	0.19
Max. Volts	0.85	
Max. Depth (%)	37.0	29.1
Avg. Depth (%)	7.7	23.4

Adjusted	T9093	Exam
Length	0.33	0.19
Max. Volts	0.85	
Max. Depth (%)	20.0	29.1
Avg. Depth (%)	4.2	23.4

Burst	T9093	Exam
Length	0.33	0.19
Max. Volts	0.85	
Max. Depth (%)	20.0	29.1
Avg. Depth (%)	4.2	23.4

PWSCC ARC Release 1.1

Figure D-53
Specimen R 39 - C 28 - 01H - Crack 1 - Year 1998
Comparison of Unadjusted, Adjusted, Burst and Voltage with Exam
NDE Depth vs. Axial Length

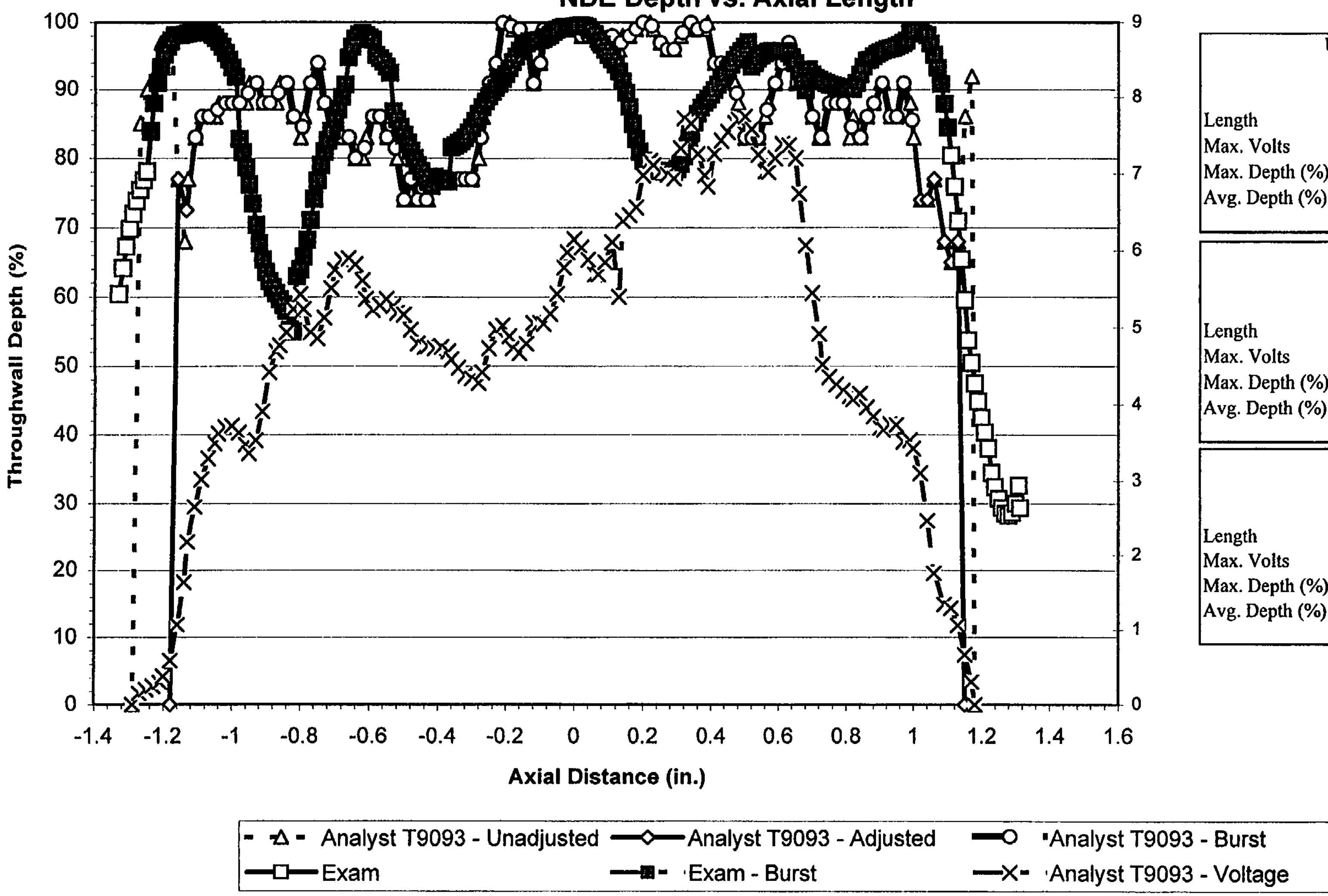

Unadjusted

	T9093	Exam
Length	2.47	2.64
Max. Volts	7.74	
Max. Depth (%)	100.0	99.6
Avg. Depth (%)	87.6	84.8

Adjusted

	T9093	Exam
Length	2.33	2.64
Max. Volts	7.74	
Max. Depth (%)	100.0	99.6
Avg. Depth (%)	87.2	84.8

Burst

	T9093	Exam
Length	2.11	2.34
Max. Volts	7.74	
Max. Depth (%)	100.0	99.6
Avg. Depth (%)	89.4	88.8

PWSCC ARC Release 1.1

Figure D-54
Specimen R 39 - C 28 - 01H - Crack 2 - Year 1998
Comparison of Unadjusted, Adjusted, Burst and Voltage with Exam NDE Depth vs. Axial Length

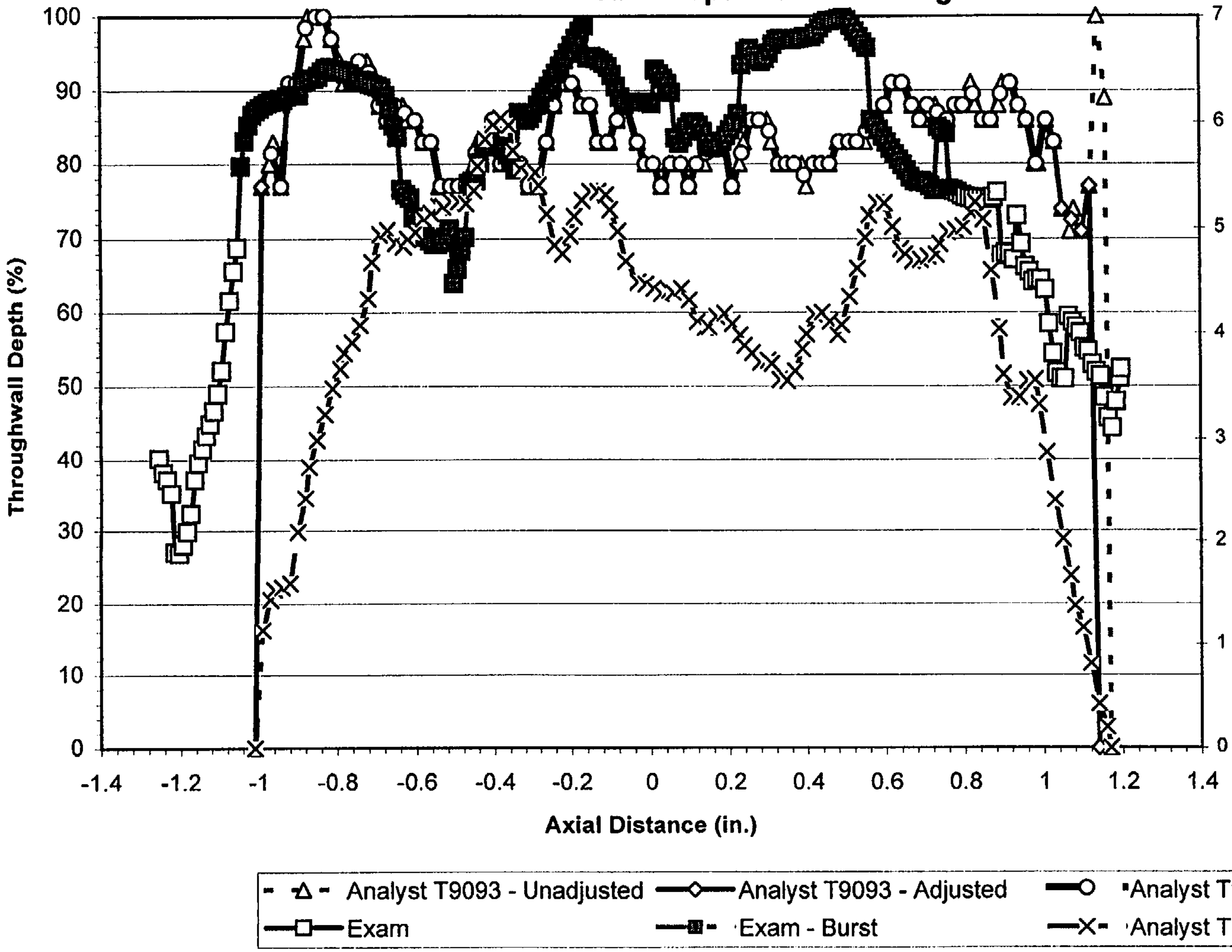

Unadjusted	T9093	Exam
Length	2.18	2.45
Max. Volts	6.04	
Max. Depth (%)	100.0	99.7
Avg. Depth (%)	83.9	79.4

Adjusted	T9093	Exam
Length	2.15	2.45
Max. Volts	6.04	
Max. Depth (%)	100.0	99.7
Avg. Depth (%)	83.5	79.4

Burst	T9093	Exam
Length	2.00	1.81
Max. Volts	6.04	
Max. Depth (%)	100.0	99.7
Avg. Depth (%)	84.9	87.4

PWSCC ARC Release 1.1

Figure D-55
Specimen R 41 - C 64 - 01H - Crack 1 - Year 1998
Comparison of Unadjusted, Adjusted, Burst and Voltage with Exam
NDE Depth vs. Axial Length

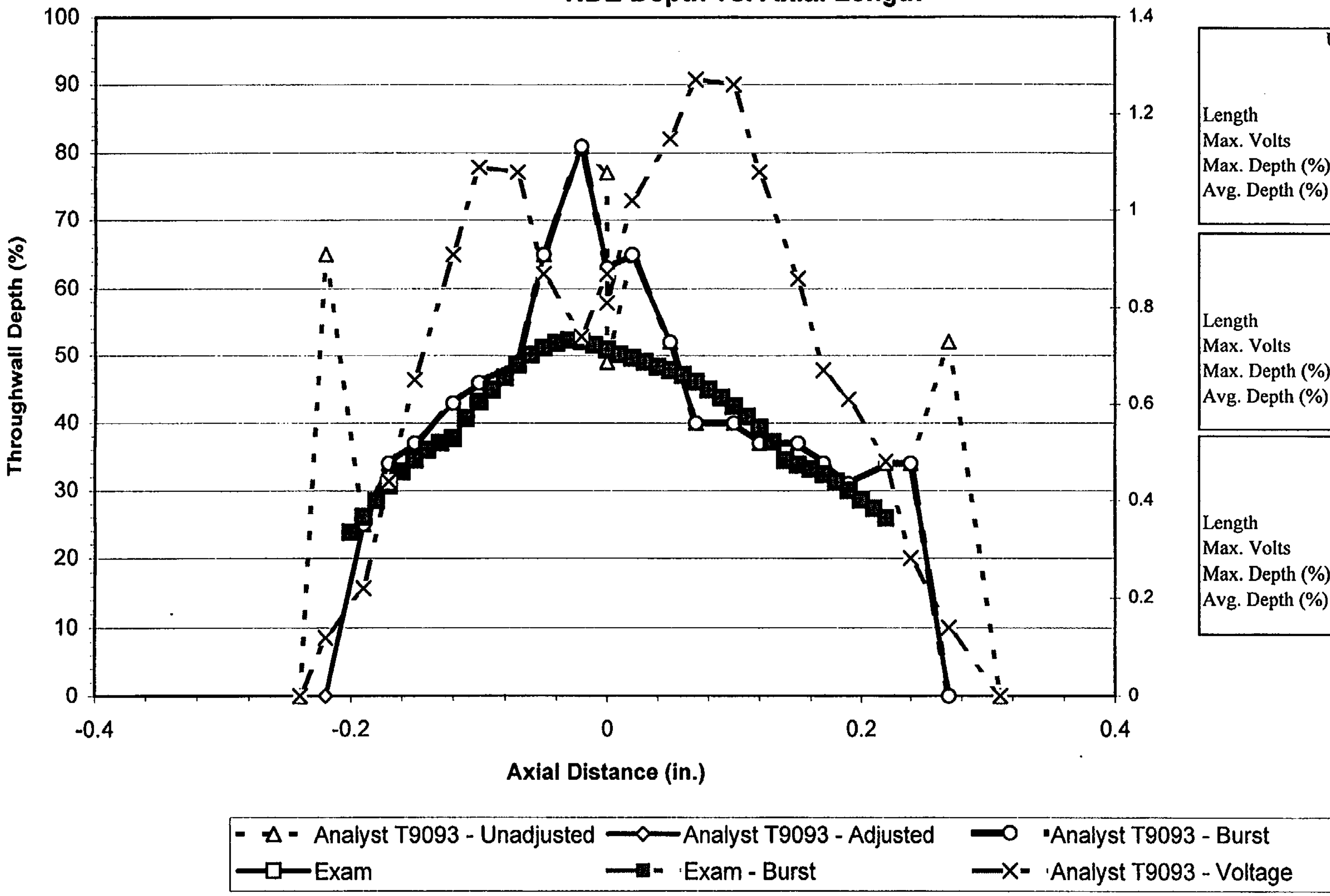

Unadjusted

	T9093	Exam
Length	0.55	0.42
Max. Volts	1.27	
Max. Depth (%)	81.0	52.2
Avg. Depth (%)	43.6	40.7

Adjusted

	T9093	Exam
Length	0.49	0.42
Max. Volts	1.27	
Max. Depth (%)	81.0	52.2
Avg. Depth (%)	41.9	40.7

Burst

	T9093	Exam
Length	0.46	0.42
Max. Volts	1.27	
Max. Depth (%)	81.0	52.2
Avg. Depth (%)	43.8	40.7

Figure D-56
Specimen R 43 - C 40 - 01H - Crack 1 - Year 1998
Comparison of Unadjusted, Adjusted, Burst and Voltage with Exam
NDE Depth vs. Axial Length

PWSCC ARC Release 1.1

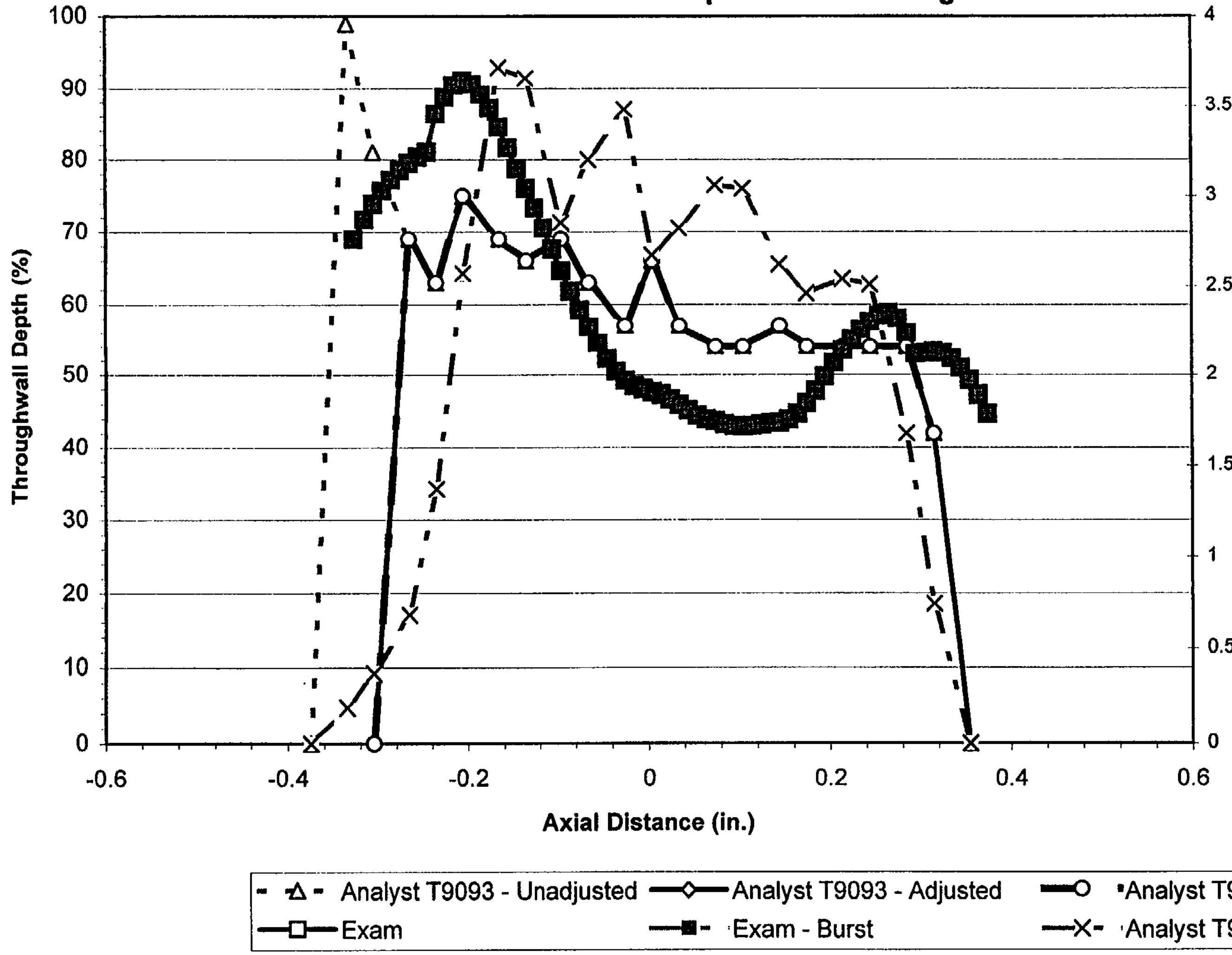

Unadjusted

	T9093	Exam
Length	0.73	0.70
Max. Volts	3.72	
Max. Depth (%)	99.0	91.1
Avg. Depth (%)	59.4	59.9

Adjusted

	T9093	Exam
Length	0.66	0.70
Max. Volts	3.72	
Max. Depth (%)	75.0	91.1
Avg. Depth (%)	56.1	59.9

Burst

	T9093	Exam
Length	0.62	0.70
Max. Volts	3.72	
Max. Depth (%)	75.0	91.1
Avg. Depth (%)	58.4	59.9